PART I: BACKBONE MODIFICATION OF N-HETEROCYCLIC CARBENES: NEW LIGANDS AND APPLICATIONS TO CATALYSIS

PART II: LARGE SCALE SYNTHESIS OF NHC PRECURSOR 2,6-DI(3-PENTYL)ANILINE

MATTHEW POMPEO

A THESIS SUBMITTED TO THE FACULTY OF GRADUATE STUDIES IN PARTIAL FULFILLMENT OF THE REQUIREMENTS FOR THE DEGREE OF

MASTER OF SCIENCE

GRADUATE PROGRAM IN CHEMISTRY

YORK UNIVERSITY

TORONTO, ONTARIO

AUGUST 2013

ABSTRACT

The first part of this research is focused on the development and application of backbone-modified N-heterocyclic carbene (NHC) ligands in palladium-catalyzed cross-coupling. Various backbone substituted imidazole-2-ylidine NHCs and their corresponding Pd-PEPPSI complexes were synthesized and S.A.R. studies were performed in a series of challenging cross-coupling reactions to determine the effect of backbone substitution on catalyst activity. Pd-PEPPSI-IPent^{Cl}, featuring chlorines on the backbone of our IPent NHC, was identified as one of the most active and selective catalysts yet reported in the literature in the secondary alkyl Negishi coupling, an important method for the installation of secondary alkyl groups onto aromatic systems. Mechanistic studies, supported by DFT calculations and IR spectroscopic analyses, indicate that the effect imparted by the backbone substituents is primarily steric in origin.

Further optimizing the architecture of the trans-ligated pyridine culminated in the development of Pd-PEPPSI-IPent^{Cl}-picoline, which we have shown to be a superior catalyst for the unprecedented *room temperature* Buchwald-Hartwig amination of aryl halides with electronically deactivated anilines using a mild carbonate base. These conditions are milder than any yet reported in the literature for the cross-coupling of anilines and represent a significant advance in the field.

The second part of this research deals with the development of a method for the large-scale preparation of 2,6-di(3-pentyl)aniline, a precursor to the IPent family of novel, highly active NHC ligands. Our newly developed synthetic route features a Pd-catalyzed cross-coupling of 3-lithio-2-pentene, derived from 3-pentanone, to readily available 2,6-dibromoaniline. This new sequence represents a significant improvement in overall process efficiency in the form of a lower step count, higher product yield, and increased reproducibility relative to earlier syntheses. Since its inception, this method has been applied successfully towards the synthesis of nearly 0.7 kg of 2,6-di(3-pentyl)aniline and has the potential for larger scale implementation.

ACKNOWLEDGEMENTS

First, I would like to express my gratitude to my supervisor, Prof. Michael G. Organ, for his constant encouragement, support, and when needed, constructive criticism. Working in an environment in which creativity and intellectual freedom were valued and encouraged has allowed me to become a much more independent and confident chemist than I would have imagined possible at the outset of my graduate work. I would also like to extend my thanks to Prof. Arturo Orellana for his honest guidance in my research and for sharing his immense knowledge of organic chemistry during the problem set sessions, from which I benefitted greatly. In addition, I would like to thank Prof. Gino Lavoie for agreeing to be on my research committee and for his suggestions and unique insight on organometallics and catalysis.

Next, I would like to thank everyone who has given me encouragement, guidance, and most of all friendship along this journey. The last few years spent in the lab would not have been as easily endured if it were not for you. Specifically, I would like to mention Dr. Selcuk Çalimsiz for patiently guiding me through my first days and months in the lab as a CHEM 4000 student and later as a graduate student, for always being open to answering questions, and for taking lab safety seriously ("face shield!"). I would also like to mention Dr. Debasis Mallik for his guidance, knowledge, and humour in the lab, especially during our arduous scale-up campaigns. Lastly, I would like to express special thanks to Dr. Howard Hunter for his willingness to share his immense knowledge and experience of NMR spectroscopy, which greatly enabled my research.

I would also like to express my appreciation to the many colleagues that I've had the pleasure of working alongside in the last few years, many of whom I now consider close friends. Specifically to Jennifer Farmer and Dr. Mahmoud Sayah for their friendship, honesty, and willingness to participate in discussion and debate on anything from chemistry to politics; to Dr. Michael "Mini-Mike" Tsimerman and Dr. Ka Hoi for accepting me into Team Carbene with open arms; to Dr. Dave Rosa for his humour, constant encouragement, and remarkable work ethic; to Dr. George Achonduh and Dr.

Niloufar Hadei for making the daily grind a little more bearable with their humour and good spirits; to Abir Khadra for her informal Arabic lessons and her rare attention to detail; to Lucas McCann ("Jesus") for demonstrating that work-life balance is indeed possible even for a graduate student; to Dr. Farman Ullah for his unique personality and perspective; to Angelika Schweinitz for serenading me with her Austrian (not German!) accent; to Dr. Toshiyuki "Toshi" Iwai for his thoroughness and curiosity; to Paul O'Brien for his mastery of the art of rotary evaporator maintenance; and to Endri Gjiri for his ingenuity and resourcefulness. I will remember you all fondly.

Finally, this section would be incomplete without mentioning my parents, without whom none of this would have been possible (literally!). Thank you for enduring my unpredictable working hours, my mercurial moods, and my evasive responses to your concerns about my future employability. Above all, thank you for providing a constant stream of warm, home-cooked meals – I will miss these immensely.

TABLE OF CONTENTS

LIST OF TABLES

Part I: Backbone Modification of N-Heterocyclic Carbenes: New Ligands and Applications to Catalysis

Part II: Towards a Scalable Synthesis of NHC Precursor 2,6-di(3-pentyl)aniline

LIST OF FIGURES

Part I: Backbone Modification of N-Heterocyclic Carbenes: New Ligands and Applications to Catalysis

Part II: Towards a Scalable Synthesis of NHC Precursor 2,6-di(3-pentyl)aniline

LIST OF SCHEMES

Part I: Backbone Modification of N-Heterocyclic Carbenes: New Ligands and Applications to Catalysis

Part II: Towards a Scalable Synthesis of NHC Precursor 2,6-di(3-pentyl)aniline

LIST OF ABBREVIATIONS

Ac	acetyl
Ad	adamantyl
BHE	β-hydride elimination
Boc	*tert*-butyl carbamate
BrettPhos	2-Dicyclohexylphosphino-3,6-dimethoxy-2′,4′,6′-triisopropylbiphenyl
°C	degree Celcius
Cat.	catalytic
cod	cyclooctadiene
CPent	1,3-bis(2,6-dicyclopentylphenyl)xvmidazole-2-ylidine
Cy	cyclohexyl
Cyoct	cyclooctyl
DME	dimethoxyethane
DMF	dimethylformamide
dppf	1,1'-Bis(diphenylphosphino)ferrocene
DFT	Density functional theory
equiv.	molar equivalents
GC/MS	Gas Chromatography/Mass Spectrometry
HRMS	High-resolution mass spectrometry
IAd	1,3-diadamantylimidazol-2-ylidine
IBiox	Bisoxazolinium-derived NHC
I^{t}Bu	1,3-di-*tert*-butylimidazol-2-ylidine

ICy	1,3-dicyclohexylimidazol-2-ylidine
IEt	1,3-bis(2,6-diethylphenyl)imidazol-2-ylidine
IHept	1,3-bis(2,6-di(4-hepty)phenyl)imidazole-2-ylidine
IMe	1,3-dimethylimidazol-2-ylidine
IMes	1,3-bis(2,4,6-trimethylphenyl)imidazol-2-ylidine
IPent	1,3-bis(2,6-di(3-pentyl)phenyl)imidazole-2-ylidine
$IPent^{Cl}$	1,3-bis(2,6-di(3-pentyl)phenyl)-4,5-dichloroimidazol-2-ylidine
$IPent^{Me}$	1,3-bis(2,6-di(3-pentyl)phenyl)-4,5-dimethylimidazol-2-ylidine
$IPent^{Quino}$	1,3-bis(2,6-di(3-pentyl)phenyl)-4,9-dioxo-4,9-dihydro-1*H*-naphtho[2,3-*d*]imidazole-2-ylidine
IPr	1,3-bis(2,6-diisopropylphenyl)imidazole-2-ylidine
IPr^{*}	1,3-bis(2,6-bis(di-*para*-tolylmethyl)phenyl)imidazole-2-ylidine
IPr^{Br}	1,3-bis(2,6-diisopropylphenyl)-4,5-dibromoimidazol-2-ylidine
IPr^{Cl}	1,3-bis(2,6-diisopropylphenyl)-4,5-dichloroimidazol-2-ylidine
IPr^{CN}	1,3-bis(2,6-diisopropylphenyl)-4,5-dicyanoimidazol-2-ylidine
IPr^{F}	1,3-bis(2,6-diisopropylphenyl)-4,5-difluoroimidazol-2-ylidine
IPr^{Me}	1,3-bis(2,6-diisopropylphenyl)-4,5-dimethylimidazol-2-ylidine
IPr^{Quino}	1,3-bis(2,6-diisopropylphenyl)-4,9-dioxo-4,9-dihydro-1*H*-naphtho[2,3-*d*]imidazole-2-ylidine
KHMDS	Potassium bis(trimethylsilyl)amide
MI	Migratory insertion
Ms	Methylsulfonyl (mesyl)
NFSI	N-fluorobenzenesulfonimide

NHC	N-heterocyclic carbene
NMR	Nuclear magnetic resonance
No-D NMR	NMR without deuterated solvent
PEPPSI	Pyridine-enhanced pre-catalyst preparation, stabilization, and initiation
QPhos	1,2,3,4,5-Pentaphenyl-1′-(di-tert-butylphosphino)ferrocene
rt	Room temperature
RE	Reductive elimination
RuPhos	dicyclohexyl(2',6'-diisopropoxybiphenyl-2-yl)phosphine
SAR	Structure-Activity Relationship
SIMes	1,3-bis(2,4,6-trimethylphenyl)imidazolidine-2-ylidine
SIPr	1,3-bis(2,6-diisopropylphenyl)imidazolidine-2-ylidine
SPhos	2-Dicyclohexylphosphino-2′,6′-dimethoxybiphenyl
TEP	Tolman's electronic parameter
Tf	Trifluoromethanesulfonyl
THF	tetrahydrofuran
TLC	Thin-layer chromatography
TMS	trimethylsilyl
TOF	Turn-over frequency
TON	Turn-over number
TPT	1,3,4-triphenyl-4*H*-1,2,4-triazol-5-ylidine
Ts	*para*-toluenesulfonyl (tosyl)
XPhos	2-Dicyclohexylphosphino-2′,4′,6′-triisopropylbiphenyl

PART I: BACKBONE MODIFICATION OF N-HETEROCYCLIC CARBENES: NEW LIGANDS AND APPLICATIONS TO CATALYSIS

CHAPTER 1: INTRODUCTION

1.1 – Palladium-Catalyzed Cross-Coupling Reactions

Palladium-catalyzed cross-coupling reactions have become some of the most widely used and versatile synthetic methods for the formation of carbon-carbon and carbon-heteroatom bonds and have revolutionized the way chemists approach complex molecule synthesis.[1] In recognition of this tremendous achievement, Akira Suzuki, Ei-ichi Negishi, and Richard Heck were awarded the 2010 Nobel Prize in Chemistry for their pioneering role in the development of these processes.[2]

Cross-coupling reactions are formally double displacement reactions in which a nucleophilic aryl, alkenyl, or alkyl organometallic reagent reacts with an electrophilic organohalide or pseudohalide, forming a new carbon-carbon bond and a metal salt by-product.[3] Unlike traditional second-order bimolecular substitution reactions that proceed in the absence of a catalyst (e.g. S_N2 reaction), the mechanism of cross-coupling reactions features at least three elementary steps, commonly: oxidative addition, transmetalation, and reductive elimination (Figure 1).[4] By partitioning the carbon-carbon bond-forming event into several smaller transition-metal mediated processes, the overall activation barrier of the transformation can be reduced relative to the uncatalyzed process. Whereas the uncatalyzed reaction requires passage through a single high-energy transition state (TS), the catalyzed version benefits from the unique ability of the transition metal to stabilize reactive intermediates thus making them more kinetically accessible.

The nature of the transmetalating agent has a profound effect on the course of the reaction and several protocols have been developed for cross-coupling various organometallics including organoboron, zinc, magnesium, and tin reagents.[1] As such, separate names are accorded to each coupling reaction depending on the specific organometallic reagent employed. For example, the most common cross-coupling, which involves the use of organoboron reagents, is known as the Suzuki-Miyaura reaction after the investigators who first demonstrated the broad transmetalating ability of these

reagents. In the absence of a suitable transmetalating agent, alkenes can behave as competent coupling partners, reacting with the oxidative addition adduct effecting a net C-H substitution with concomitant extrusion of a Brønsted acid (Figure 1, Cycle 2). Known as the Mizoroki-Heck reaction, this transformation is significant in that it was one of the first widely used metal-catalyzed "C-H activation" processes.[5]

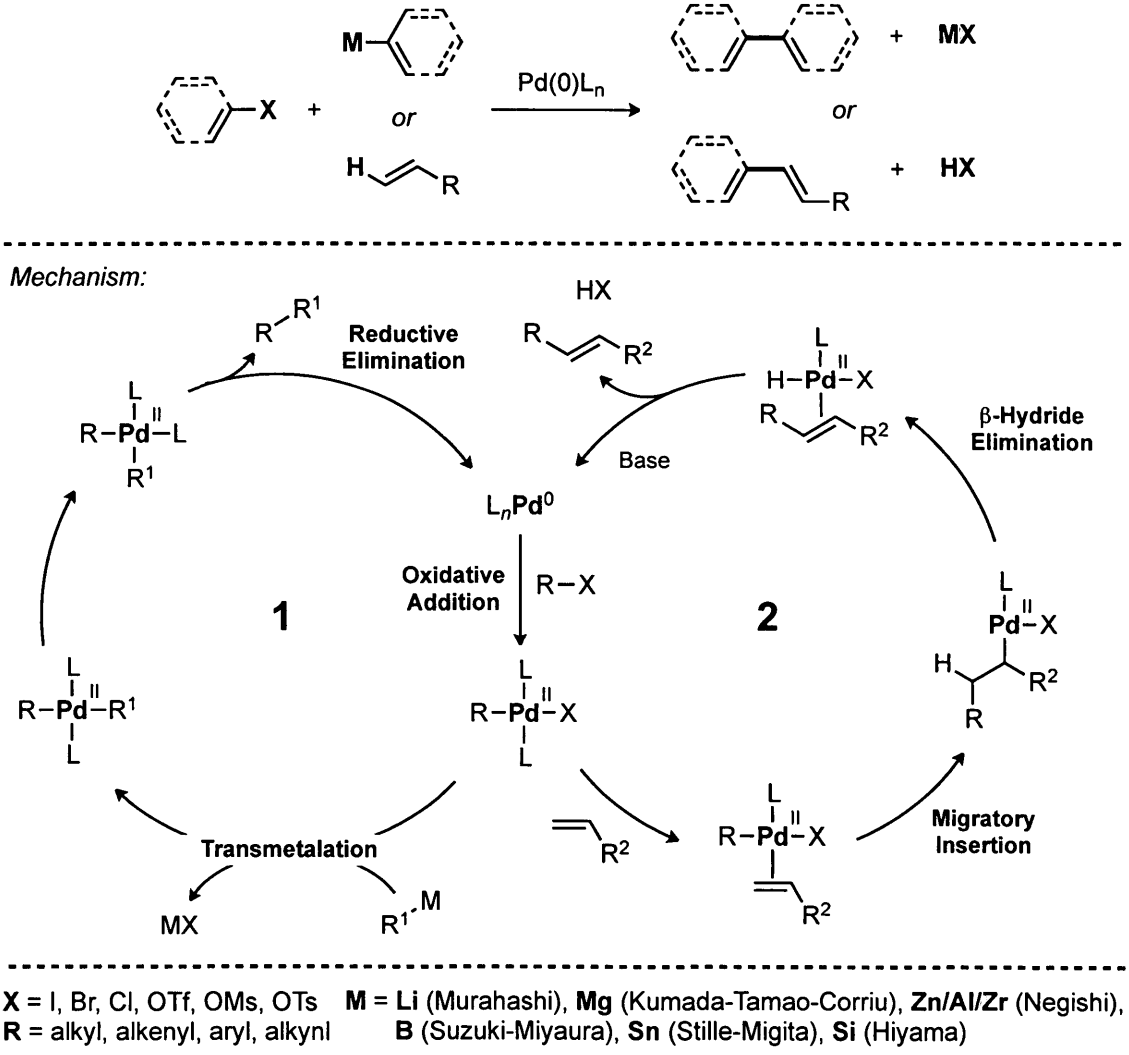

Figure 1. Simplified general mechanisms for Pd-catalyzed cross-coupling reactions forming C-C bonds. Cycle 1: with organometallic transmetalator; Cycle 2: with alkene.

Cross-coupling of heteroatom nucleophiles has also been the subject of intense study over the last twenty years.[6] Protocols have been developed for the Pd-catalyzed formation of C-O,[7-8] C-S,[9] and C-P[10] bonds, however by far the most common of these carbon-heteroatom bond-forming reactions is the Buchwald-Hartwig amination which involves the preparation of the pharmaceutically relevant C-N bond.[11] The putative mechanism of this transformation is similar to that of a typical cross-coupling reaction except that an amine replaces the organometallic transmetalator as the nucleophile (Figure 2).[4,6] After oxidative addition, the amine coordinates to the metal forming Pd-ammonium species **B**, which is deprotonated by exogenous base to furnish a Pd-amido intermediate **C**, which then undergoes reductive elimination to generate the cross-coupled product.

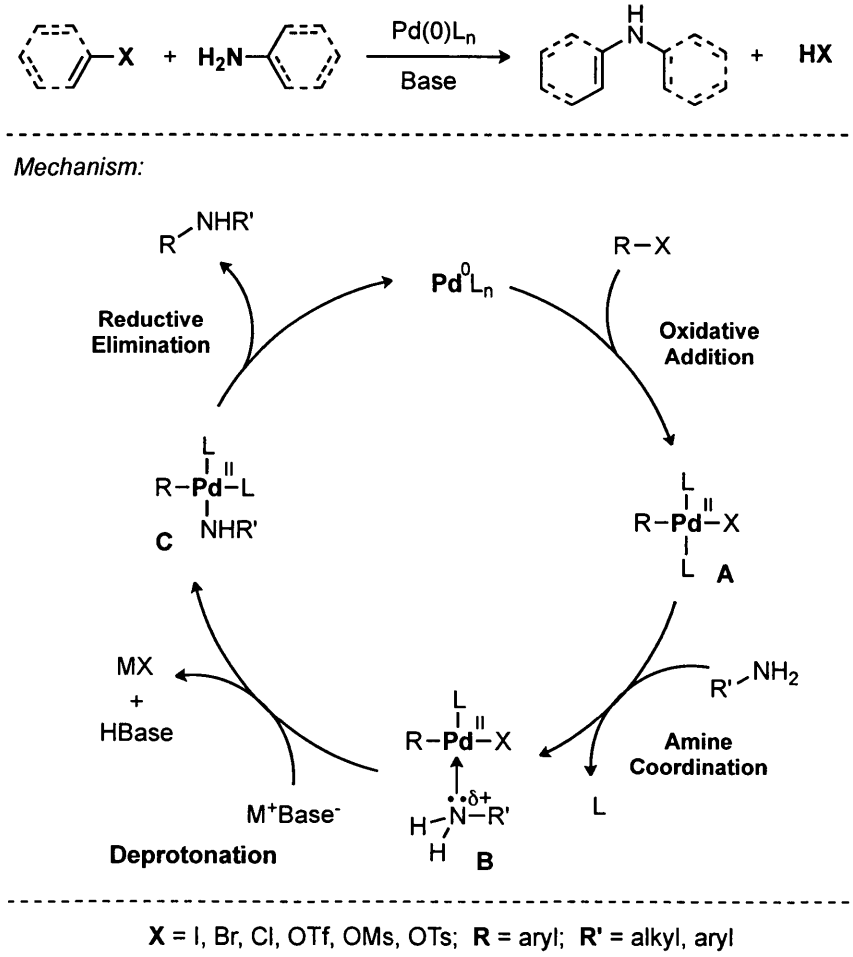

Figure 2. Putative mechanism for the Pd-catalyzed Buchwald-Hartwig Amination

1.2 – Importance of Cross-Coupling Chemistry

In organic chemistry, the ultimate measure of a new synthetic method is in its uptake by chemists. Even a cursory glance at the synthetic routes employed for the preparation of important natural products, agrochemicals, and drug molecules reveals the high degree to which Pd-catalyed cross-coupling has been and continues to be used to prepare C-C and C-heteroatom bonds.[12] A summary of some notable applications of cross-coupling is outlined below and summarized in Figure 3.[13]

The literature is replete with examples of cross-coupling in the preparation of active pharmaceutical ingredients (APIs) on multi-gram to tonne scale. The industrial synthesis of Losartan (Merck),[14] used to treat high blood pressure, and Crizotinib (Pfizer),[15] used to treat non-small lung carcinoma, feature key Suzuki-Miyaura disconnections to assemble two sp^2-hybridized aryl fragments. Notably, both of these routes are routinely carried out on multi-kg scales. The Novartis route to Gleevec (Imatinib), a tyrosine kinase inhibitor used to treat Leukemia, relies on a Buchwald-Hartwig amination to install the heteroaryl amine unit, which was found to be critical for biological activity. Merck's process route to prepare Singulair, a leukotriene receptor antagonist used for the treatment of asthma and seasonal allergies, makes effective use of a Heck coupling.[16]

The use of cross-coupling chemistry in the synthesis of more complex natural products is also a staple in total synthesis. A gram-scale sp^2-sp^3 Negishi coupling was employed by the Smith group to assemble two highly functionalized fragments towards the total synthesis of discodermolide, a clinically-relevant microtubule stabilizer of extraordinary structural complexity.[17] The synthesis of marine natural-product diazonamide A, another microtubule stabilizer and anti-cancer agent, was completed by the Nicolaou group using a Suzuki-Miyaura coupling.[18] Finally, a remarkable use of both the Stille and Heck coupling reactions was demonstrated by Overman and co-workers towards the synthesis of tetrameric quadrigemine C, a potent antibacterial.[19] Needless to say, most of these impressive achievements would have been impossible in the absence of cross-coupling chemistry and the novel molecular architectures that it has allowed chemists to access.

Active Pharmaceutical Ingredients (APIs):

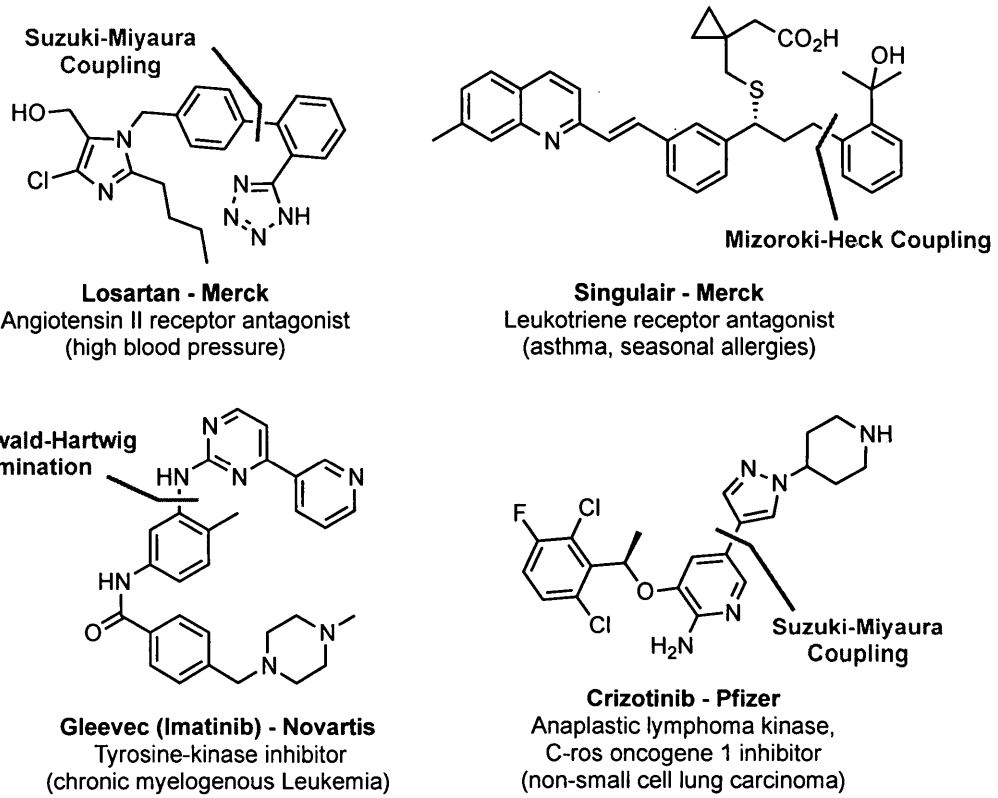

Biologically Active Natural Products:

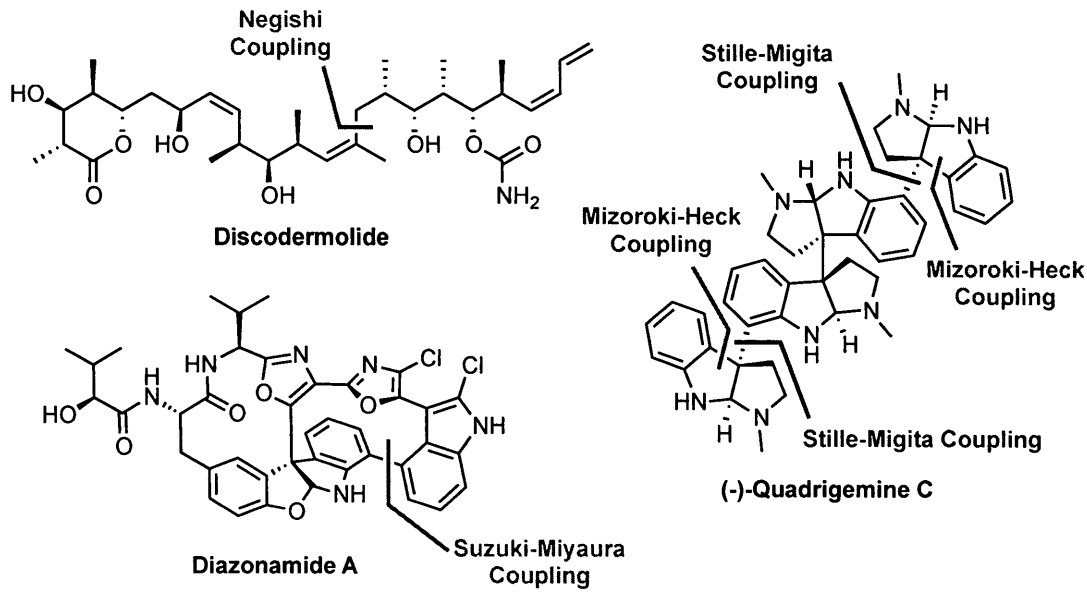

Figure 3. Selected applications of cross-coupling in total synthesis[13-19]

1.3 – Ancillary Ligands in Palladium Catalysis

Ancillary ligands are critically important to the success of most cross-coupling reactions since they allow for predictable modulation of the steric and electronic environment around the metal centre without being consumed during the course of the reaction. By systematically varying these steric and electronic parameters, researchers have come to better understand the stereoelectronic requirements of each elementary process in the catalytic cycle. For example, it is now well appreciated that the rate of oxidative addition is positively correlated with an increasingly electron rich metal centre compared to reductive elimination, which is enhanced by a sterically crowded metal. This knowledge is indispensable because it allows chemists to implement rational design elements into new ligands that are explicitly tailored to improve the efficiency of specific cross-coupling reactions. As such, the majority of modern studies aimed at improving the efficiency and scope of cross-coupling chemistry are focused on the design and optimization of ligand architectures.[20]

To measure the performance of various catalyst systems, two quantitative parameters are used: *Turn-Over Number (TON)* and *Turn-Over Frequency (TOF)* (Equations 1 and 2). *TON* measures the number of catalytic cycles a complex can pass through before decomposing or becoming deactivated. Industrial-scale catalytic processes such as Rh-catalyzed hydroformylation proceed with *TON*s > 1.0 x 10^5, whereas newly developed processes might only occur with *TON*s < 50.[3] Conversely, *TOF* can be used as a good measure of the *rate* at which each cycle proceeds. The aim of ligand design is to increase both the stability of the active catalyst (leading to a higher *TON*) and the rate at which the catalyst produces product (leading to a higher *TOF*).

$$TON = \frac{mols\ product}{mols\ catalyst} \tag{1}$$

$$TOF = \frac{TON}{time} \tag{2}$$

1.4 – Phosphine Ligands

1.4.1 – Steric and Electronic Parameters of Phosphine Ligands

For many years, simple tertiary phosphine ligands, such as PPh_3, dominated the landscape of transition metal catalysis due to their electron rich character and ability to impart significant steric shielding to the metal coordination sphere. The steric and electronic nature of these ligands can be predictably tuned by varying the substituent attached to phosphorus. Quantitative parameters for measuring the relative donating ability and steric footprint of various phosphine ligands were developed by Tolman in a seminal 1977 review.[21] Tolman noted that, although sterics and electronics are intimately related and difficult to separate, a practical disambiguation could be achieved through the steric parameter (θ) and the electronic parameter (ν) associated with $[(PR_3)Ni(CO)_3]$ complexes (Figure 4).

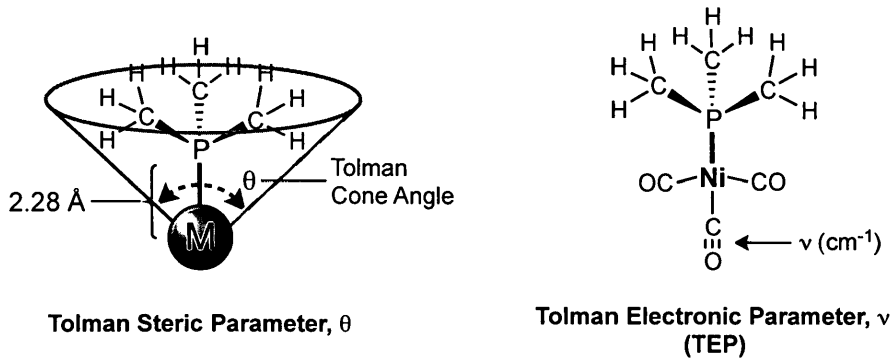

Figure 4. Commonly used quantitative parameters for measuring stereoelectronic effects of phosphine ligands.

The steric parameter quantifies the degree of phosphine steric bulk using the well-known ligand cone angle, which is defined as the apex angle of a cone centred at a distance of 2.28 Å from the phosphorus and extended to touch the Vander-Waals radii of the outermost ligand atoms. Conversely, the electronic parameter quantifies the electronic nature of the metal centre independent of the steric parameter using the A_1 IR stretching frequency of the trans-oriented carbonyl ligand.[22] This electronic parameter is now

known as Tolman's electronic parameter or TEP (θ) and has become one of the most widely accepted methods for measuring the relative σ-electron donating properties of phosphine and related ancillary ligands. The values of the TEP correlate with the *net* donor ability of the phosphine ligands, thereby allowing for an assessment of the relative electron "richness" of the associated metal centre. This is of critical importance in catalysis as the reactivity of many metal complexes towards organic molecules is invariably influenced by the electronic properties of the metal centre.

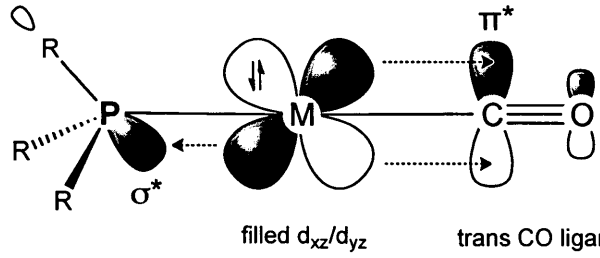

Figure 5. Simplified bonding schematic of phosphine-metal-CO complexes

When ligated to a transition metal, there are two main interactions between the phosphine and the metal centre that can be used to determine a qualitative bond order: (1) Phosphine to Metal σ-donation ($sp^3 \rightarrow d_z^2$) forming a formal sigma bond; and (2) Metal to Phosphine π back-donation ($d_\pi \rightarrow \sigma^*$), an interaction that depends highly on the nature of the substituent attached to the P atom. As illustrated in Figure 5, a trans-oriented carbonyl group can be used to probe the electronic content of the metal centre given its nature as a π-acceptor ligand.[23] As the electron density in the metal d-orbitals changes in response to the varying donating ability of the ligated phosphine, metal to carbonyl back donation into the π^* orbital of the CO ligand will change resulting in a fluctuation of the CO bond order. This variation in CO bond strength can be analyzed by infrared spectroscopy according to equation (3) which describes the wavenumber of absorbance in cm^{-1} as a function of the force constant, k, and the reduced mass of the system, μ:[24]

$$\nu = \frac{1}{2\pi c}\sqrt{\frac{k}{\mu}} \qquad (3)$$

Since the force constant, k, is directly proportional to the bond strength of the carbonyl group, it is expected that as the phosphine ligand becomes more electron donating and the CO bond weaker, the wavenumber of absorbance should decrease.

1.4.2 – Trends in the Development of Modern Phosphines

The general trend in the development of modern phosphine architectures for use in C-C bond-forming reactions is, predictably, towards ligands that render the metal more electron rich and deliver increased steric shielding.[20] The aim of these ligand enhancements is twofold. First, to expand the scope of Pd-catalyzed cross-couplings to include less expensive and more readily available aryl chlorides as electrophilic coupling partners, which have traditionally been reluctant to couple due to the high bond-dissociation energy of the C-Cl bond (95 kcal/mol) relative to their Br or I congeners (80 and 65 kcal/mol, respectively). By systematically varying the phosphine substituents, it was discovered that more electron-rich trialkyl phosphines significantly enhanced the rate-limiting oxidative addition of Pd(0) into these substrates.[25] The second target of these modifications is to improve the efficiency of coupling sterically-encumbered substrates, for example to form tri- or tetra-ortho-substituted biaryls. These processes often suffer from a slow reductive elimination step due to the considerable strain energy that develops in the transition state leading to the product. This limitation can be overcome by increasing the steric bulk of the ancillary ligand, which increases the rate of reductive elimination.

A selection of commonly used state-of-the-art phosphine ligands is shown below in Figure 6. Notable examples include the use of Pd/P^{t}Bu$_3$-based catalysts by Fu and Koie,[26] Beller's diadamantyl phosphines (CataCXium family),[27] dialkyl ferrocene phosphines employed by Hartwig (Q-Phos and JosiPhos),[28] and Buchwald's family of tunable dialkylbiaryl phosphine ligands,[29] all of which have dramatically expanded the scope of C-C and C-heteroatom couplings with aryl chlorides.

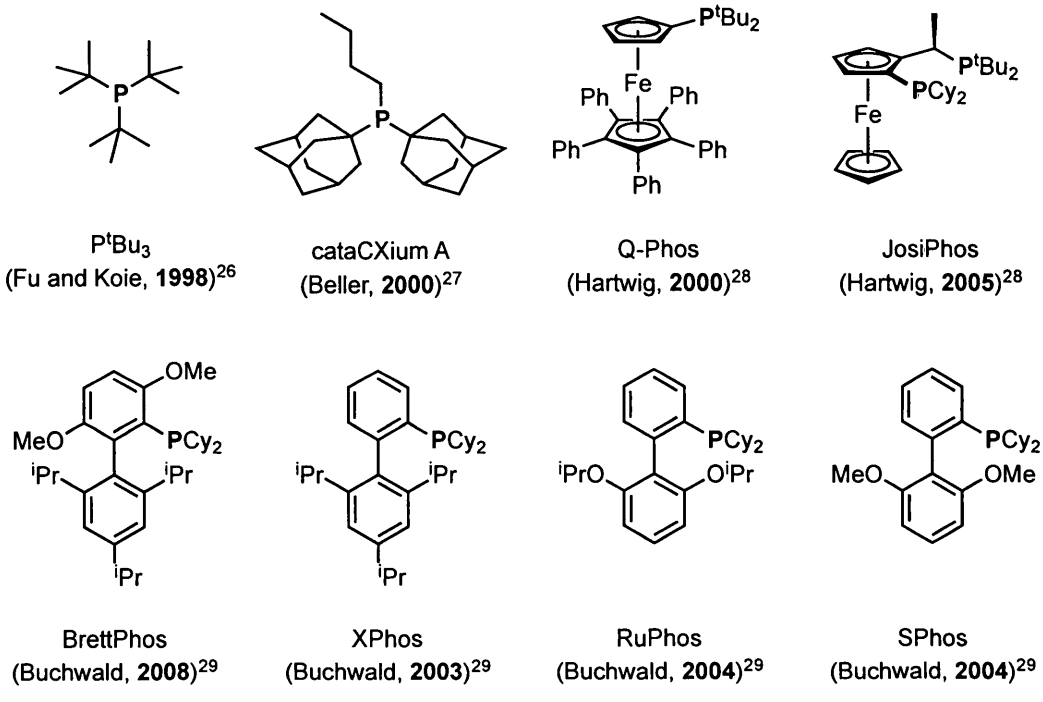

P^tBu_3 (Fu and Koie, **1998**)[26] | cataCXium A (Beller, **2000**)[27] | Q-Phos (Hartwig, **2000**)[28] | JosiPhos (Hartwig, **2005**)[28]

BrettPhos (Buchwald, **2008**)[29] | XPhos (Buchwald, **2003**)[29] | RuPhos (Buchwald, **2004**)[29] | SPhos (Buchwald, **2004**)[29]

Figure 6. A selection of state-of-the-art phosphine ligands used in palladium catalysis

1.4.3 – Deficiencies of Phosphine Ligands

Although phosphines are undoubtedly the most commonly used family of ancillary ligands in palladium catalysis, there are a number of disadvantages associated with their use. The first concerns the steric topology of a typical triaryl or trialkyl-phosphine, which is oriented away from the metal centre thus preventing optimal steric shielding of the metal. Next, many state-of-the-art trialkyl phosphines are highly pyrophoric due to their propensity to oxidize in air, thus requiring handling in an inert-atmosphere glovebox, which greatly detracts from their use. Finally, even the most strongly σ-donating phosphine ligands, such as P^tBu_3, are relatively labile leading to a dissociative tendency that is liable to disrupt the catalytic cycle in a significant and catastrophic way if the reaction is carried out in the absence of excess ligand. To demonstrate this lability, Hartwig reported in 2005 that treating tricoordinate [(P^tBu_3)Pd(o-tol)Br] (**1**) with an excess of pyridine resulted in complete substitution of the phosphine by the significantly

less donating pyridine (Equation 4).[28b] These deficiencies contributed to the development of alternative ligand platforms, of which N-heterocyclic carbenes (NHCs) have emerged as the predominant challeger to the supremacy of phosphines in Pd-catalyzed cross-coupling.

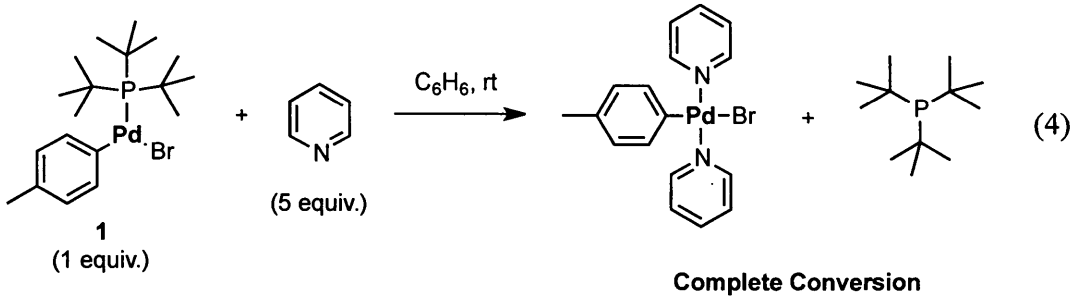

(4)

1.5 – N-Heterocyclic Carbene (NHC) Ligands

Since the isolation and characterization of the first stable free N-heterocyclic carbene (**2**) by Arduengo, et al. in 1991,[30] these compounds have undergone a remarkable evolution from academic curiosities to widely used ancillary ligands for transition-metal complexes. In the field of homogeneous catalysis, NHC-metal complexes have been demonstrated to effectively facilitate synthetically useful transformations including ruthenium-mediated olefin metathesis,[31] iridium-catalyzed hydrogenation,[32] platinum-catalyzed hydrosilylation,[33] and more recently palladium-catalyzed C-C[34] and C-N[35] cross-coupling reactions.

The most commonly employed NHC ligands are based on five-membered nitrogen-containing heterocycles in which the name of the ligand reflects the number and type of heteroatom contained in the ring (Figure 7).[36] The vast majority of NHCs used in Pd-catalyzed cross-coupling are derived from the imidazole and imidazolidine family. A selection of important NHCs is summarized in Figure 7. Noteworthy examples include Arduengo's IMes (**7**) and IPr (**8**) ligands, which remain the "go-to" NHCs for use in cross-coupling and their saturated counterparts SIMes (**11**) and SIPr (**12**), which are staples in Ru-catalyzed olefin metathesis.[37] More recent sterically hindered NHCs

developed by Glorius (**5** and **6**)[38], Organ (**10**)[39], Markó (**9**)[40], and Dorta (**13** and **14**)[41] have also made a significant impact in improving the scope of modern cross-coupling chemistry.

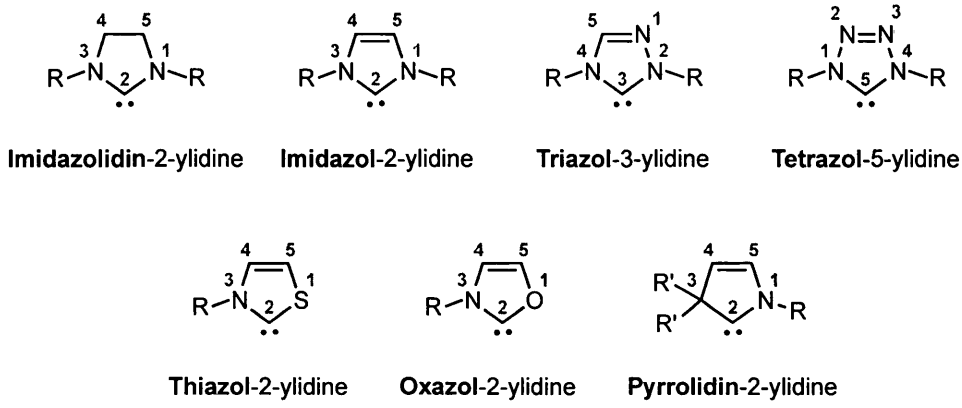

Figure 7. Five-membered N-heterocyclic carbene ligands and selected imidazole and imidazolidine NHCs used in cross-coupling

After the synthesis and characterization of the first NHC-metal complexes in 1968 by Wanzlick[42] and Öfele,[43] these ligands were considered simple tertiary phosphine mimics. This notion remained largely unchallenged until Arduengo's breakthrough in 1991 rekindled interest in NHCs and led to new synthetic strategies for their synthesis. In subsequent years, NHC-ligated transition metal complexes have been shown to be superior in many ways to their phosphine-based counterparts in terms of both scope and catalytic activity.

1.5.1 – Steric Parameters of NHC Ligands

Unlike phosphines, the steric bulk of NHC ligands is projected downward towards the metal centre, thus measurement of NHC steric bulk using Tolman's cone angle was deemed insufficient (Figure 8).[36]

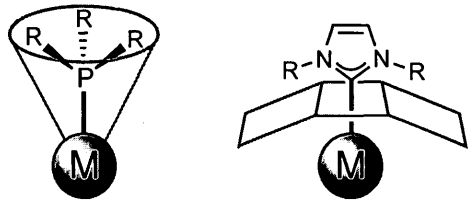

Figure 8. General steric topology of phosphine ligands and NHC ligands.

To address this difficulty, Nolan, Cavallo, and co-workers introduced the percent buried volume, $\%V_{Bur}$, a steric parameter specifically tailored to the steric topology of NHCs. The $\%V_{Bur}$ is defined as the fraction of the volume of the first coordination sphere around a metal occupied by a given ligand (Figure 9).[44] The value of the parameter can be computed from DFT-optimized structures or from X-ray crystal structures of the desired NHC metal complex. The standard NHC-metal complex from which the parameter could be computed was initially the same $[(L)Ni(CO)_3]$-type complexes from which the Tolman cone angle of phosphines was calculated, however difficulties were encountered in the preparation of some bulkier NHC-ligated congeners.[45] As a result, it was determined that

[(NHC)Ir(CO)$_2$Cl] complexes were optimal for the determination of NHC %V_{Bur} since they are readily accessible square planar complexes that simulate a reasonably bulky environment that might be encountered during a cross-coupling catalytic cycle, for example. The %V_{Bur} parameter was found to be sufficiently generic that the steric properties of phosphines could also be quantified using this technique.[46] The %V_{Bur} of some common NHCs is show in Figure 9.

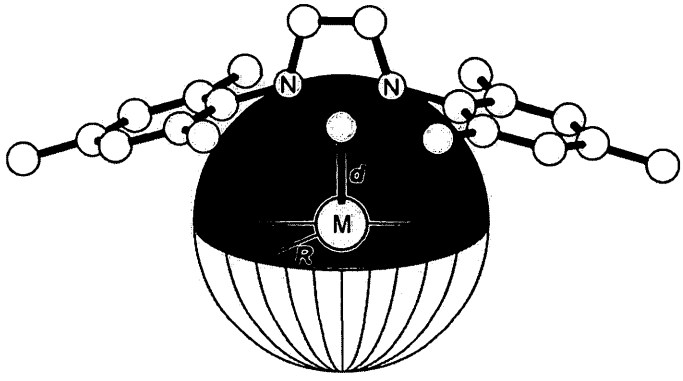

NHC	%V_{Bur}
IAd (**2**)	36.1
I^{t}Bu (**4**)	35.5
IMes (**7**)	31.6
IPr (**8**)	33.6
SIMes (**11**)	32.7
SIPr (**12**)	35.7
PPh_3	30.5
PCy_3	35.3

Figure 9. Percent buried volume, %V_{Bur} steric parameter of some common NHC ligands computed from the DFT-optimized geometries of [(NHC)Ir(CO)$_2$Cl] complexes in which d = 2.10 Å and R = 3.5 Å.[44b] For comparison purposes, the %V_{Bur} of two popular phosphines is also listed. Image reproduced from Ref. 36a.

1.5.2 – Electronic Parameters of NHC Ligands

Since Tolman's seminal 1977 review, the use of IR spectroscopy in concert with a coordinated trans carbonyl (CO) ligand as a "reporting group" has become a standard approach for probing the electronic properties of transition metals in complexes of widely varying structure.[21] It is not surprising then that a number of workers have sought to extend Tolman's phosphine methodology to NHC ligands. In 2003, Crabtree and co-workers reported on the use of [(L)Ir(CO)$_2$Cl] complexes in order to compare a series of phosphine and NHC ligands in terms of their electron donating ability.[47] It was noted that by correlating the average IR stretching frequency of the Ir system and the A_1 stretching

frequency from Tolman's [(L)Ni(CO_3)] complexes, a linear relationship was obtained for a series of ligands where data was available for both systems. Using this correlation, it was then possible to evaluate the Tolman electronic parameter (TEP) for these new NHC ligands by simple extrapolation. Crabtree's discovery was instrumental in that it allowed evaluation of the TEP without the need for the corresponding [(NHC)Ni($CO)_3$] complexes whose synthesis requires the extremely toxic [Ni($CO)_4$] precursor. Crabtree,[48] Glorius,[49] and Hermann[50] expanded on this work in 2004 and used the same Ir system to explore the donating properties of other NHC ligands including the bisoxazoline-derived NHCs (**5-6**) found to be highly active in challenging Suzuki-Miyaura couplings. The most significant contribution to date in this area was made by Nolan and co-workers, who in 2008 published a detailed account of the correlation between the TEP and mean CO stretching frequencies of [(NHC)Ir($CO)_2$Cl] complexes bearing a variety of structurally diverse NHC ligands.[51] The larger sample size enabled the calculation of a more accurate linear regression equation between the two parameters (Figure 8).

From these studies, Crabtree and Nolan confirmed that typical imidazole-2-ylidine NHCs are significantly more donating than even the most electron-rich phosphines, such as PCy_3, thus rendering the metal to which they are coordinated much more electron rich relative to their phosphine counterparts. In addition, it became evident that the nature of the *ortho*-alkyl substituents on the aryl ring did not significantly affect the donating ability of the carbene, demonstrating independent tunability of NHC steric and electronic properties. For example, a difference of only 0.8 cm^{-1} was observed between the TEP of IMes (**7**) and the profoundly more bulky IPr (**8**). This electronic invariability of NHC ligands starkly contrasts with trialkylphosphines, whose donor abilities vary greatly as the substituent on the P atom is varied. For example, comparing PEt_3 and $P(^iPr)_3$, a simple change from ethyl to isopropyl substituents results in a much larger change in the TEP of 2.8 cm^{-1}. This can be rationalized by considering that the substituents that confer steric bulk to an NHC are far removed from the carbene carbon, whereas in phosphines, they are bonded directly to the phosphorus atom. In this way, the steric and electronic

parameters of this class of phosphine are intimately linked in a way that limits the tunability of the ligand class.

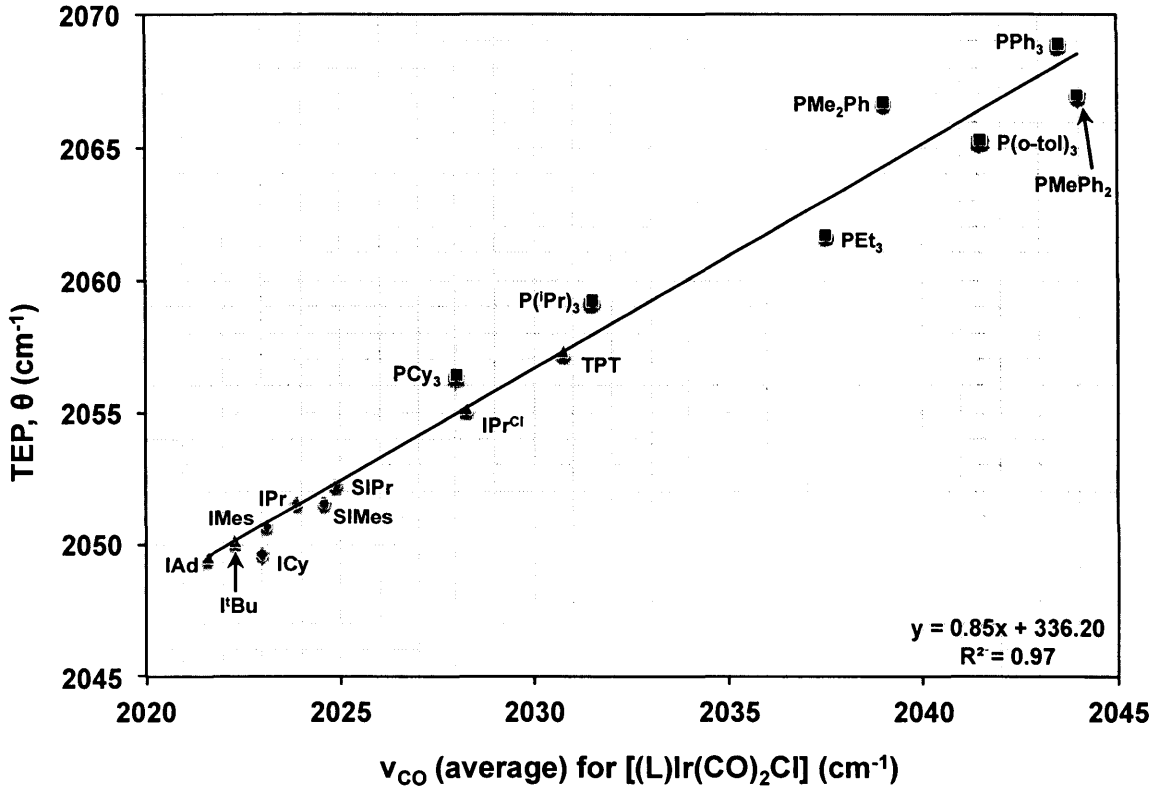

Figure 8. Nolan's correlation of average ν_{CO} values for $[(L)Ir(CO)_2Cl]$ complexes with the Tolman electronic parameter (TEP).[51] (■) Experimental values for phosphines; (•) Experimental values for NHCs; (▲) Values obtained by linear regression.

1.5.3 – Tuning the Electronic Properties of NHC Ligands

Unlike steric tuning of NHCs, which has largely been focused on increasing the size of the N-substituents (compare NHCs **7**, **8**, and **10**), electronic modification has been relatively less explored.[52] The critical structural parameters that can be modified to tune the donating ability of NHCs are: (a) the NHC skeleton; (b) the nature of the substituents on the ligand backbone; and (c) the N-substituents. From the TEP studies by Nolan, it is evident that alterations to the ligand backbone result in the most significant changes to

ligand donicity. For example, the IPr^{Cl} ligand **15** with electron-withdrawing Cl atoms on the ligand backbone and the triazole-based NHC **16** were found to be significantly less donating than their unmodified counterparts (Figure 9). Biewlawski and co-workers also observed a similar trend when systematically varying the backbone substituent of related NHC ligands.[53] Interestingly, Plenio and co-workers discovered that the donating ability of these ligands could be similarly modulated by varying the *para*-substituents on the aryl ring of the N-substituents, a somewhat unexpected finding considering that the imidazole ring of the NHC is not in conjugation with the N-aryl substituent.[54] It is important to note that in all cases, the electronic effects observed during these modifications are significant and result in changes in the TEP of up to 9 cm^{-1} in the case of backbone modification.

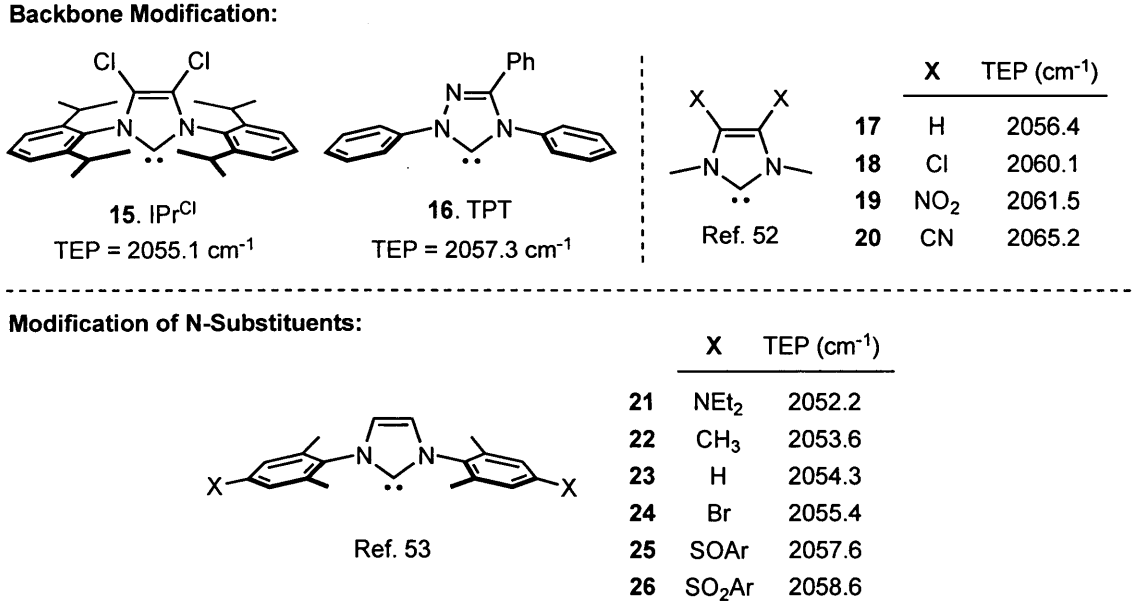

Figure 9. Electronic modification of NHC ligands

1.6 – The Pd-PEPPSI Family of Pre-Catalysts

Unlike phosphines, NHC ligands form exceptionally stable bonds with most transition metals.[36] As a result, the use of pre-formed NHC-Pd pre-catalysts has become a staple in modern cross-coupling.[55] Arguably the most popular NHC-based Pd pre-catalyst was

introduced by Organ and co-workers in 2006 and features an NHC-Pd(II) complex with a trans-ligated 3-chloropyridine ligand (Figure 10). Coined PEPPSI (Pyridine-Enhanced Pre-catalyst Preparation, Stabilization, and Initiation), these pre-catalysts have proven attractive since they are air and moisture-stable, are easily prepared on large-scale under ambient conditions, and are easily reduced to the active NHC-Pd(0) species under typical cross-coupling conditions.

In a series of publications, Organ and co-workers reported that while evaluating PEPPSI-based catalysts in Negishi,[56] Suzuki-Miyaura,[57] Kumada-Tamao-Corriu,[58] and Buchwald-Hartwig amination[59] reactions, those employing the PEPPSI-IPr catalyst (**29**) resulted in much higher yields than those employing the less sterically bulky PEPPSI-IMes (**27**) or IEt (**28**) catalysts. Since the σ-donor ability of both the IMes and IPr carbenes are very similar, it was thought that varying sterics must be responsible for the improved yields.

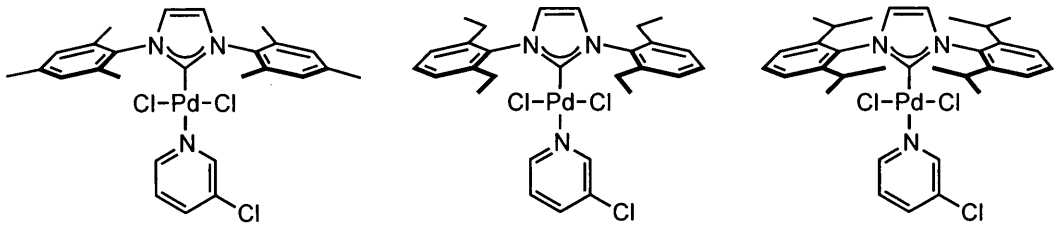

27 Pd-PEPPSI-IMes | **28** Pd-PEPPSI-IEt | **29** Pd-PEPPSI-IPr

Figure 10. A selection of first generation Pd-PEPPSI pre-catalysts

Based on this information, the Organ group proceeded to synthesize a second generation of Pd-PEPPSI complexes featuring a series of new, more sterically-demanding NHCs: Pd-PEPPSI-CPent (**30**), Pd-PEPPSI-IPent (**31**) and Pd-PEPPSI-IHept (**32**) (Figure 11).[60] These new catalysts were systematically evaluated in a series of difficult Suzuki-Miyaura reactions and **31** was identified as the most active. Since 2009, the Organ group has published a number of accounts detailing the superior activity of **31** in the Suzuki-Miyaura,[61] Negishi,[62] Stille-Migita,[63] and Buchwald-Hartwig[64] cross-coupling reactions.

This complex has proven to be the most active of the Pd-PEPPSI family of pre-catalysts as well as one of the most effective NHC-based palladium catalysts in cross-coupling chemistry published to date.

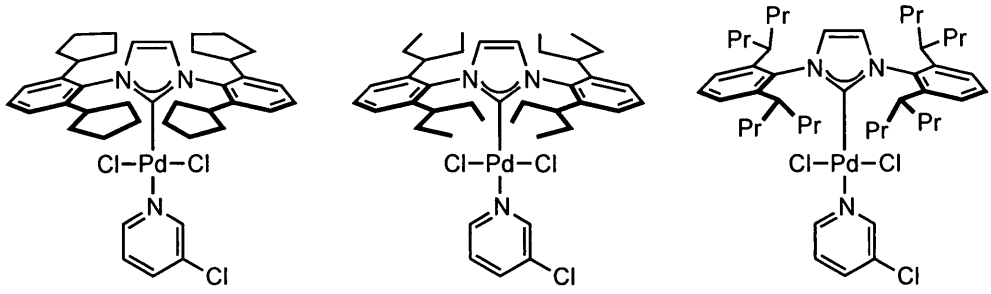

30
Pd-PEPPSI-cPent

31
Pd-PEPPSI-IPent

32
Pd-PEPPSI-IHept

Figure 11. A selection of second-generation Pd-PEPPSI pre-catalysts

Interestingly, when comparing the activities of **30-32**, two important structure-activity relationships were observed. First, it appeared that **31** was much more active than **30** despite the fact that the NHC *ortho*-alkyl substituents were almost identical (cyclopentyl vs. 3-pentyl). This led the Organ group to confirm the notion of "flexible steric bulk" coined in 2003 by Glorius and co-workers, which suggests that for high catalytic activity, a sterically demanding yet conformationally flexible environment about the palladium metal is required.[49] Second, by further increasing the size of the *ortho*-substituent from 3-pentyl (**31**) to 4-heptyl (**32**), less significant increases in reactivity were observed, indicating that the steric limit has been reached with this ligand motif, beyond which extra steric bulk does not translate into additional catalytic activity.[65]

1.7 – Plan of Study

Despite the heightened activity of Pd-PEPPSI-IPent (**31**) relative to the less bulky IPr congener (**29**), its reactivity still lagged behind state-of-the-art phosphines in two important cross-coupling reactions: the Buchwald-Hartwig amination of deactivated

aniline substrates[64b] and the Negishi coupling of secondary alkylzinc reagents.[62b] In order to address these deficiencies, we set out to design a series of new ligands specifically tailored for improved activity in these reactions. However, given the similar activity of catalysts **31** and **32** in the Suzuki-Miyaura reaction, we reasoned that further modification of the NHC steric profile via the *ortho*-alkyl substituents would most likely not furnish profoundly more reactive catalysts. As a result, we thought it prudent to examine the effect of modifications elsewhere on the NHC core, specifically on the backbone of the imidazole ring, which would allow for systematic variation of *both* NHC steric and electronic properties. Although a number of 4,5-disubstituted imidazol-2-ylidine NHCs have been reported in the last two decades, there have been remarkably few reports on the application of these ligands in Pd-catalyzed cross-coupling.

In this context, the aim of this research is to prepare various analogues of backbone-modified NHC ligands and their corresponding Pd-PEPPSI complexes and systematically evaluate their efficacy in the Buchwald-Hartwig amination reaction and in the secondary alkyl Negishi coupling. Furthermore, mechanistic studies will be performed in order to determine whether observed reactivity differences can be attributed to changes in ligand donating ability or steric topology.

CHAPTER 2: Synthesis of Backbone-Modified NHCs and Evaluation of their Steric and Electronic Properties

2.1 – Synthesis of 4,5-disubstituted IPr NHCs

In order to determine the effect of NHC backbone modification on catalytic activity in cross-coupling, we opted to focus first on modifying the more readily available IPr core. Both 4,5-dichloro-IPr (**34**) and 4,5-dimethyl-IPr (**38**) ligand precursors were prepared according to procedures developed by Arduengo,[66] and Nolan,[67] respectively (Figure 12).

Synthesis of IPr^{Cl}·HCl and IPr^{Br}·HCl (Adapted from Ref. 66):

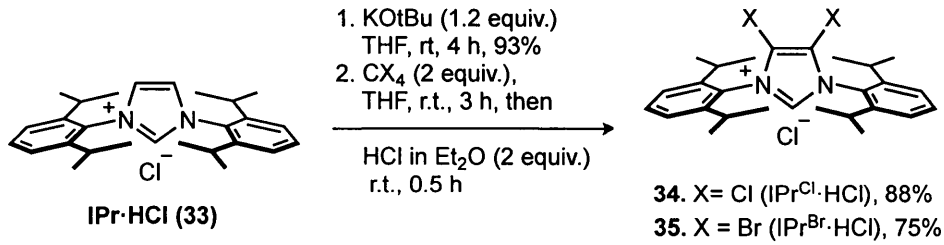

Synthesis of IPr^{Me}·HCl (Adapted from Ref. 67):

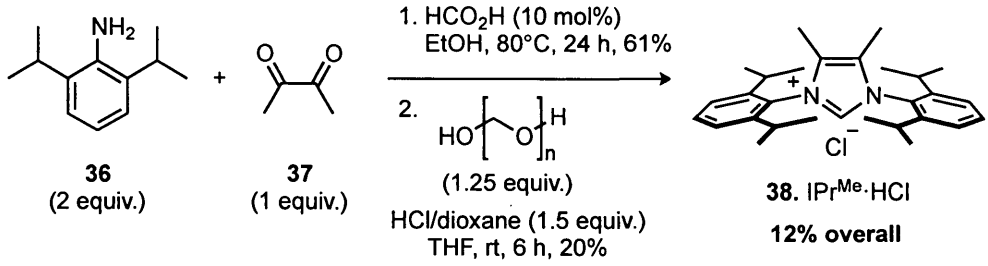

Synthesis of IPr^{Quino}·HCl (Adapted from Ref. 68):

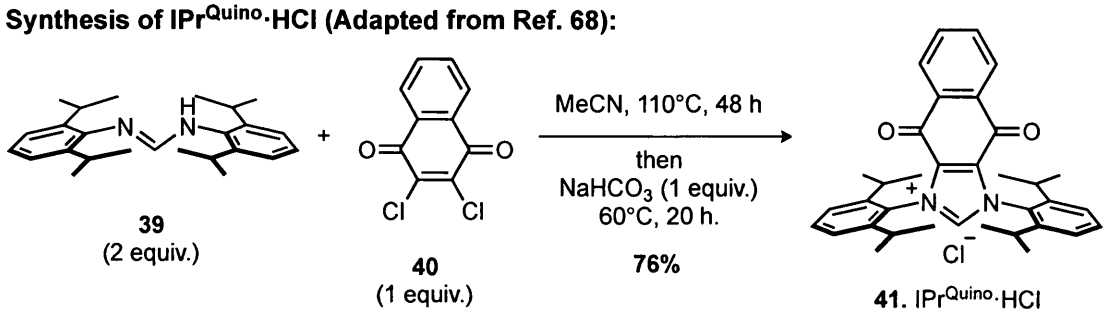

Figure 12. Synthesis of 4,5-disubstituted IPr NHC precursors: IPr^{Cl}, IPr^{Me}, and IPr^{Quino}.

The corresponding dibrominated ligand precursor IPr^{Br}·HCl (**35**) was also prepared successfully using a modification of the Arduengo procedure. With these known ligand precursors in hand, we looked to prepare other derivatives in which the backbone substituent might have a more profound impact on the steric and electronic nature of the NHC. To this end, the quinone-fused NHC precursor IPr^{Quino}·HCl (**41**) was prepared using a modification of Biewlawski's procedure for the IMes congener.[68] In this report, the π-acceptor character of the quinone-fused IMes ligand was noted to be significantly higher than unmodified IMes, which presents two opportunities for catalysis. First, the metal to which the ligand is coordinated will be rendered much more electrophilic due to decreased ligand donicity, a property which may be beneficial in certain cross-coupling reactions. Second, the increased π-acceptor character of the ligand will result in a shorter metal-ligand bond length thus projecting the steric bulk closer to the metal coordination sphere (Figure 13).

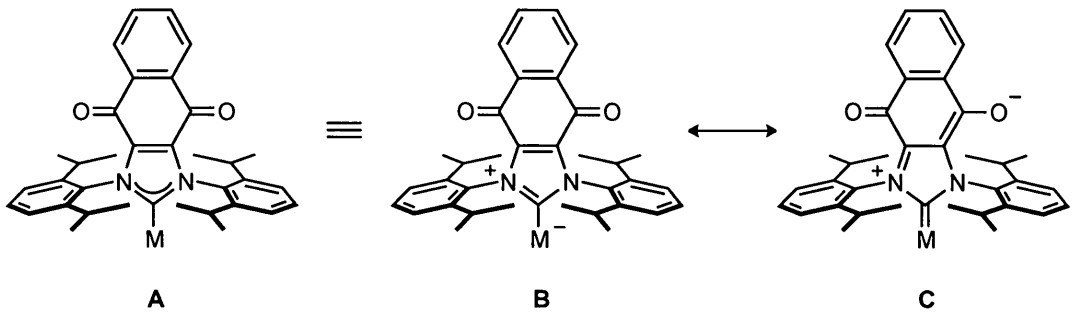

Figure 13. Selected bonding representations in an IPr^{Quino}-metal complex.

2.2 – Attempted Synthesis of Novel 4,5-disubstituted IPr NHCs

2.2.1 – Towards 4,5-difluoro-IPr (42)

One persistent uncertainty that arises in evaluating the activity of 4,5-dihalo NHCs **34** and **35** in cross-coupling is the susceptibility of the backbone halogens to oxidative addition. If the halogens do indeed undergo cross-coupling during the catalytic cycle, it then becomes impossible to correlate changes in catalytic activity solely to the effect of the halogen. With this in mind, the corresponding 4,5-difluorinated NHC ligand

precursor, IPr^F·HCl (**42**) was targeted, since the carbon-fluorine bond is generally inert to oxidative addition.

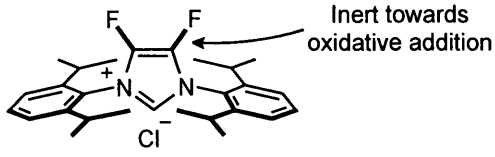

42. IPr^F·HCl

Figure 14. IPr^F·HCl (**42**)

Unfortunately, the method used to synthesize ligands **34** and **35** cannot be applied to the synthesis of the fluorinated analogue since CF_4 is a gas at room temperature and is likely much less reactive towards nucleophilic attack than CCl_4 (BDE(C-F) = 118 vs. BDE(C-Cl) = 81 kcal/mol). Accordingly, we opted to make use of Bertrand's recently reported stepwise strategy for the 4,5-difunctionalization of NHCs.[69] This method begins from the 4,5-unsubstituted free carbene **A** that upon treatment with a suitable electrophile forms imidazolium salt **B** (Scheme 1). Backbone deprotonation of this adduct with a strong base leads to intermolecular attack of the resulting anion at the 2-position of another molecule of **B**, generating mono-functionalized carbene **C**. This can be repeated to generate the 4,5-difunctionalized carbene **D**. It should be noted that this is essentially the same mechanism proposed by Arduengo for the 4,5-dichlorination of IPr with CCl_4,[66a] however with CCl_4, the trichloromethyl anion that is generated after carbene nucleophilic attack also serves the role as the base, thus the reaction can occur *in situ* from **A** – **D**.

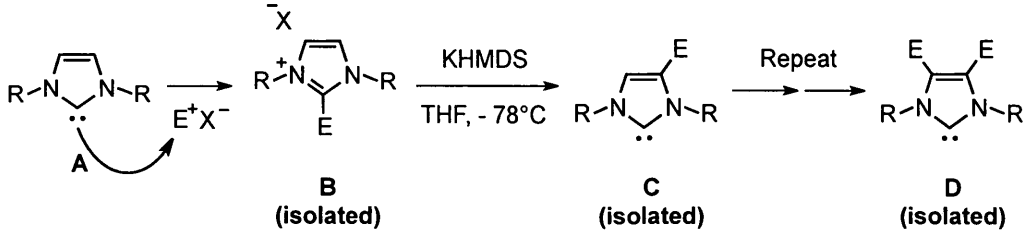

Scheme 1. Summary of Bertrand's methodology for NHC 4,5-difunctionalization[69]

Content with this strategy, the synthesis of precursor **43** was attempted by treating IPr carbene **8** with a variety of F^+ sources (Table 1).[70] Unfortunately, treating **8** with commercially available *N*-fluoropyridinium salts **44-46** in solvent mixtures of THF and acetonitrile resulted in clean recovery of the protonated carbenes (Entries 1-4). It has been reported that exposure of N-fluoropyridinium triflate **44** to strong bases results in deprotonation at the 2-position generating a carbene that decomposes by reacting with THF.[71] Similarly, one can envision deprotonation of **45** at the methyl groups in the 2- or 4-positions to generate the corresponding N-fluoro-dihydropyridine. Indeed, a set of vinyl resonances was observed between 5 – 6 ppm in the crude ^{1}H-NMR spectra that may be indicative of such a species. In these cases, the carbene was behaving as a base rather than a nucleophile as intended.

Table 1. Attempted Synthesis of Imidazolium Adduct **42**[a]

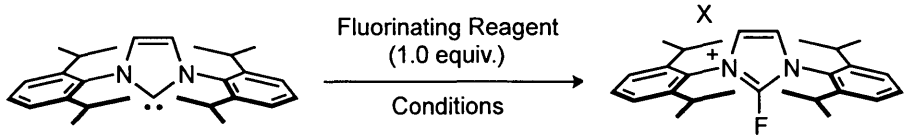

8. IPr

43. 2-F-IPr·HX

Entry	Fluorinating Reagent	Conditions	Products	Notes
1	**44**	1:1 THF:MeCN, r.t., 2h	IPr·HOTf	
2	**45**	1:1 THF:MeCN, r.t., 3h	IPr·HBF_4	2 vinyl singlets in ^{1}H-NMR
3	**45**	1:4 THF:hexanes r.t., 17h	IPr·HBF_4	Cleaner than Entry 2 but vinyl resonances still present
4	**46**	1:1 THF:MeCN, r.t., 17h	IPr·HBF_4	**46** completely consumed
5	**47**	MeCN, r.t., 49h	~1:1 Mixture of IPr·HBF_4 and unknown NHC	Inseparable Mixture

6	**48**	MeCN, r.t., 1.5h	**8**	No Reaction, IPr·HBF_4 recovered after MeOD quench
7	**48**	THF, r.t., 20h	**8**	
8	**48**	MeCN, 80°C, 49h	IPr·HBF_4 (major)	
9	**48**	THF, 80°C, 49h	IPr·HBF_4 (major)	
10	**49**	MeCN, r.t., 18.5h	IPr·HBF_4 (major), other NHC (major)	Inseparable Mixture
11	**50**	THF, r.t., 16h	Complex Mixture	
12	**50**	MeCN, r.t., 16h	Complex Mixture	

[a] All reactions performed on 1.0 mmol scale; [b] Product composition determined by ^{1}H-NMR spectroscopic analysis in CD_3CN.

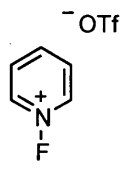

44

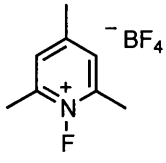

45

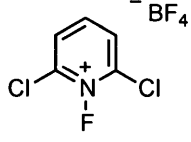

46

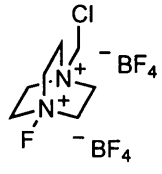

47

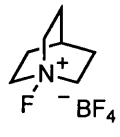

48

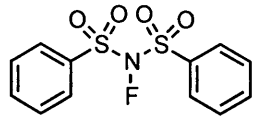

49

XeF_2

50

Switching to less acidic F^+ reagents such as SelectFluor™ (**47**) did result in the formation of a new imidazolium species however separation from the protonated carbene and N-defluorinated **47** proved difficult (Entry 5). Unexpectedly, no reaction was observed with quinuclidine-derived **48** (Entries 6 and 7). Heating the mixture to 80°C led to formation

of the protonated carbene (Entries 8 and 9), however the source of the proton in this case is unclear. Finally, the use of reagents **49** and **50** resulted in complex reaction mixtures, which could not be purified by crystallization or chromatography (Entries 10-12).

In light of our failure to intercept **8** with various F^+ sources, we wondered if **43**·BF_4 could be accessed via BF_3-mediated abstraction of a fluoride ion from 2,2-difluoro-IPr (**51**) (Scheme 2).

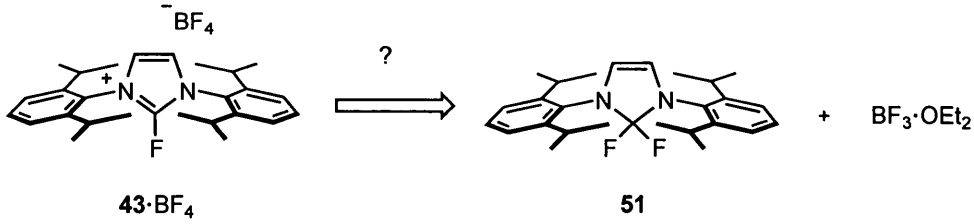

43·BF_4 **51**

Scheme 2. Proposed synthesis of **43**·BF_4 from 2,2-difluoro-IPr (**51**)

To prepare **51**, we adapted a literature procedure for the preparation of 2,2-difluoro-IMe (**53**), which has been used as a nucleophilic fluorinating reagent (Scheme 3).[72] Deprotonation and electrophilic quench of **30** with hexachloroethane generated 2-chloroimidazolium salt **54**, which was then treated with a twofold excess of anhydrous CsF in refluxing acetonitrile. Unfortunately, only urea **55** was isolated, which likely formed from hydrolysis of **51** with adventitious water. Since the CsF was rigorously dried under high vacuum at 200°C for 5 days then stored in a glovebox before use, it became clear that hydrolysis of **51** must have occurred during the work-up, which consisted of a simple Celite filtration in air. Thus, in light of the apparent sensitivity of **51** to atmospheric moisture, this route was abandoned. However, some months after these initial attempts, the preparation and use of **51** as a superior nucleophilic fluorination reagent was disclosed by Ritter, et al.[73] Interestingly, their published synthetic procedure was nearly identical to the one we attempted earlier (CsF, 3 equiv., acetonitrile, 60°C, 24h). Although the susceptibility of **51** to hydrolysis was noted, no requirements for special preparative techniques were indicated. However, in discussions with various members of the Ritter research group, it became clear that **51** could only be reliably

prepared if the entire operation were conducted in an inert-atmosphere glovebox. Since we have no provision for conducting filtrations and solvent-removal operations in our glovebox, we made no further attempts to prepare **51**.

Literature Precedent (Ref. 72):

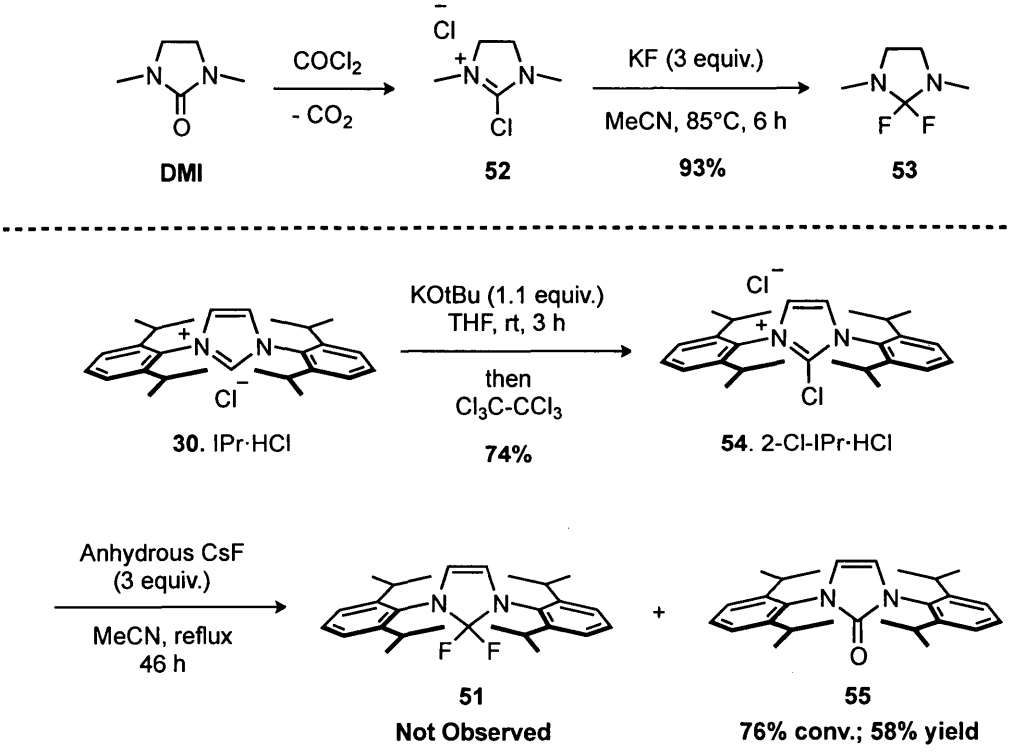

Scheme 3. Attempted preparation of **51**.

Having exhausted all efforts to prepare **42** via the Arduengo/Bertrand methodology, our final approach relied on Curran's recently disclosed technique for direct backbone functionalization of NHC-boranes.[74] This is a protecting group strategy that employs BH_3 in order to cap the reactive free carbene, thus allowing for backbone deprotonation by a strong base, such as nBuLi, followed by electrophilic quench of the resulting anion to generate variously functionalized NHCs (**A**, Scheme 4). Removal of the protecting group was shown to proceed quantitatively using one equivalent of a Brønsted acid in the presence of methanol.

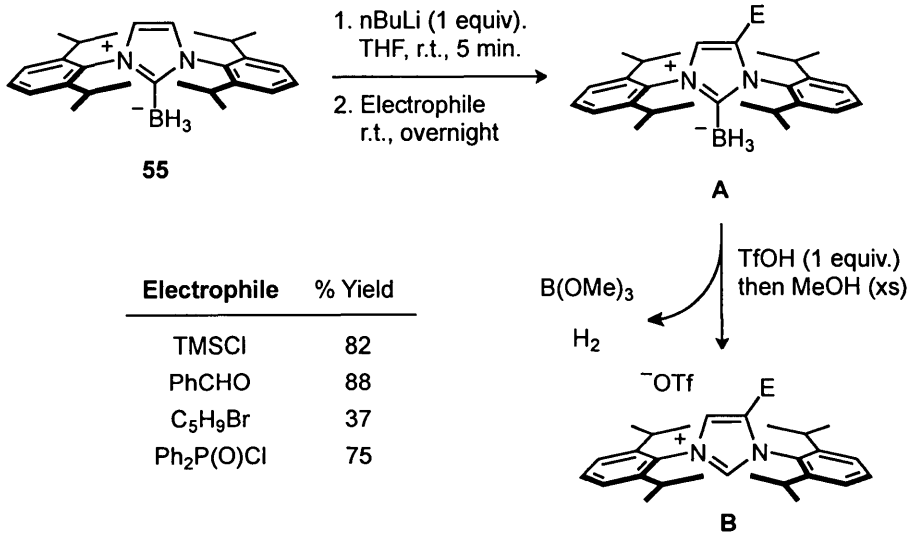

Electrophile	% Yield
TMSCl	82
PhCHO	88
C_5H_9Br	37
$Ph_2P(O)Cl$	75

Scheme 4. Curran's backbone functionalization of NHC-boranes[74]

IPr·BH_3 (**55**) was prepared by treating *in situ*-generated IPr carbene with BH_3·THF (Equation 5).[75] By removing the residual ^{t}BuOH and performing a solvent switch to hexanes before addition of BH_3·THF, **55** was isolated in 87% yield in excellent purity by simple filtration.

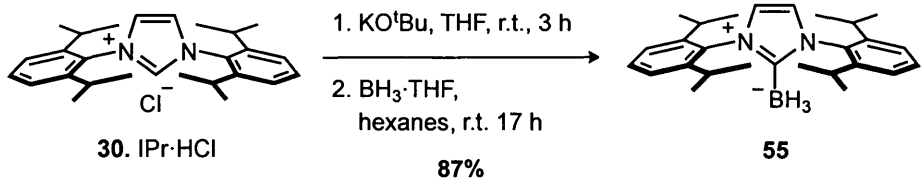

(5)

With **55** in hand, it was treated with 1.0 equiv. of nBuLi in THF at room temperature for 10 min. after which 1.2 equiv. of fluorinating reagent **49** were added.[76] Interestingly, four new products were detected and determined to be **56-59** (Equation 6). Along with 34% of recovered starting material, desired di-fluorinated product **57** was isolated in only 11% yield along with 13% of fluoro-sulfonylated product **59**. Mono-fluorinated **56** and sulfonylated **58** were also formed in 6% and 4% yield, respectively, however in light of purification difficulties, **58** could not be obtained in pure form. In an attempt to improve the yield of **57**, an optimization study was performed in which the solvent, temperature,

and equivalents of **49** were varied, monitoring for conversion by ^{19}F-NMR spectroscopy (Table 2).

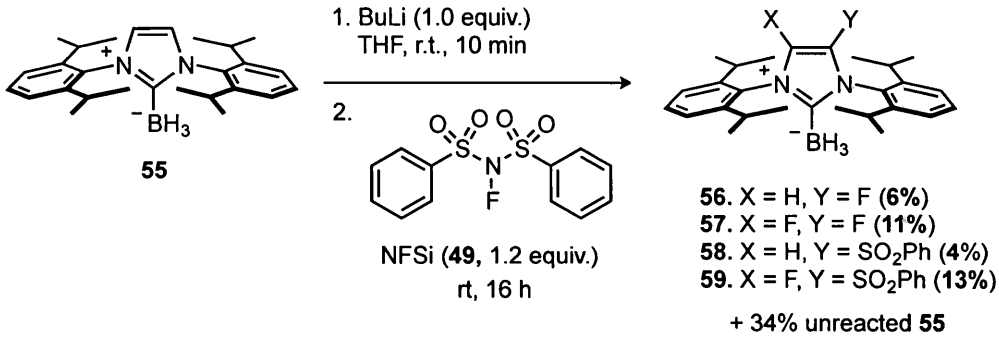

(6)

While reducing the temperature from rt (Entry 1) to -78°C (Entry 2) had little effect on the reaction outcome, introducing a non-polar co-solvent dramatically reduced the degree to which backbone sulfonylation was occurring (Entries 3 and 4). Despite this, as the polarity of the solvent mixture decreased, the selectivity of **57** over **56** deteriorated. Switching to DME or 1,4-dioxane resulted in the formation of unidentified side-products, perhaps due to the poor stability of organolithium reagents in these solvents (Entries 5 and 6).[77] Finally, employing Et_2O as the solvent improved the overall consumption of **55** to 79% but resulted in the formation of undesired mono-fluorinated product **56** in high selectivity (Entry 7). Doubling the amount of **49** to 2.4 equiv. further improved the selectivity of **56**, however some additional by-products were formed, likely decomposition products resulting from prolongued exposure of **56** to **49** (Entry 8).

Since we were able to generate **56** selectively, we attempted to isolate the product and subject it to another round of deprotonation/fluorination, however separating **56** from **57** and unreacted **55** proved prohibitively difficult on scale-up. As a result, preparation of **42** was abandoned.

Table 2. Yield optimization of **57**[a]

Entry	Solvent	Temp (°C)	Equiv. 49	% Unreacted IPr.BH_3[b]	^{19}F-NMR Ratio		
					56	**57**	**59**
1	THF	r.t.	1.2	52	20	**35**	45
2	THF	-78 (2h) - r.t.	1.2	50	12	**36**	52
3	1:1 THF/hexanes	r.t.	1.2	44	30	**48**	22
4	1:3 THF/hexanes	r.t.	1.2	67	79	**18**	4
5	DME	r.t.	1.2	15	0	**0**	0
6	1,4-Dioxane	r.t.	1.2	7	0	**0**	0
7	**Et_2O**	**r.t.**	**1.2**	**79**	**89**	**8**	**3**
8	Et_2O	r.t.	2.4	86	94	**3**	3

[a] Reactions conducted on a 0.2 mmol scale at a concentration of 0.04 M in **55**; [b] Determined by ^{1}H-NMR spectroscopic analysis of the crude reaction mixture following silica filtration.

2.2.2 – Towards 4,5-dicyano-IPr (64)

In light of the excellent electron-withdrawing ability and minimal steric profile of nitrile substituents, our next target became 4,5-dicyano-IPr NHC precursor **64**, whose preparation we invisaged to proceed via a double addition-elimination reaction of IPr formamidine (**39**) with 2,3-dibromofumaronitrile (**63**) (Scheme 5). Electrophile **63** was prepared via bromination of dimethyl acetylenedicarboxylate (**60**)[78] furnishing diester **61**, which was converted to bis-amide **62** via aminolysis with aqueous ammonia. After significant experimentation, dehydration of **62** with TsCl/pyridine in a binary solvent system of CH_2Cl_2/DMF was found to be optimal to provide **63**, albeit in a yield of only 25%. With **63** in hand, we then attempted the key double displacement reaction using conditions similar to those used for the preparation of IPr^{Quino}·HCl (**41**). Although a

number of downfield singlets were observed in the ^{1}H-NMR spectra of the crude reaction mixture, which may correspond to **64**, these conditions furnished an intractable black tar from which no product could be isolated. As a result, the preparation of **64** was abandoned.

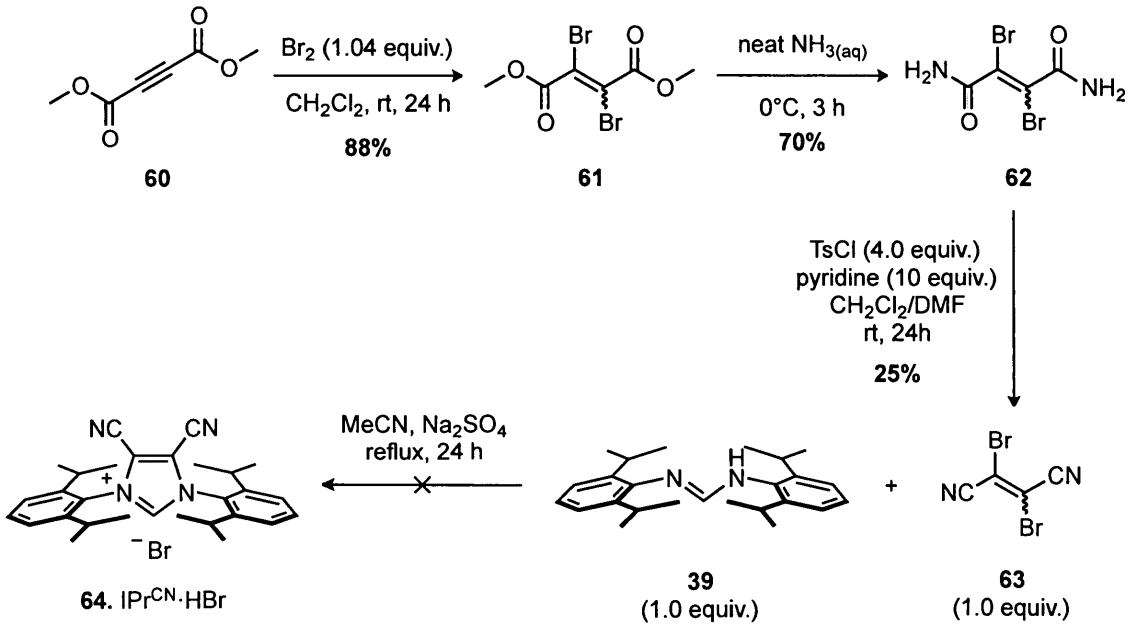

Scheme 5. Attempted preparation of IPr^{CN}·HBr (**64**)

2.3 – Synthesis of 4,5-disubstituted IPent NHCs

2.3.1 – 4,5-dichloro-IPent (IPent^{Cl})

With a selection of backbone-modified NHC precursors in hand, the synthesis of a series of bulkier IPent analogues was attempted. IPent^{Cl}·HCl (**66**) was prepared by heating IPent free carbene generated from **65** and KO^{t}Bu, with a large excess of CCl_4 followed by protonation with ethereal HCl (Equation 7). Unlike the IPr congener (**34**), the use of stoichiometric CCl_4 at room temperature furnished inseparable mixtures of monochlorinated IPent and desired **66**, which may be attributed to a reduction in the reaction rate due to the increased steric bulk of the ligand.

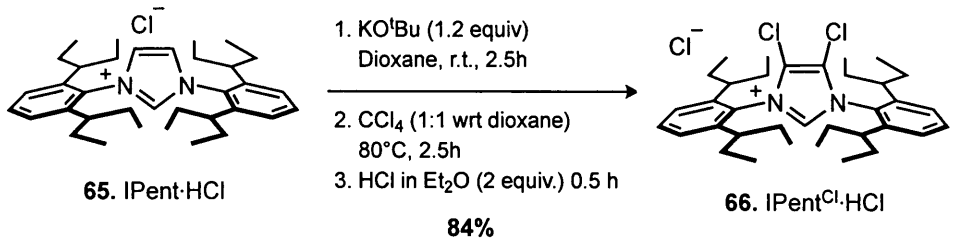

65. IPent·HCl

66. IPent^{Cl}·HCl

(7)

2.3.2 – 4,5-dimethyl-IPent (IPent^{Me})

The synthesis of IPent^{Me}·HCl had previously been attempted in our group.[79] Condensation of aniline **67**[80] with 2,3-butanedione (**37**) under standard conditions did not proceed to completion, but diimine **69** was isolated in 21% yield after flash chromatography (Scheme 6). Unfortunately, when **69** was subjected to standard cyclization conditions known to work well for the synthesis of IPent·HCl (**65**),[81] complete decomposition of **69** was observed and no product was detected. Evidently, the steric interactions between the backbone methyl groups render **70** kinetically inaccessibly under these conditions, thus no further attempts were made to prepare this ligand.

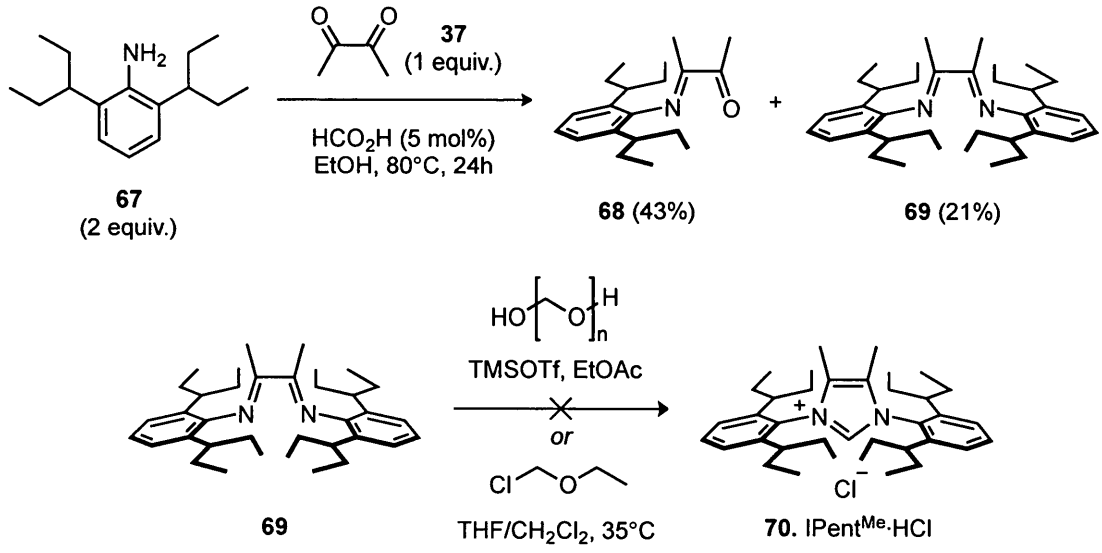

67
(2 equiv.)

68 (43%)

69 (21%)

69

70. IPent^{Me}·HCl

Scheme 6. Previously attempted synthesis of IPent^{Me}·HCl (**70**)

2.3.3 – Miscellaneous 4,5-disubstituted IPent Ligands

In light of previous unsuccessful attempts to prepare IPent^{Me}·HCl (**70**), no attempt was made to synthesize the diethyl counterpart. The preparation of the quinone-fused IPent ligand (IPent^{Quino}·HCl, **72**) was then targeted, however the steric bulk of aniline **67** foiled our attempts to generate the required IPent formamidine precursor (**71**) (Scheme 7).

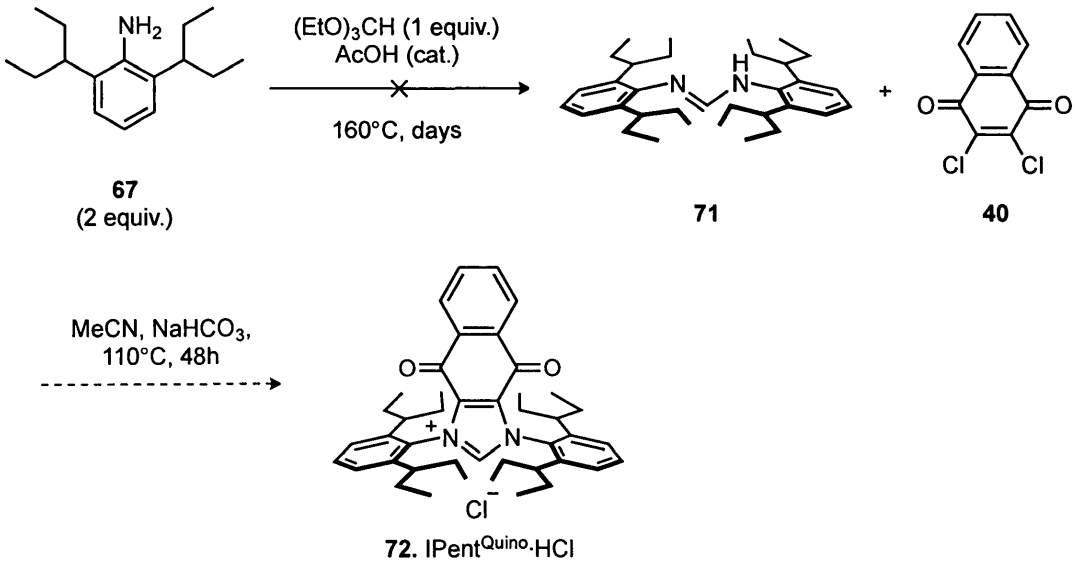

Scheme 7. Attempted preparation of IPent^{Quino}·HCl (**72**)

2.4 – Preparation of Pd-PEPPSI Complexes

With the ligand precursors of IPr^{Cl}, IPr^{Br}, IPr^{Me}, IPr^{Quino}, and IPent^{Cl} in hand, the corresponding Pd-PEPPSI complexes were prepared in order to evaluate their activity in cross-coupling. Applying the standard complexation conditions ($PdCl_2$, K_2CO_3, neat 3-chloropyridine, 80°C) furnished Pd-PEPPSI-IPr^{Cl} (**73**) and Pd-PEPPSI-IPr^{Me} (**76**) in good yields, however Pd-PEPPSI-IPr^{Br} (**75**) and Pd-PEPPSI-IPr^{Quino} (**77**) could not be prepared using this method (Scheme 8). In the first case, the chloride counter-ion from IPr^{Br}·HCl (**35**) displaced the backbone Br atoms, forming mostly scrambled complex **74**, whose structure was confirmed unambiguously by X-ray crystallography (Figure 15). Unfortunately, desired complex **75** and halogen-scrambled complex **74** could not be sepa-

Pd-PEPPSI-IPr^{Cl} (73):

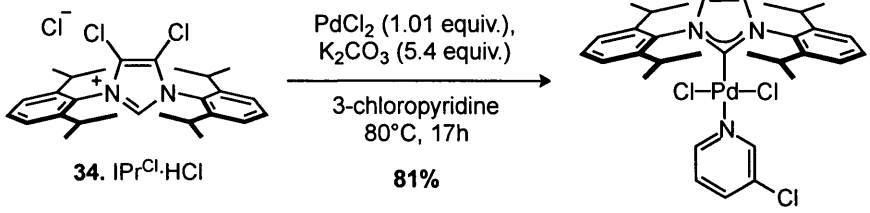

34. IPr^{Cl}·HCl

73. Pd-PEPPSI-IPr^{Cl}

Pd-PEPPSI-IPr^{Br} (75):

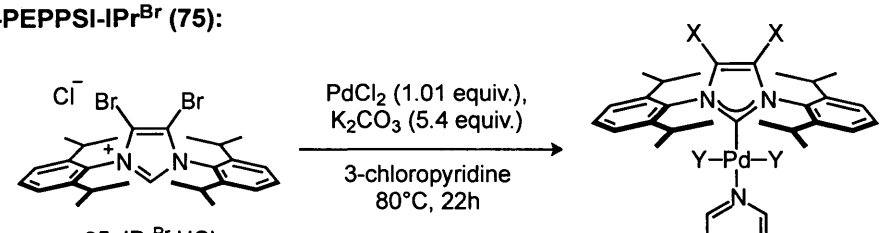

35. IPr^{Br}·HCl

74. X = Cl, Y = Br (Major)

75. X = Br, Y = Cl, Pd-PEPPSI-IPr^{Br} (Minor)

Pd-PEPPSI-IPr^{Me} (76):

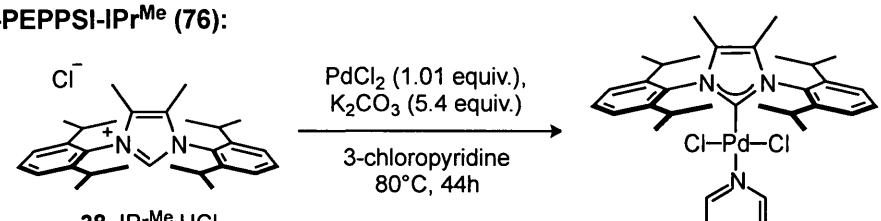

38. IPr^{Me}·HCl

76. Pd-PEPPSI-IPr^{Me}

Pd-PEPPSI-IPr^{Quino} (77):

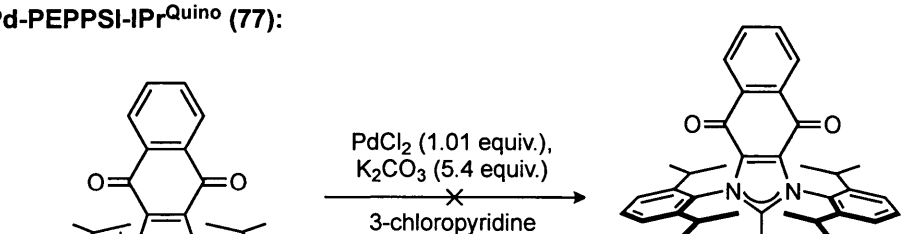

41. IPr^{Quino}·HCl

77. PEPPSI-IPr^{Quino}

Scheme 8. Synthesis of Pd-PEPPSI complexes with backbone-modified IPr ligands

rated by fractional crystallization or flash chromatography. The ratio of Br to Cl on the imidazole ring was determined crystallographically to be 79:21. In the second case, a number of inseparable by-products were formed in addition to desired complex **77**, which were not identified.

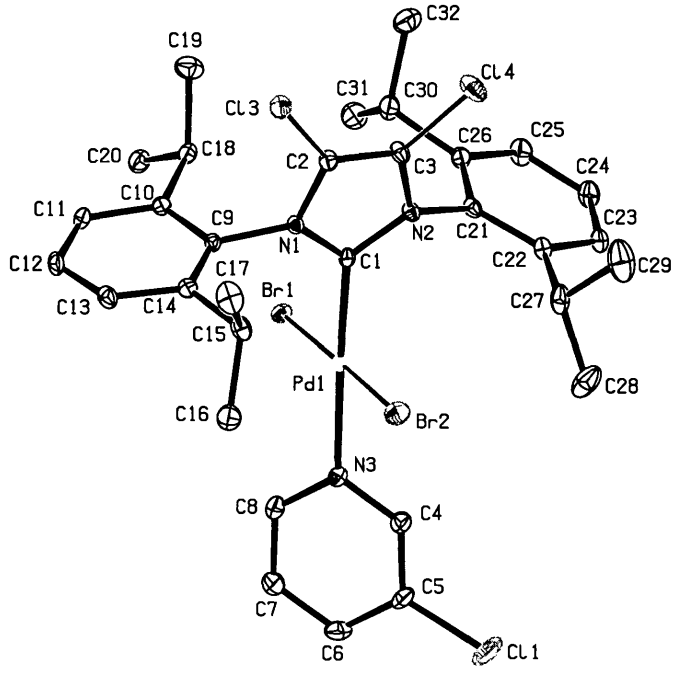

Figure 15. ORTEP diagram of complex **74** with thermal ellipsoids at a 50% probability level. Hydrogen atoms are omitted for clarity.

In light of our inability to prepare complexes **75** and **77** due to the sensitivity of NHC precursors **35** and **41**, a milder synthetic protocol was developed (Equation 9). Treating **41** with a slight excess of KO^{t}Bu in THF generated the free carbene *in situ*, which was then complexed with an equimolar amount of $PdCl_2(MeCN)_2$ to form chloro-bridged dimer $[(IPr^{Quino})Pd(\mu\text{-}Cl)Cl]_2$.[82] After stirring for 2 h, the dimer was cleaved with a slight excess of 3-chloropyrine to furnish **77** in good yield after flash chromatography. The generality and modularity of this procedure allows for the preparation of any Pd-PEPPSI complex with any trans-ligated pyridine in high yields without heating or extended reaction times. Although confident that this procedure would work well for the

preparation of Pd-PEPPSI-IPr^{Br} (**75**), we opted to omit this complex from our structure-activity studies due to the susceptibility of the backbone Br atoms to substitution.

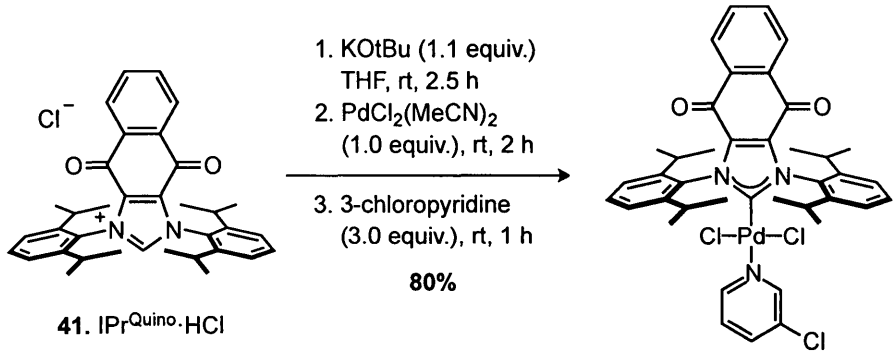

41. IPr^{Quino}·HCl

77. PEPPSI-IPr^{Quino}

(9)

Pd-PEPPSI-IPent^{Cl} (**78**) was prepared successfully in good yield using complexation conditions developed earlier for the non-chlorinated congener Pd-PEPPSI-IPent (**31**)[83] (Equation 10). Purification of the complex was achieved by simple silica filtration and pentane trituration. The structure of each new Pd-PEPPSI complex was determined unambiguously via X-ray crystallography (Figure 16).

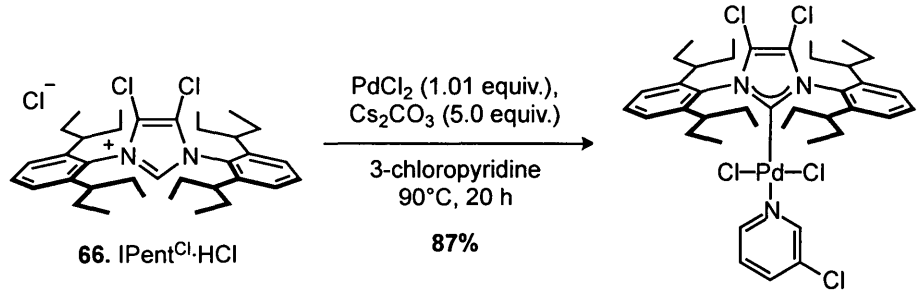

66. IPent^{Cl}·HCl

78. Pd-PEPPSI-IPent^{Cl}

(10)

2.5 – Steric Properties of 4,5-disubstituted NHC Ligands

In order to make a comprehensive appraisal of the steric topology of these new ligands, their %V_{Bur} values were computed using the acquired X-ray data (Table 3).[44b] The %V_{Bur} values of IPent^{Cl} and IPent were within 0.5% of each other, implying that the role of the backbone substituents is small in this particular Pd(II) complex. The %V_{Bur} values of the

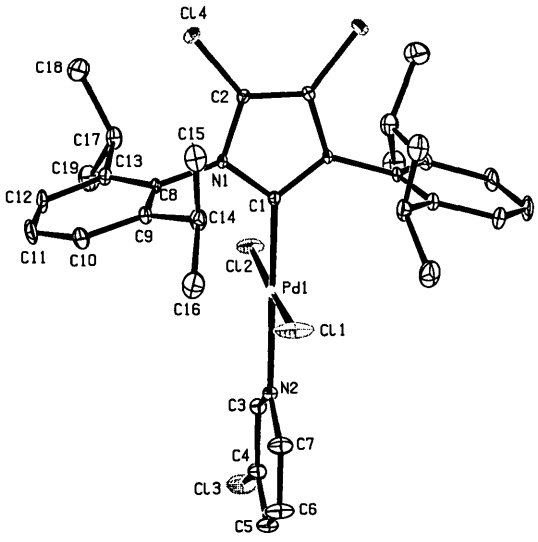

(a) Pd-PEPPSI-IPr^{Cl} **(73)**

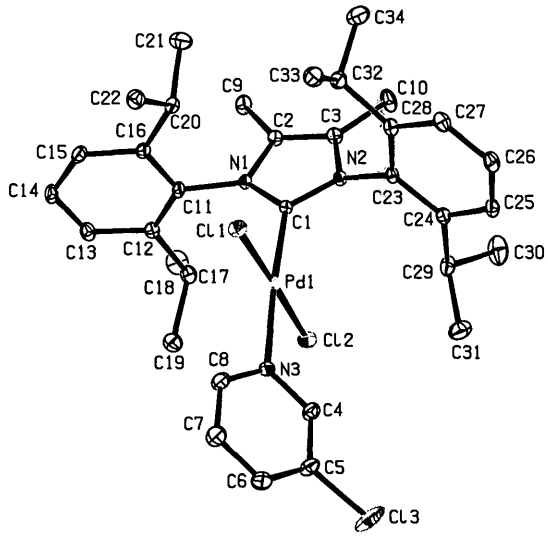

(b) Pd-PEPPSI-IPr^{Me} **(76)**

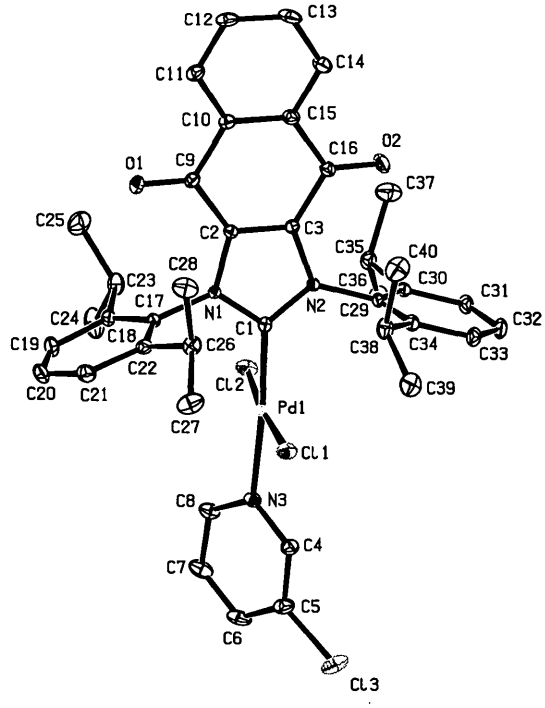

(c) Pd-PEPPSI-IPr^{Quino} **(77)**

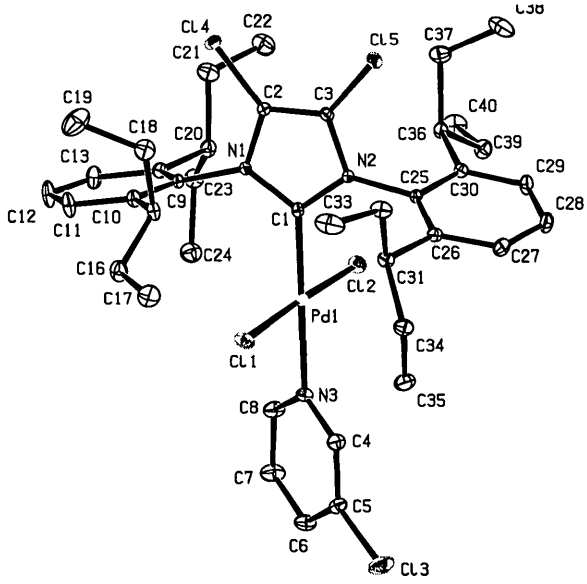

(d) Pd-PEPPSI-IPent^{Cl} **(78)**

Figure 16. ORTEP diagrams of complexes **73**, **76**, **77**, **78** with thermal ellipsoids at a 50% probability level. Hydrogen atoms are omitted for clarity.

IPr^{Me} and IPr^{Quino} ligands were found to be larger than substituted IPr whereas that of IPr^{Cl} was slightly lower, regardless if the Pd-C(1) bond lengths were normalized to 2.00 Å or set to their crystallographically-determined lengths. This contrasts with Nolan's report in which the $\%V_{Bur}$ value of IPr^{Cl} was significantly higher (>4%) than either IPr^{Me} or IPr in the corresponding [(NHC)Pd(η^3-allyl)Cl] complexes.[84] Evidently, the nature of the other ligands in the metal coordination sphere profoundly impacts the degree to which the NHC can project its bulk towards the metal centre.[85] As a result, the $\%V_{Bur}$ values calculated using the solid-state structures of the Pd-PEPPSI pre-catalysts are likely poorly representative of the complexes that would be encountered in solution during the catalytic cycle.

Table 3. Calculated $\%V_{Bur}$ values of NHCs in Pd-PEPPSI Complexes[a]

Entry	Pd-PEPPSI Complex	Pd-C(1) Bond Length (Å)[b]	$\%V_{Bur}$	
			Pd-C(1) = 2.0 Å[c]	Pd-C(1) = actual[d]
1	IPr (**29**)	1.969(3)	34.3	34.9
2	IPr^{Cl} (**73**)	1.966(3)	33.6	34.3
3	IPr^{Me} (**76**)	1.965(2)	35.4	36.0
4	IPr^{Quino} (**77**)	1.959(2)	34.9	35.6
5	IPent (**31**)	1.974(3)	37.9	38.3
6	$IPent^{Cl}$ (**78**)	1.978(2)	38.4	38.8

[a] $\%V_{Bur}$ values were calculated with hydrogen atoms omitted, a sphere radius of 3.5 Å, 0.05 mesh spacing, and scaled bond radii using the application described in ref. 44b; [b] Value in parentheses refers to the error in the last decimal point; [c] Values calculated with Pd-C(1) bond lengths normalized to 2.0 Å; [d] Values calculated with crystallographically determined Pd-C(1) bond lengths.

2.6 – Electronic Properties of 4,5-disubstituted NHC Ligands

To understand the effect of the backbone substituents on the donating ability of the carbene, the Tolman electronic parameter (TEP) associated with these ligands was computed from the average IR stretching frequency of the carbonyl ligands in the corresponding [(NHC)Ir(CO)$_2$Cl] complexes. Carbonyl complexes **83** – **86** were prepared in good yield by displacement of cyclooctadiene (cod) from the [(NHC)Ir(cod)Cl] precursors **79** – **82** under 1 atm of $CO_{(g)}$ (Table 4).[51] IR spectroscopic analyses were performed in freshly distilled CH_2Cl_2 using an IR liquid cell.

Table 4. Synthesis and TEP Analysis of [(NHC)Ir(CO)$_2$Cl] Complexes

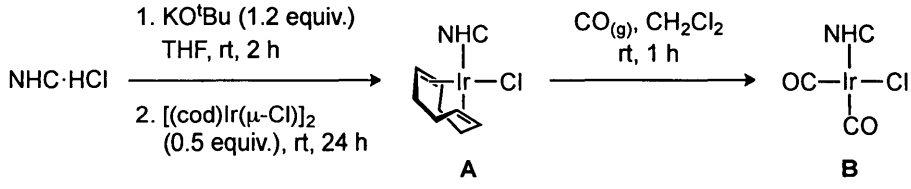

Entry	NHC	Yield A (%)	Yield B (%)	ν_{CO} (CH_2Cl_2, cm^{-1})	ν_{CO} (avg)	TEP (cm^{-1})[a]
1	IPr	-	-	2066.8, 1981.0	2023.9	2051.5[b]
2	IPr^{Cl}	-	-	2071.4, 1985.1	2028.3	2055.1[b]
3	IPr^{Me}	43 (**79**)	96 (**83**)	2064.5, 1978.2	2021.3	2049.3
4	IPr^{Quino}	82 (**80**)	83 (**84**)	2073.7, 1987.3	2030.5	2057.1
5	IPent	51 (**81**)	80 (**85**)	2064.7, 1978.6	2021.7	2049.6
6	IPent^{Cl}	71 (**82**)	62 (**86**)	2069.3, 1982.2	2025.8	2053.0

[a] TEP computed using the linear regression: TEP (cm^{-1}) = 0.8475*(ν_{CO}(avg)) + 336.2 described in ref. 51; [b] These complexes and their TEP values have been reported previously, see ref. 51.

As expected, the TEP of IPr^{Me} (2049.3 cm^{-1}) was found to be the lowest of the IPr series (most donating), whereas IPr^{Quino} (2057.1 cm^{-1}) was the highest (least donating). Interestingly, the IPent ligand was found to be more donating than IPr with a TEP similar

to that of IPr^{Me} (2049.6 cm^{-1}). Consistent with Nolan's observation that backbone chlorination leads to a less donating ligand, the TEP of $IPent^{Cl}$ (2053.0 cm^{-1}) was shown to be 3.4 cm^{-1} higher than that of IPent. From this data, the donating ability of these NHCs can be ranked in order of decreasing donicity: IPr^{Me} ~ IPent > IPr > $IPent^{Cl}$ > IPr^{Cl} > IPr^{Quino}.

2.7 – Conclusions

Backbone modified NHC precursors IPr^{Cl} (**34**), IPr^{Me} (**38**), IPr^{Quino} (**41**), $IPent^{Cl}$ (**66**) and their corresponding Pd-PEPPSI complexes were prepared in order to evaluate their activity in cross-coupling chemistry. The synthesis of novel NHC precursors IPr^{F} (**42**), IPr^{CN} (**64**), $IPent^{Me}$ (**69**), and $IPent^{Quino}$ (**72**) were also attempted but were ultimately unsuccessful.

Analysis of the X-ray crystal structures of these new Pd-PEPPSI complexes using Nolan's $\%V_{Bur}$ steric parameter revealed that, with the exception of IPr^{Cl}, the addition of substituents on the NHC backbone resulted in a more sterically hindered metal centre. To understand the effect of the backbone substituent on the donating ability of these carbenes, the Tolman electronic parameter was computed from the average IR stretching frequency of the carbonyl ligands in the corresponding [(NHC)Ir$(CO)_2$Cl] complexes. Consistent with previously reported trends, placing an electron withdrawing group on the backbone (Cl/quinone) led to a less donating carbene, whereas placing an electron-donating group in the backbone (CH_3) resulted in a more donating carbene.

CHAPTER 3: Evaluation of Backbone-Modified NHC Ligands in Secondary Alkyl Negishi Cross-Coupling

3.1 – General Background

Aromatic secondary alkyl substituents are common motifs in many top-selling active pharmaceutical ingredients (APIs) (Figure 17).[86] Some notable examples include Crestor and Lipitor used for the treatment of high-cholesterol, and Cialis, used for the treatment of erectile dysfunction. Indeed, a statistical analysis of all drug candidates since 1980 revealed that molecules with higher alkyl content were more likely to make the transition from the discovery phase, through clinical trials, and into successful drugs.[87] The increased three-dimensional topology associated with greater alkyl composition is thought to result in improved target specificity and greater bioavailability.

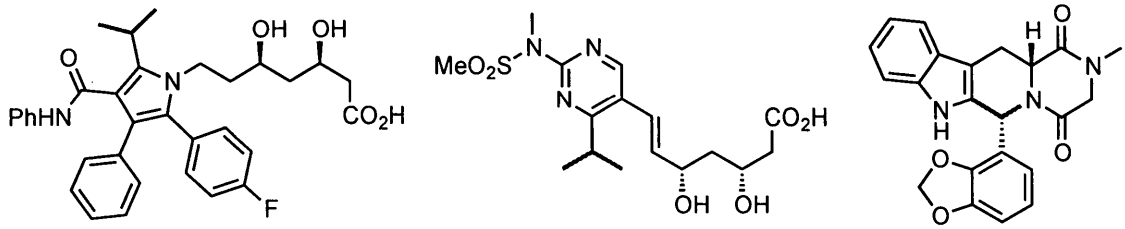

Lipitor - Pfizer
HMG-CoA Reductase Inhibitor
(High cholesterol)

Crestor - AstraZeneca
HMG-CoA Reductase Inhibitor
(High cholesterol)

Cialis - Eli Lilly
PDE5 Inhibitor
(Erectile Dysfunction)

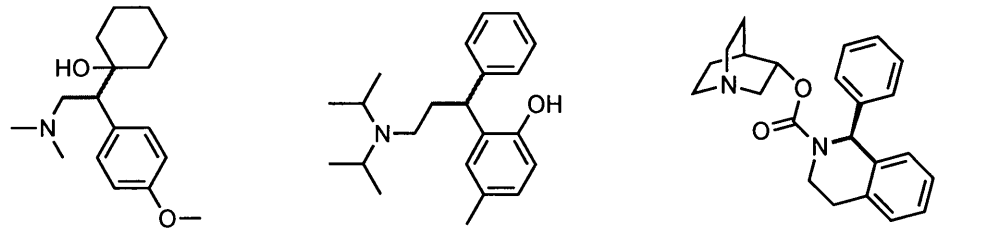

Effexor - Pfizer
Serotonin-Norepinephrine
Reuptake Inhibitor (SNRI)
(Anti-depressant)

Detrol LA - Pfizer
Antimuscarinic
(Urinary Incontinence)

Vesicare - Astellas
Cholinergic Receptor Antagonist
(Overactive Bladder)

Figure 17. Selection of popular drugs containing aromatic secondary alkyl substituents

In light of the growing importance of aromatic secondary alkyl groups, there is a significant impetus for the development of synthetic methods that enable efficient access to these substituents. Palladium-catalyzed cross-coupling of secondary alkyl nucleophiles with aryl halides has emerged as one of the most applicable and atom-economical techniques for this purpose.[88] Unfortunately, despite the high utility of this reaction, the regiochemical outcome of secondary alkyl cross-couplings is often difficult to control and has not been widely adopted as a result. As depicted in Figure 18, the regiochemical uncertainty arises from a process of β-hydride elimination (BHE) and migratory insertion (MI) following transmetalation (TM) that competes with reductive elimination (RE). If the RE step is slow relative to BHE, then linear alkyl complex **E** will predominate in solution thus resulting in selective formation of the isomeric or "linear" cross-coupled product, $\mathbf{P_L}$, over the desired "branched" product $\mathbf{P_B}$.

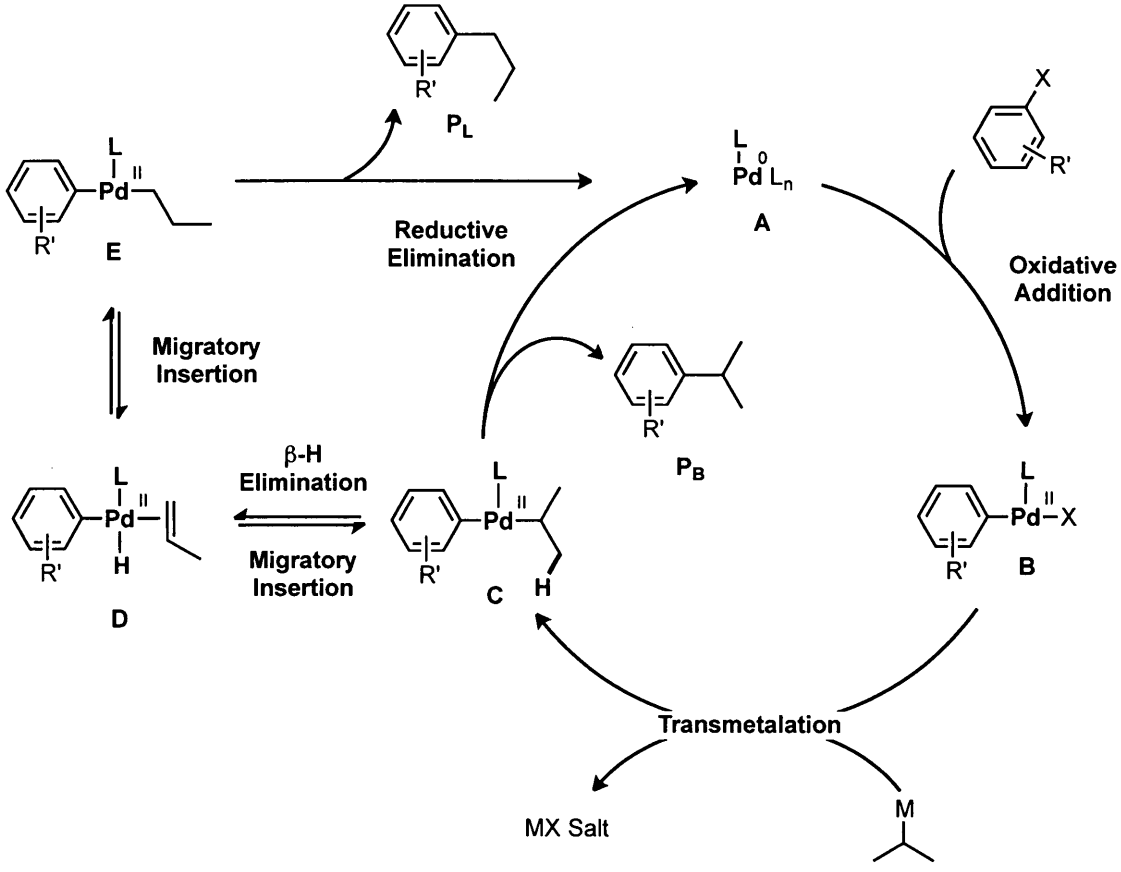

Figure 18. General mechanism for the cross-coupling of secondary alkyl organometallics

The general strategy for imparting better regiocontrol has been centred around the use of sterically hindered phosphine ligands, which serve to increase the rate of RE relative to BHE, thus favouring the formation of $\mathbf{P_B}$. In 1984, Hayashi and co-workers reported that secondary alkyl Grignard reagents could be coupled with aryl bromides with little or no observed isomerization using dppf, a new bidendate phosphine ligand (Figure 19).[89] Despite this, the reported substrate scope was very limited and the functional group tolerance low given the high reactivity and basicity of organomagnesium reagents.

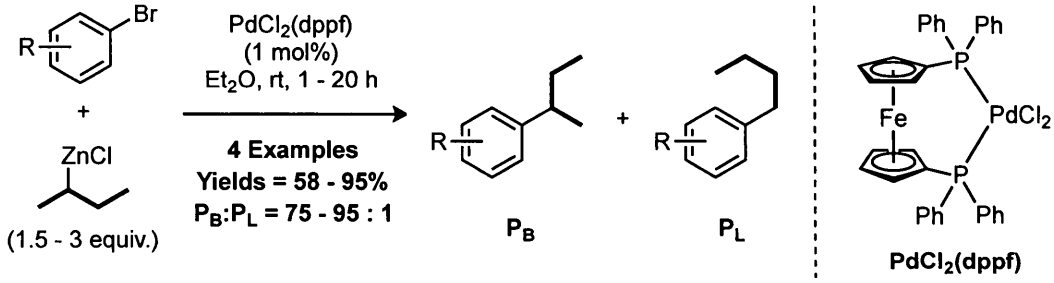

Figure 19. The use of $PdCl_2$(dppf) in early Pd-catalyzed secondary alkyl cross-couplings

The field remained nearly dormant until 2008, when Molander and co-workers revealed that potassium isopropyl trifluoroborate could be successfully coupled with aryl chlorides using ^{n}BuPAd$_2$ and ^{t}Bu$_2$PPh ligands (Figure 20).[90] Unfortunately, the substrate scope was limited to only two aryl chlorides and regioselectivity was poor in both cases. Later that year, van den Hoogenband and co-workers reported on the use of the RuPhos ligand in a similar coupling of potassium 2-butyltrifluoroborate with aryl bromides.[91] Although no isomerization was observed in the four substrates that were screened, a high catalyst loading and extended reaction times were required to achieve acceptable product yields. Shortly thereafter in 2009, Han and Buchwald published an account detailing the superior activity of CPhos in the Negishi cross-coupling of secondary alkylzinc reagents with a variety of aryl halides with good regioselectivities (>20:1).[92] Although the BHE pathway could not be fully suppressed, the authors demonstrated for the first time that the cross-coupling of secondary alkyl nucleophiles could be used as a viable method for the predictable installation of aromatic secondary alkyl substituents.

Molander, et al. **2008** (Ref. 90):

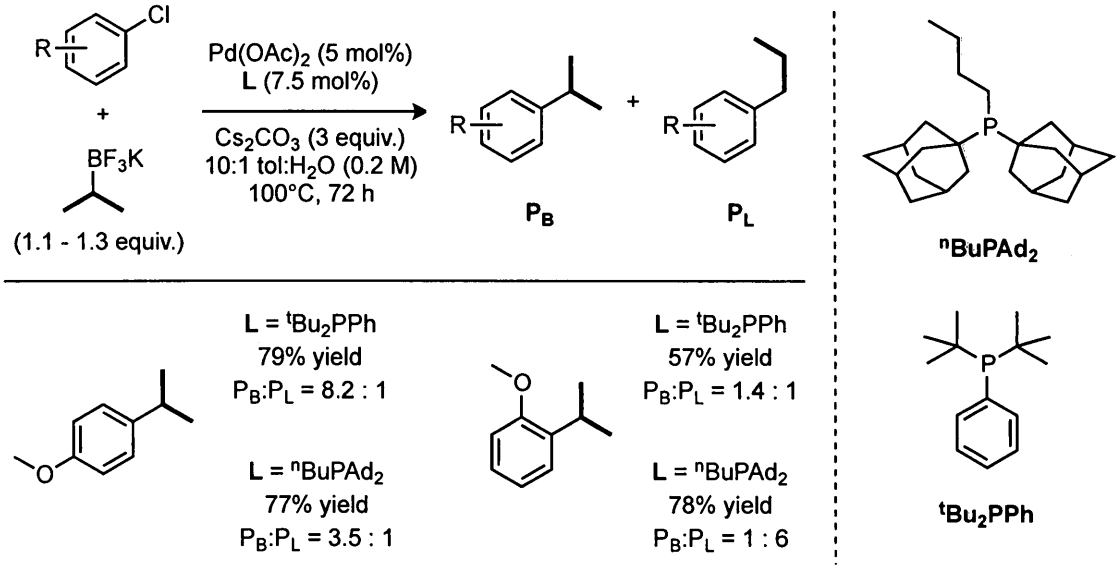

van Den Hoogenband, et al. **2008** (Ref. 91):

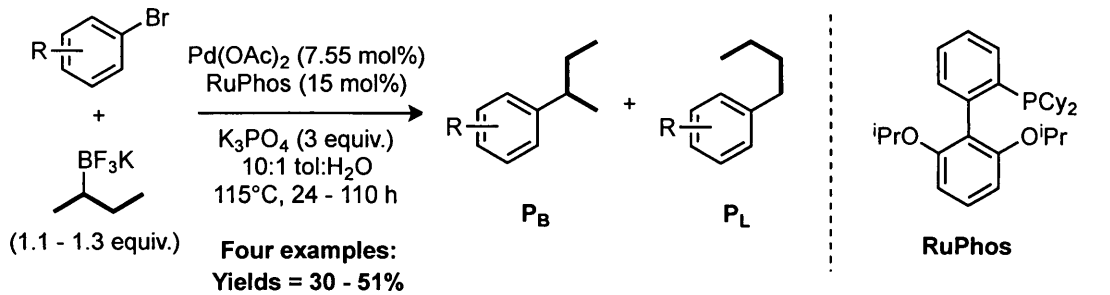

Han and Buchwald, **2009** (Ref. 92):

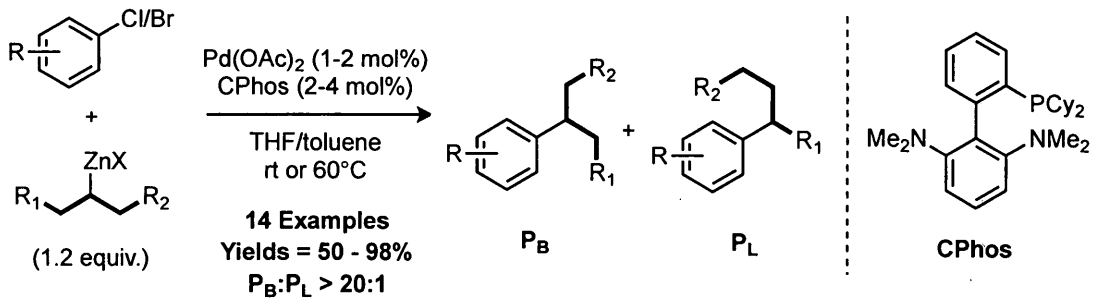

Figure 20. Selected phosphine ligands for cross-coupling secondary alkyl nucleophiles

3.2 – Pd-PEPPSI and the Secondary Alkyl Negishi Coupling

Although Buchwald's CPhos ligand represented a groundbreaking achievement in the field of secondary alkyl cross-coupling, the regiochemical outcome of the reaction was still highly dependent on the structure of the electrophile. For example, when employing sterically hindered aryl halides, such as 2-bromobenzonitrile, the regioselectivity fell to 20:1 due to a reduction in the rate of RE. This prompted the Organ group to evaluate the Pd-PEPPSI family of pre-catalysts in this coupling, hoping to capitalize on the unique steric topology of NHC ligands. In 2011, Çalimsiz and Organ reported that Pd-PEPPSI-IPent (**31**) could effectively catalyze the Negishi coupling of a variety of secondary alkylzinc reagents with aryl halides, significantly outperforming the less bulky Pd-PEPPSI-IPr (**29**).[93] Despite this, the regioselectivity imparted by **31** was found to be inferior to CPhos, especially when coupling sterically hindered and electron rich aryl halides, such as 2-bromoanisole (Figure 21). In this case, the regioselectivity deteriorated to 2:1 in favour of the desired isomer indicating a significant reduction in the rate of RE relative to BHE. Considering that isomers $\mathbf{P_B}$ and $\mathbf{P_L}$ cannot be separated via chromatography, this limitation severely detracted from the usefulness of **31.**

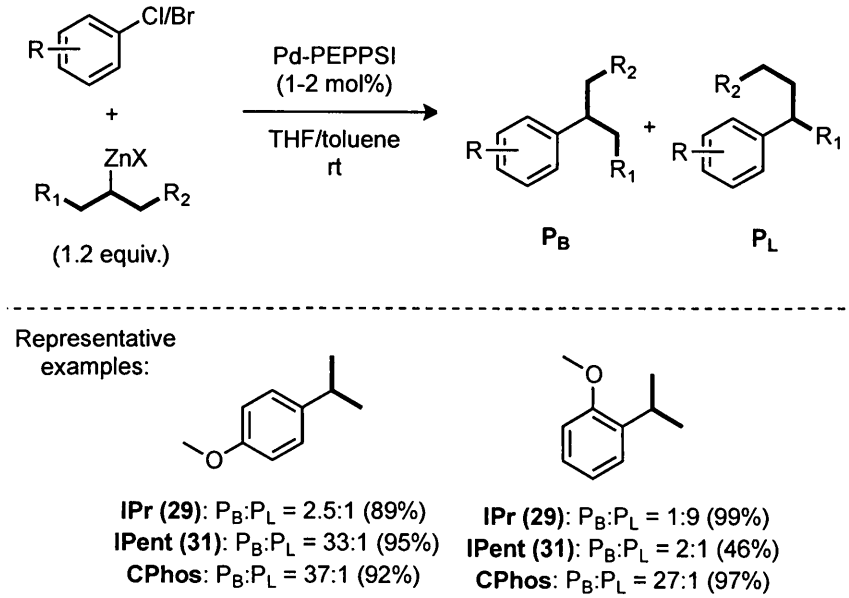

Figure 21. Evaluation of pre-catalysts **29** and **31** in the secondary alkyl Negishi coupling

3.3 – Evaluation of Pd-PEPPSI Complexes with Backbone-Modified NHC ligands

In light of the limited performance of both Pd-PEPPSI-IPr (**29**) and Pd-PEPPSI-IPent (**31**) in the Negishi coupling of secondary alkylzinc reagents, we opted to evaluate our new Pd-PEPPSI complexes derived from backbone-modified NHCs. Since RE tends to occur faster from electron-deficient metals coordinated to sterically demanding ancillary ligands,[3] we hypothesized that bulky NHCs containing electron-withdrawing groups (EWGs) on the backbone, such as IPr^{Cl} and $IPent^{Cl}$, might be uniquely suited for this chemistry. To test this hypothesis, the coupling of 3-bromobenzonitrile with isopropylzinc bromide was chosen as the model reaction in which the new Pd-PEPPSI complexes would be screened (Table 5). This particular organozinc was selected due to its susceptibility to undergo BHE, thus ensuring that any products arising from the BHE/MI process could be easily detected and quantified.

Table 5. Evaluation of Pd-PEPPSI Complexes with Backbone-Modified NHCs[a-c]

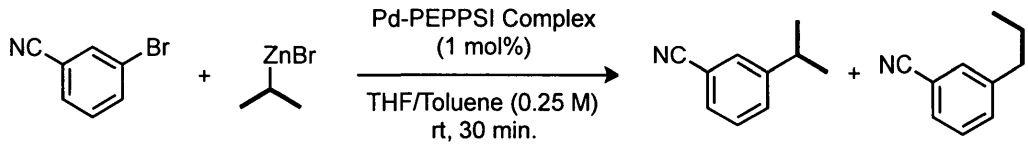

87 (1.0 equiv.) + **88** (1.2 equiv.) → **89** + **90**

Entry	Pd-PEPPSI Complex	Yield (%)	89 : 90
1	IPr (**29**)	82	1 : 1.4
2	IPr^{Cl} (**73**)	81	15 : 1
3	IPr^{Me} (**76**)	70	15 : 1
4	IPr^{Quino} (**77**)	78	13 : 1
5	IPent (**31**)	66	11 : 1
6	$IPent^{Cl}$ (**78**)	81	**61 : 1**

[a] Reactions were conducted on a 0.5 mmol scale at a concentration of 0.25 M in **87**; [b] Isolated yields are reported on products purified by flash chromatography and were averaged over two runs; [c] The ratio of inseparable isomers was determined by ^{1}H-NMR spectroscopy after purification

Consistent with the results disclosed by Çalimsiz and Organ, the selectivity imparted by the IPr catalyst (**29**) was a dismal 1.4:1 in favour of the undesired, isomeric product **90** (Entry 1). Applying Pd-PEPPSI complexes with less donating NHCs IPr^{Cl} (**73**) and IPr^{Quino} (**77**) resulted in a significant improvement in regioselectivity to 15:1 and 13:1 respectively (Entries 2 and 4), supporting our hypothesis. However, we were surprised to find that the complex with the most donating NHC, IPr^{Me} (**76**), also led to a similar improvement in selectivity (Entry 3), implying that regioselectivity is independent of the electron withdrawing or releasing ability of the backbone substituent. Switching to the IPent NHC core, we discovered that Pd-PEPPSI-$IPent^{Cl}$ (**78**) resulted in a remarkable selectivity of 61:1 (Entry 6), drastically outperforming the unmodified IPent congener (**31**) (Entry 5) and all backbone-modified IPr catalysts.

Having identified Pd-PEPPSI-$IPent^{Cl}$ (**78**) as the most selective catalyst in the model reaction, we proceeded to couple the same organozinc reagent with a variety of sterically and electronically diverse aryl bromides in order to determine the extent to which the regiochemical outcome is influenced by the structure of the electrophile (Table 6). Selectivities imparted by both **78** and Buchwald's state-of-the-art CPhos ligand, were observed to decline as the aryl substituent moved closer to the reaction site, implying a reduction in the rate of RE. The performance of **78** was shown to be essentially independent of the electronic nature of the aryl halide, furnishing $\mathbf{P_B}$ with excellent regioselectivity with both electron rich (Entries 4, 6, 6) and electron-deficient electrophiles (Entries 1-3, 5, 7). Notably, with the exception of 2-bromoanisole, selectivities imparted by **78** were on par with or slightly higher than CPhos.

Table 6. Substituent Effect Studies: Pd-PEPPSI-IPent^{Cl} (**78**) vs. CPhos[a-c]

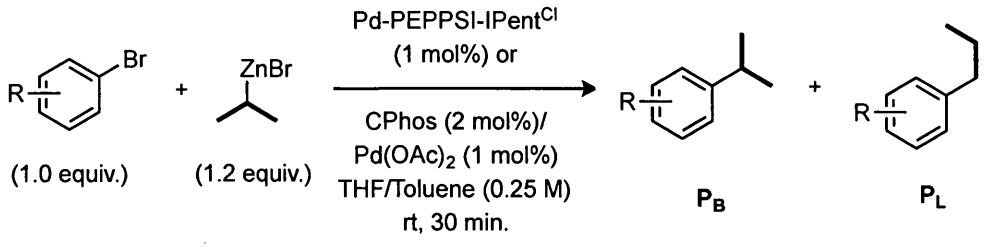

Entry	R	Product	Catalyst	Yield (%)	P_B : P_L
1	4-CN	**91**	**78**	92	59:1
			CPhos/Pd	87	59:1
2	4-CHO	**92**	**78**	92	59:1
			CPhos/Pd	89	43:1
3	4-CO_2Me	**93**	**78**	94	56:1
			CPhos/Pd	94	46:1
4	4-OMe	**94**	**78**	79	46:1
			CPhos/Pd	92	37:1
5	3-CHO	**95**	**78**	84	48:1
6	3-OMe	**96**	**78**	66	39:1
7	2-CN	**97**	**78**	56	28:1
			CPhos/Pd	89	20:1
8	2-OMe	**98**	**78**	54	23:1
			CPhos/Pd	97	27:1

[a] Reactions were conducted on a 0.5 mmol scale at a concentration of 0.25 M; Results associated with CPhos/Pd(OAc)$_2$ were reproduced from ref. 92. [b] Isolated yields are reported on products purified by flash chromatography and were averaged over two runs; [c] The ratio of inseparable isomers P_B:P_L was determined by ^{1}H-NMR spectroscopy after purification (d1 = 5 s).

3.4 – Substrate Scope Study of Secondary Alkyl Couplings with Pd-PEPPSI-IPent^{Cl}

With these promising results in hand, the substrate scope of this transformation using **78** was then investigated, with the aim of preparing a broad range of functionalized compounds of biological and medicinal-relevance (Table 7). All organozinc reagents used were prepared as solutions in THF from the corresponding bromoalkanes via Knochel's LiCl-mediated direct Zn(0)-insertion.[94] The isomeric ratios of normal (n) to rearranged (r) products were determined by integrating the resonances corresponding to the benzylic protons of all respective regioisomers in the ^{1}H-NMR spectra after chromatographic purification. In most cases, the multiplicities of the benzylic resonances were sufficiently well resolved to make confident structural assignments, however when isomer differentiation was ambiguous, all additional isomers were prepared independently and their ^{1}H-NMR spectra cross-referenced. A representative example with substrate **107** is shown below in Figure 22.

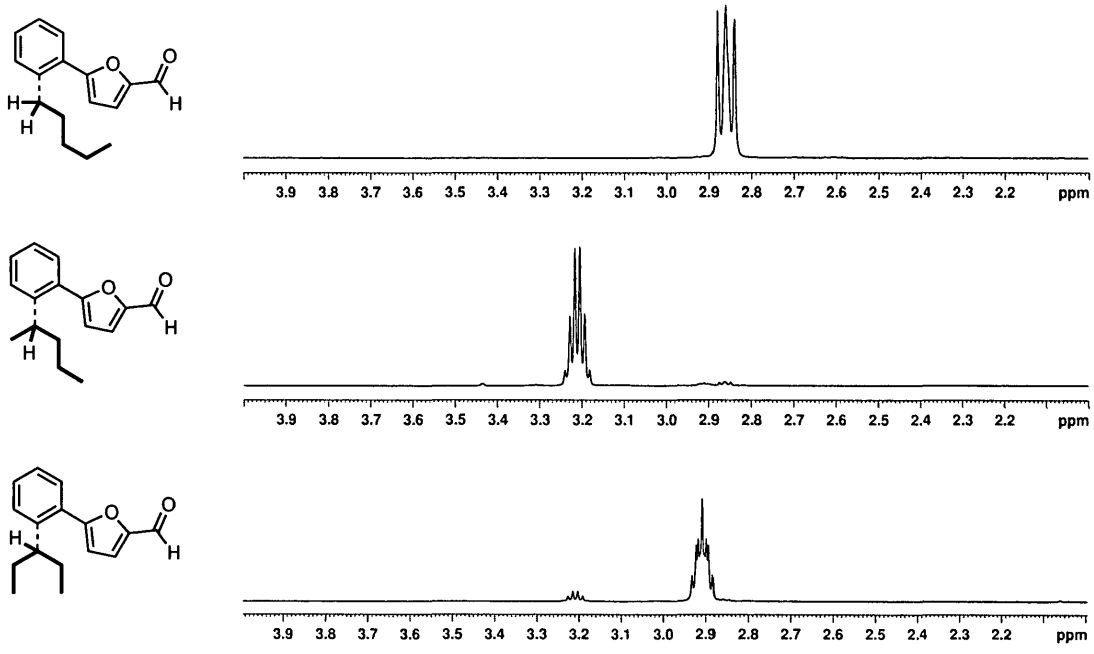

Figure 22. Representative example of regioisomer disambiguation with substrate **107** using ^{1}H-NMR data of individually prepared regioisomers

Remarkably, when coupling 2-butylzinc bromide to a variety of electronically diverse aryl chorides and bromides, no isomeric products were detected by ^{1}H-NMR spectroscopy (**99–102**). Similarly, a piperidine-derived organozinc also coupled with very little or no observed isomerization, furnishing biologically-relevant heterocycles in a single step (**103**, **104**, **110**). Complex **78** was also found to be effective in coupling 3-pentylzinc bromide, which is statistically more likely to generate isomeric products relative to 2-butylzinc bromide.[95] All *para*-substituted halides tested with this organozinc furnished only the desired regioisomer (**108**, **111**, **112**) in excellent yields. Very good selectivites (>30:1) were achieved for *meta*-substituted halides **105** and **106**, regardless of the electronic nature of the substituent, however a slight reduction in regioselectivity to 17:1 was observed for *ortho*-substituted **107**.

The scope and functional group compatibility of these conditions allowed for the coupling of electrophiles containing aldehydes, ketones, esters, amides and even free amines, alcohols, and carboxylic acids if excess organozinc was used. Higher molecular-weight, drug-like electrophiles were also successfully coupled, notable examples of which include **108**, derived from Haloperidol, an anti-psychotic drug, and **110–112**, derived from Indomethacin, a common non-steroidal anti-inflammatory drug (NSAID). In general, catalyst **78** exhibits very high reactivity, broad functional group tolerance, and most importantly, virtually exclusive selectivity for the desired, non-rearranged product.[96]

Table 7. Scope Study of Secondary Alkyl Couplings with Pd-PEPPSI-IPent^{Cl} (**78**)[a-c]

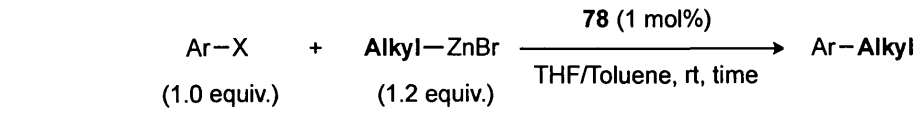

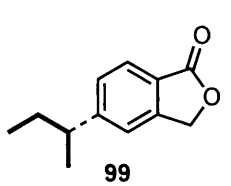

99

30 min, X = Br
quant., **n/r: >99:1**

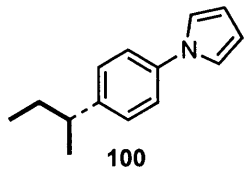

100

30 min, X = Cl
quant., **n/r: >99:1**

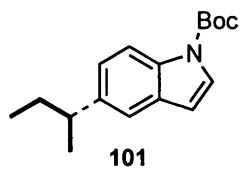

101

30 min, X = Br
quant., **n/r: >99:1**

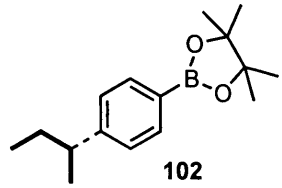

102

30 min, X = Cl
quant., **n/r: >99:1**

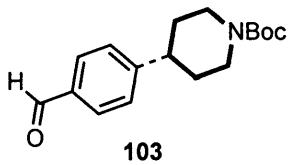

103

45 min., X = Br
98%, **n/r: >99:1**

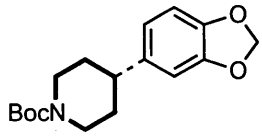

104

5 h, X = OTf,
96%, **n/r: >99:1**

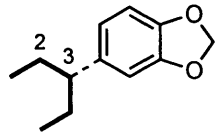

105

5 h, X = OTf, 85%
n(C3)/r(C2): 31:1

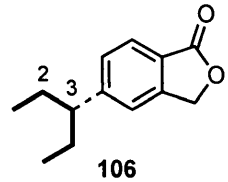

106

30 min., X = Br, 94%
n(C3)/r(C2): 35:1

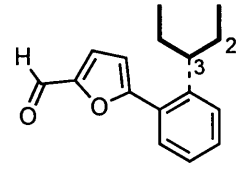

107

16 h, X = Cl 64%
n(C3)/r(C2): 17:1

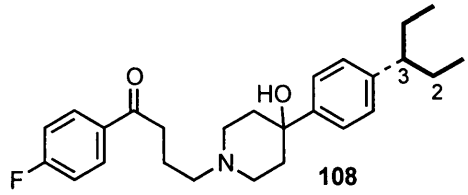

108

16 h, X = Cl, 68%
n(C3)/r(C2): >99:1
(2.2 equiv AlkZnBr)

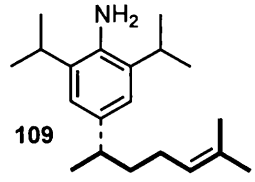

109

2 h, X = Br
66%, **n/r: 58:1**
(2 equiv. AlkZnX)

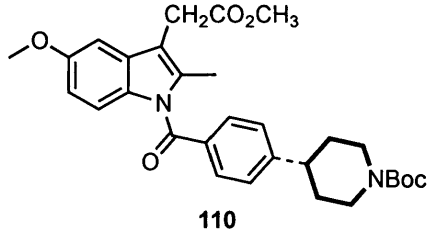

110

1 h, X = Cl
95%, **n/r: >99:1**

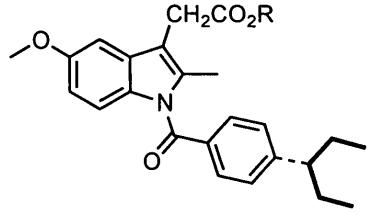

111 (R = H)
2 h, X = Cl,
76%, **n/r: >99:1**
(2 equiv. AlkZnX)

112 (R = CH_3)
1 h, X = Cl,
93%, **n/r: >99:1**

[a] Reactions were conducted on a 0.5 mmol scale at a concentration of 0.25 M; [b] Isolated yields are reported on products purified by flash chromatography and were averaged over two runs; [c] The ratio of inseparable regioisomers n:r was determined by ^{1}H-NMR spectroscopy after purification (d1 = 5 s). A ratio of >99:1 means that no minor isomers were detected at all. n = normal product, r = rearranged product.

Heteroaryl halides could also be successfully cross-coupled using **78**, however the regiochemical outcome was found to be highly dependent on the structure of the heteroaryl unit (Table 8). While coupling various organozinc reagents with 6-membered nitrogen-containing heterocycles furnished excellent selectivities for the desired product (**113–116**), switching to 5-membered heterocycles led to a precipitous decline in selectivity. This deterioration was found to be independent of the type of heteroatom or the position in the five-membered ring that underwent coupling. This increased aptitude for isomerization was especially evident when 3-pentylzinc bromide was used as the nucleophile as all three regioisomers were often generated (3-pentyl, 2-pentyl, and 1-pentyl). Remarkably, in the case of thiophene **126**, the linear (1-pentyl) isomer predominated, demonstrating a profound reduction in the rate of RE relative to BHE.

To determine whether the electronic effect of the heteroatom or the steric topology of 5-membered ring was responsible for the observed decline in selectivity, 1-bromoindene, a heteroatom-free analogue, was prepared and cross-coupled with 3-pentylzinc bromide. Compound **122** was generated with an excellent selectivity of 91:1 for the desired 3-pentyl isomer, thus implicating the heteroatom as the cause of the reduction in the rate of RE.

The notorious difficulty of coupling 5-membered heterocycles in the Buchwald-Hartwig amination due to a slow reductive elimination step has been repeatedly noted.[97] In an effort to understand the origins of this effect, Hartwig and co-workers prepared and characterized a series of (dppf)Pd(heteroaryl)(amido) complexes with various 2 an 3-substituted heterocycles.[97a] The Pd-C bond lengths associated with the heteroaryl substituents were found to be slightly shorter than that of a typical electron-rich aryl substituent (2.000 – 2.046 Å vs. 2.048 Å), prompting Hartwig to conclude that this increase in bond order would lead to a more difficult reductive elimination step (Figure 23a). This reduction in bond length can be rationalized by considering the degree to which the heteroatom can mesomerically transfer electron density to Pd via the aromatic system (Figure 23b). Since this type of delocalization is not possible in 6-membered

heterocycles, these substrates couple with predictably high regioselectivities. As a result of this inherent electronic property of 5-membered heterocycles, the cross-coupling of this class of electrophile using complex **78** remains a challenge.

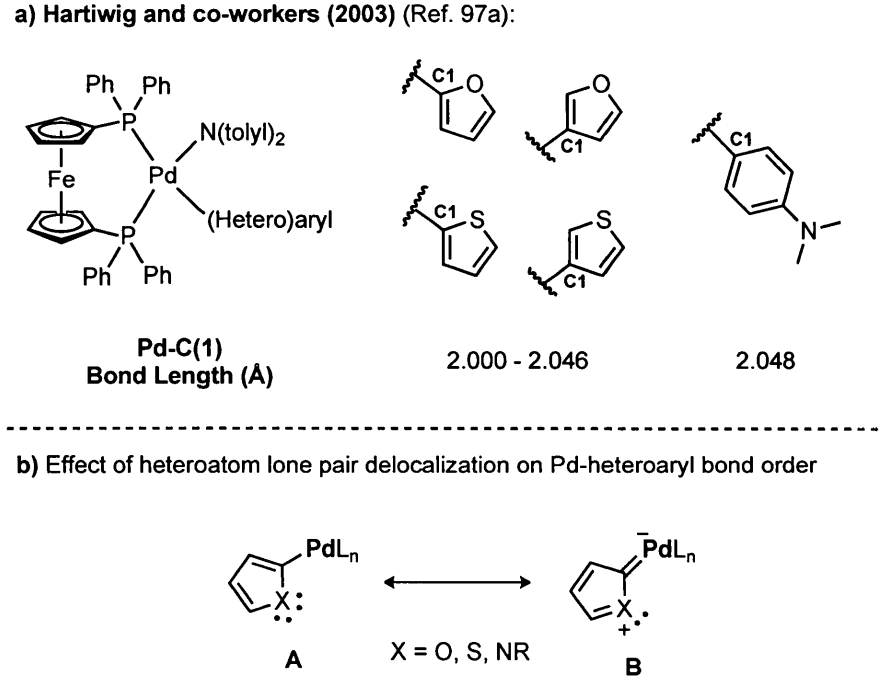

Figure 23. Effect of 5-membered heteroaromatic substituent on Pd-heteroaryl bond order

Table 8. Coupling Heteroaryl Halides with Pd-PEPPSI-IPent^{Cl} (**78**)[a-c]

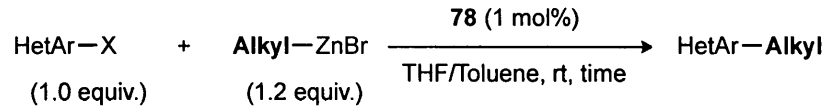

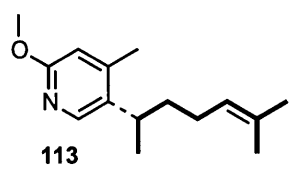

113

4 h, X = Br
84%, **n/r: >99:1**

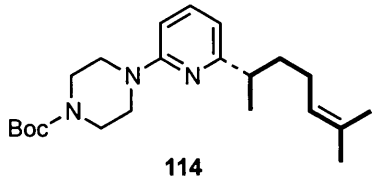

114

30 min, X = Br
94%, **n/r: >99:1**

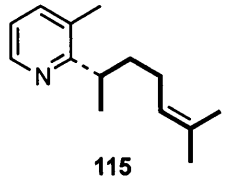

115

4 h, X = Cl
84%, **n/r: >99:1**

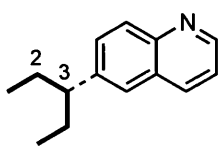

116

3 h, X = OTf
85%, **n(C3)/r(C2): >49:1**

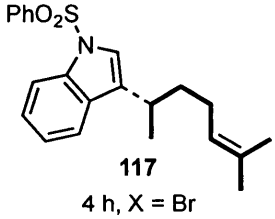

117

4 h, X = Br
88%, **n/r: 29:1**

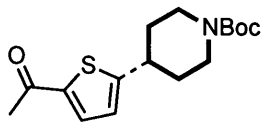

118

4.5 h, X = Cl, 97%
n/r: 15:1

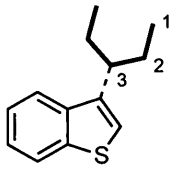

119

0.5 h, X = Br, 85%
C3 : C2 : C1 =
1.0 : 0.5 : 0

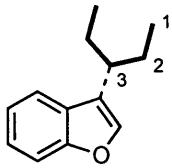

120

1 h, X = Br, 88%
C3 : C2 : C1 =
1.0 : 2.0 : 0.4

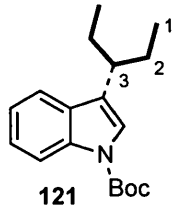

121

17 h, X = Br, 90%
C3 : C2 : C1 =
1.0 : 0.6 : 0

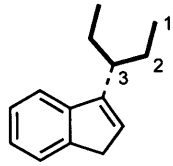

122

2h, X = Br, 65%
C3 : C2 : C1 =
91 : 1 : 0

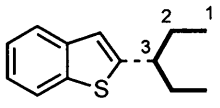

123

2h, X = Br, 93%
C3 : C2 : C1 =
1.0 : 4.1 : 2.9

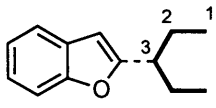

124

1 h, X = Br, 90%
C3 : C2 : C1 =
1.0 : 1.6 : 0.2

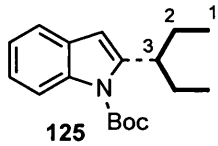

125

17 h, X = Br, 72%
C3 : C2 : C1 =
1.0 : 1.1 : 1.0

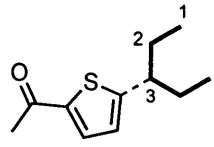

126

16 h, X = Cl, 85%
C3 : C2 : C1 =
0.2 : 0.7 : 1.0

[a] Reactions were conducted on a 0.5 mmol scale at a concentration of 0.25 M; [b] Isolated yields are reported on products purified by flash chromatography and were averaged over two runs; [c] The ratio of inseparable regioisomers (n:r) was determined by ^{1}H-NMR spectroscopy after purification. A ratio of >99:1 means that no minor isomers were detected at all. n = normal product, r = rearranged product.

3.5 – Mechanistic Studies on the Effect of Backbone Substitution

In order to better understand the improved selectivity furnished by Pd-PEPPSI-IPent^{Cl} (**78**) and related Pd-PEPPSI complexes containing backbone-modified NHC ligands, density functional theory (DFT) calculations were performed by our collaborator Dr. Rob Froese at The Dow Chemical Company.[98] The calculated potential energy surface (PES) for the selectivity associated with the formation of the branched (**B**) and linear products (**E**) is shown in Figure 24. To simplify the calculations, only the Pd-PEPPSI complexes featuring the IPr (**29**) and IPr^{Cl} (**73**) ligands were studied.

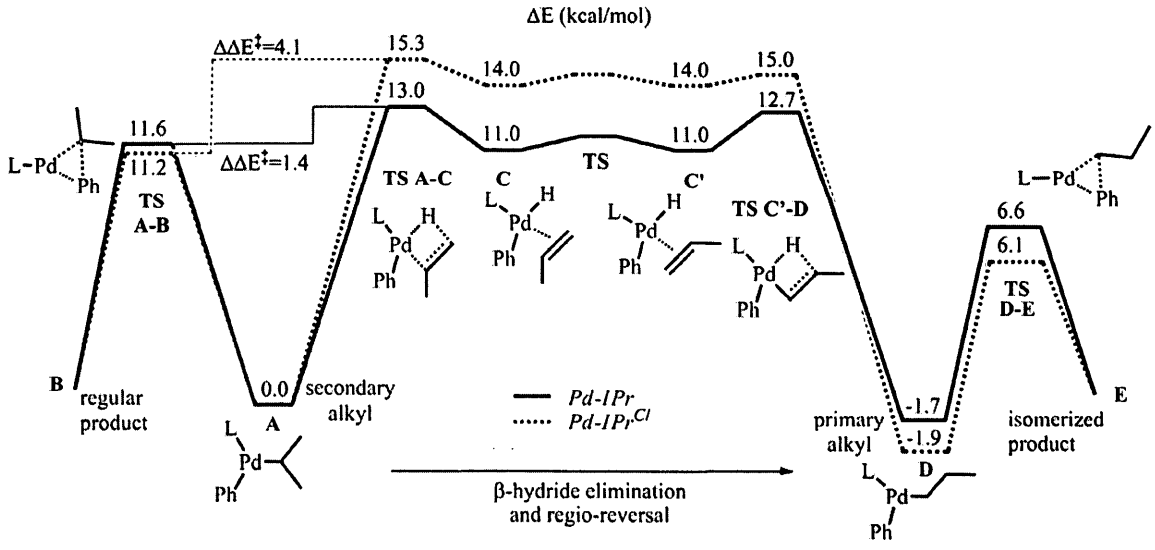

Figure 24. The DFT potential energy surface for RE vs. BHE for the coupling of PhBr and isopropylzinc halide with pre-catalysts **29** (——) and **73** (·····). Free energies are expressed in kcal/mol. Image reproduced from ref. 96.

Consistent with the mechanism presented in Figure 18, after transmetalation, complex **A** can directly undergo RE to generate branched product **B** or undergo BHE, forming olefin hydrido complex **C**. Re-insertion of the hydride ligand into the adjacent olefin carbon atom yields **D** from which linear isomer **E** is formed after RE. Notably, n-propyl complex **D** was found to be lower in energy than isopropyl complex **A** with both **29** and **73**,

implying that once BHE has occurred to form **C/C'**, MI will occur preferentially to form **D** rather than reverting back to **A**. Furthermore, since the barrier leading from **D** to isomeric product **E** is low (6.1 or 6.6 kcal/mol), irreversible RE to form **E** will occur rapidly. As a result, the regiochemical outcome of the reaction is determined by the relative heights of **TS A-C** vs. **TC A-B**. This can be expressed as $\Delta\Delta E^{\ddagger}$, the energy difference between the two transition states: $\Delta\Delta E^{\ddagger} = \Delta E^{\ddagger}_{E} - \Delta E^{\ddagger}_{B}$ – a positive $\Delta\Delta E^{\ddagger}$ implies that desired product **B** is favoured over isomeric product **E**. As shown in Figure 24, when employing Pd-PEPPSI-IPr (**29**), $\Delta\Delta E^{\ddagger}$ = 1.4 kcal/mol, implying a slight preference for **B**, however when the backbone chlorinated IPr^{Cl} is used (**73**), this energy difference increases significantly to 4.1 kcal/mol, resulting in a jump in selectivity for **B**. The computed values of $\Delta\Delta E^{\ddagger}$ were found to correlate well to experimentally observed selectivites for a variety of aryl halides when employing pre-catalysts **29** and **73**, as well as the other backbone-modified IPr complexes **76** and **77**.[96,99]

Since the calculations were found to correlate well with observed regioselectivites, a series of other backbone modified NHCs (including virtual ones) were examined in order to determine the effect of backbone substitution on selectivity. An interesting linear correlation was discovered between the average C-N-Ar angles of the NHC ligand and the regiochemical outcome of the reaction, measured by $\Delta\Delta E^{\ddagger}$ (Figure 25). Apparently, as the C-N-Ar angle increases in response to growing steric pressure from the backbone substituents, the $\Delta\Delta E^{\ddagger}$ value also increases, predicting very high selectivities with large ^{t}Bu and TMS backbone substituents. We initially rationalized this by assuming that the increased steric profile of the ligand caused by large backbone substituents resulted in a decreased barrier for RE, hence improving regioselectivity. However upon close inspection of the PES, this justification appeared to be inadequate since the RE barrier was only calculated to decrease by 0.4 kcal/mol when switching from **29** to **73**, whereas the barrier for BHE was found to increase by 2.3 kcal/mol. This can be justified by considering that regioselectivity is a function of the *difference* between the barriers for RE, having a 3-center transition state (eg. **TS A-B**), and BHE, having a 4-centred

transition state (eg. **TS A-C**). Thus, larger backbone substituents, which push the aryl groups closer to the metal coordination sphere, destabilize the four-centred TS of BHE much more than the three-centred TS of RE, resulting in increased selectivity for the desired branched isomer.

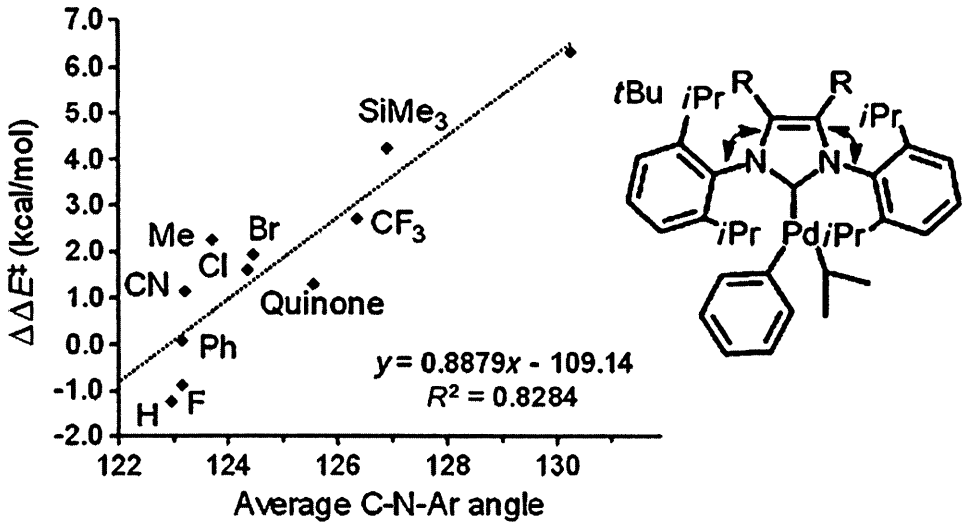

Figure 25. A comparison of the computed $\Delta\Delta E^{\ddagger}$ value of between RE and BHE vs. the average of the two computed C-N-Ar bond angles (see arrows on structure) of the NHC. Each point on the graph corresponds to an individual substituent, R, on the NHC backbone. Image reproduced from ref. 96.

3.6 – Conclusions

A series of novel NHC-based Pd-PEPPSI pre-catalysts were developed featuring a number of backbone-substituted NHC ligands rationally designed for improved performance in the cross-coupling of secondary alkyl nucleophiles. We hypothesized that backbone substituents which increase the steric footprint of the NHC and render the metal slightly more electron deficient would improve the regiochemical outcome of the reaction by increasing the rate of RE relative to BHE. We performed S.A.R. studies on these complexes in the Negishi coupling of secondary alkylzinc reagents with variously

substituted aryl and heteroaryl halides and discovered that whether the backbone substituents render the metal centre more electron rich (eg. **76**) or deficient (eg. **73** or **77**), selectivity for the branched, non-isomeric product is favoured, partially invalidating our hypothesis. Furthermore, we identified air-stable and easily synthesized Pd-PEPPSI-IPent^{Cl} (**78**) as the most active and selective NHC-based Pd catalyst yet reported for this transformation, rivaling and usually surpassing state-of-the-art phosphane-based technology. Using **78** allowed for the cross-coupling of a wide variety of electrophiles containing aldehydes, ketones, esters, amides and even free amines, alcohols, and carboxylic acids, leading to virtually one desired regioisomer. However, despite this improved activity, 5-membererd heterocyclic halides were found to be recalcitrant substrates, furnishing cross-coupled products with dismal regioselectivities. Consistent with previous accounts in the literature, this can be rationalized by considering the innate ability of the heteroatom to mesomerically transfer electron density to the metal centre, resulting in a stronger metal-carbon bond and a concomitant reduction in the rate of RE.

In order to better understand the improved regioselectivity associated with **78**, we performed computational studies, which revealed that the relative barrier difference between RE and BHE correlated very well with observed selectivities. Moreover, it appears that the effect imparted by the backbone substituent is primarily steric in origin and essentially independent of the donating ability of the NHC, verifying experimental observations.

CHAPTER 4: Evaluation of Backbone-Modified NHC Ligands in the Buchwald-Hartwig Amination Reaction

4.1 – General Background

The Pd-catalyzed amination of aryl halides has become one of the most widely used methods for the construction of C-N bonds.[11] As a result, much effort has been invested in the development of more active ancillary ligands to improve the scope and efficiency of this transformation. Electron-rich, bulky tertiary phosphines have emerged as the ligands of choice due to their high activity and easy tunability. Some notable highly active phosphine ligands include Fu and Koie's P^tBu_3,[26] Verkade's amino-phosphines,[100] Beller's indolyl phosphines,[101] Hartwig's ferrocene-based phosphines,[28] Buchwald's[29] and Kwong's[102] biaryl phosphines, and Stradiotto's P,N-ligands[103] (Figure 26).

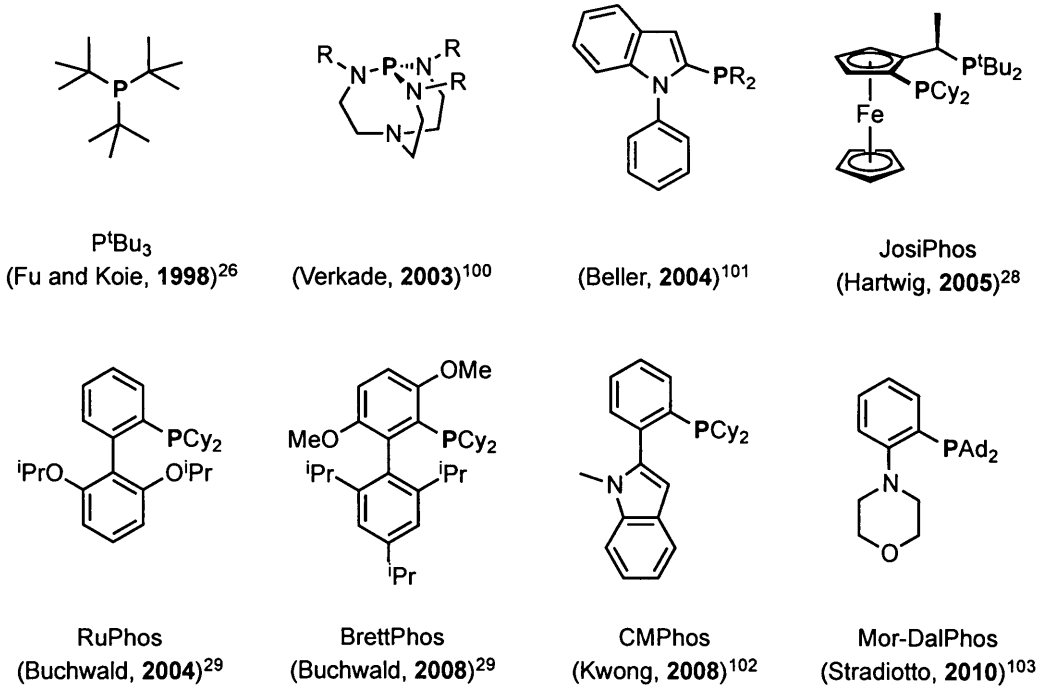

Figure 26. A selection of state-of-the-art phosphine ligands used in the Buchwald-Hartwig amination reaction

The mechanism for this transformation is shown in Figure 2 (Page 4, *vida supra*). The amine-coordination/deprotonation step has frequently been identified as challenging[104] thus many early amination protocols required the use of a strong metal alkoxide or amide base to obtain acceptable product yields.[105] However, in light of the aggressive reactivity of these bases, the tolerance of the reaction conditions to various sensitive functional groups, such as ketones and esters, was limited. As a result, the goal of modern ligand design has become to enable this cross-coupling to proceed efficiently in the presence of weaker bases thus expanding the substrate scope of the transformation.[106] Although weak bases such as Cs_2CO_3 had been used previously,[107] one of the first general protocols for the coupling of aryl chlorides with anilines using K_2CO_3 was disclosed by Buchwald and co-workers in 2008 using the XPhos ligand (Figure 27).[108] Since then, a number of conditions have been developed by the same group for the coupling of anilines, primary and secondary aliphatic amines, and primary amides that employ weak carbonate bases.[109]

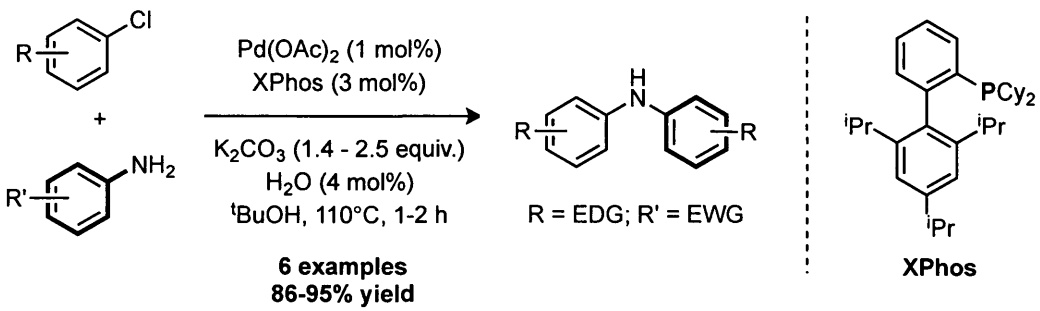

Figure 27. An aryl amination using a weak base

4.2 – Pd-PEPPSI Complexes in the Buchwald-Hartwig Amination

In 2008, Organ and co-workers disclosed that Pd-PEPPSI-IPr (**29**) was an effective pre-catalyst for the amination of aryl chlorides and bromides with anilines and secondary amines using KO^tBu as the base.[59] In the report, Cs_2CO_3 was also demonstrated to be effective when coupling secondary amines, however the authors noted that only electron-deficient aryl halides coupled effectively under these mildly basic conditions. The

electron-withdrawing group was thought necessary in order to sufficiently reduce the pKa of the Pd-ammonium complex (**B** in Figure 2) to be deprotonated by Cs_2CO_3. In 2011 and 2012, the same group disclosed that the bulkier Pd-PEPPSI-IPent pre-catalyst (**31**) vastly outperformed **29** in the coupling of secondary amines[64a] and anilines[64b] with electronically deactivated aryl chlorides using Cs_2CO_3 as the base (Figure 28).

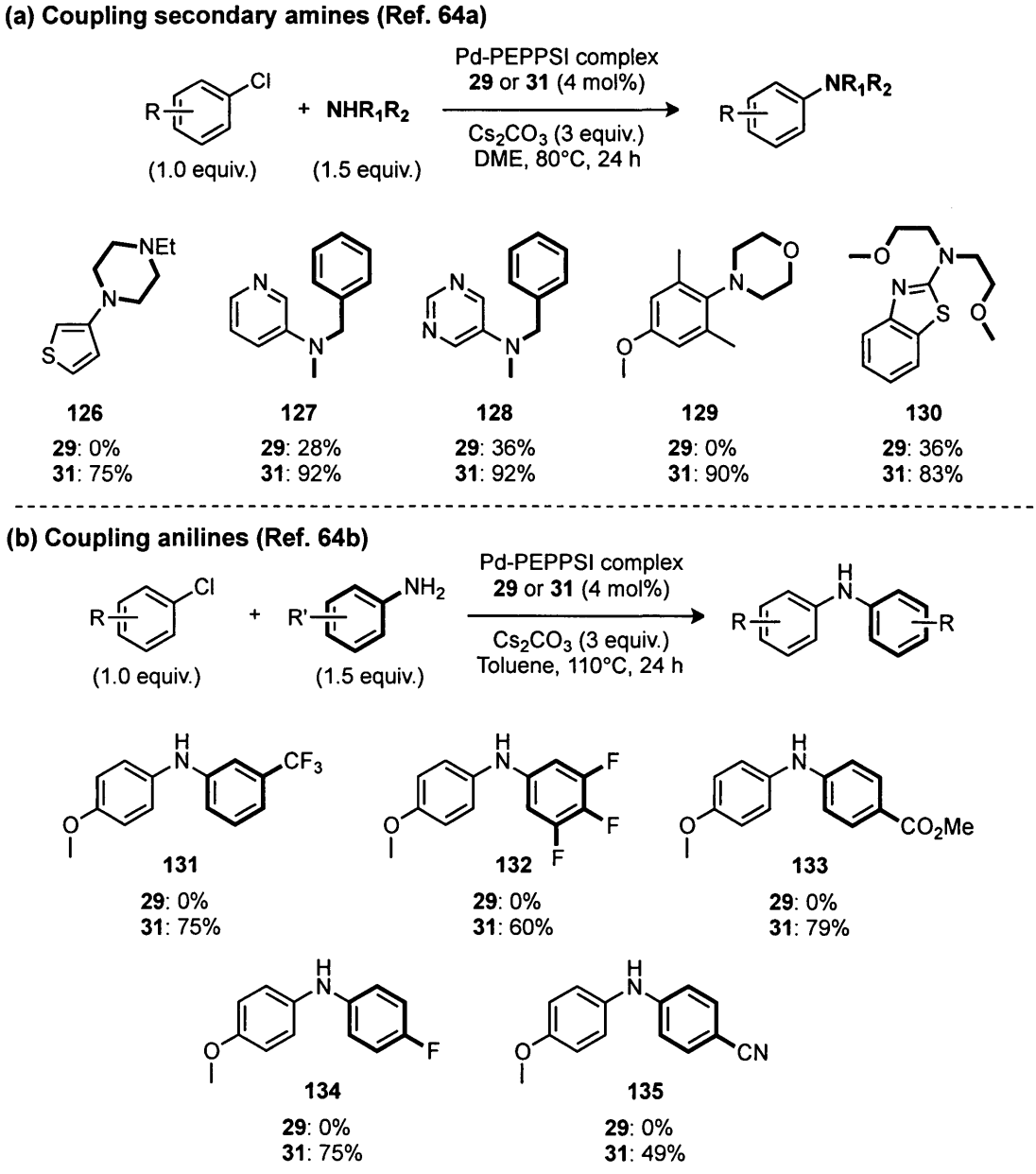

Figure 28. Coupling (a) secondary amines and (b) anilines with Pd-PEPPSI-IPent (**31**)

Pd-PEPPSI-IPent (**31**) effectively promoted the cross-coupling of various secondary amines with a wide variety of aryl halides at 80°C (**126 – 130**, Figure 28a). Notably, even sterically hindered and electronically deactivated substrates coupled in high yields (**129**). This pre-catalyst was also able to effectively promote the coupling of a diverse array aniline substrates compared to **29**, which was almost completely inactive in these cases (Figure 28b). However, despite its superior activity, the coupling of non-nucleophilic anilines using **31** was noted to be problematic even at elevated temperatures (110°C).

To shed light on the mechanistic underpinnings of these aminations involving aniline derivatives, rate and computational studies were performed.[64b] First, the reaction was determined to be zero-order in aryl chloride (implying that oxidative addition (OA) is not rate-limiting) and first order in both aniline and base (suggesting a slow amine coordination/deprotonation step). However, by systematically varying the electronic nature of the aryl halide and the aniline, Organ discovered that the reaction was accelerated by both an electron-deficient aryl halide and an electron-rich aniline, which is more consistent with RE as the rate-limiting step rather than deprotonation. An updated mechanistic picture of the Pd-PEPPSI catalyzed Buchwald-Hartwig amination is shown in Figure 29a, accounting for these observations.

In light of the modest reactivity of **31** in coupling electron-deficient anilines, we thought it worthwhile to investigate the use of Pd-PEPPSI pre-catalysts with backbone-modified NHC ligands. We hypothesized that placing electron-withdrawing groups on the backbone would render the metal centre more electrophilic thus enhancing the amine coordination equilibrium and the rate of deprotonation (Figure 29b). More importantly, the additional steric bulk proffered by the backbone substituents would serve to improve the rate of the crucial RE step.

(a) Updated Mechanistic Picture with Pd-PEPPSI complexes (Adapted from ref. 64b):

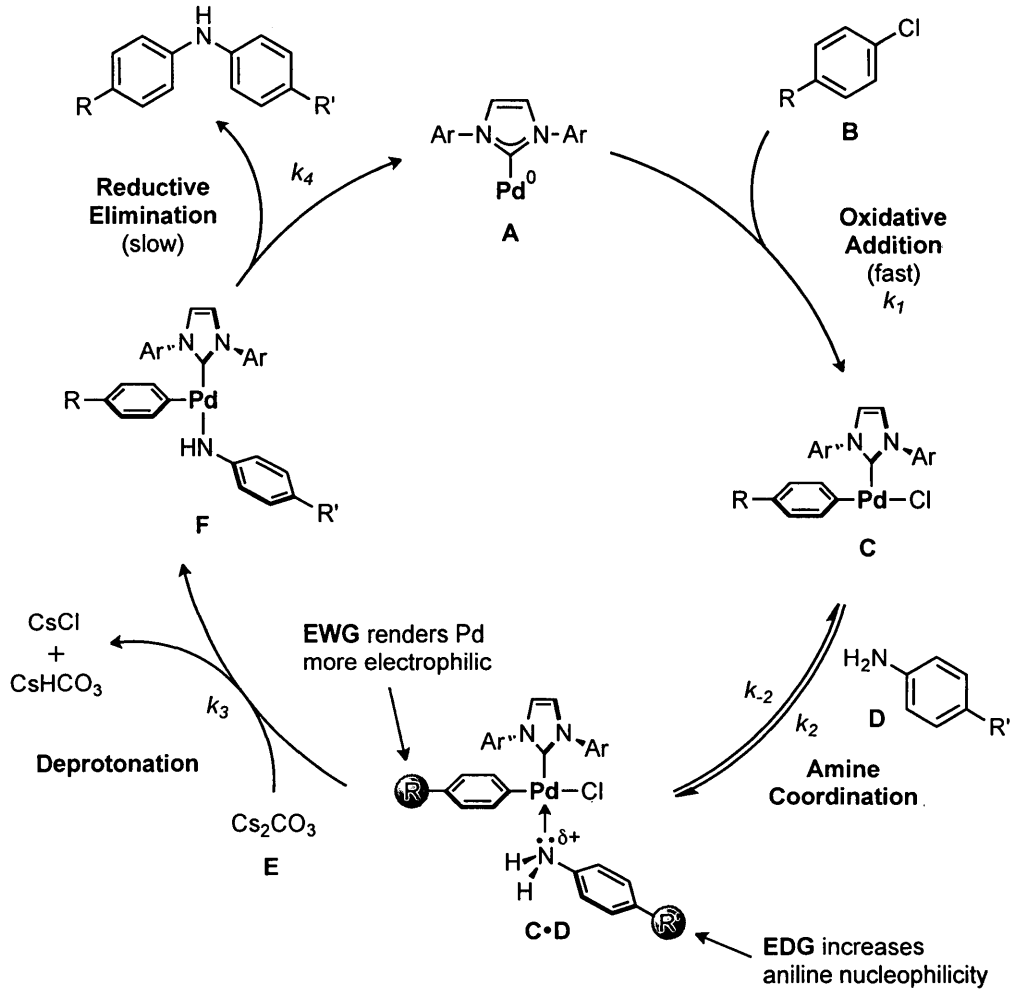

(b) Using Backbone-Modified NHCs to Modulate Reactivity:

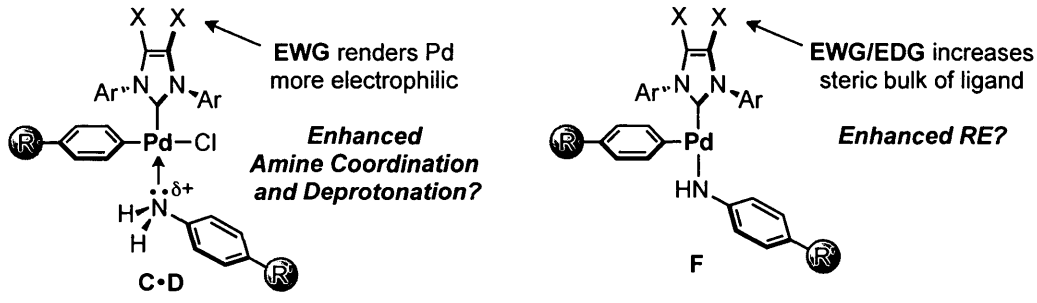

Figure 29. (a) Updated mechanism of the Pd-PEPPSI catalyzed Buchwald-Hartwig Amination; and (b) Proposed applications of backbone-modified NHCs.

4.3 – Evaluation of Backbone-Modified Pd-PEPPSI Complexes in Aryl Amination

Pd-PEPPSI-IPr (**29**) and the backbone-modified IPr derivatives IPr^{Cl} (**73**), IPr^{Me} (**76**), and IPr^{Quino} (**77**) were first tested for efficacy by coupling aniline with various *para*-substituted aryl chlorides under the standard amination conditions developed earlier (DME, Cs_2CO_3, 80°C) (Table 9). Not surprisingly, all catalysts performed poorly when electron-rich 4-chloroanisole was used as the electrophile, however **73** and **76** were the most reactive, producing product in 10% and 16% yield, respectively. Switching to chlorobenzene resulted in a marked improvement in reactivity for all backbone-modified catalysts yielding product in 36-55% yield, however **29** remained essentially inactive. Finally, when employing an electron-deficient chloride, all catalysts furnished product quantitatively. These results demonstrate that backbone-modified NHC ligands are more active in aryl amination with anilines than their unmodified counterpart **29** and more importantly, that the increase in catalytic activity is essentially independent of the donating ability of the substituent. Thus, the effect of the backbone substituent appears to be steric in origin and corroborates Organ's conclusion that RE is rate-limiting.

Table 9. Evaluation of Backbone-Modified IPr ligands in Aryl Amination[a]

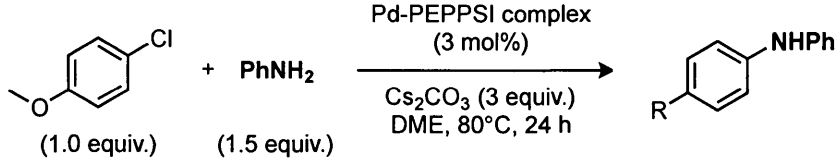

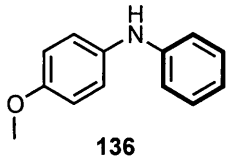	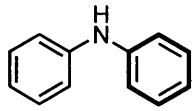	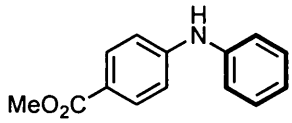
136	**137**	**138**
29: 0%	**29**: 5%	**29**: 95%
73: 10%	**73**: 55%	**73**: 97%
76: 16%	**76**: 46%	**76**: 96%
77: 2%	**77**: 36%	**77**: 96%

[a] Reactions were conducted on a 0.5 mmol scale at a concentration of 1 M; [b] Isolated yields are reported on products purified by flash chromatography and were averaged over two runs.

We opted next to evaluate the bulkier IPent (**31**) and IPent^{Cl} (**78**) analogues in the coupling of electron-deficient anilines electron-rich aryl chlorides, the most challenging electronic combination (Table 10). Pd-PEPPSI-IPent^{Cl} (**78**) was found to be significantly more active than the unmodified IPent complex (**31**), effectively coupling both 3-trifluoromethylaniline and 3,4,5-trifluoroaniline with 4-chloroanisole, furnishing **131** and **132** in 96 and 94% yield, respectively. Remarkably, even profoundly deactivated pentafluoroaniline could be cross-coupled to 4-chloroanisole using **78** in a 58% yield, whereas no reaction was observed with **31**. This is the first example of Pd-catalyzed arylation of pentafluoroaniline, demonstrating the unprecedented reactivity of **78**. Surprisingly, when we attempted to couple 4-nitroaniline, a much more commonly used aniline, only traces of product (<5%) were observed with both catalysts.

Next, coupling sterically hindered 2,6-dimethylaniline with 2-chloropyridine yielded **140** in 78% yield using **78** and only 55% yield with **31**. Notably, 11% of triarylamine **141** was also observed when employing **78**, again demonstrating the significant improvement in reactivity relative to **31**. Diarylamines are much more challenging coupling partners than even the most deactivated anilines due to the presence of the second aryl ring, which severely curtails the nucleophilicity of the amine. This promising result prompted a colleague, Ka Hoi, to investigate the synthesis of triarylamines using **78** and a set of general conditions were discovered that allowed for the preparation of a wide variety of these useful substrates.[110]

Table 10. Coupling Electron-deficient anilines with aryl halides with **31** and **78**[a,b]

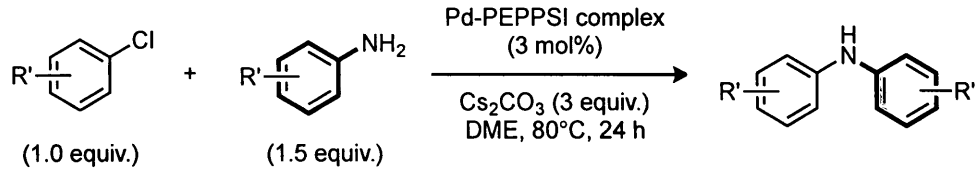

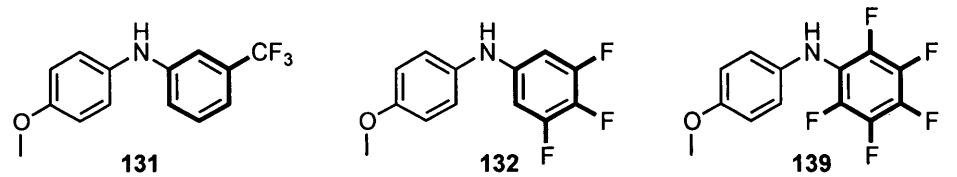

131
31: 62%
78: 96%

132
31: 51%
78: 94%

139
31: 0%
78: 58%

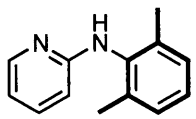

140
31: 55%
78: 78% + 11% **141**

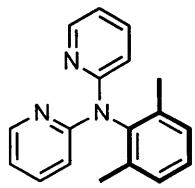

141

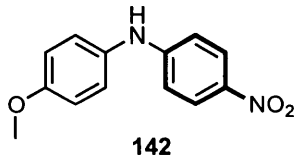

142
31: 0%
78: traces

[a] Reactions were conducted on a 0.5 mmol scale at a concentration of 1 M; [b] Isolated yields are reported on products purified by flash chromatography and were averaged over two runs.

4.4 – Low Temperature Aryl Aminations with Pd-PEPPSI-IPent^{Cl} (78)

Given the superior activity of **78** relative to **31** and all other reported NHC-based Pd catalysts, we wondered if it would be possible to conduct these amination reactions at lower temperature. If successful, the combination of a mild base and low temperature offers unique opportunities for cross-coupling substrates containing highly sensitive functional groups. In approaching this challenge, we took a page from our group's recent work on the low temperature Pd-PEPPSI-catalyzed sulfination chemistry in which the structure of the pyridine ligand in the pre-catalyst was found to have a profound impact on catalyst performance.[111] Although the pre-catalyst activation pathways and catalytic cycles are somewhat different, we were curious to learn if a similar dependence on the pyridine topology might be manifested in low temperature amination chemistry. To this

end, a number of Pd-PEPPSI-IPent^{Cl} precatalysts with various pyridine ligands were prepared and screened in the coupling of 4-chloroanisole with 3,4,5-trifluoroaniline at *room temperature* – an extremely challenging coupling for **31** even at 110°C! (Table 11).

Table 11. Pyridine Optimization in the Room Temperature Aryl Amination[a]

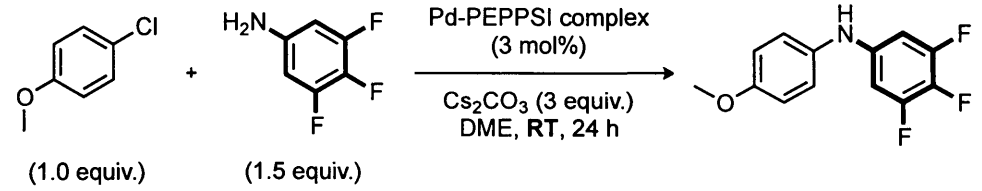

(1.0 equiv.) (1.5 equiv.)

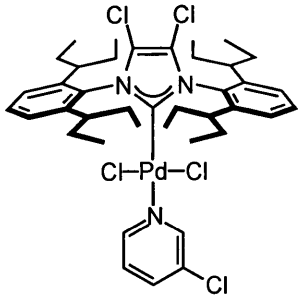

78
55% conv.

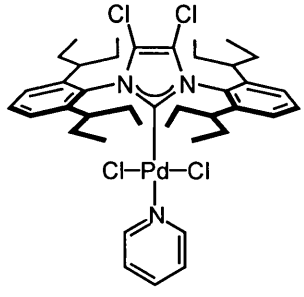

143
70% conv.

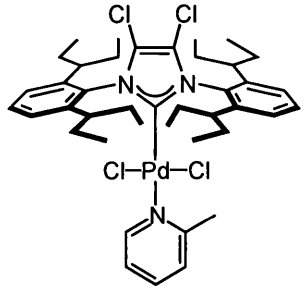

144
82% conv.

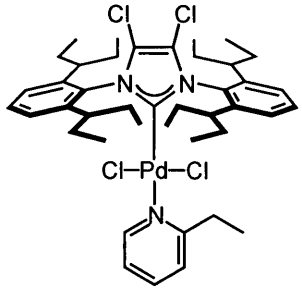

145
81% conv.

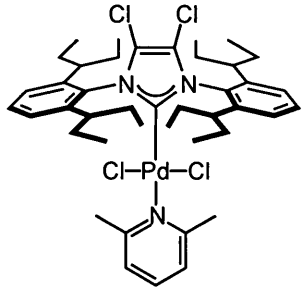

146
39% conv.[c]

[a] Reactions were set up in a glovebox using degassed DME on a 0.5 mmol scale at a concentration of 1 M; [b] Percent conversion to product determined by ^{1}H-NMR spectroscopic analysis of the crude reaction mixture following filtration; [c] 92% of **146** was left unreacted after 24 h.

To our delight, the 3-chloropyridine catalyst (**78**) exhibited good reactivity at this temperature, furnishing 55% conversion to product after 24 h. The fact that **78** is as reactive at *room temperature* as **31** is at 80°C is a testament to the profound effect that backbone substitution has on modulating the performance of this NHC ligand. Switching to pyridine complex **143** resulted in a 15% jump in conversion to 70%. Placing a methyl or ethyl group in the *ortho*-position of the pyridine resulted in another 10% improvement in conversion (**144** and **145**), however employing pre-catalyst **146** with bulkier 2,6-dimethylpyridine resulted in only 39% conversion to product. Interestingly, 92% of **146** was recovered unreacted after 24 h, thus only 8% of the 3 mol% of catalyst added was responsible for the observed catalysis, which corresponds to just 0.0024 mol% Pd. This implies that activation of **146** is slow but that once activated, proceeds to catalyze product formation at a very high rate. From this study, Pd-PEPPSI-IPent^{Cl}-picoline (**144**) was identified as the most reactive pre-catalyst for room temperature aryl amination, which is coincidentally the same complex that was identified as the most active for room temperature aryl sulfination.[111] The exact role of the pyridine ligand in improving catalyst reactivity is currently unknown.

Unexpectedly, these reactions were found to be somewhat sensitive to the level of dissolved O_2 in commercially available anhydrous DME. The initial pyridine optimization studies were successfully conducted using standard Schlenk techniques and commercial anhydrous DME purchased from Sigma-Aldrich. However, when switching to a new solvent bottle from the same supplier, the reactions essentially shut down. Reactivity could only be recovered if the solvent was degassed via three cycles of freeze-pump-thaw and the entire reaction set up in an Ar-filled glovebox. Thus to ensure consistently reproducible results, all room temperature aryl aminations were conducted under a strictly O_2-free environment. This increased sensitivity might be due to competitive oxidative ligation of molecular oxygen towards (NHC)Pd(0)L_n, forming unreactive (NHC)Pd(O_2)L complexes which have been documented in the literature. For example, Fantasia and Nolan recently reported that peroxo complex (IPr)Pd(PPh_3)(O_2)

forms rapidly and irreversibly from (IPr)Pd(PPh_3) upon exposure to atmospheric O_2 and is stable as such for many days without observable decomposition.[112] The stability of these off-cycle intermediates at room temperature may account for the heightened O_2-sensitivity of aminations conducted at this temperature relative to those conducted at elevated temperatures in which sufficient thermal energy is available to drive off the Pd-bound O_2.

To demonstrate the scope of this new catalyst at room temperature, a variety of functionalized, electron-rich aryl chlorides were coupled with a series of electron-deficient anilines (Table 12). Good to excellent yields were achieved when coupling 4-chloroanisole with polyfluorinated anilines (**131** and **132**) and methyl 4-aminobenzoate (**147**). An impressive chemoselective amination of 4-chlorophenylboronic acid pinacol ester was also achieved, yielding **149** in good yield without a trace of biaryl side-products that might be observed at higher temperatures. Finally, higher molecular weight aryl chlorides with medicinal value were coupled with 3-trifluoromethylaniline, forming cross-coupled products **150** and **151** in excellent yields. Due to the limited solubility of the aryl chloride from which **151** was derived, this reaction was heated gently at 45°C to ensure complete conversion to product.

Table 12. Examining the Substrate Scope of Room Temperature Aryl Aminations catalyzed by Pd-PEPPSI-IPent^{Cl}-picoline[a-b]

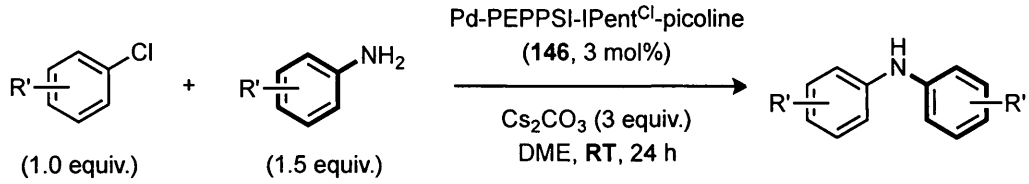

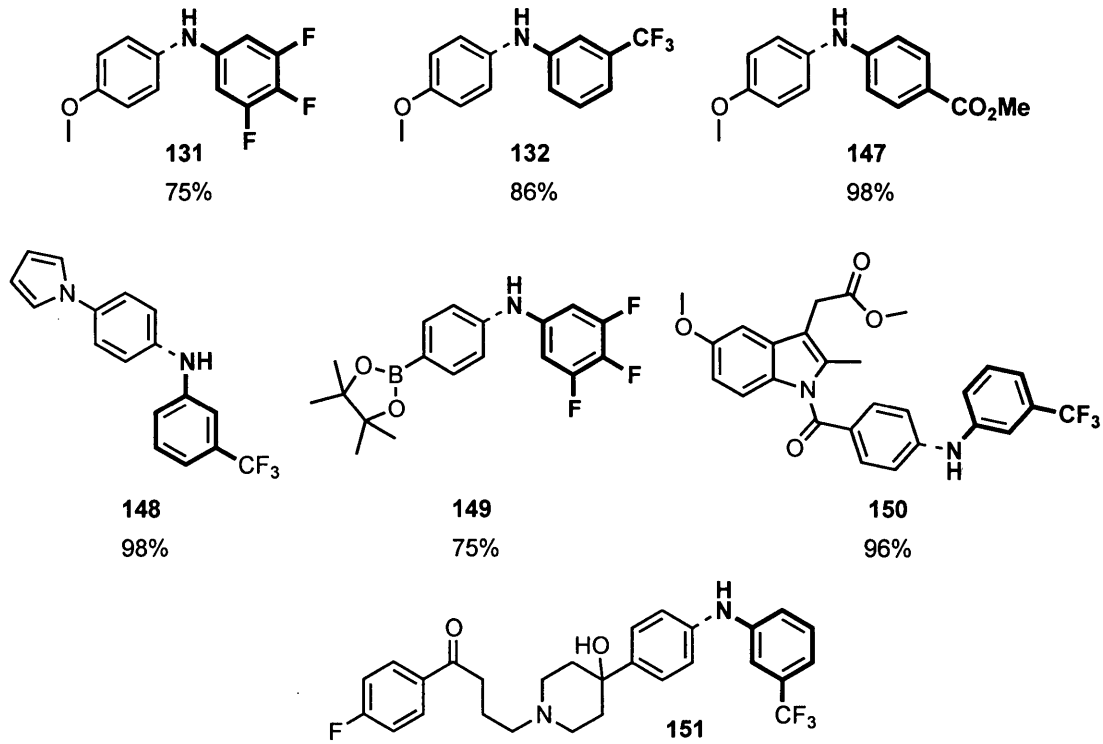

[a] Reactions were set up in a glovebox using degassed DME on a 0.5 mmol scale at a concentration of 1 M; [b] Isolated yields are reported on products purified by flash chromatography and were averaged over two runs.

4.5 – Conclusions

A series of Pd-PEPPSI complexes featuring backbone-modified NHC ligands were evaluated for activity in the Buchwald-Hartwig amination of deactivated aniline substrates. All backbone-modified complexes exhibited enhanced reactivity relative to their unmodified counterparts, regardless of the electron withdrawing or releasing ability of the backbone substituents. This implies that the effect imparted by the substituents is primarily steric in origin and seems to corroborate Organ's mechanistic assertion that the rate-limiting step in these aryl aminations is reductive elimination.

Pd-PEPPSI-IPent^{Cl} (**78**) was identified as the most active pre-catalyst and could effectively promote even the most difficult aminations in which Pd-PEPPSI-IPent (**31**) was completely inactive. Further optimizing the architecture of the trans-ligated pyridine culminated in the development of Pd-PEPPSI-IPent^{Cl}-picoline (**144**), which was demonstrated to be highly effective for the unprecedented *room temperature* amination of electron rich aryl halides with electronically deactivated anilines using a mild carbonate base. The scope and functional group compatibility of these conditions allowed for the efficient coupling of electrophiles containing ketones, esters, amides, alcohols, and boronic acid derivatives. Higher molecular-weight, drug-like electrophiles were also successfully coupled, notable examples of which include **151**, derived from Haloperidol, an anti-psychotic drug, and **150**, derived from Indomethacin, a common non-steroidal anti-inflammatory drug (NSAID). These conditions are milder than any yet reported in the literature for the cross-coupling of deactivated anilines and represent a significant advance in the field.

CHAPTER 5: Experimental Procedures

5.1 – General Experimental

All experiments were conducted under an atmosphere of dry argon in oven-dried or flame-dried glassware using standard Schlenk techniques unless noted otherwise. Experiments performed in an oil bath were done using Fisher Scientific silicone oil in a Pyrex crystallizing dish on top of an IKA RCT basic model magnetic hotplate stirrer with an ETS-D5 electronic contact thermometer. Glovebox manipulations were performed in an MBraun Unilab glove-box under an atmosphere of dry argon. All reagents were purchased from Sigma-Aldrich, Alfa Aesar, or Strem and were used without further purification unless noted otherwise. THF and Et_2O were distilled under argon over sodium-benzophenone ketyl prior to use whereas toluene and dichloromethane were distilled under argon over calcium hydride prior to use. All reaction vials (screw-cap threaded, caps attached, 15x45 mm) were purchased from Fisher Scientific. Analytical Thin Layer Chromatography (TLC) was performed on EMD 60 F254 pre-coated glass plates and spots were visualized with UV light (254 nm) or a $KMnO_4$ staining solution. Column chromatography purifications were carried out using the flash technique on EMD silica gel 60 (230 - 400 mesh).[113] NMR spectra were recorded on Bruker 300 AVANCE, Bruker 400 AVANCE, and Bruker 600 DRX spectrometers. The chemical shifts for ^{1}H-NMR spectra are given in parts per million (ppm) referenced to the residual proton signal of the deuterated solvent; coupling constants are expressed in Hertz (Hz). ^{13}C-NMR spectra were referenced to the carbon signals of the deuterated solvent. The following abbreviations are used to describe peak multiplicities: s = singlet, br s = broad singlet, d = doublet, br d = broad doublet, t = triplet, br t = broad triplet, q = quartet, quint = quintet, sext = sextet, sept = septet, dd = doublet of doublets, tt = triplet of triplets, qt = quartet of triplets, qd = quartet of doublets, and m = multiplet. For ^{13}C-APT NMR spectra, quaternary carbons and carbons with an even number of attached protons produce a positive (+) signal whereas peaks with a negative (–) signal arise from carbons attached to an odd number of protons. Gas chromatographic analysis was performed on

Varian Series GC/MS/MS 4000 System. Melting points were determined using a Fisher-Johns melting point apparatus and are uncorrected. High Resolution Mass Spectrometry (HRMS) analysis was performed by the Mass Spectrometry and Proteomics Unit at Queen's University in Kingston, Ontario.

5.2 – Preparation of Backbone-modified NHCs and their Pd-PEPPSI Complexes

Preparation of IPr^{Cl}·HCl (8):

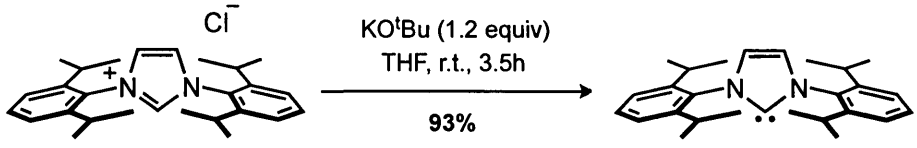

33. IPr·HCl **8.** IPr

In a glovebox, a 100 mL round-bottom flask equipped with a magnetic stir bar was charged with KO'Bu (1.42 g, 12 mmol) then removed from the glovebox. In air, IPr·HCl (**33**)[114] (4.25 g, 10 mmol) was quickly added and the flask evacuated and backfilled with Ar (x3). THF (40 mL) was added *via* syringe and the resulting pale-brown suspension stirred at rt. After 3.5 h, the turbid light-green solution was concentrated *in vacuo* to yield an off-white solid to which 50 mL dry toluene were added. The resulting suspension was heated gently with a heat gun until it became nearly homogeneous. Dry hexanes (50 mL) were then added and the suspension was filtered through a thin pad of oven-dried (140°C for 3 h) Celite, washing with small portions of dry hexanes. The light-yellow filtrate was concentrated *in vacuo* and subsequently dried under high vacuum to yield IPr carbene (**8**) as a flocculent off-white solid (3.65 g, 93%) that was quickly transferred to a glovebox and used directly in the next step. ^{1}H-NMR (400 MHz, C_6D_6) δ 7.40 (t, J = 7.6 Hz, 2H), 7.29 (d, J = 7.6 Hz, 4H), 6.71 (s, 2H), 3.06 (sept, J = 6.8 Hz, 4H), 1.41 (d, J = 6.8 Hz, 12H), 1.30 (d, J = 6.8 Hz, 12H). Spectral data are in accordance with those reported in the literature.[66b]

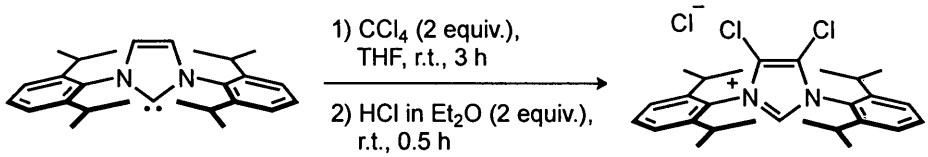

8. IPr

95%

34. IPr^{Cl}·HCl

In a glovebox, a 25 mL round-bottom flask equipped with a magnetic stir bar was charged with IPr (**8**) (974 mg, 2.5 mmol) then sealed with a rubber septum and moved outside the glovebox. THF (12 mL) was added *via* syringe and to the resulting yellow solution at rt was slowly added anhydrous CCl_4 (484 μL, 5 mmol). After stirring for 3 h, ^{1}H-NMR spectroscopic analysis (C_6D_6) of a 100 μL aliquot revealed complete consumption of **8**, thus a 2.0 M solution of HCl in Et_2O (2.5 mL, 5 mmol) was added slowly to the brown solution over 2 min resulting in precipitation of a heavy white solid. After vigorous stirring for an additional 30 min, the precipitate was collected in a medium-porosity fritted glass funnel and washed with portions of Et_2O (30 mL total) to yield 1.08 g of a white solid (Batch 1). The filtrate was re-filtered and an additional 105 mg was collected (Batch 2). A total of 1.19 g (95%) of **34** were collected after drying *in vacuo* for 24 h at 60°C. ^{1}H-NMR (300 MHz, CD_3CN) δ 10.07 (br s, 1H), 7.75 (t, J = 7.8 Hz, 2H), 7.55 (d, J = 7.8 Hz, 4H), 2.49 (sept, J = 6.6 Hz, 4H), 1.31 (d, J = 6.6 Hz, 12H), 1.20 (d, J = 6.9 Hz, 12H); ^{13}C-NMR (100 MHz, CD_3CN) δ 146.0, 138.0, 132.9, 126.8, 125.1, 122.6, 28.8, 23.9, 22.3. Spectral data are in accordance with those reported in the literature.[66b]

Preparation of Pd-PEPPSI-IPr^{Cl} (73):

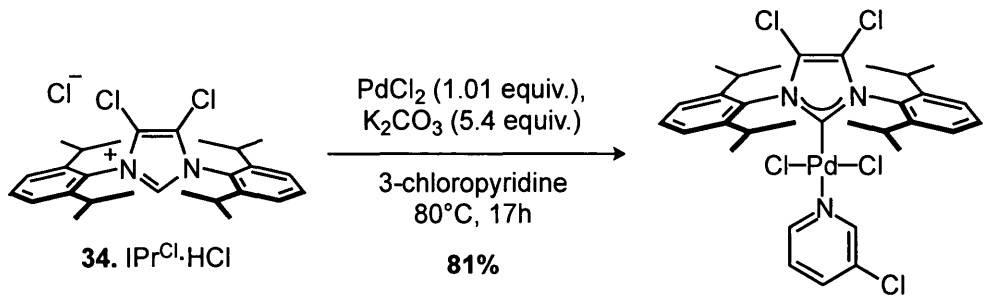

34. IPr^{Cl}·HCl

73

A 25 mL round-bottom flask equipped with magnetic stir bar was charged with $PdCl_2$ (358 mg, 2.02 mmol, 1.01 equiv.), IPr^{Cl}·HCl (**34**, 994 mg, 2.0 mmol, 1.0 equiv.), and crushed anhydrous K_2CO_3 (1.5 g, 10.8 mmol, 5.4 equiv.) then evacuated and backfilled with Ar (x3). 3-Chloropyridine (8 mL) was added *via* syringe and the flask was subsequently sealed, immersed in a pre-heated 80°C oil bath, and allowed to stir ***vigorously*** for 17 h. At this time, ^{1}H-NMR spectroscopic analysis of a 100 μL aliquot ($CDCl_3$) revealed complete consumption of **34**, thus the reaction was cooled to rt and diluted with 5 mL CH_2Cl_2. The resulting suspension was filtered through a well-packed 1.5 cm pad of Silica Gel H covered with a 1 cm pad of Celite in a 30 mL medium-porosity fritted glass funnel, washing with CH_2Cl_2 until the filtrate became colourless (ca. 50 – 60 mL). CH_2Cl_2 and excess 3-chloropyridine were evaporated *in vacuo* (rotovap, bath T = 65°C) and the resulting yellow/orange solid was dried under high vacuum for 1 h with occasional gentle heating with a heat gun to drive off any remaining 3-chloropyridine. Trituration with pentane (10 mL x 3) followed by recrystallization from CH_2Cl_2/pentane (3 batches) furnished 1.22 g (81%) of **73** as a yellow solid. Crystals suitable for X-ray diffraction were grown by slow diffusion of pentane into a concentrated CH_2Cl_2 solution of **73**. Mp: > 300°C; ^{1}H-NMR (400 MHz, $CDCl_3$) δ 8.58 (s, 1H), 8.51 (d, J = 5.2 Hz, 1H), 7.60 (t, J = 8.0 Hz, 3H), 7.42 (d, J = 8.0 Hz, 4H), 7.10 (dd, J = 7.8, 6.2 Hz, 1H), 3.06 (sept, J = 6.6 Hz, 4H), 1.49 (d, J = 6.8 Hz, 12H), 1.21 (d, J = 6.8 Hz, 12H); ^{13}C-NMR (75 MHz, $CDCl_3$) δ 157.7, 150.4, 149.4, 147.7, 137.6, 132.1,

131.9, 131.2, 124.8, 124.4, 120.7, 28.9, 25.4, 24.7; HRMS (ESI) $[M+H]^+$ calcd. for $C_{32}H_{39}N_3PdCl_5$ 746.0621; found 746.0620.

Preparation of IPr^{Br}·HCl (35):

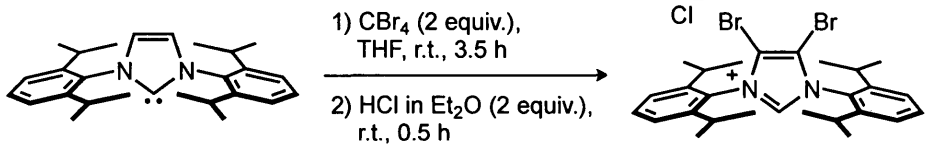

8. IPr **35.** IPr^{Br}·HCl

In a glovebox, a 50 mL round-bottom flask equipped with a magnetic stir bar was charged with IPr (**8**) (1.50 g, 3.85 mmol) then sealed with a rubber septum and moved outside the glovebox. THF (10 mL) was added *via* syringe and to the resulting yellow solution at rt was added a solution of CBr_4 (2.55 g, 7.70 mmol, 2.0 equiv) in 10 mL THF dropwise over 10 min. After stirring for 3 h, ^{1}H-NMR spectroscopic analysis (C_6D_6) of a 200 μL aliquot revealed complete consumption of **8**, thus a 2.0 M solution of HCl in Et_2O (3.9 mL, 7.70 mmol, 2.0 equiv.) was added slowly to the brown solution over 5 min resulting in precipitation of a heavy white solid. After diluting with 5 mL THF, the suspension was stirred vigorously for an additional 30 min, at which point the precipitate was collected in a medium-porosity fritted glass funnel and washed with portions of Et_2O. Triturating successively with 1:1 CH_2Cl_2/pentane (10 mL x 5) then pentane (20 mL x 2) yielded 1.69 g (75%) of **35** as a white solid after drying in vacuo for 16 h. ^{1}H-NMR (400 MHz, DMSO-d_6) δ 10.99 (s, 1H), 7.74 (t, J = 7.8 Hz, 2H), 7.59 (d, J = 8.0 Hz, 4H), 2.37 (quint, J = 6.4 Hz, 4H), 1.29 (d, J = 6.8 Hz, 12H), 1.15 (d, J = 6.8 Hz, 12H); ^{13}C-NMR (100 MHz, DMSO-d_6) δ 145.8, 141.0, 133.1, 128.6, 125.5, 115.3, 29.1, 24.8, 23.0; HRMS (ESI) $[M-Cl]^+$ calc'd. for $C_{27}H_{35}Br_2N_2$ 545,1167; found 545.1172.

Preparation of Pd-PEPPSI-IPr^{Me} (76):

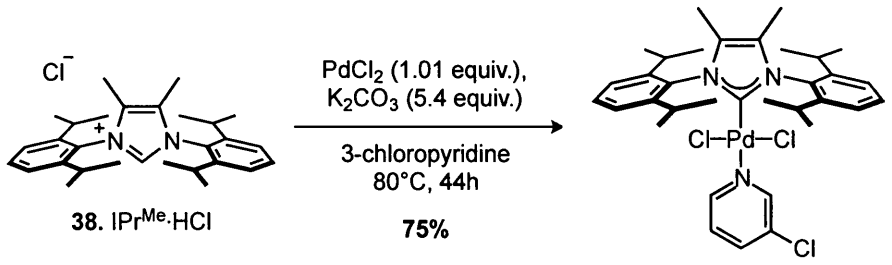

38. IPr^{Me}·HCl

76. Pd-PEPPSI-IPr^{Me}

A 10 mL round-bottom flask equipped with magnetic stir bar was charged with $PdCl_2$ (197.5 mg, 1.114 mmol, 1.01 equiv.), IPr^{Me}·HCl[67] (**38**, 500 mg, 1.103 mmol, 1.0 equiv.), and crushed anhydrous K_2CO_3 (821 mg, 5.94 mmol, 5.4 equiv.) then evacuated and backfilled with Ar (x3). 3-Chloropyridine (5.5 mL) was added *via* syringe and the flask was subsequently sealed, immersed in a pre-heated 80°C oil bath, and allowed to stir ***vigorously*** for 44 h. At this time, the reaction was cooled to rt and diluted with CH_2Cl_2. The resulting suspension was filtered through a well-packed 1.5 cm pad of silica gel covered with a 1.5 cm pad of Celite in a 30 mL medium-porosity fritted glass funnel, washing with CH_2Cl_2 until the filtrate became colourless (ca. 50 – 60 mL). CH_2Cl_2 and excess 3-chloropyridine were evaporated *in vacuo* (rotovap, bath T = 65°C) then dried under high vacuum. The residue thus obtained was taken up in CH_2Cl_2 and filtered through a 6 cm x 3.5 cm column of silica gel, eluting with CH_2Cl_2 until the filtrate became colourless. The filtrate was concentrated and dried for 16 h *in vacuo* to yield 625 mg of **76** as a light-yellow solid, which contained ca. 6% by weight of CH_2Cl_2 as determined by ^{1}H-NMR spectroscopy (75%). Crystals suitable for X-ray diffraction were grown by slow evaporation of a concentrated CH_2Cl_2 solution of **76**. Mp: decomposition over 300°C; ^{1}H-NMR (400 MHz, $CDCl_3$) δ 8.63 (d, J = 2.0 Hz, 1H), 8.55 (d, J = 6.0 Hz, 1H), 7.54 (t, J = 7.8 Hz, 3H), 7.40 (d, J = 7.6 Hz, 4H), 7.07 (dd, J = 8.0, 5.2 Hz, 1H), 3.12 (sept, J = 6.8 Hz, 4H), 1.97 (s, 6H), 1.49 (d, J = 6.8 Hz, 12H), 1.12 (d, J = 6.8 Hz, 12H); ^{13}C-NMR (100 MHz, $CDCl_3$) δ 150.5, 150.1, 149.5, 147.5, 137.2, 133.4, 131.8, 130.2, 129.1, 124.6, 124.2, 28.4, 25.3, 25.1, 11.0; HRMS (ESI) $[M+H]^+$ calcd. for $C_{34}H_{45}Cl_3N_3Pd$ 706.1713; found 706.1744.

Preparation of IPr^{Quino}·HCl (41):

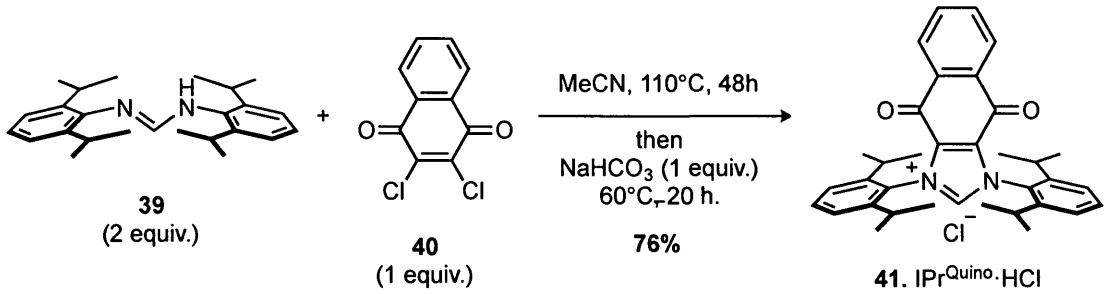

To a 20 mL Biotage microwave vial were added 0.15 g of 2,3-dichloro-1,4-naphthoquinone (0.68 mmol, 1.0 equiv.), 0.50 g of *N,N'*-Bis(2,6-diisopropylphenyl) formamidine[115] (**39**, 1.36 mmol, 2.0 equiv), and 7 mL acetonitrile. The vial was sealed and the solution was heated to 110 °C for 48 h. After cooling to rt, 57 mg of $NaHCO_3$ (0.68 mmol, 1.0 equiv.) were added and the reaction mixture heated at 60 °C for 20 h. After cooling, the resulting slurry was filtered through a pad of Celite and the filtrate was concentrated on a rotary evaporator. Et_2O was added to the residue and the resulting yellow crystals were collected by filtration and dried under high vacuum providing 290 mg (76%) of **41**. Mp: decomposition above 300°C; ^{1}H-NMR (300 MHz, $CDCl_3$) δ 13.91 (s, 1H), 8.22-8.19 (m, 2H), 7.93-7.90 (m, 2H), 7.66 (t, J = 7.8 Hz, 2H), 7.42 (d, J = 7.8 Hz, 4H), 2.40 (sept, J = 6.9 Hz 4H), 1.40 (d, J = 6.9 Hz, 12H), 1.22 (d, J = 6.9 Hz, 12H); ^{13}C-NMR (100 MHz, $CDCl_3$) δ 173.3, $149.4, 135.5, 132.2, 131.7, 131.3, 128.3, 127.8, 124.6, 29.8, 24.6, 23.1; HRMS (E I) $[M-Cl]^+$ calcd. For $C_{35}H_{39}ClN_2O_2$ 519.3012; found 519.3026.

Preparation of Pd-PEPPSI-IPr^{Quino} (77):

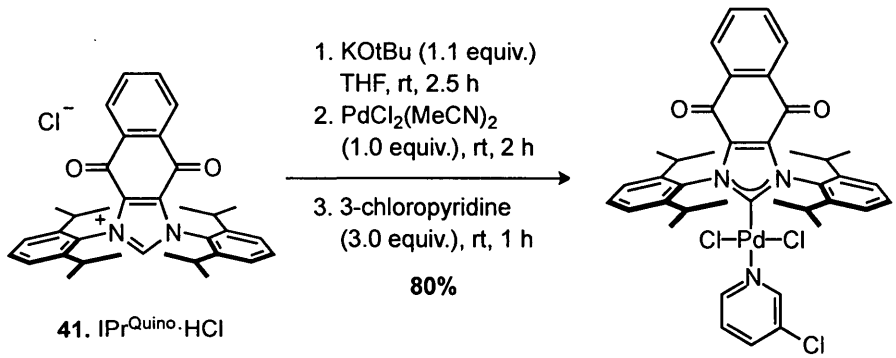

41. IPr^{Quino}·HCl

77. PEPPSI-IPr^{Quino}

In a glovebox, a 2-neck 25 mL round-bottom flask was charged with 70.2 mg of KO^{t}Bu (0.594 mmol, 1.1 equiv.) then with 300 mg of **41** (0.54 mmol, 1.0 equiv.) in air. The flask was evacuated and backfilled with Ar (x3) then THF (5.4 mL) was added. The resulting green suspension was stirred at rt for 2.5 at which time 140.1 mg of $PdCl_2(MeCN)_2$ (0.54 mmol, 1.0 equiv.) was added in one shot under positive Ar pressure. After 2 h, 154 μL of 3-chloropyridine was injected and the suspension further stirred for 1 h before diluting with Et_2O and filtering through a pad of silica gel. The burgundy solid obtained after solvent removal was triturated with pentane (x2) then purified via flash chromatography (CH_2Cl_2, R_f = 0.72) to yield 350 mg (80%) of **77** as a yellow solid. Crystals suitable for X-ray diffraction were grown by slow diffusion of pentane into a CH_2Cl_2 solution of **77**. ^{1}H-NMR (400 MHz, $CDCl_3$) δ 8.60 (d, J = 2.4 Hz, 1H), 8.52 (d, J = 5.6 Hz, 1H), 8.10-8.06 (m, 2H), 7.79-7.75 (m, 2H), 7.67 (dd, J = 8.0, 7.6 Hz, 2H), 7.60 (d, J = 8.4 Hz, 1H), 7.47 (d, J = 8.0 Hz, 4H), 7.14-7.11 (m, 1H) 3.07 (sept, J = 6.8 Hz 4H), 1.51 (d, J = 6.4 Hz, 12H), 0.91 (d, J = 6.8 Hz, 12H); ^{13}C-NMR (100 MHz, $CDCl_3$) δ 174.1 (+), 171.6 (+), 150.4 (–), 149.4 (–), 146.2 (+), 137.7 (–), 134.9 (+), 134.8 (–), 133.2 (+), 132.1 (+), 131.6 (+), 131.1 (–), 127.3 (–), 124.7 (–), 124.5 (–), 29.2 (–), 25.1 (–), 24.5 (–); HRMS (ESI) $[M\text{-}Cl]^+$ calcd. for $C_{40}H_{43}Cl_2N_3O_2Pd$ 772.1688; found 772.1682.

Preparation of IPent^{Cl}·HCl (66):

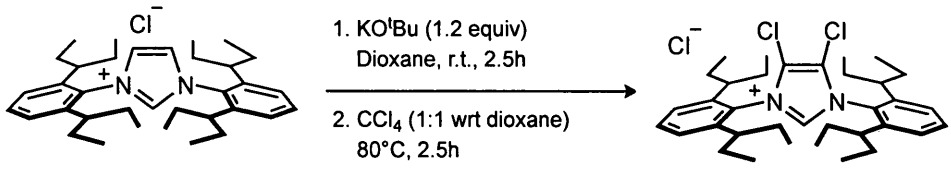

65. IPent·HCl

84%

66. IPent^{Cl}·HCl

In an unoptimized procedure, a 50 mL round-bottom flask equipped with magnetic stir bar and rubber septum was charged with KOtBu (95%, 283 mg, 2.4 mmol, 1.2 equiv.) in a glovebox. The flask was further charged with IPent·HCl (**65**, 1.07 g, 2.0 mmol, 1.0 equiv.) in air, then evacuated and backfilled with Ar (x3). Anhydrous 1,4-dioxane (10 mL) was added *via* syringe and the resulting light-beige suspension was stirred at rt for 2.5 h. At this time, the light-orange, nearly homogeneous solution was charged with anhydrous CCl_4 (10 mL) and the flask was sealed with vinyl tape then immersed in a pre-heated 80°C oil bath and allowed to stir at this temperature under a static Ar atmosphere. After 2.5 h, ^{1}H-NMR spectroscopic analysis (C_6D_6) of a 250 μL aliquot revealed the disappearance of the backbone protons, thus the mixture was cooled to rt and a 2.0 M solution of HCl in Et_2O (2.0 mL, 4 mmol, 2.0 equiv.) was added slowly to the brown solution over 2 min resulting in precipitation of a beige solid. After vigorous stirring for an additional 30 min, the mixture was diluted with ca. 15 mL CH_2Cl_2 and filtered through a pad of Celite washing with CH_2Cl_2 until the filtrate became colourless (ca. 30 mL). The orange filtrate was concentrated under reduced pressure and the resulting beige solid was triturated successively with pentane (30 mL x 3), 1:1 Et_2O/pentane (8 mL x 3), and Et_2O (4 mL x 3) then dried for 16 h under high vacuum to yield S5 (1.02 g, 84%) as an off-white solid. Mp: 230-232°C; ^{1}H-NMR (400 MHz, $CDCl_3$) δ 12.86 (s, 1H), 7.61 (t, J = 7.8 Hz, 2H), 7.31 (d, J = 7.8 Hz, 4H), 2.01 (quint, J = 6.6 Hz, 4H), 1.89-1.75 (m, 8H), 1.69 (quint, J = 7.2 Hz, 8H), 0.95-0.87 (m, 24H); ^{13}C-NMR (100 MHz, CDCl3) δ 143.1, 142.1, 131.9, 129.4, 125.8, 121.5, 43.1, 28.0, 27.0, 12.2, 11.5; HRMS (ESI) [M-Cl]+ calcd. for $C_{35}H_{51}Cl_3N_2$ 569.3429; found 569.3425.

Preparation of Pd-PEPPSI-IPent^{Cl} (78):

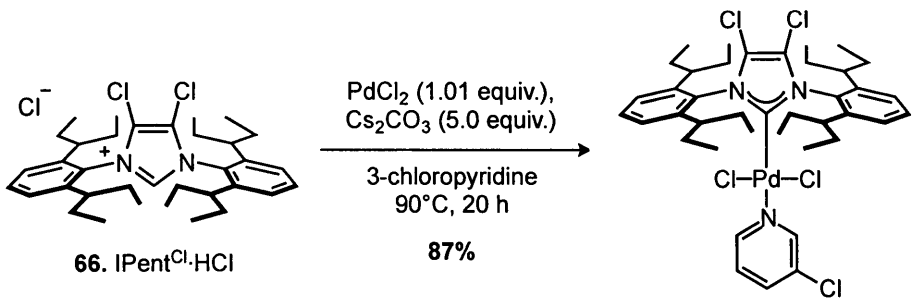

66. IPent^{Cl}·HCl

78. Pd-PEPPSI-IPent^{Cl}

In a glovebox, a 1-dram vial equipped with magnetic stir bar and Teflon-lined screwcap was charged with 489 mg Cs_2CO_3 (1.5 mmol, 5.0 equiv.) then removed from the glovebox after which 181.1 mg of **66** (0.3 mmol, 1.0 equiv.) and 53.7 mg of $PdCl_2$ (0.303 mmol, 1.01 equiv.) were added in air. The vial was evacuated and backfilled with Ar (x3) then charged with 3-chloropyridine (2.6 mL) *via* syringe. The vial was subsequently sealed with a rubber septum and vinyl tape then immersed in a pre-heated 90°C oil bath and allowed to stir at this temperature for 20 h at which time ^{1}H-NMR spectroscopic analysis ($CDCl_3$) of a 100 μL aliquot revealed complete consumption of **66**. The reaction was cooled to r.t. then filtered through a 1.5 cm pad of silica gel covered with a 1 cm pad of Celite in a 30 mL medium-porosity fritted glass funnel, washing with CH_2Cl_2 until the filtrate became colourless (ca. 50-75 mL). The filtrate was stripped of CH_2Cl_2 and excess 3-chloropyridine *in vacuo* (rotovap, bath T = 60°C) then dried under high vacuum for 2 h. The light-brown solid thus obtained was taken up in CH_2Cl_2 and filtered through a short pad of silica gel, eluting with CH_2Cl_2 until the filtrate became colourless. The filtrate was concentrated *in vacuo* and the resulting solid was triturated with pentane (3 mL x 3). Drying under high vacuum for 16 h furnished 223.5 mg (87%) of **78** as a light-yellow solid. Crystals suitable for X-ray diffraction were grown by slow diffusion of pentane into a concentrated EtOAc solution of **78**. Mp: decomposition above 275-280°C; ^{1}H-NMR (600 MHz, $CDCl_3$) δ 8.58 (d, J = 2.4 Hz, 1H), 8.49 (d, J = 5.4 Hz, 1H), 7.57 (d, J = 8.4 Hz, 1H), 7.53 (t, J = 7.5 Hz, 2H), 7.32 (d, J = 7.8 Hz, 4H), 7.09 (dd, J = 8.1, 5.7 Hz, 1H), 2.98-2.90 (m, 4H), 2.05-2.00 (m, 4H), 1.95-1.88 (m, 4H), 1.72-1.67 (m, 4H), 1.55-

1.50 (m, 4H), 1.15 (t, J = 7.2 Hz, 12H), 0.86 (t, J = 7.5 Hz, 12H); ^{13}C-NMR (75 MHz, $CDCl_3$) δ 155.9 (+), 150.6 (–), 149.52 (–), 145.3 (+), 137.5 (–), 133.5 (+), 132.0 (+), 129.8 (–), 126.4 (–), 124.4 (–), 121.1 (+), 40.9 (–), 27.6 (+), 26.8 (+), 12.6 (–), 11.0 (–); HRMS (ESI) $[M\text{-}Cl]^+$ calcd. for $C_{40}H_{54}N_3Cl_5Pd$ 822.2111; found: 822.2138; Elemental analysis calcd. for $C_{40}H_{54}Cl_5N_3Pd$: C 55.83, H 6.32, N 4.88; found C 55.80, H 6.12, N 4.51.

Attempted Preparation of IPr^F·HCl (42) using NHC-Boranes

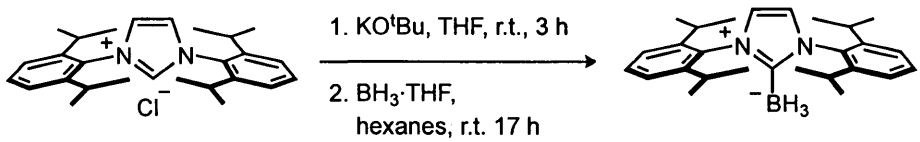

30. IPr·HCl

87%

55

In a glovebox, a 100 mL round-bottom flask equipped with stir bar was charged with 780 mg of KO^{t}Bu (6.6 mmol, 1.1 equiv.) then it was sealed with a rubber septum and moved outside the glovebox where 2.55 g of **30** (6.0 mmol, 1.0 equiv.) were added. The flask was evacuated and backfilled with Ar (x3) then charged with 36 mL THF, forming a light- yellow suspension. After vigorous stirring for 3 h, the suspension was carefully concentrated and then dried under high vacuum to yield an off-white solid to which 30 mL of hot anhydrous toluene were added followed by 20 mL anhydrous hexanes were. The turbid solution was filtered through a pad of oven-dried Celite under a cone of Ar into a dry 100 mL round-bottom flask, washing the filter cake with an additional 30 mL of anhydrous hexanes. The clear, light-yellow filtrate was concentrated and then dried under high vacuum to yield a flocculent, off-white solid (IPr free carbene). The flask was charged with a stir bar then evacuated and backfilled with Ar (x3) at which point 40 mL of anhydrous hexanes was added, ensuring that no solid particles remained stuck to the upper walls. To this suspension was added 6.0 mL of BH_3·THF (1.0 M in THF, 6 mmol, 1.0 equiv.) over 5 min. After stirring for 17 h, the colourless suspension was filtered and the collected solid washed with 20 mL of pentane. The filtrate was concentrated to one

third of its original volume and the solid that precipitated was collected and combined with the first batch. Drying under high vacuum furnished 2.10 g (87%) of **55** as a white solid in >98% purity as determined by ^{1}H-NMR spectroscopic analysis. ^{1}H-NMR (400 MHz, $CDCl_3$) δ 7.48 (t, J = 7.6 Hz, 2H), 7.31 (d, J = 8.0 Hz, 4H), 7.05 (s, 2H), 2.59 (sept, J = 6.8 Hz, 4H), 1.31 (d, J = 6.8 Hz, 12H), 1.20 (d, J = 7.2 Hz, 12H), 0.58 (broad q, J_{HB} = 81.0 Hz, 3H); ^{13}C-NMR (100 MHz, $CDCl_3$) δ 145.4, 134.3, 129.9, 123.9, 121.5, 28.7, 24.5, 23.0 [the ^{13}C resonance of the carbon attached to B was not detected]. The spectral data are consistent with those reported in the literature.[75]

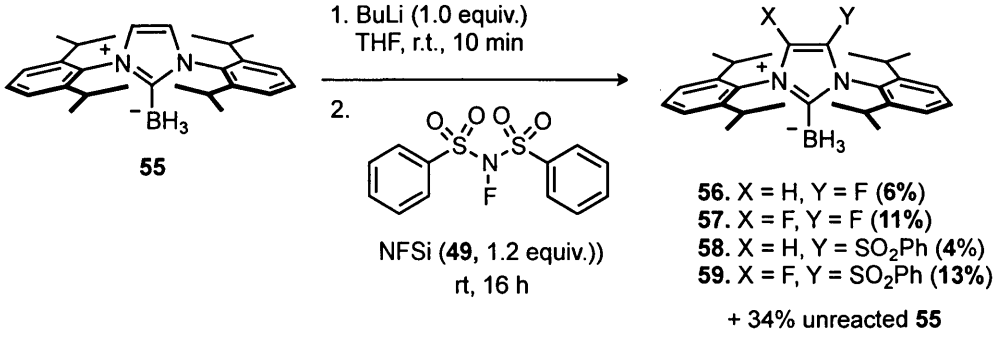

Representative procedure: A 10 mL round-bottom flask equipped with rubber septum and stir bar was charged with 80.5 mg of **55** (0.2 mmol, 1.0 equiv.) then evacuated and backfilled with Ar (x3). THF (2 mL) was then added and to the resulting colourless solution was added 81 μL of nBuLi (2.47 M in hexanes, 0.2 mmol, 1.0 equiv.) over 15 s. After stirring at rt for 10 min, a solution of 76 mg of **49** in 1 mL THF was added dropwise over 2 min, resulting in a colour change to orange. After stirring for 16 h, the orange homogenous solution was concentrated to yield 175 mg of a thick orange oil, which solidified on sonication with pentane. The crude product was adsorbed onto silica gel and purified via flash chromatography (SiO_2, gradient elution: 2.5%→15% EtOAc/hexanes) to yield 34 mg (34%) of unreacted **55** (R_f = 0.20, 10% EtOAc/hexanes) and compounds **56** – **59**. However, **58** could not be completely separated from **59** hence structural details were inferred from the ^{1}H-NMR spectrum of the mixture.

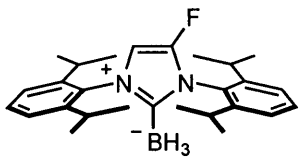

56

(1,3-bis(2,6-diisopropylphenyl)-5-fluoro-1*H*-imidazol-3-ium-2-yl) trihydroborate (56): 5.1 mg (6%) of compound **56** was isolated as a colourless film. R_f = 0.34 (10% EtOAc/hexanes); ^{1}H-NMR (300 MHz, $CDCl_3$) δ 7.53 (t, J = 7.8 Hz, 1H), 7.49 (t, J = 7.8 Hz, 1H), 7.34 (d, J = 7.8 Hz, 2H), 7.30 (d, J = 7.8 Hz, 2H), 6.70 (d, J_{CF} = 6.3 Hz, 1H), 2.69 – 2.56 (m, 4H), 1.33 (d, J = 6.7 Hz, 6H), 1.32 (d, J = 6.7 Hz, 6H), 1.23 (d, J = 6.8 Hz, 6H), 1.22 (d, J = 6.8 Hz, 6H), 0.55 (broad q, $J_{H\text{-}B}$ = 84.2 Hz, 3H); ^{13}C-NMR (75 MHz, $CDCl_3$) δ 147.8 (d, $^1J_{CF}$ = 261.9 Hz), 146.0, 145.3, 133.8, 130.7, 130.2, 128.7, 124.1, 124.0, 100.4 (d, $^2J_{CF}$ = 21.1 Hz), 29.1, 28.8, 24.5, 24.1, 23.0, 22.9 [the ^{13}C resonance of the carbon attached to B was not detected]; ^{19}F-NMR (376 MHz, $CDCl_3$) δ -148.2; ^{11}B-NMR (96 MHz, $CDCl_3$) δ -36.2 (q, J = 88.6 Hz); HRMS (EI) $[M]^+$ calcd. for $C_{27}H_{38}BFN_2$ 420.3112; found 420.3125.

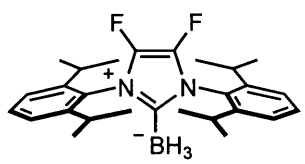

57

(1,3-bis(2,6-diisopropylphenyl)-4,5-difluoro-1*H*-imidazol-3-ium-2-yl)trihydroborate (57): 9.6 mg (11%) of compound **57** was isolated as a white solid. R_f = 0.38 (10% EtOAc/hexanes); ^{1}H-NMR (400 MHz, $CDCl_3$) δ 7.53 (t, J = 7.8 Hz, 2H), 7.34 (d, J = 7.6 Hz, 4H), 2.63 (sept, J = 6.4 Hz, 4H), 1.33 (d, J = 6.8 Hz, 12H), 1.24 (d, J = 6.8 Hz, 12H), 0.53 (broad q, J_{HB} = 88.0 Hz, 3H); ^{13}C-NMR (75 MHz, $CDCl_3$) δ 146.1 (+), 131.0 (–), 128.2 (+), 128.1 (+, dd, J_{CF} = 260.0 and 17.0 Hz), 124.2 (–), 29.2 (–), 24.1 (–), 22.9 (–) [the ^{13}C resonance of the carbon attached to B was not detected]; ^{19}F-NMR (376 MHz, $CDCl_3$) δ -160.5; ^{11}B-NMR (128 MHz, $CDCl_3$) δ -36.6 (q, J = 86.0 Hz); HRMS (ESI) $[M+H]^+$ calcd. for $C_{27}H_{38}BF_2N_2$ 439.3091; found 439.3097.

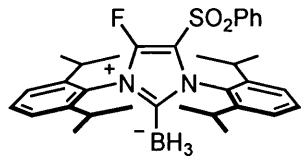

59

(1,3-bis(2,6-diisopropylphenyl)-4-fluoro-5-(phenylsulfonyl)-1*H*-imidazol-3-ium-2-yl)trihydroborate (59): 14.8 mg (13%) of compound **59** was isolated as a white solid. R_f = 0.09 (10% EtOAc/hexanes); ^{1}H-NMR (400 MHz, $CDCl_3$) δ 7.6 (t, J = 7.6 Hz, 1H), 7.61 (d, J = 8.0 Hz, 2H), 7.58 – 7.46 (m, 4H), 7.35 (d, J = 7.6 Hz, 2H), 7.26 (d,

J = 8.0 Hz, 2H), 2.48 (sept, J = 6.8 Hz, 2H), 2.36 (sept, J = 6.6 Hz, 2H), 1.33 (d, J = 6.8 Hz, 6H), 1.22 (d, J = 6.8 Hz, 6H), 1.19 (d, J = 7.2 Hz, 6H), 1.00 (d, J = 6.8 Hz, 6H), 0.54 (broad q, J_{HB} = 87.6 Hz, 3H); ^{13}C-NMR (75 MHz, $CDCl_3$) δ 148.2 (+, d, $^1J_{CF}$ = 278.5 Hz), 146.0 (+), 145.7 (+), 139.9 (+), 134.7 (–), 131.4 (–), 131.2 (+), 130.9 (–), 129.5 (–), 128.0 (–), 127.3 (+), 124.5 (–), 123.9 (–), 112.3 (+, d, $^2J_{CF}$ = 12.1 Hz), 29.6 (–), 29.3 (–), 24.5 (–), 24.3 (–), 22.7 (–), 22.5 (–); ^{19}F-NMR (376 MHz, $CDCl_3$) δ -127.3; ^{11}B-NMR (128 MHz, $CDCl_3$) δ -36.5 (q, J = 86.2 Hz); HRMS (ESI) $[M+Na]^+$ calcd. for $C_{33}H_{42}BFN_2O_2Na$ 583.2942; found 583.2961.

Attempted Preparation of IPr^{CN}·HBr (64):

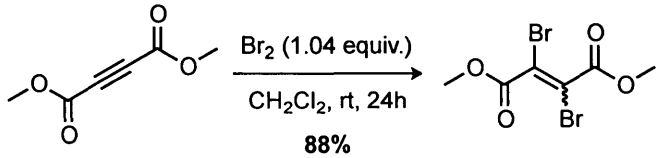

60 **61**

A solution of **60** (6.14 mL, 50 mmol) in 100 mL CH_2Cl_2 was charged with Br_2 (2.67 mL, 52 mmol, 1.04 equiv.) slowly over 2 min and the resulting dark red homogeneous solution was allowed to stir in the dark under a static Ar atmosphere. After 24 h, the reaction was quenched with 100 mL of saturated aqueous $Na_2S_2O_3$ and the organic layer removed. The aqueous layer was extracted with CH_2Cl_2 (x3) then the combined organic extracts were washed with brine, dried over anhydrous $MgSO_4$, filtered, and concentrated to yield a yellow oil. Filtration of this crude oil through a 13 cm x 4.5 cm column of silica gel eluting with 20% EtOAc/hexanes yielded 13.7 g (88%) of **61** as a light-yellow oil after solvent removal as a mixture of geometric isomers in a ratio of 1.6:1. Major isomer: ^{1}H-NMR (400 MHz, $CDCl_3$) δ 3.92 (s, 3H); ^{13}C-NMR (100 MHz, $CDCl_3$) δ 162.2, 112.7, 53.9. Minor isomer: ^{1}H-NMR (400 MHz, $CDCl_3$) δ 3.89 (s, 3H); ^{13}C-NMR (100 MHz, $CDCl_3$) δ 162.6, 125.0, 53.7. HRMS (EI) $[M]^+$ calcd. for $C_6H_6Br_2O_4$ 299.8633; found 299.8635.

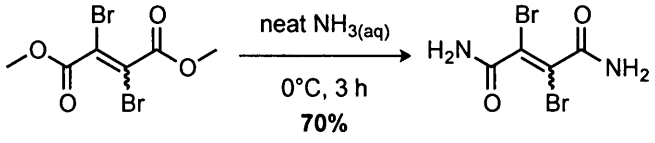

61 **62**

To 35 mL of a 15 M solution of aqueous NH_3 (525 mmol, 15 equiv.) cooled to 0°C in air was added 10.5 g of **61** (34.8 mmol, 1.0 equiv.) dropwise over 5 min, resulting in a yellow biphasic mixture. After 20 min, a light-yellow solid began to precipitate from solution, necessitating addition of an additional 5 mL of $NH_{3(aq)}$ to improve stirring. After 3 h, the heavy suspension was warmed to rt over 30 min then the solid was collected over a medium-porosity frit washing with H_2O until the filtrate became colourless. After drying under high vacuum over P_2O_5 for 4 h, the crude solid was triturated and washed with Et_2O (15 mL x3) then dried under high vacuum over P_2O_5 for 16 h yielding 6.61 g (70%) of bisamide **62** as a free-flowing white solid as a mixture of geometric isomers in a ratio of 1.5:1. Major isomer: ^{1}H-NMR (300 MHz, DMSO-d_6, 50°C) δ 7.72 (s, 4H); ^{13}C-NMR (75 MHz, DMSO-d_6, 23°C) δ 164.9, 111.6. Minor isomer: ^{1}H-NMR (300 MHz, DMSO-d_6, 50°C) δ 8.01 (s, 4H); ^{13}C-NMR (75 MHz, DMSO-d_6, 23°C) δ 164.3, 124.4; HRMS (EI) $[M]^+$ calcd. for $C_4H_4Br_2N_2O_2$ 269.8639; found 269.8651.

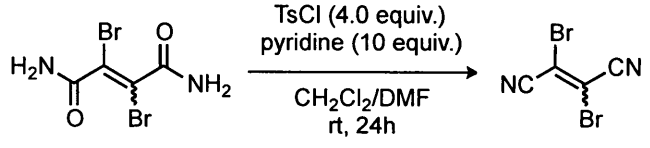

62 **63**

To a rt suspension of 1.0 g of **62** (3.68 mmol, 1.0 equiv.) and 2.8 g of TsCl (14.72 mmol, 4 equiv.) in 7.5 mL of CH_2Cl_2 and 7.5 mL of DMF was slowly added 3.0 mL of pyridine (36.8 mmol, 10 equiv.). The resulting dark brown solution was allowed to stir for 24 h at which point the reaction was diluted with 15 mL Et_2O and quenched with 10 mL of a 10% solution of $NH_{3(aq)}$ saturated with NH_4Cl. The biphasic mixture was stirred vigorously until all excess TsCl had been completely consumed (30 min). The dark red solution was transferred to a separatory funnel, washing with CH_2Cl_2, however no phase

cut was observed, necessitating filtration of the entire mixture through an 8.5 cm x 10 cm column of basic alumina gel, eluting with Et_2O (1.5 L) until the filtrate was clear of product by TLC analysis. The filtrate was concentrated to yield a dark purple oil which was washed with brine, dried over anhydrous Na_2SO_4, then filtered through a pad of silica gel with Et_2O and concentrated to yield a brown solid. Purification via flash chromatography (SiO_2, gradient elution: hexanes→2.5%→5% EtOAc/hexanes) afforded 221 mg (25%) of **63** as a light-yellow solid and single geometric isomer. ^{1}H-NMR (400 MHz, $CDCl_3$): no resonances observed; ^{13}C-NMR (100 MHz, $CDCl_3$) δ 112.9, 102.6; HRMS (EI) $[M]^+$ calcd. for $C_4Br_2N_2$ 233.8428; found: 233.8437.

5.3 – Preparation of (NHC)IrCl(CO)$_2$ Complexes for TEP Studies

General Procedure for the Synthesis of (NHC)IrCl(cod) complexes: In a glovebox, a 25 mL round-bottom flask equipped with a magnetic stir bar and rubber septum was charged with KO^{t}Bu (95%, 1.2 equiv.) then removed from the glovebox and the corresponding imidazolium salt (1.0 equiv.) was added in air. The flask was evacuated and backfilled with Ar (x3) after which THF (1 mL per 0.1 mmol imidazolium salt) was added. The resulting suspension was stirred at rt for 2-3 h at which time $[(cod)Ir(\mu\text{-}Cl)]_2$ (0.5 equiv.) was added in one shot under a cone of Ar. After stirring for 24 h, the suspension was filtered through a pad of silica gel, washing with CH_2Cl_2 until the filtrate became colourless. The filtrate was then concentrated and the residue thus obtained was purified via flash chromatography to yield the desired (NHC)IrCl(cod) complexes.

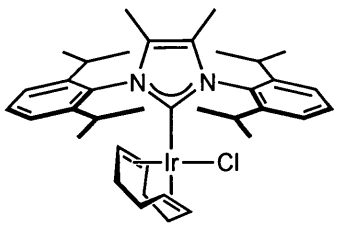

(IPr^{Me})IrCl(cod), 79: Following the general procedure on a 0.75 mmol scale, 242 mg (43%) of complex **79** were obtained after flash chromatography (CH_2Cl_2) as a yellow-orange solid. Mp: Decomposition above 255°C; R_f = 0.66 (CH_2Cl_2); The ^{1}H-NMR spectrum of **79** at rt contained broad signals due to rotamers resulting from restricted rotation of the N-2,6-diisopropylphenyl

bonds. Consequently, NMR spectra were acquired at 80°C to obtain acceptable resolution. ^{1}H-NMR (400 MHz, toluene-d_8, 80°C) δ 7.31 (t, J = 7.6 Hz, 2H), 7.22 (d, J = 7.6 Hz, 4H), 4.55-4.49 (m, 2H), 3.23-3.09 (m, 5H), 1.70-1.57 (m, 10H), 1.46 (d, J = 6.4 Hz, 12H), 1.36-1.24 (m, 5H), 1.04 (d, J = 6.8 Hz, 12 H); ^{13}C-NMR (100 MHz, toluene-d_8, 80°C) δ 183.9, 147.3, 134.5, 129.4, 127.2, 124.0, 81.6, 49.6, 33.5, 28.6, 28.2, 24.9, 24.5, 10.0. HRMS (EI) $[M]^+$ calcd. for $C_{37}H_{52}N_2ClIr$ 752.3447; found: 752.3472.

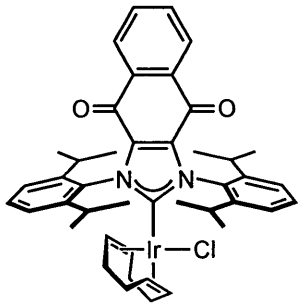

(IPr^{Quino})IrCl(cod), 80: Following the general procedure on a 0.675 mmol scale, 513 mg (82%) of complex **80** were obtained as a 1:1 adduct with CH_2Cl_2 following flash chromatography (75→90% CH_2Cl_2/pentane gradient) as a dark-burgundy solid. Mp: decomposition above 275°C; R_f = 0.69 (75% CH_2Cl_2/ pentane); ^{1}H-NMR (400 MHz, $CDCl_3$) δ 8.06-8.02 (m, 2H), 7.75-7.71 (m, 2H), 7.63 (t, J = 7.6 Hz, 2H), 7.52 (d, J = 8.0 Hz, 2H), 7.31 (d, J = 8.0 Hz, 2H), 4.46-4.41 (m, 2H), 3.65 (sept, J = 6.6 Hz, 2H), 3.06-3.03 (m, 2H), 2.38 (sept, J = 6.6 Hz, 2H), 1.71-1.66 (m, 2H), 1.53-1.41 (m, 10H), 1.32-1.25 (m, 8H), 1.11 (d, J = 6.8 Hz, 6H), 0.91 (d, J = 6.8 Hz, 6H); ^{13}C-NMR (100 MHz, $CDCl_3$) δ 198.1, 174.3, 147.6, 144.1, 135.0, 134.3, 134.0, 131.5, 130.3, 126.8, 125.4, 123.1, 86.5, 52.1, 33.3, 29.2, 29.1, 28.4, 25.2, 25.1, 25.0, 23.2; HRMS (EI) $[M]^+$ calcd. for $C_{43}H_{50}ClIrN_2O_2$ 854.3190; found: 854.3157.

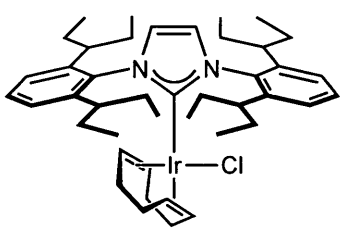

(IPent)IrCl(cod), 81: Following the general procedure on a 0.42 mmol scale, 179 mg (51%) of complex **81** were obtained after filtration through a plug of silica gel (60% CH_2Cl_2/pentane) as a yellow-orange solid. Mp: 169-171°C; ^{1}H-NMR (400 MHz, $CDCl_3$) δ 7.42 (t, J = 7.6 Hz, 2H), 7.21 (d, J = 7.6 Hz, 4H), 6.99 (s, 2H), 4.22-4.17 (m, 2H), 2.97-2.95 (m, 2H), 2.69 (br s, 4H), 2.20-1.77 (m, 10H), 1.67-1.49 (m, 10H), 1.40-1.33 (m, 2H), 1.20-1.14 (m, 2H), 1.06 (t, J = 7.0 Hz, 12 H), 0.76 (t, J = 7.4 Hz, 12H); ^{13}C-NMR (100 MHz, $CDCl_3$) δ 179.6, 144.4,

137.4, 128.5, 124.9, 124.4, 82.6, 51.3, 41.1, 33.2, 28.7, 28.1, 26.5, 12.5, 10.8. HRMS (EI) [M^+] calcd. for $C_{43}H_{64}ClIrN_2$ 836.4387; found 836.4362.

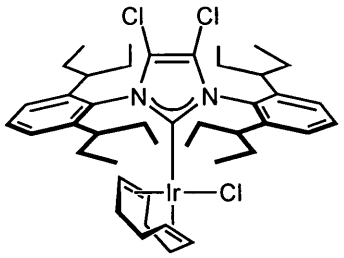

(IPent^{Cl})IrCl(cod), 82: In a deviation from the general procedure, a 25 mL round-bottom flask equipped with magnetic stir bar and rubber septum was charged with KO^{t}Bu (95%, 142 mg, 1.2 mmol) in a glovebox. The flask was further charged with *IPent* HCl (537 mg, 1.0 mmol) in air, then evacuated and backfilled with Ar (x3). Anhydrous 1,4-dioxane (6 mL) was added *via* syringe and the resulting suspension was stirred at rt for 3 h. At this time, anhydrous CCl_4 (5 mL) was added and the flask was sealed with vinyl tape then allowed to stir in a pre-heated 80°C oil bath under a static Ar atmosphere. After 2.5 h, ^{1}H-NMR spectroscopic analysis (C_6D_6) of a 200 μL aliquot revealed the disappearance of the backbone protons, thus the mixture was cooled to rt then filtered through a pad of oven-dried Celite into a 50 mL round-bottom flask, washing with dry THF until the filtrate became colourless (ca. 15 mL). The filtrate was concentrated and dried under high vacuum to yield a brown semi-solid, which was taken up in THF (10 mL) and stirred until homogeneous. Under a cone of Ar, [(cod)Ir(μ-Cl)]$_2$ (336 mg, 0.5 mmol) was added in one shot and the resulting homogeneous solution was stirred overnight at rt. After 23 h, the solvent was evaporated and the brown solid thus obtained was purified via flash chromatography (35→40% CH_2Cl_2/pentane gradient) to yield 644 mg (71%) of complex **82** as a bright-orange solid. Mp: decomposition over 220°C; R_f = 0.25 (35% CH_2Cl_2/pentane); ^{1}H-NMR (600 MHz, $CDCl_3$) δ 7.47 (t, J = 7.8 Hz, 2H), 7.25 (d, J = 7.8 Hz, 4H), 4.30-4.27 (m, 2H), 3.04-3.03 (m, 2H), 2.80 (br s, 4H), 1.87-1.76 (m, 10H), 1.70-1.62 (m, 6H), 1.57-1.50 (m, 4H), 1.42-1.38 (m, 2H), 1.24-1.19 (m, 2H), 1.07 (t, J = 7.2 Hz, 12H), 0.83 (t, J = 7.5 Hz, 12H); ^{13}C-NMR (100 MHz, $CDCl_3$) δ 181.6 (+), 145.0 (+), 134.4 (+), 129.2 (–), 126.1 (–), 120.2 (+), 84.2 (–), 52.1 (–), 41.0 (–), 33.2 (+), 28.7 (+), 26.7 (+), 26.2 (+), 12.2 (–), 10.8 (–); HRMS (EI) [M^+] calcd. for $C_{43}H_{62}Cl_3IrN_2$ 904.3608;

found 904.3622; Elemental analysis calcd. for $C_{43}H_{62}Cl_3IrN_2$: C 57.03 H 6.90 N 3.09; found C 56.52 H 6.33 N 3.28.

General Procedure for the Synthesis of (NHC)IrCl(CO)$_2$ complexes

A 25 mL round-bottom flask equipped with magnetic stir bar and rubber septum was charged with (NHC)IrCl(cod) complex then evacuated and backfilled with Ar (x3). THF (1 mL per 0.05 mmol complex) was then added *via* syringe and the flask was purged with $CO_{(g)}$ (1 atm, balloon) for 1 min. The resulting solution was allowed to stir at rt under an atmosphere of $CO_{(g)}$ for the indicated time, at which point the solvent was evaporated. The residue thus obtained was triturated with pentane then dried under high vacuum for 16 h to yield pure (NHC)IrCl(CO)$_2$ complexes. IR spectroscopic analyses were performed in freshly distilled CH_2Cl_2 at ~0.06 M concentration using an IR liquid cell, with the exception of **79** which was run at 0.03 M due to poor CH_2Cl_2 solubility. Spectra were acquired in duplicate.

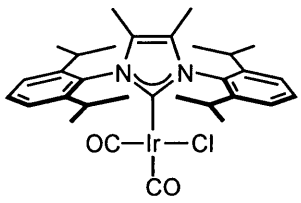

(IPr^{Me})IrCl(CO)$_2$, 83: Following the general procedure (t = 1 h) on a 0.265 mmol scale, 179 mg (96%) of **83** were obtained after trituration with pentane (3 mL x 3) as a pale-orange solid. Mp: decomposition above 265°C; ^{1}H-NMR (400 MHz, $CDCl_3$) δ 7.53 (t, J = 7.6 Hz, 2H), 7.35 (d, J = 7.6 Hz, 4H), 2.87 (sept, J = 6.7 Hz, 4H), 1.95 (s, 6H), 1.40 (d, J = 6.8 Hz, 12H), 1.14 (d, J = 6.8 Hz, 12H); ^{13}C-NMR (100 MHz, $CDCl_3$) δ 179.7, 175.5, 169.1, 146.4, 133.1, 130.4, 128.5, 124.6, 28.5, 25.1, 24.4, 10.6; IR ν_{CO} (CH_2Cl_2, cm^{-1}): 2064.5, 1978.2; HRMS (EI) [M$^+$] calcd. for $C_{31}H_{40}ClIrN_2O_2$ 700.2408; found 700.2387.

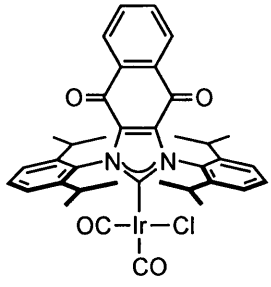

(IPr^{Quino})IrCl(CO)$_2$, 84: Following the general procedure (t = 3 h) on a 0.265 mmol scale, 177 mg (83%) of **84** were obtained after trituration with pentane (5 mL x 4) as a bright-yellow solid. Mp: decomposition above 215°C; ^{1}H-NMR (400 MHz, $CDCl_3$) δ 8.11-8.08 (m, 2H), 7.81-7.78 (m, 2H), 7.67 (t, J = 7.6 Hz, 2H), 7.44 (d, J = 7.6 Hz, 4H), 2.84 (sept, J = 6.6 Hz, 4H), 1.44 (d, J = 6.8 Hz, 12H), 1.03 (d, J = 6.8 Hz, 12H); ^{13}C-NMR (100 MHz, $CDCl_3$) δ 189.6, 178.7, 174.3, 168.2, 145.2, 134.9, 134.5, 132.9, 131.7, 131.2, 127.3, 124.6, 29.3, 25.1, 23.7; IR ν_{CO} (CH_2Cl_2, cm^{-1}): 2073.7, 1987.3; HR-MS (EI) [M$^+$] calcd. for $C_{37}H_{38}ClIrN_2O_4$ 802.2150; found 802.2163.

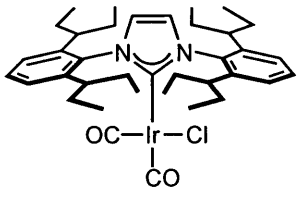

(IPent)IrCl(CO)$_2$, 85: Following the general procedure (t = 0.5 h) on a 0.179 mmol scale, 113 mg (80%) of **85** were obtained after trituration with pentane (1 mL x 3) as a pale-yellow solid. Mp: 164-166°C; ^{1}H-NMR (400 MHz, $CDCl_3$) δ 7.47 (t, J = 7.8 Hz, 2H), 7.27 (d, J = 8.0 Hz, 4H), 7.16 (s, 2H), 2.50-2.44 (m, 4H), 2.12-2.02 (m, 4H), 1.84-1.73 (m, 4H), 1.70-1.60 (m, 4H), 1.57-1.48 (m, 4H), 1.03 (t, J = 7.4 Hz, 12H), 0.78 (t, J = 7.4 Hz, 12H); ^{13}C-NMR (100 MHz, $CDCl_3$) δ 179.3 (+), 177.2 (+), 168.1 (+), 144.1 (+), 136.2 (+), 129.4 (–), 125.2 (–), 124.8 (–), 41.9 (–), 28.3 (+), 27.2 (+), 12.7 (–), 11.3 (–); IR ν_{CO} (CH_2Cl_2, cm^{-1}): 2064.7, 1978.6; HRMS (EI) [M$^+$] calcd. for $C_{37}H_{52}ClIrN_2O_2$ 784.3347; found 784.3366.

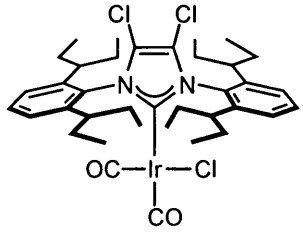

(IPent^{Cl})IrCl(CO)$_2$, 86: Following the general procedure (t = 1 h) on a 0.276 mmol scale, 146 mg (62%) of **86** were obtained after trituration with pentane (1 mL x 1 at -15°C due to high pentane solubility) as a pale-yellow solid. Mp: 175-177°C; ^{1}H-NMR (400 MHz, $CDCl_3$) δ 7.51 (t, J = 7.8 Hz, 2H), 7.27 (d, J = 8.0 Hz, 4H), 2.58-2.52 (m, 4H), 2.03-1.93 (m, 4H), 1.87-1.76 (m, 4H), 1.69-1.60 (m, 8H), 1.02 (t, J = 7.4 Hz, 12H), 0.84 (t, J = 7.6 Hz, 12H); ^{13}C-NMR (100 MHz, $CDCl_3$) δ

178.0 (+), 177.1 (+), 167.7 (+), 144.4 (+), 133.5 (+), 130.0 (–), 126.3 (–), 120.9 (+), 41.7 (–), 27.1 (+), 26.3 (+), 12.0 (–), 11.2 (–); IR ν_{CO} (CH_2Cl_2, cm^{-1}): 2069.3, 1982.2; HRMS (EI) [M^+] calcd. for $C_{37}H_{50}Cl_3IrN_2O_2$ 852.2567; found 852.2581; Elemental analysis calcd. for $C_{37}H_{50}Cl_3IrN_2O_2$: C 52.07 H 5.91 N 3.28; found C 51.62 H 5.37 N 3.34.

5.4 – Compound Characterization Data for Secondary Alkyl Negishi Couplings

Preparation of Secondary Alkylzinc Halides[94]

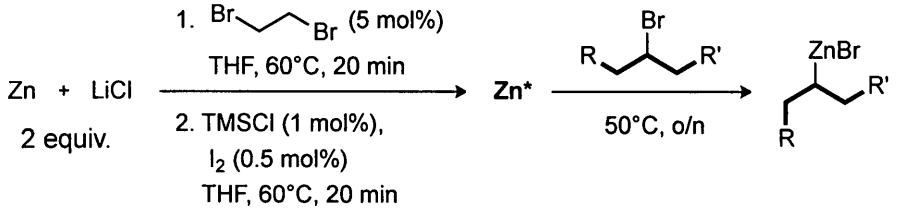

In a glovebox, a 50 mL round-bottom flask equipped with a magnetic stir bar was charged with LiCl (2.12 g, 50 mmol) and zinc dust (3.27 g, 50 mmol) then sealed with a rubber septum and moved outside the glovebox. Under high vacuum, the flask was heated with a heat gun for 15 min with occasional stirring then cooled to rt and carefully backfilled with Ar. After repeating this process once more, THF (24 mL) and 1,2-dibromoethane (108 μL, 1.25 mmol) were added via syringe and the reaction mixture was heated at 60 °C for 20 min. After cooling to rt, TMSCl (32 μL, 0.25 mmol) and a solution of iodine (32 mg, 0.125 mmol) in THF (1 mL) were added via syringe. The reaction mixture was heated at 60 °C for 20 min and then cooled to rt. The corresponding alkyl halide (25 mmol) was added dropwise over 5 min after which the flask was sealed with vinyl tape and allowed to stir at 50 °C for 20 – 24 h at which time it was cooled to rt and allowed to stand for 24 h. The concentration of the organozinc solution was determined by iodometric titration of the resulting supernatant using Knochel's procedure.[116] The solutions thus prepared are shown below with their measured titer.

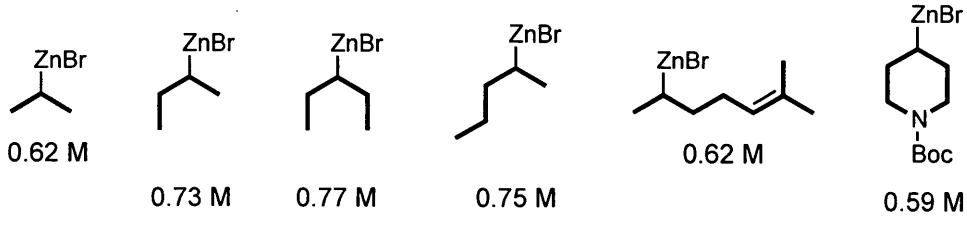

General Procedure for the Secondary Alkyl Negishi Coupling: An oven-dried 15x45 mm (1 dram) vial, equipped with stir bar and Teflon-lined screw cap was charged with 4.3 mg of Pd-PEPPSI-IPent^{Cl} (**79**, 0.005 mmol, 1 mol%) and, if solid, the aryl halide or pseudo-halide (0.5 mmol, 1.0 equiv.) after which it was evacuated and backfilled with Ar (x3). If liquid, the aryl halide or pseudo-halide was added via microliter syringe after the evacuation/backfilling process. Toluene (enough to bring the final reaction volume to 2 mL) was added and the resulting mixture was cooled to 0°C in an ice bath for 5 min. A THF solution of secondary alkylzinc bromide (0.6 mmol, 1.2 equiv.) was then added dropwise *via* syringe over 2 min. The vial was removed from the ice bath, capped with a 14/20 rubber septum, and allowed to stir at ambient temperature under a static Ar atmosphere for the indicated time, monitoring for completion by TLC. Once completed, the reaction was quenched by the addition of aqueous 1 M HCl (0.6 mL, 1.2 equiv.) and the resulting biphasic mixture stirred vigorously until a satisfactory phase cut was achieved (2 min). The organic layer was removed and the aqueous layer extracted with EtOAc (x3). The combined organic extracts were washed with brine (x1), dried over anhydrous Na_2SO_4, filtered through a short plug of Celite, and concentrated *in vacuo*. The residue thus obtained was purified via flash chromatography to yield pure cross-coupled product. Where applicable, the ratio of desired product to isomeric product was readily determined by ^{1}H-NMR spectroscopy after chromatography. In those cases where identification of isomeric products was ambiguous, all additional isomers were synthesized independently and their NMR spectra cross-referenced (see Figure 22).

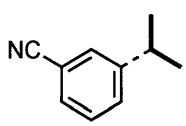

3-Isopropylbenzonitrile (**89**, Table 5, Entry 6): Following the general procedure (t = 0.5 h), 61 mg (84%) of **89** were isolated by flash chromatography (2.5→5% EtOAc/hexanes) as a clear, colourless oil. R_f = 0.41 (5% EtOAc/hexanes); ^{1}H-NMR (300 MHz, $CDCl_3$) δ 7.52 (s, 1H), 7.49-7.46 (m, 2H), 7.42-7.37 (m, 1H), 2.95 (sept, J = 6.9 Hz, 1H), 1.27 (d, J = 6.9 Hz, 6H); ^{13}C-NMR (75 MHz, $CDCl_3$) δ 145.0 (+), 131.1 (–), 130.0 (–), 129.5 (–), 129.0 (–), 119.1 (+), 112.2 (+), 33.8 (–), 23.5 (–). The spectral data of the major isomer are in accordance with those

reported in the literature.[93] The ratio of the branched to linear cross-coupled products was determined to be 61:1.

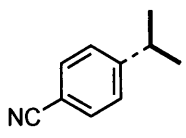

4-Isopropylbenzonitrile (**91**, Table 6, Entry 1): Following the general procedure (t = 0.5 h), 67 mg (92%) of **91** were isolated by flash chromatography (3→5% EtOAc/hexanes) as a light-yellow oil. R_f = 0.29 (5% EtOAc/hexanes); ^{1}H-NMR (300 MHz, $CDCl_3$) δ 7.59 (d, J = 8.4 Hz, 2H), 7.34 (d, J = 8.1 Hz, 2H), 2.98 (sept, J = 6.9 Hz, 1H), 1.27 (d, J = 6.9 Hz, 6H); ^{13}C-NMR (75 MHz, $CDCl_3$) δ 154.3, 132.2, 127.2, 119.1, 109.5, 34.32, 23.5. The spectral data of the major isomer are in accordance with those reported in the literature.[117] The ratio of the branched to linear cross-coupled products was determined to be 59:1.

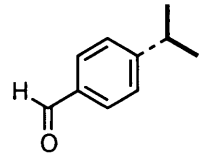

4-Isopropylbenzaldehyde (**92**, Table 6, Entry 2): Following the general procedure (t = 0.5 h), 68 mg (92%) of **92** were isolated by flash chromatography (5% EtOAc/hexanes) as a yellow oil. R_f = 0.26 (5% EtOAc/hexanes); ^{1}H-NMR (300 MHz, $CDCl_3$) δ 9.98 (s, 1 H), 7.83 (d, J = 8.1 Hz, 2H), 7.40 (d, J = 8.1 Hz, 2H), 3.00 (sept, J = 6.9 Hz, 1H), 1.29 (d, J = 6.9 Hz, 6H); ^{13}C-NMR (75 MHz, $CDCl_3$) δ 192.0, 156.2, 134.5, 130.0, 127.1, 34.4, 23.6. The spectral data of the major isomer are in accordance with those reported in the literature.[117] The ratio of branched to linear cross-coupled product was determined to be 59:1.

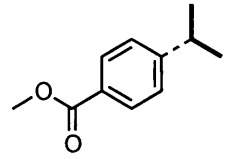

Methyl 4-isopropylbenzoate (**93**, Table 6, Entry 3): Following the general procedure (t = 0.5 h), 84 mg (94%) of **93** were isolated by flash chromatography (2.5→5% EtOAc/hexanes) as a light-yellow oil. R_f = 0.29 (5% EtOAc/hexanes); ^{1}H-NMR (400 MHz, $CDCl_3$) δ 7.99 (d, J = 8.0 Hz, 2H), 7.31 (d, J = 8.0 Hz, 2H), 3.92 (s, 3H), 2.98 (sept, J = 6.8 Hz, 1H), 1.28 (d, J = 7.2 Hz, 6H); ^{13}C-NMR (100 MHz, $CDCl_3$) δ 167.1, 154.2, 129.7, 127.7, 126.4, 51.9, 34.2, 23.6. The spectral data of the major isomer are in accordance with those reported in the

literature.[92] The ratio of branched to linear cross-coupled product was determined to be 56:1.

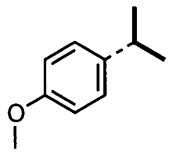

1-Isopropyl-4-methoxybenzene (**94**, Table 6, Entry 4): Following the general procedure (t = 0.5 h), 60 mg (79%) of **94** were isolated by flash chromatography (2→4% EtOAc/hexanes) as a clear, colourless oil. R_f = 0.34 (5% EtOAc/hexanes); ^{1}H-NMR (400 MHz, $CDCl_3$) δ 7.22 (d, J = 8.8 Hz, 2H), 6.91 (d, J = 8.8 Hz), 3.85 (s, 3H), 2.93 (sept, J = 6.9 Hz, 1H), 1.30 (d, J = 6.8 Hz, 6H); ^{13}C-NMR (100 MHz, $CDCl_3$) δ 157.6, 141.0, 127.2, 113.6, 55.2, 33.2, 24.2. The spectral data of the major isomer are in accordance with those reported in the literature.[117] The ratio of branched to linear cross-coupled product was determined to be 46:1.

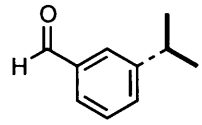

3-Isopropylbenzaldehyde (**95**, Table 6, Entry 5): Following the general procedure (t = 0.5 h), 62 mg (84%) of **95** were isolated by flash chromatography (5% EtOAc/hexanes) as a light-yellow oil. R_f = 0.25 (5% EtOAc/hexanes); ^{1}H-NMR (400 MHz, $CDCl_3$) δ 10.02 (s, 1H), 7.78 (s, 1H), 7.71 (d, J = 7.2 Hz, 1H), 7.52 (d, J = 7.2 Hz, 1H), 7.47 (t, J = 7.4 Hz, 1H), 3.01 (sept, J = 6.8 Hz, 1 H), 1.31 (d, J = 6.8 Hz, 6H); ^{13}C-NMR (100 MHz, $CDCl_3$) δ 192.6, 149.8, 136.5, 132.9, 128.9, 127.7, 127.2, 33.9, 23.8. The spectral data of the major isomer are in accordance with those reported in the literature.[117] The ratio of the branched to linear cross-coupled products was determined to be 48:1.

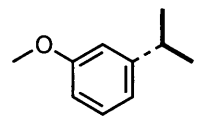

1-Isopropyl-3-methoxybenzene (**96**, Table 6, Entry 6): Following the general procedure (t = 0.5 h), 50 mg (66%) of **96** were isolated by flash chromatography (2% EtOAc/hexanes) as a clear, colourless oil. R_f = 0.23 (5% EtOAc/hexanes); ^{1}H-NMR (300 MHz, $CDCl_3$) δ 7.27 (t, J = 7.8 Hz, 1H), 6.89 (app d, J = 7.5 Hz, 1H), 6.85-6.84 (m, 1H), 6.78 (dd, J = 8.0, 2.0 Hz, 1H), 3.86 (s, 3H), 2.94 (sept, J = 6.9 Hz, 1H), 1.31 (d, J = 6.9 Hz, 6H); ^{13}C-NMR (75 MHz, $CDCl_3$) δ 159.6, 150.6, 129.2, 118.9, 112.5, 110.7, 55.1, 34.2, 23.9. The spectral data of the major

isomer are in accordance with those reported in the literature.[118] The ratio of the branched to linear cross-coupled products was determined to be 39:1.

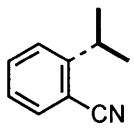

2-Isopropylbenzonitrile (**97**, Table 6, Entry 7): Following the general procedure (t = 0.5 h), 55 mg (76%) of **97** were isolated by flash chromatography (5% EtOAc/hexanes) as a light-yellow oil. R_f = 0.27 (5% EtOAc/hexanes); ^{1}H-NMR (300 MHz, $CDCl_3$) δ 7.62 – 7.53 (m, 2H), 7.41 (d, J = 7.8 Hz, 1H), 7.28 (dt, J = 7.6, 1.1 Hz, 1H), 3.40 (sept, J = 6.9 Hz, 1H), 1.33 (d, J = 6.9 Hz, 6H); ^{13}C-NMR (75 MHz, $CDCl_3$) δ 152.4, 132.9, 132.8, 126.3, 125.9, 118.1, 111.6, 32.4, 23.2. The spectral data of the major isomer are in accordance with those reported in the literature.[117] The ratio of the branched to linear cross-coupled products was determined to be 28:1.

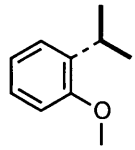

1-Isopropyl-2-methoxybenzene (**98**, Table 6, Entry 8): Following the general procedure (t = 0.5 h), 40 mg (54%) of **98** were isolated by flash chromatography (2% EtOAc/hexanes) as a clear, colourless oil. R_f = 0.26 (5% EtOAc/hexanes); ^{1}H-NMR (300 MHz, $CDCl_3$) δ 7.27 (dd, J = 7.7, 1.4 Hz, 1H), 7.22 (dt, J = 7.9, 1.7 Hz, 1H), 6.98 (dt, J = 0.8, 7.4 Hz, 1H), 6.90 (app d, J = 7.8 Hz, 1H), 3.88 (s, 3H), 3.39 (sept, J = 6.9 Hz, 1H), 1.66 (d, J = 6.9 Hz, 6H); ^{13}C-NMR (75 MHz, $CDCl_3$) δ 156.8, 137.0, 126.5, 126.0, 120.5, 110.3, 55.3, 26.7, 22.7. The spectral data of the major isomer are in accordance with those reported in the literature.[117] The ratio of the branched to linear cross-coupled products was determined to be 23:1.

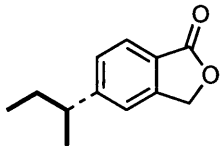

5-sec-Butylisobenzofuran-1(3H)-one (**99**): Following the general procedure (t = 0.5 h), 94 mg (99%) of **99** were isolated by flash chromatography (10% EtOAc/hexanes) as a yellow oil. R_f = 0.2 (10% EtOAc/hexanes); ^{1}H-NMR (600 MHz, $CDCl_3$) δ 7.82 (d, J = 7.8 Hz, 1H), 7.34 (d, J = 7.8 Hz, 1H), 7.30 (s, 1H), 5.30 (s, 2H), 2.76-2.71 (m, 1H), 1.67-1.61 (m, 2H), 1.27 (d, J = 6.6 Hz, 3H), 0.83 (t, J = 7.2 Hz, 3H); ^{13}C-NMR (150 MHz, $CDCl_3$) δ 171.1, 155.1, 147.1,

128.4, 125.5, 123.6, 120.4, 69.5, 42.2, 31.0, 21.9, 12.1; HRMS (EI) [M^+] calcd. for $C_{12}H_{14}O_2$ 190.0994; found 190.0997. No isomeric products were detected by ^{1}H-NMR spectroscopy.

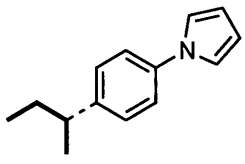

1-(4-sec-Butylphenyl)-1H-pyrrole (100): Following the general procedure (t = 0.5 h), 99 mg (99%) of **100** were isolated by flash chromatography (5% EtOAc/hexanes) as yellow oil. R_f = 0.3 (5% EtOAc/hexanes); ^{1}H-NMR (600 MHz, $CDCl_3$) δ 7.40 (d, J = 9.6 Hz, 2H), 7.30 (d, J = 8.4 Hz, 2H), 7.15 (d, J = 2.4 Hz, 2H), 6.43 (t, J = 1.8 Hz, 2H), 2.73-2.70 (m, 1H), 1.71-1.69 (m, 2H), 1.35 (d, J = 7.2 Hz, 3H), 0.94 (m, 3H); ^{13}C-NMR (150 MHz, $CDCl_3$) δ 145.2, 138.8, 128.1, 120.6, 119.4, 110.1, 41.2, 31.3, 21.9, 12.3; HRMS (EI) [M^+] calcd. for $C_{14}H_{17}N$ 199.1361; found 199.1366. No isomeric products were detected by ^{1}H-NMR spectroscopy.

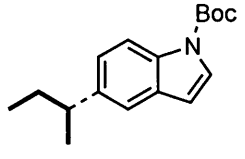

tert-Butyl 5-sec-butyl-1H-indole-1-carboxylate (101): Following the general procedure (t = 0.5 h), 136 mg (99%) of **101** were isolated by flash chromatography (5% EtOAc/hexanes) as a yellow oil. R_f = 0.2 (5% EtOAc/hexanes); ^{1}H-NMR (600 MHz, $CDCl_3$) δ 8.07 (br s, 1H), 7.60 (s, 1H), 7.39 (s, 1H), 7.19 (dd, J = 7.8, 0.6 Hz, 1H) 6.56 (d, J = 3.0 Hz, 1H), 2.74-2.70 (m, 1H), 1.70 (s, 9H), 1.69-1.66 (m, 2H), 1.32 (d, J = 6.6 Hz, 3H), 0.86 (m, 3H); ^{13}C-NMR (150 MHz, $CDCl_3$) δ 149.9, 142.1, 133.6, 130.7, 125.9, 123.6, 118.9, 114.9, 107.2, 83.4, 41.6, 31.5, 28.2, 22.4, 12.3; HRMS (EI) [M^+] calcd. for $C_{17}H_{23}NO_2$ 273.1729; found 273.1719. No isomeric products were detected by ^{1}H-NMR spectroscopy.

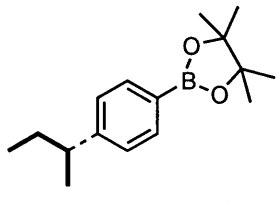

2-(4-sec-butylphenyl)-4,4,5,5,-tetramethyl-1,3,2-dioxaborolane (102): Following the general procedure (t = 0.5 h), 129 mg (99%) of **102** were isolated by flash chromatography (5% EtOAc/hexanes) as a yellow solid. Mp: 90-92°C; R_f = 0.3 (5% EtOAc/hexanes); ^{1}H-NMR (400 MHz, $CDCl_3$) δ 7.76 (d, J = 7.6 Hz, 2H), 7.25 (d, J = 7.6

Hz, 2H), 2.63-2.61 (m, 1H), 1.62 (m, 2H), 1.36 (s, 12H), 1.25 (d, J = 7.2 Hz, 3H), 0.83 (t, J = 7.4 Hz, 3H). ^{13}C-NMR (75 MHz, $CDCl_3$) δ 151.12, 134.8, 126.5, 83.5, 41.9, 30.9, 24.8, 21.7, 12.2. The carbon adjacent to boron was not detected. Spectral data were in accordance with those reported in the literature.[15] No isomeric products were detected by ^{1}H-NMR spectroscopy.

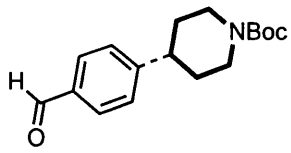

***tert*-Butyl 4-(4-formylphenyl)piperidine-1-carboxylate (103)**: Following the general procedure with the exception that the reaction was quenched with saturated $NH_4Cl_{(aq)}$ solution instead of 1 M HCl (t = 0.75 h), 141 mg (98%) of **103** were isolated after flash chromatography (10→20% EtOAc/hexanes) as a pale-yellow viscous oil that solidified on standing. Mp: 58-60°C; R_f = 0.26 (20% EtOAc/hexanes); ^{1}H-NMR (400 MHz, $CDCl_3$) δ 9.98 (s, 1H), 7.84 (d, J = 8.0 Hz, 2H), 7.38 (d, J = 7.6 Hz, 2H), 4.28 (br s, 2H), 2.82-2.72 (m, 3H), 1.85 (br d, J = 12.3 Hz, 2H), 1.65 (qd, J = 12.3, 3.8 Hz, 2H), 1.49 (s, 9H); ^{13}C-NMR (100 MHz, $CDCl_3$) δ 191.9 (–), 154.8 (+), 152.9 (+), 134.9 (+), 130.1 (–), 127.5 (–), 79.6 (+), 44.4 (broad, +), 43.0 (–), 32.8 (+), 28.5 (–). The spectral data are in accordance with those reported in the literature.[119] No isomeric products were detected by ^{1}H-NMR spectroscopy.

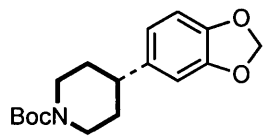

***tert*-Butyl 4-(benzo[*d*][1,3]dioxol-5-yl)piperidine-1-carboxylate (104)**: Following the general procedure with the exception that the reaction was quenched with saturated $NH_4Cl_{(aq)}$ solution instead of 1 M HCl (t = 5 h), 147 mg (96%) of **104** were isolated by flash chromatography (5→10% Et_2O/pentane) as a light-yellow, viscous oil. R_f = 0.07 (5% Et_2O/pentane); ^{1}H-NMR (400 MHz, $CDCl_3$) δ 6.76 (d, J = 8.0 Hz, 1H), 6.72-6.70 (m, 1H), 6.67-6.65 (m, 1H), 5.93 (s, 2H), 4.24 (br s, 2H), 2.78 (br t, J = 11.5 Hz, 2H), 2.58 (tt, 12.2, 3.4 Hz, 1H), 1.79 (br d, J = 12.2 Hz, 2H), 1.65-1.49 (m, 11H); ^{13}C-NMR (100 MHz, $CDCl_3$) δ 154.8, 147.6, 145.8, 139.9, 119.5, 108.2, 107.2, 100.8, 79.4, 44.4 (broad), 42.4, 33.4, 28.4; HRMS (EI) [M^+]

calcd. for $C_{17}H_{23}NO_4$ 305.1617; found 305.1627. No isomeric products were detected by ^{1}H-NMR spectroscopy.

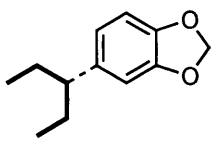

5-(Pentan-3-yl)benzo[*d*][1,3]dioxole (105): Following the general procedure (t = 5 h), 81 mg (85%) of **105** were isolated by flash chromatography (pentane) as a clear, colourless oil. R_f = 0.21 (pentane); ^{1}H-NMR (400 MHz, $CDCl_3$) δ 6.76 (d, J = 7.6 Hz, 1H), 6.67 (d, J = 1.2 Hz, 1H), 6.61 (dd, J = 8.2, 1.5 Hz, 1H), 5.95 (s, 2H), 2.29-2.23 (m, 1H), 1.73-1.63 (m, 2H), 1.56-1.45 (m, 2H), 0.80 (t, J = 7.3 Hz, 6H); ^{13}C-NMR (100 MHz, $CDCl_3$) δ 147.6 (+), 145.5 (+), 139.8 (+), 120.9 (–), 107.8 (–), 107.6 (–), 100.7 (+), 49.5 (–), 29.5 (+), 12.2 (–); HRMS (EI) [M^+] calcd. for $C_{12}H_{16}O_2$ 192.1144; found 192.1150. The ratio of desired to isomeric (2-pentyl) product was determined to be 31:1.

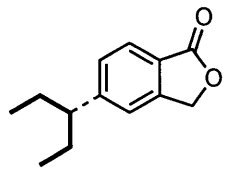

5-(Pentan-3-yl)isobenzofuran-1(3*H*)-one (106): Following the general procedure (t = 0.5 h), 96 mg (94%) of **106** were isolated by flash chromatography (5→15% EtOAc/hexanes) as a light-yellow oil. R_f = 0.17 (10% EtOAc/hexanes); ^{1}H-NMR (400 MHz, $CDCl_3$) δ 7.83 (d, J = 8.0 Hz, 1H), 7.32 (d, J = 7.9 Hz, 1H), 7.26 (s, 1H), 5.30 (s, 2H), 2.52-2.45 (m, 1H), 1.81-1.71 (m, 2H), 1.64-1.53 (m, 2H), 0.78 (t, J = 7.4 Hz, 6H); ^{13}C-NMR (100 MHz, $CDCl_3$) δ 171.2 (+), 153.5 (+), 147.0 (+), 129.0 (–), 125.5 (–), 123.7 (+), 121.2 (–), 69.6 (+), 50.2 (–), 29.2 (+), 12.1 (–); HRMS (EI) [M^+] calcd. for $C_{13}H_{16}O_2$ 204.1150; found 204.1142. The ratio of desired to isomeric (2-pentyl) product was determined to be 35:1.

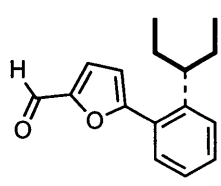

5-(2-(Pentan-3-yl)phenyl)furan-2-carbaldehyde (107): Following the general procedure (t = 16 h), 83 mg (68%) of **107** were isolated by flash chromatography (10% EtOAc/hexanes) as a yellow oil. R_f = 0.4 (10% EtOAc/hexanes); ^{1}H-NMR (600 MHz, $CDCl_3$) δ 9.70 (s, 1H), 7.55-7.27 (m, 5H), 6.63 (d, J = 3.6 Hz, 1H), 2.92-2.89 (m, 1H), 1.74-1.60 (m, 4H), 0.80-

0.77 (m, 6H); ^{13}C-NMR (150 MHz, $CDCl_3$) δ 177.5, 160.3, 152.3, 145.0, 130.0, 129.9, 129.6, 126.7, 125.8, 122.0, 111.5, 44.0, 29.3, 12.0; HRMS (EI) [M^+] calcd. for $C_{16}H_{18}O_2$ 242.1307; found 242.1298. The ratio of the desired to isomeric (2-pentyl) product was determined to be 17:1.

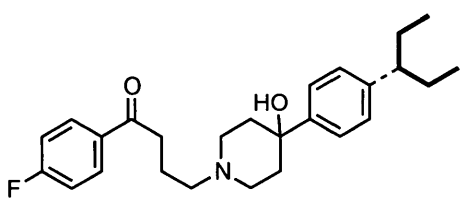

1-(4-Fluorophenyl)-4-(4-hydroxy-4-(4-(pentan-3-yl)phenyl)piperidin-1-yl)butan-1-one (108): Following the general procedure using 2.2 equiv. 3-pentylzinc bromide (t = 16 h), 181 mg (88%) of **108** were isolated by flash chromatography (0.5% $MeOH/CH_2Cl_2$) as a white solid. Mp: 242-244°C; R_f = 0.3 (0.5% $MeOH/CH_2Cl_2$); ^{1}H-NMR (600 MHz, $CDCl_3$) δ 11.59 (br s, 1H), 7.98-7.96 (m, 2H), 7.43 (d, J = 8.4 Hz, 2H), 7.13-7.09 (m, 2H), 7.06 (d, J = 8.4 Hz, 2H), 3.48-3.41 (m, 4H), 3.18 (t, J = 6.6 Hz, 2H), 3.09 (t, J = 7.2 Hz, 2H), 2.80-2.77 (m, 2H), 2.31-2.24 (m, 3H), 2.00-1.98 (m, 2H), 1.65-1.47 (m, 4H), 0.70 (m, 6H); ^{13}C-NMR (150 MHz, $CDCl_3$) δ 196.6, 165.6 (d, $^1J_{C,F}$ = 254.9 Hz), 145.3, 143.4, 132.7, 130.8 (d, $^3J_{C,F}$ = 8.0 Hz), 127.9, 124.3, 115.9 (d, $^2J_{C,F}$ = 21.1 Hz), 69.1, 56.6, 49.1, 49.0, 35.5, 35.3, 29.0, 18.2, 12.1; HRMS (EI) [M^+] calcd. for $C_{26}H_{34}FNO_2$ 411.2574; found 411.2586. No isomeric products were detected by ^{1}H-NMR spectroscopy.

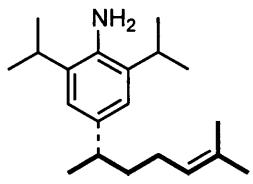

2,6-Diisopropyl-4-(6-methylhept-5-en-2-yl)aniline (109): Following the general procedure using 2.0 equiv. of the organozinc reagent (t = 2 h), 95 mg (66%) of **109** were isolated by flash chromatography (5% EtOAc/hexanes) as a light orange oil. R_f = 0.4 (5% EtOAc/hexanes); ^{1}H-NMR (400 MHz, $CDCl_3$) δ 6.91 (s, 2H), 5.19 (dd, J = 7.6, 7.2 Hz, 1H), 3.63 (br s, 2H), 2.63 (sext, J = 6.8 Hz, 1H), 2.00-1.95 (m, 2H), 1.74 (s, 3H), 1.68-1.59 (m, 5H), 1.34 (d, J = 6.8 Hz, 12H), 1.28 (d, J = 7.2 Hz, 3H); ^{13}C-NMR (100 MHz, $CDCl_3$) δ 138.0 (+), 137.6 (+), 132.4 (+), 131.2 (+), 124.9 (–), 121.3 (–), 39.2 (–), 38.7 (+), 28.0 (–), 26.4 (+), 25.8 (–), 22.6 (–, two overlapping signals), 17.7 (–); HRMS

(EI) [M^+] calcd. for $C_{20}H_{33}N$ 287.2613; found 287.2624. The ratio of desired to linear product was determined to be 58:1.

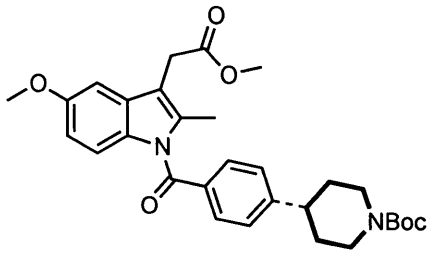

***tert*-Butyl 4-(4-(5-methoxy-3-(2-methoxy-2-oxoethyl)-2-methyl-1*H*-indole-1-carbonyl)phenyl)-piperidine-1-carboxylate (110)**: Following the general procedure (t = 1 h), 248 mg (95%) of **110** were isolated by flash chromatography (50% Et_2O/pentane) as a light-yellow solid. Mp: 50-52°C; R_f = 0.2 (50% Et_2O/pentane); ^{1}H-NMR (400 MHz, $CDCl_3$) δ 7.68 (d, J = 8.0 Hz, 2H), 7.33 (d, J = 8.0 Hz, 2H), 6.97 (d, J = 2.4 Hz, 1H), 6.91 (d, J = 9.2 Hz, 1H), 6.67 (dd, J = 9.0, 2.6 Hz, 1H), 4.29 (br s, 2H), 3.85 (s, 3H), 3.72 (s, 3H), 3.69 (s, 2H), 2.84-2.74 (m, 3H), 2.39 (s, 3H), 1.89 (d, J = 12.4 Hz, 2H), 1.73-1.62 (m, 2H), 1.50 (s, 9H); ^{13}C-NMR (100 MHz, $CDCl_3$) δ 171.4, 169.2, 155.8, 154.7, 151.2, 136.0, 133.5, 130.9, 130.4, 130.1, 127.1, 114.9, 111.9, 111.4, 101.0, 79.5, 55.6, 52.1, 44.2 (broad), 42.7, 32.8, 30.1, 28.4, 13.2; HRMS (EI) [M^+] calcd. for $C_{30}H_{36}N_2O_6$ 520.2573; found 520.2592. No isomeric products were detected by ^{1}H-NMR.

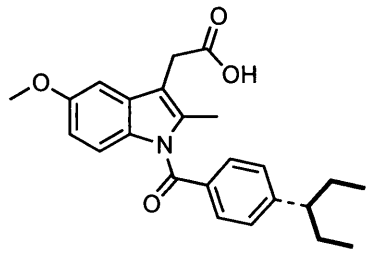

2-(5-Methoxy-2-methyl-1-(4-(pentan-3-yl)benzoyl)-1*H*-indol-3-yl)acetic acid (111): Following the general procedure (t = 2 h) using 2.2 equiv. organozinc reagent, 150 mg (76%) of **111** were isolated after trituration with hexanes as an off-white solid. Mp: 75-77 °C; ^{1}H-NMR (400 MHz, $CDCl_3$) δ 7.65 (d, J = 8.0 Hz, 2H), 7.27 (d, J = 8.0 Hz, 2H), 6.98 (s, 1H), 6.92 (d, J = 8.8 Hz, 1H), 6.67 (dd, J = 6.8, 1.8 Hz, 1H), 3.85 (s, 3H), 3.71 (s, 2H), 2.46-2.42 (m, 1H), 2.38 (s, 3H), 1.80-1.72 (m, 2H), 1.69-1.57 (m, 2H), 0.82 (t, J = 7.2 Hz, 6H); ^{13}C-NMR (100 MHz, $CDCl_3$) δ 177.2 (+), 169.6 (+), 155.8 (+), 151.7 (+), 136.3 (+), 133.1 (+), 131.1 (+), 130.3 (+), 129.8 (–), 128.2 (–), 115.0 (–), 111.6 (–), 111.3 (+), 100.9 (–), 55.7 (–), 49.8 (–), 30.2 (+), 29.1 (+), 13.2 (–), 12.1 (–); HRMS (EI) [M^+] calcd. for

$C_{24}H_{27}NO_4$ 393.1940; found 393.1953. No isomeric products were detected by ^{1}H-NMR spectroscopy.

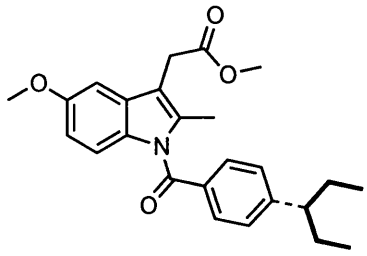

Methyl 2-(5-methoxy-2-methyl-1-(4-(pentan-3-yl)benzoyl)-1*H*-indol-3-yl)acetate (112): Following the general procedure (t = 1 h), 190 mg (93%) of **112** were isolated by flash chromatography (15% EtOAc/hexanes) as a viscous, light-yellow oil. R_f = 0.27 (15% EtOAc/hexanes); ^{1}H-NMR (600 MHz, $CDCl_3$) δ 7.66 (d, J = 7.8 Hz, 2H), 7.28 (d, J = 8.4 Hz, 2H), 6.99 (d, J = 2.4 Hz, 1H), 6.93 (d, J = 9.0 Hz, 1H), 6.68 (dd, J = 8.7, 2.4 Hz, 1H), 3.86 (s, 3H), 3.73 (s, 3H), 3.70 (s, 2H), 2.48-2.43 (m, 1H), 2.40 (s, 3H), 1.81-1.74 (m, 2H), 1.66-1.58 (m, 2H), 0.84-0.81 (t, J = 7.5 Hz, 6H); ^{13}C-NMR (100 MHz, $CDCl_3$) δ 171.4 (+), 169.6 (+), 155.8 (+), 151.6 (+), 136.0 (+), 133.1 (+), 131.0 (+), 130.4 (+), 129.8 (–), 128.1 (–), 114.9 (–), 111.8 (+), 111.4 (–), 101.0 (–), 55.6 (–), 52.1 (–), 49.8 (–), 30.1 (+), 29.1 (+), 13.2 (–), 12.1 (–); HRMS (EI) [M^+] calcd. for $C_{25}H_{29}NO_4$ 407.2097; found 407.2093. The ratio of desired to isomeric (2-pentyl) product was determined to be >99:1.

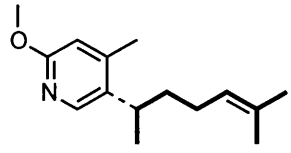

2-Methoxy-4-methyl-5-(6-methylhept-5-en-2-yl)pyridine (113): Following the general procedure (t = 4 h), 98 mg (84%) of **113** were isolated by flash chromatography (3% EtOAc/hexanes) as a yellow oil. R_f = 0.1 (3% EtOAc/hexanes); ^{1}H-NMR (600 MHz, $CDCl_3$) δ 7.96 (s, 1H), 6.51 (s, 1H), 5.08 (t, J = 7.2 Hz, 1H), 3.90 (s, 3H), 2.86 (sext, J = 7.2 Hz, 1H), 2.25 (s, 3H), 1.95-1.93 (m, 2H), 1.69-1.59 (m, 5H), 1.50 (s, 3H), 1.23 (d, J = 6.6 Hz, 3H); ^{13}C-NMR (150 MHz, $CDCl_3$) δ 162.4, 147.9, 144.0, 134.2, 131.7, 124.2, 111.1, 53.0, 37.5, 31.9, 26.0, 25.6, 21.6, 19.0, 17.6; HRMS (EI) [M^+] calcd. for $C_{15}H_{23}NO$ 233.1780; found 233.1774. No isomeric products were detected by ^{1}H-NMR spectroscopy.

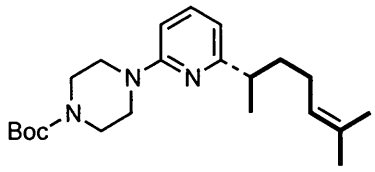

***tert*-Butyl 4-(6-(6-methylhept-5-en-2-yl)piperazine-1-carboxylate (114)**: Following the general procedure (t = 0.5 h), 175 mg (94%) of **114** were isolated by flash chromatography (10% EtOAc/hexanes) as a clear, colourless oil. R_f = 0.2 (10% EtOAc/hexanes); ^{1}H-NMR (600 MHz, $CDCl_3$) δ 7.41 (t, *J* = 7.8 Hz, 1H), 6.50 (d, *J* = 7.2 Hz, 1H), 6.45 (d, *J* = 8.4 Hz, 1H), 5.13-5.11 (m, 1H), 3.54 (s, 8H), 2.74-2.71 (m, 1H), 1.94-1.88 (m, 2H), 1.81-1.77 (m, 1H), 1.68 (s, 3H), 1.56-1.53 (m, 13H), 1.24 (d, *J* = 6.6 Hz, 3H); ^{13}C-NMR (150 MHz, $CDCl_3$) δ 164.7, 158.9, 154.9, 137.6, 131.1, 124.8, 111.5, 104.2, 79.7, 45.2, 41.3, 37.0, 28.4, 26.1, 25.7, 20.8, 17.6; HRMS (EI) [M^+] calcd. for $C_{22}H_{35}N_3O_2$ 373.3729; found 373.2715. No isomeric products were detected by ^{1}H-NMR spectroscopy.

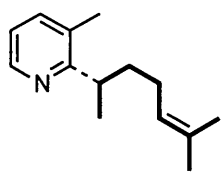

3-Methyl-2-(6-methylhept-5-en-2-yl)pyridine (115): Following the general procedure (t = 4 h), 85 mg (84%) of **115** were isolated by flash chromatography (5% EtOAc/hexanes) as a clear, colourless oil. R_f = 0.2 (5% EtOAc/hexanes); ^{1}H-NMR (600 MHz, $CDCl_3$) δ 8.44 (d, *J* = 4.8 Hz, 1H), 7.39 (d, *J* = 7.2 Hz, 1H), 6.99 (dd, *J* = 4.8, 3.0 Hz, 1H), 5.11-5.09 (m, 1H), 3.11-3.09 (m, 1H), 2.30 (s, 3H), 1.93-1.87 (m, 3H), 1.66 (s, 3H), 1.62-1.61 (m, 1H), 1.48 (s, 3H), 1.25 (d, *J* = 6.6 Hz, 3H); ^{13}C-NMR (150 MHz, $CDCl_3$) δ 164.3, 146.9, 137.5, 131.3, 130.5, 124.7, 120.6, 36.3, 35.9, 26.0, 25.7, 20.1, 18.8, 17.5; HRMS (EI) [M^+] calcd. for $C_{14}H_{21}N$ 203.1674; found 203.1679. No isomeric products were detected by ^{1}H-NMR spectroscopy.

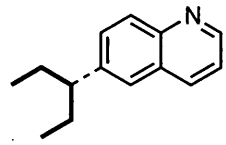

6-(Pentan-3-yl)quinoline (116): Following the general procedure (t = 3 h), 84 mg (85%) of **116** were isolated by flash chromatography (2.5% EtOAc/hexanes + 2% NEt_3) as a light-yellow oil. R_f = 0.19 (2.5% EtOAc/hexanes + 2% NEt_3); ^{1}H-NMR (600 MHz, $CDCl_3$) δ 8.86-8.85 (m, 1H), 8.09 (d, *J* = 8.4 Hz, 1H), 8.06 (d, *J* = 9.0 Hz, 1H), 7.56-7.54 (m, 2H), 7.36-7.34 (m, 1H), 2.54-2.49 (m, 1H), 1.81-1.74 (m, 2H), 1.69-1.61 (m, 2H), 0.79 (t, *J* = 7.5 Hz, 6H); ^{13}C-

NMR (100 MHz, $CDCl_3$) δ 149.5 (–), 147.4 (+), 144.1 (+), 135.6 (–), 129.6 (–), 129.3 (–), 128.2 (+), 126.2 (–), 120.9 (–), 49.7 (–), 29.2 (+), 12.2 (–); HRMS (EI) [M^+] calcd. for $C_{14}H_{17}N$ 199.1364; found 199.1361. The ratio of desired to isomeric (2-pentyl) product was determined to be 49:1.

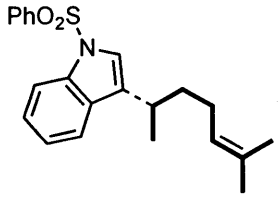

3-(6-Methylhept-5-en-2-yl)-1-(phenylsulfonyl)-1H-indole (**117**): Following the general procedure (t = 4 h), 162 mg (88%) of **117** were isolated by flash chromatography (3% EtOAc/hexanes) as a colourless oil. R_f = 0.1 (3% EtOAc/ hexanes); ^{1}H NMR (600 MHz, $CDCl_3$) δ 8.02 (d, J = 8.4 Hz, 1H), 7.87 (d, J = 7.8 Hz, 2H), 7.55-7.51 (m, 2H), 7.74-7.41 (m, 2H), 7.33-7.31 (m, 3H), 5.11 (t, J = 7.2 Hz, 1H), 2.99-2.95 (m, 1H), 1.99-1.95 (m, 2H), 1.81-1.59 (m, 5H), 1.49 (s, 3H), 1.32 (d, J = 7.2 Hz, 3H); ^{13}C NMR (150 MHz, $CDCl_3$) δ 138.4, 135.7, 133.6, 131.8, 130.6, 129.2, 129.1, 126.6, 124.5, 124.1, 122.9, 121.7, 119.9, 113.9, 36.7, 30.1, 25.8, 25.6, 20.6, 17.6; HRMS (EI) [M^+] calcd. for $C_{22}H_{25}NO_2S$ 367.1606; found 367.1617. The ratio of the desired to isomeric (linear) product was determined to be 29:1.

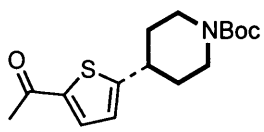

***tert*-Butyl 4-(5-acetylthiophen-2-yl)piperidine-1-carboxylate** (**118**): Following the general procedure (t = 4.5 h), 151 mg (97%) of **118** were isolated by flash chromatography (gradient: 30%→40% Et_2O/pentane) as a light-yellow, viscous oil that solidified on standing. Mp: 63-65°C; R_f = 0.25 (40% Et_2O/pentane); ^{1}H-NMR (400 MHz, $CDCl_3$) δ 7.55 (d, J = 3.8 Hz, 1H), 6.86 (d, J = 3.7 Hz, 1H), 4.20 (br s, 2H), 2.97 (tt, J = 11.7, 3.5 Hz, 1H), 2.83 (br t, J = 11.2 Hz, 2H), 2.52 (s, 3H), 1.99 (br d, J = 13.0 Hz, 2H), 1.63 (dq, J = 12.5, 4.0 Hz, 2H), 1.45 (s, 9H); ^{13}C-NMR (100 MHz, $CDCl_3$) δ 190.2 (+), 159.1 (+), 154.4 (+), 141.7 (+), 132.5 (–), 123.7 (–), 79.4 (+), 43.6 (broad, +), 38.0 (–), 33.5 (+), 28.2 (–), 26.2 (–); HRMS (EI) [M]$^+$ calcd. for $C_{16}H_{23}NO_3S$ 309.1399; found 309.1412. The ratio of desired to isomeric product was determined to be 15:1.

Compounds **119 – 121** and **123 – 126** were contaminated with significant quantities of the corresponding 2-pentyl and 3-pentyl regioisomers. The characterization of only the 3-pentyl isomer is reported, which was confirmed by 1D-COSY, 2D-HSQC, and 2D-HMBC NMR experiments.

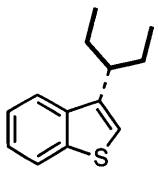

3-(Pentan-3-yl)benzo[*b*]thiophene (119): Following the general procedure (t = 0.5 h) 88 mg (86%) of **119** were isolated by flash chromatography (hexanes) as a clear, colourless oil. R_f = 0.6 (hexanes); ^{1}H-NMR (600 MHz, $CDCl_3$) δ 7.93 (d, J = 7.8 Hz, 1H), 7.86 (d, J = 7.8 Hz, 1H), 7.44-7.38 (m, 2H), 7.11 (s, 1H), 3.02-2.97 (m, 1H), 1.88-1.80 (m, 4H), 0.89 (t, J = 10.8 Hz, 6H); ^{13}C NMR (150 MHz, $CDCl_3$) δ 140.6, 139.4, 124.0, 123.6, 122.9, 122.0, 121.9, 120.3, 42.2, 27.7, 11.9; HRMS (EI) [M^+] calcd. for $C_{13}H_{16}S$ 204.0973; found 204.0966. The ratio of desired to isomeric products was determined to be 1.0 (3-pentyl): 0.5 (2-pentyl).

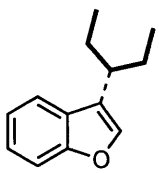

3-(Pentan-3-yl)benzofuran (120): Following the general procedure (t = 1 h) using 3-bromobenzofuran,[120] 83 mg (88%) of **120** were isolated by flash chromatography (hexanes) as a clear, colourless oil. R_f = 0.43 (hexanes); ^{1}H-NMR (600 MHz, $CDCl_3$) δ 7.65 (t, J = 7.2 Hz, 1H), 7.52 (d, J = 7.8 Hz, 1H), 7.43 (s, 1H), 7.35-7.31 (m, 1H), 7.30-7.24 (m, 1H), 2.69-2.63 (m, 1H), 1.85-1.76 (m, 4H), 0.91 (t, J = 7.5 Hz, 6H); ^{13}C-NMR (100 MHz, $CDCl_3$) δ 155.7 (+), 141.3 (–), 127.7 (+), 123.9 (–), 123.4 (+), 121.9 (–), 120.3 (–), 111.5 (–), 39.2 (–), 27.2 (+), 12.0 (–). HRMS (EI) [M^+] calcd. for $C_{13}H_{16}O$ 188.1201; found 188.1206. The ratio of desired to isomeric products was determined to be 1.0 (3-pentyl): 2.0 (2-pentyl): 0.4 (1-pentyl).

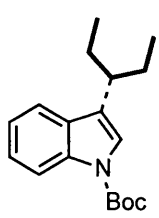

***tert*-Butyl 3-(pentan-3-yl)-1*H*-indole-1-carboxylate (121)**: Following the general procedure (t = 17 h) using *tert*-butyl 3-bromo-1*H*-indole-1-carboxylate,[121] 129 mg (90%) of **121** were isolated by flash chromato-

graphy (gradient: hexanes→1% EtOAc/hexanes) as a colourless, viscous oil. R_f = 0.1 (1% EtOAc/hexanes); ^{1}H-NMR (400 MHz, $CDCl_3$) δ 8.32-8.08 (m, 1H), 7.61 (d, J = 7.7 Hz, 1H), 7.38 (s, 1H), 7.36-7.30 (m, 1H), 7.27-7.23 (m, 1H), 2.74-2.67 (m, 1H), 1.81-1.76 (m, 4H), 1.72 (s, 9H), 0.91 (t, J = 7.4 Hz, 6H); ^{13}C-NMR (100 MHz, $CDCl_3$) δ 149.9 (+), 130.7 (+), 127.0 (+), 124.5 (+), 124.0 (–), 122.0 (–), 119.6 (–), 119.4 (–), 115.3 (–), 83.2 (+), 39.9 (–), 28.2 (–), 27.4 (+), 12.1 (–); HRMS (EI) $[M]^+$ calcd. for $C_{18}H_{25}NO_2$ 287.1885; found 287.1891. The ratio of desired to isomeric (2-pentyl) product was determined to be 1:0.6.

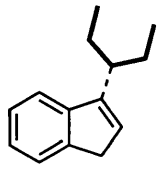

3-(Pentan-3-yl)-1*H*-indene (122): Following the general procedure (t = 2 h) using 1-bromoindene,[122] 61 mg (65%) of **122** were isolated by flash chromatography (hexanes) as a clear, colourless oil. R_f = 0.63 (hexanes); ^{1}H-NMR (400 MHz, $CDCl_3$) δ 7.52 (d, J = 7.2 Hz, 1H), 7.46 (d, J = 7.6 Hz, 1H), 7.33 (t, J = 7.6 Hz, 1H), 7.24 (t, J = 7.6 Hz, 1H), 6.23 (s, 1H), 3.40 (s, 2H), 2.63 (quint, J = 6.8 Hz, 1H), 1.79-1.71 (m, 4H), 0.92 (t, J = 7.4 Hz, 6H); ^{13}C-NMR (100 MHz, $CDCl_3$) δ 147.6 (+), 145.5 (+), 144.9 (+), 127.6 (–), 125.8 (–), 124.3 (–), 123.8 (–), 119.5 (–), 41.5 (–), 37.6 (+), 26.3 (+), 11.9 (–); HRMS (EI) $[M^+]$ calcd. for $C_{14}H_{18}$ 186.1409; found 186.1412. The ratio of desired to isomeric (2-pentyl) product was determined to be 91:1.

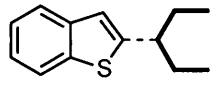

2-(Pentan-3-yl)benzo[*b*]thiophene (123): Following the general procedure (t = 2 h) using 2-bromobenzo[*b*]thiophene,[123] 95 mg (93%) of **123** were isolated by flash chromatography (hexanes) as a clear, colourless oil. R_f = 0.55 (hexanes); ^{1}H-NMR (400 MHz, $CDCl_3$) δ 7.85-7.82 (m, 1H), 7.73 (d, J = 7.6 Hz, 1H), 7.37 (t, J = 7.6 Hz, 1H), 7.31 (t, J = 8.0 Hz, 1H), 7.07 (s, 1H), 2.79 (tt, J = 9.3, 4.8 Hz, 1H), 1.88-1.65 (m, 4H), 0.96 (t, J = 7.6 Hz, 6H); ^{13}C-NMR (100 MHz, $CDCl_3$) δ 151.0 (+), 139.9 (+), 139.1 (+), 123.9 (–), 123.2 (–), 122.6 (–), 122.2 (–), 120.5 (–), 45.8 (–), 31.3 (+), 12.0 (–); HRMS (EI) $[M^+]$ calcd. for $C_{13}H_{16}S$ 204.0973; found 204.0979.

The ratio of desired to isomeric products was determined to be 1.0 (3-pentyl): 4.1 (2-pentyl): 2.9 (1-pentyl).

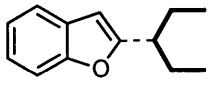

2-(Pentan-3-yl)benzofuran (124): Following the general procedure (t = 1 h) using 2-bromobenzofuran,[124] 85 mg (90%) of **124** were isolated by flash chromatography (hexanes) as a clear, colourless oil. R_f = 0.61 (hexanes); ^{1}H-NMR (400 MHz, $CDCl_3$) δ 7.57-7.54 (m, 1H), 7.48 (d, *J* = 7.6 Hz, 1H), 7.28-7.21 (m, 2H), 6.45 (s, 1H), 2.73-2.66 (m, 1H), 1.89-1.76 (m, 4H), 0.95 (t, *J* = 7.6 H, 6H); ^{13}C-NMR (100 MHz, $CDCl_3$) δ 162.1 (+), 154.6 (+), 128.7 (+), 123.0 (–), 122.2 (–), 120.1 (–), 110.8 (–), 102.3 (–), 42.9 (–), 26.3 (+), 11.8 (–); HRMS (EI) [M^+] calcd. for $C_{13}H_{16}O$ 188.1201; found 188.1207. The ratio of desired to isomeric products was determined to be 1.0 (3-pentyl): 1.6 (2-pentyl): 0.2 (1-pentyl).

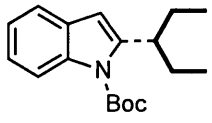

***tert*-Butyl 2-(pentan-3-yl)-1*H*-indole-1-carboxylate (125)**: Following the general procedure (t = 17 h) using *tert*-butyl 2-bromo-1*H*-indole-1-carboxylate, [125] 103 mg (72%) of **125** were isolated by flash chromatography (gradient: pentane→1% Et_2O/pentane) as a light-pink oil. R_f = 0.27 (1% Et_2O/pentane); ^{1}H-NMR (400 MHz, $CDCl_3$) δ 8.16 (d, *J* = 8.0 Hz, 1H), 7.53-7.49 (m, 1H), 7.29-7.21 (m, 2H), 6.42 (s, 1H), 3.66 (quint, *J* = 6.8 Hz, 1H), 1.86-1.77 (m, 4H), 1.74 (s, 9H), 0.95 (t, *J* = 7.6 Hz, 6H); ^{13}C-NMR (100 MHz, $CDCl_3$) δ 150.7 (+), 142.6 (+), 136.6 (+), 129.4 (+), 123.1 (–), 119.7 (–), 115.5 (–), 106.0 (–), 105.1 (–), 83.6 (+), 40.0 (–), 28.2 (–), 26.8 (+), 11.1 (–); HRMS (EI) $[M]^+$ calcd. for $C_{18}H_{25}NO_2$ 287.1885; found 287.1893. The ratio of desired to isomeric products was determined to be 1.0 (3-pentyl): 1.1 (2-pentyl): 1.0 (1-pentyl).

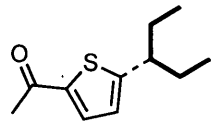

1-(5-(Pentan-3-yl)thiophen-2-yl)ethanone (126): Following the general procedure (t = 16 h) using 87 mg (88%) of **126** were isolated by flash chromatography (5% EtOAc/hexanes) as a yellow oil. R_f = 0.3 (5% EtOAc/hexanes); ^{1}H-NMR (600 MHz, $CDCl_3$) δ 7.56-7.53 (m, 1H), 6.83-6.81 (m,

1H), 2.70-2.65 (m, 1H), 2.51 (s, 3H), 1.75-1.68 (m, 4H), 0.91-0.84 (m, 6H); ^{13}C NMR (150 MHz, $CDCl_3$) δ: 190.5, 162.3, 142.0, 132.9, 124.1, 45.6, 31.1, 26.2, 11.9; HRMS (EI) [M^+] calcd. for $C_{11}H_{16}OS$ 196.0922; found 196.0917. The ratio of desired to isomeric products was determined to be 0.2 (3-pentyl): 0.7 (2-pentyl): 1.0 (1-pentyl).

5.5 – Preparation of Pd-PEPPSI-IPent^{Cl} Complexes for use in the room temperature Buchwald-Hartwig Reaction

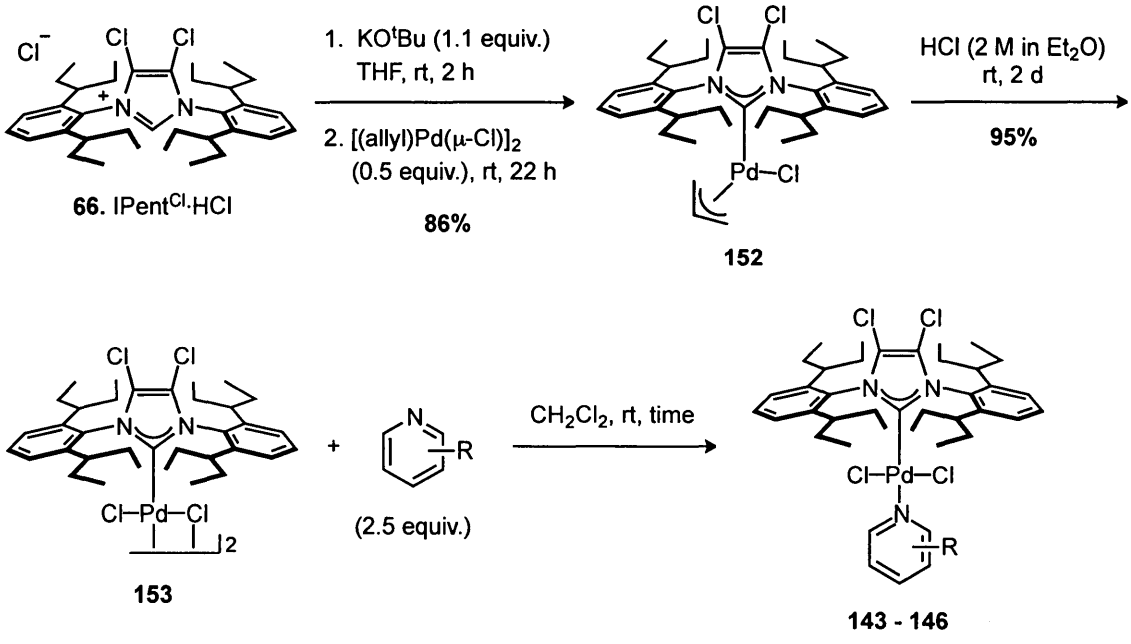

Scheme 9. General Route for the Synthesis of Pd-PEPPSI-IPent^{Cl} Complexes **143 – 146**

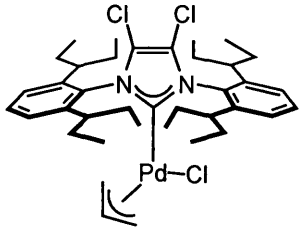

(IPent^{Cl})Pd(η^3-allyl)Cl (152): A 25 mL round-bottom flask was charged with 150 mg KO^{t}Bu (1.27 mmol, 1.1 equiv.) in a glovebox then with 700 mg **66** (1.15 mmol, 1.0 equiv.) in air. The flask was evacuated and backfilled with Ar (x3) then THF (11.5 mL) was added forming a light-brown, nearly homogeneous solution. After stirring for 2 h at rt, 212.2 mg of [(η^3-allyl)Pd(μ-Cl)]$_2$ (0.58 mmol, 0.5 equiv.) was added in one shot under a cone of Ar. After 22 h, the dark-brown

suspension was diluted with Et_2O, filtered through a pad of silica gel, washing the filter cake copiously with Et_2O. The filtrate was concentrated to yield an orange oil that solidified after repeated sonication with pentane. Washing with cold pentane furnished 742 mg (86%) of **152** as an off-white solid. ^{1}H-NMR (400 MHz, C_6D_6) δ 7.33 (t, J = 7.6 Hz, 2H), 7.18 (d, J = 8.0 Hz, 4H), 4.78 – 4.67 (m, 1H), 4.10 (d, J = 7.2 Hz, 1H), 3.07 (d, J = 13.2 Hz, 1H), 2.97 (m, 2H), 2.85 – 2.78 (m, 3H), 2.30 – 2.08 (m, 4H), 1.90 (sept, J = 7.6 Hz, 4H), 1.77 – 1.70 (m, 9H), 1.20 (q, J = 6.8 Hz, 12H), 0.95 (t, J = 7.3 Hz, 12H); ^{13}C-NMR (100 MHz, C_6D_6) δ 186.7, 144.4, 144.1, 135.0, 129.4, 126.0, 125.6, 119.7, 113.6, 73.2, 52.1, 41.5, 41.4, 27.1, 26.9, 26.2, 25.9, 25.8, 25.7, 12.1, 11.8, 11.2, 11.0; HRMS (EI) $[M]^+$ calcd. for $C_{38}H_{55}N_2Cl_3Pd$ 750.2466; found: 750.2493.

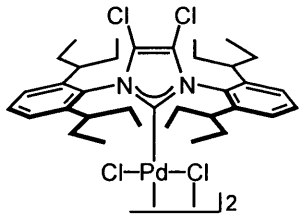

[{(IPent^{Cl})PdCl$_2$}$_2$] (153): A solution of 700 mg of **152** (0.93 mmol) in 9.5 mL HCl (2 M in Et_2O) was stirred for 48 h under a static atmosphere of Ar, during which time an orange solid precipitated from the reaction mixture. The solvent was then removed yielding 660 mg (95%) of **153** as a dark-orange solid, which was used without further purification. ^{1}H-NMR (400 MHz, $CDCl_3$) δ 7.53 (t, J = 7.6 Hz, 4H), 7.27 (d, J = 8.4 Hz, 8H), 2.46 (m, 8H), 1.95 – 1.80 (m, 8H), 1.80 – 1.68 (m, 8H), 1.62 – 1.50 (m, 8H), 1.48 – 1.32 (m, 8H), 0.95 (t, J = 7.2 Hz, 24H), 0.75 (t, J = 7.4 Hz, 24H); ^{13}C-NMR (75 MHz, $CDCl_3$) δ 150.1, 145.1, 132.6, 129.8, 126.4, 121.1, 40.8, 27.2, 26.3, 12.6, 10.8; HRMS (ESI) $[M\text{-}Cl]^+$ calcd. for $C_{70}H_{100}N_4Cl_7Pd_2$ 1453.3837; found: 1453.3827.

General Procedure for the Synthesis of Pd-PEPPSI Complexes 143 – 146 from 153: A solution of **153** in CH_2Cl_2 (2 mL per 0.5 mmol complex) was charged with the appropriately substituted pyridine derivative (2.5 equiv.) then allowed to stir at rt for the indicated time. The solvent was then evaporated and the residue purified via flash chromatography on silica gel to yield pure complex.

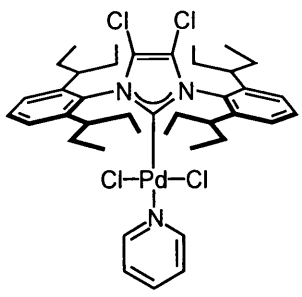

Pd-PEPPSI-IPent^{Cl}-pyr (**143**): Following the general procedure (t = 2 h) on a 0.0523 mmol scale using 11 μL (0.13 mmol) of pyridine furnished 76 mg (88%) of **143** as a light-yellow solid after flash chromatography (1:1 CH_2Cl_2/pentane, R_f = 0.37). Mp: 285–290°C (decomp.); ^{1}H-NMR (400 MHz, $CDCl_3$) δ 8.53 (d, J = 5.2 Hz, 2H), 7.58 – 7.49 (m, 3H), 7.31 (d, J = 7.6 Hz, 4H), 7.12 (t, J = 6.6 Hz, 2H), 3.03 – 2.90 (m, 4H), 2.12 – 1.97 (m, 4H), 1.97 – 1.85 (m, 4H), 1.76 – 1.62 (m, 4H), 1.58 – 1.45 (m, 4H), 1.15 (t, J = 7.2 Hz, 12H), 0.85 (t, J = 7.5 Hz, 12H); ^{13}C-NMR (100 MHz, $CDCl_3$) δ 157.3 (+), 151.5 (–), 145.3 (+), 137.4 (–), 133.6 (+), 129.7 (–), 126.4 (–), 124.1 (–), 120.9 (+), 40.8 (–), 27.5 (+), 26.7 (+), 12.6 (–), 10.9 (–); HRMS (ESI) $[M\text{-}CH_3]^+$ calc'd for $C_{39}H_{52}N_3Cl_4Pd$: 808.1954; found: 808.1971.

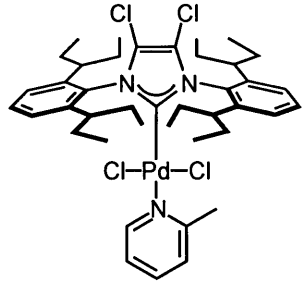

Pd-PEPPSI-IPent^{Cl}-picoline (**144**): Following the general procedure (t = 2 h) on a 0.1 mmol scale using 25 μL (0.25 mmol) of 2-methylpyridine furnished 144 mg (86%) of **144** as a light-yellow solid after flash chromatography (CH_2Cl_2, R_f = 0.78). Mp: 185–190°C (decomp.); ^{1}H-NMR (400 MHz, $CDCl_3$) δ 8.21 (d, J = 6.0 Hz, 1H), 7.54 (t, J = 7.8 Hz, 2H), 7.41 (t, J = 7.4 Hz, 1H), 7.35 (d, J = 8.0 Hz, 4H), 6.98 (d, J = 8.0 Hz, 1H), 6.93 (t, J = 6.6 Hz, 1H), 3.05 – 2.93 (m, 4H), 2.53 (s, 3H), 2.08 – 1.84 (m, 8H), 1.75 – 1.58 (m, 4H), 1.56 – 1.47 (m, 4H), 1.12 (t, J = 7.2 Hz, 12H), 0.84 (t, J = 7.2 Hz, 12H); ^{13}C-NMR (100 MHz, $CDCl_3$) δ 159.8, 159.4, 150.4, 145.7, 137.0, 133.2, 129.5, 126.4, 125.5, 121.5, 120.8, 40.4, 27.0, 25.8, 25.0, 12.4, 10.4. The spectral data are consistent with those reported in the literature.[111]

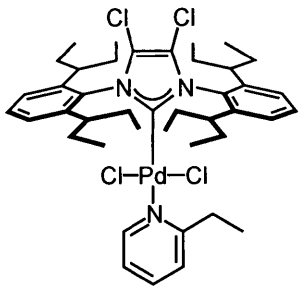

Pd-PEPPSI-IPent^{Cl}-2-Etpyr (**145**): Following the general procedure (t = 1 h) on a 0.06 mmol scale using 17 μL (0.15 mmol) of 2-ethylpyridine furnished 77.9 mg (76%) of **145** as a light-yellow solid after flash chromatography (60% CH_2Cl_2/pentane, R_f = 0.29). Mp: 190–195°C (decomp.); ^{1}H-NMR (400 MHz, $CDCl_3$) δ 8.23 (d, J = 5.6 Hz, 1H), 7.56 (t, J = 7.8 Hz, 2H), 7.46 (dt, J = 7.7 and 1.3 Hz, 1H), 7.37 (d, J = 7.8 Hz, 4H), 7.03 (d, J = 7.8 Hz, 1H), 6.94 (t, J = 6.5 Hz, 1H), 3.09 (q, J = 7.6 Hz, 2H), 3.04 – 2.94 (m, 4H), 2.01 – 1.84 (m, 8H), 1.75 – 1.65 (m, 4H), 1.54 – 1.44 (m, 4H), 1.08 (t, J = 7.2 Hz, 12H), 1.01 (t, J = 7.6 Hz, 3H), 0.83 (t, J = 7.5 Hz, 12H); ^{13}C-NMR (75 MHz, $CDCl_3$) δ 164.2, 159.7, 150.3, 145.8, 137.1, 133.1, 129.5, 126.5, 123.5, 121.6, 120.8, 40.3, 31.4, 26.9, 25.7, 12.6, 12.3, 10.4; HRMS (ESI) $[M+H]^+$ calc'd for $C_{42}H_{60}N_3Cl_4Pd$: 852.2571; found: 852.2546.

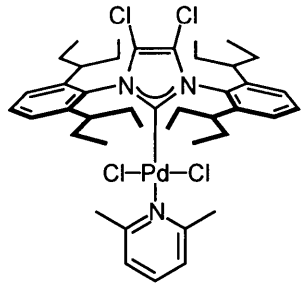

Pd-PEPPSI-IPent^{Cl}-lutidine (**146**): Following the general procedure (t = 22 h) on a 0.0219 mmol scale using 10 μL (0.086 mmol) of 2,6-lutidine furnished 25 mg (67%) of **146** as a light-yellow solid after flash chromatography (1:1 CH_2Cl_2/pentane, R_f = 0.3). Mp: 180–185°C (decomp.); ^{1}H-NMR (400 MHz, $CDCl_3$) δ 7.53 (t, J = 7.8 Hz, 2H), 7.37 (d, J = 7.8 Hz, 4H), 7.29 (t, J = 7.7 Hz, 1H), 6.78 (d, J = 7.7 Hz, 2H), 3.05 – 2.92 (m, 4H), 2.56 (s, 6H), 2.0 – 1.83 (m, 8H), 1.77 – 1.66 (m, 4H), 1.57 – 1.46 (m, 4H), 1.05 (t, J = 7.2 Hz, 12H), 0.81 (t, J = 7.4 Hz, 12H); ^{13}C-NMR (100 MHz, $CDCl_3$) δ 161.4 (+), 158.9 (+), 146.2 (+), 137.5 (–), 132.7 (+), 129.4 (–), 126.4 (–), 122.4 (–), 120.7 (+), 40.1 (–), 26.8 (+), 25.0 (+), 24.9 (–), 12.2 (–), 10.1 (–); HRMS (ESI) $[M+H]^+$ calc'd for $C_{42}H_{60}N_3Cl_4Pd$ 852.2570; found 852.2602.

5.6 – Compound Characterization Data for Buchwald-Hartwig Reactions

General Amination Procedure A - Evaluation of backbone-modified IPr and IPent complexes: In a glovebox, a 15x45 mm 1-dram vial equipped with magnetic stir bar and Teflon-lined screw-cap was charged with 489 mg of Cs_2CO_3 (1.5 mmol, 3.0 equiv.) then with 3 mol% of Pd-PEPPSI-IPr (**29**, 10.2 mg), Pd-PEPPSI-IPr^{Cl} (**73**, 11.2 mg), Pd-PEPPSI-IPr^{Me} (**76**, 10.5 mg), Pd-PEPPSI-IPr^{Quino} (**77**, 12.1 mg), Pd-PEPPSI-IPent (**31**, 11.9 mg) or Pd-PEPPSI-IPent^{Cl} (**78**, 12.9 mg) in air. The vial was evacuated and backfilled with Ar (x3) then aryl halide (0.5 mmol, 1.0 equiv.) and amine (0.75 mmol, 1.5 equiv.) were added via microliter syringe followed by anhydrous DME (0.5 mL). Alternatively, if the aryl halide or amine were solids at room temperature, they were added to the vial with the other solids prior to evacuation. The vial was then sealed, immersed in a pre-heated 80°C oil bath and allowed to stir under a static Ar atmosphere at 1150 – 1200 rpm. After 24 h, the reaction was cooled to rt, diluted with Et_2O, filtered through a plug of Celite, and the filtrate concentrated *in vacuo*. The residue thus obtained was purified via flash chromatography on silica gel to yield pure cross-coupled product.

General Amination Procedure B – Room Temperature Amination with Pd-PEPPSI-IPent^{Cl}-picoline: In a glovebox, a 15x45 mm 1-dram vial equipped with magnetic stir bar and Teflon-lined screw-cap was charged with 12.6 mg of Pd-PEPPSI-IPent^{Cl}-picoline (0.015 mmol, 3 mol%), 489 mg of Cs_2CO_3 (1.5 mmol, 3.0 equiv.), aryl halide (0.5 mmol, 1.0 equiv.), substituted aniline (0.75 mmol, 1.5 equiv.), and anhydrous DME (0.5 mL) degassed via three cycles of freeze-pump-thaw. The resulting suspension was stirred in the glovebox for 24 h at ambient temperature (24 – 28°C) at which time the reaction was taken out of the glovebox, diluted with CH_2Cl_2, and filtered through a plug of Celite. The filtrate was concentrated *in vacuo* and the residue thus obtained was purified by flash chromatography on silica gel (unless noted otherwise) to yield pure cross-coupled product.

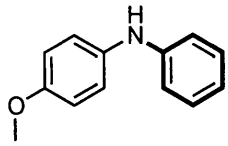

4-Methoxy-*N*-phenylaniline (136): Following general procedure A, 10 mg (10%), 16 mg (16%), and 2 mg (2%) were obtained using catalysts **73**, **76**, and **77**, respectively. Compound **136** was isolated by flash chromatography (5% Et_2O/pentane, $R_f = 0.21$) as a white solid. Mp: 104-106°C (lit. mp: 105-106°C);[127] ^{1}H-NMR (400 MHz, $CDCl_3$) δ 7.24 (t, J = 7.6 Hz, 2H), 7.10 (d, J = 7.6 Hz, 2H), 6.93 (d, J = 8.4 Hz, 2H), 6.91 – 6.83 (m, 3H), 5.51 (br s, 1H), 3.83 (s, 3H); ^{13}C-NMR (100 MHz, $CDCl_3$) δ 155.2, 145.1, 135.7, 129.3, 122.2, 119.5, 115.6, 114.6, 55.6. The spectral data are consistent with those reported in the literature.[126]

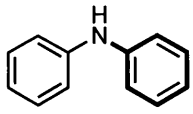

Diphenylamine (137): Following general procedure A, 4 mg (5%), 46 mg (55%), 39 mg (46%), and 30 mg (36%) were obtained using catalysts **29**, **73**, **76**, and **77**, respectively. Compound **137** was isolated by flash chromatography (5% Et_2O/pentane, R_f = 0.19) as an off-white solid. Mp: 52-53°C (lit. mp: 54-55°C);[127] ^{1}H-NMR (400 MHz, $CDCl_3$) δ 7.33 (t, J = 7.8 Hz, 4H), 7.13 (d, J = 8.0 Hz, 4H), 6.99 (t, J = 7.4 Hz, 2H), 5.74 (br s, 1H); ^{13}C-NMR (100 MHz, $CDCl_3$) δ 143.1, 129.3, 120.9, 117.8. The spectral data are consistent with those reported in the literature.[127]

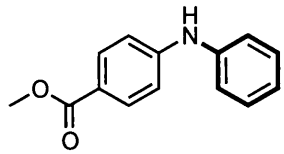

Methyl 4-(phenylamino)benzoate (138): Following general procedure A, 108 mg (95%), 110 mg (97%), 109 mg (96%), and 109 mg (96%) were obtained using catalysts **29**, **73**, **76**, and **77**, respectively. Compound **138** was isolated by flash chromatography (5% Et_2O/pentane, R_f = 0.19) as an off-white solid. Mp: 104-105°C (lit. mp: 108-110°C);[128] ^{1}H-NMR (400 MHz, $CDCl_3$) δ 7.95 (d, J = 8.8 Hz, 2H), 7.36 (t, J = 7.8 Hz, 2H), 7.20 (d, J = 8.0 Hz, 2H), 7.09 (t, J = 7.4 Hz, 1H), 7.02 (d, J = 8.4 Hz, 2H), 6.25 (br s, 1H), 3.90 (s, 3H); ^{13}C-NMR (100 MHz, $CDCl_3$) δ 167.0 (+), 148.1 (+), 140.8 (+), 131.4 (–), 129.4 (–), 122.9 (–), 120.8 (+), 120.3 (–), 114.4 (–), 51.7 (–). The spectral data are consistent with those reported in the literature.[128]

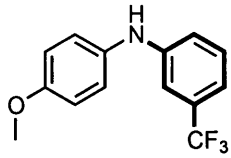

***N*-(4-methoxyphenyl)-3-(trifluoromethyl)aniline (131)**: Following general procedure A, 83 mg (62%) and 128 mg (96%) of **131** were obtained using **31** and **78**, respectively. Following general procedure B, 115 mg (86%) of **131** were obtained. Compound **131** was isolated by flash chromatography (10% EtOAc/hexanes, $R_f = 0.26$) as a beige solid. Mp: 57-59°C (lit. mp: 58-60°C);[108] ^{1}H-NMR (300 MHz, $CDCl_3$) δ 7.32 (t, J = 8.0 Hz, 1H), 7.16 – 7.11 (m, 3H), 7.09 (d, J = 7.9 Hz, 1H), 7.03 (dd, J = 8.1, 1.7 Hz, 1H), 6.98 – 6.92 (m, 2H), 5.68 (br s, 1H), 3.86 (s, 3H); ^{13}C-NMR (75 MHz, $CDCl_3$) δ 156.1, 146.0, 134.2, 131.6 (q, $^2J_{CF}$ = 31.7 Hz), 129.7, 124.2 (q, $^1J_{CF}$ = 272.5 Hz), 123.4, 117.8, 115.5 (q, $^3J_{CF}$ = 3.8 Hz), 114.8, 111.2 (q, $^3J_{CF}$ = 3.8 Hz), 55.5. ^{19}F-NMR (282 MHz, $CDCl_3$) δ -62.8 (s, 3F). The spectral data are consistent with those reported in the literature.[129]

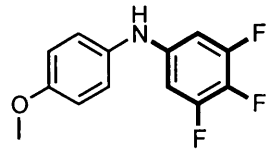

3,4,5-trifluoro-*N*-(4-methoxyphenyl)aniline (132): Following general procedure A, 65 mg (51%) and 120 mg (94%) of **132** were obtained using **31** and **78**, respectively. Following general procedure B, 95 mg (75%) of **132** were obtained. Compound **132** was isolated by flash chromatography (10% EtOAc/hexanes, R_f = 0.26) as a beige solid. Mp: 107-108°C (lit. mp: 108-109°C);[129] ^{1}H-NMR (400 MHz, $CDCl_3$) δ 7.08 (d, J = 9.2 Hz, 2H), 6.92 (d, J = 8.8 Hz, 2H), 6.46 – 6.37 (m, 2H), 5.49 (br s, 1H), 3.84 (s, 3H); ^{13}C-NMR (75 MHz, $CDCl_3$) δ 156.5, 151.8 (ddd, J_{CF} = 246.0, 10.4, and 6.0 Hz), 141.1 (dt, J_{CF} = 11.0 and 2.0 Hz), 133.7, 133.1 (dt, J_{CF} = 241.1 and 15.8 Hz), 124.0, 114.9, 98.3 (m), 55.5. ^{19}F-NMR (282 MHz, $CDCl_3$) δ -134.4 (d, J = 19.8 Hz, 2F), -173.6 (t, J = 21.2 Hz, 1F). The spectral data are consistent with those reported in the literature.[129]

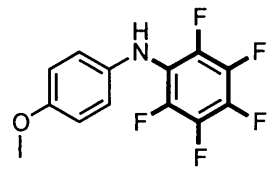

2,3,4,5,6-pentafluoro-*N*-(4-methoxyphenyl)aniline (139): Following general procedure A, 83 mg (58%) of **139** were obtained using **78**. No product was observed when **31** was used. Compound **139** was isolated by flash chromatography (2.5% EtOAc/hexanes, R_f = 0.21) as a brown oil which solidified upon cooling. ^{1}H-NMR (300 MHz, $CDCl_3$) δ

6.91 – 6.84 (m, 4H), 5.37 (br s, 1H), 3.82 (s, 3H); ^{13}C-NMR (75 MHz, $CDCl_3$) δ 155.6, 135.1, 119.7, 114.4, 55.5 [Resonances from carbons on the pentafluoroaryl ring are not reported due to complex C-F coupling]; ^{19}F-NMR (282 MHz, $CDCl_3$) δ -151.5 – -151.6 (m, 2F), -162.9 (app dt, J = 21.6 and 5.2 Hz, 2F), -165.9 (tt, J = 21.7 and 4.0 Hz, 1F). HRMS (EI) [M^+] calcd. for $C_{13}H_8F_5NO$ 289.0530; found 289.0526.

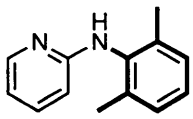

140

***N*-(2,6-Dimethylphenyl)pyridin-2-amine (140)**: Following general procedure A, 55 mg (55%) and 77 mg (78%) of **140** were obtained using **31** and **78**, respectively. Compound **140** was isolated by flash chromatography (gradient: 10→15% EtOAc /hexanes, R_f = 0.20 in 20% EtOAc/hexanes) as an off-white solid. Mp: 115–116°C; ^{1}H-NMR (300 MHz, $CDCl_3$) δ 8.16 (d, J = 3.9 Hz, 1H), 7.38 (dt, J = 7.8, 1.8 Hz, 1H), 7.16 (s, 3H), 6.64 (dd, J = 6.6, 5.4 Hz, 1H), 6.28 (br s, 1H), 6.02 (d, J = 8.4 Hz, 1H), 2.26 (s, 6H); ^{13}C-NMR (75 MHz, $CDCl_3$) δ 157.8, 148.5, 137.8, 136.7, 136.4, 128.5, 126.7, 113.6, 105.6, 18.3. HRMS (EI) [M^+] calcd. for $C_{13}H_{14}N_2$ 198.1157; found 198.1149.

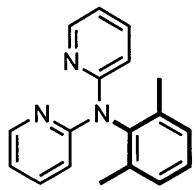

141

When **78** was used, 7.2 mg (11%) of triarylamine **141** was also isolated as an off-white solid. R_f = 0.11 (20% EtOAc/hexanes); Mp: 165-167°C; ^{1}H-NMR (300 MHz, $CDCl_3$) δ 8.33 (d, J = 3.6 Hz, 2H), 7.54 (dt, J = 7.8, 2.0 Hz, 2H), 7.28 – 7.16 (m, 3H), 6.97 (d, J = 8.4 Hz, 2H), 6.86 (dd, J = 7.2, 4.8 Hz, 2H), 2.06 (s, 6H); ^{13}C-NMR (75 MHz, $CDCl_3$) δ 156.2, 148.1, 141.2, 137.6, 137.4, 129.0, 127.8, 117.0, 114.2, 18.4. HRMS (EI) [M^+] calcd. for $C_{18}H_{17}N_3$ 275.1422; found 275.1425.

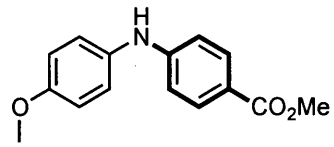

Methyl 4-((4-methoxyphenyl)amino)benzoate (147): Following general procedure B, 126 mg (98%) of **147** were isolated by flash chromatography (gradient: hexanes →5%→10% EtOAc/hexanes, R_f = 0.13 in 10% EtOAc/hexanes) as a white solid. Mp: 74–75°C; ^{1}H-NMR (300 MHz, $CDCl_3$) δ 7.89 (app d, J = 8.7 Hz, 2H), 7.14 (d, J = 8.8 Hz, 2H), 6.92 (app d, J = 8.9 Hz, 2H), 6.83 (app d, J = 8.7 Hz, 2H), 6.06 (br s, 1H), 3.87

(s, 3H), 3.83 (s, 3H); ^{13}C-NMR (75 MHz, $CDCl_3$) δ 167.1, 156.3, 149.8, 133.3, 131.4, 124.2, 119.7, 114.6, 113.1, 55.4, 51.5. The spectral data are consistent with those reported in the literature.[64b]

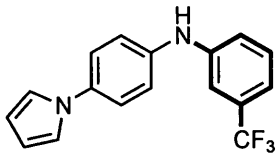

***N*-(4-(1*H*-Pyrrol-1-yl)phenyl)-3-(trifluoromethyl)aniline (148)**: Following general procedure B, 145 mg (96%) of **148** were isolated as a white solid by triturating the crude residue with pentane (x3). Mp: 107–108°C; ^{1}H-NMR (400 MHz, $CDCl_3$) δ 7.43 – 7.37 (m, 3H), 7.31 (s, 1H), 7.23 – 7.17 (m, 4H), 7.13 – 7.12 (m, 2H), 6.43 (t, J = 1.6 Hz, 2H), 5.85 (s, 1H); ^{13}C-NMR (100 MHz, $CDCl_3$) δ 144.0 (+), 139.5 (+), 135.7 (+), 131.8 (+, q, $^2J_{CF}$ = 32.2 Hz), 129.9 (–), 124.0 (+, q, $^1J_{CF}$ = 272.7 Hz), 121.9 (–), 120.1 (–), 119.6 (–), 119.4 (–), 117.0 (–, q, $^3J_{CF}$ = 4.0 Hz), 113.0 (–, q, $^3J_{CF}$ = 4.0 Hz), 110.1 (–); HRMS (EI) [M^+] calcd. for $C_{17}H_{13}F_3N_2$; 302.1031; found 302.1036.

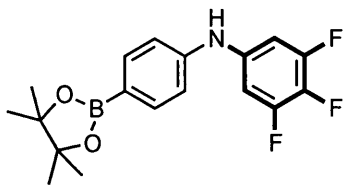

3,4,5-trifluoro-*N*-(4-(4,4,5,5-Tetramethyl-1,3,2-dioxaborolan-2-yl)phenyl)aniline (149): Following general procedure B, 131 mg (75%) of **149** were isolated by flash chromatography (gradient: hexanes→5%→10% EtOAc/hexanes, R_f = 0.32 in 10% EtOAc/hexanes) as a light-yellow solid. ^{1}H-NMR (300 MHz, $CDCl_3$) δ 7.77 (d, J = 8.4 Hz, 2H), 7.03 (d, J = 8.4 Hz, 2H), 6.75 – 6.64 (m, 2H), 5.84 (s, 1H), 1.37 (s, 12H); ^{13}C-NMR (75 MHz, $CDCl_3$) δ 151.7 (ddd, J_{CF} = 247.6, 10.6, 6.0 Hz), 144.3, 138.4 (dt, J_{CF} = 11.0, 3.0 Hz), 136.4, 134.6 (dt, J_{CF} = 244.5, 15.3 Hz), 117.0, 102.0 – 101.7 (m), 83.7, 24.8 [quaternary carbon adjacent to B not detected]; HRMS (EI) [M^+] calcd. for $C_{18}H_{19}BF_3NO_2$ 349.1461; found 349.1474.

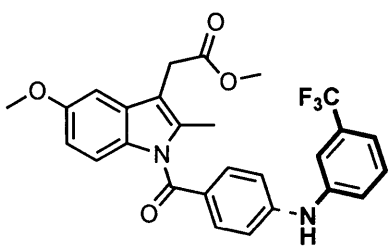

Methyl 2-(5-methoxy-2-methyl-1-(4-((3-(trifluoromethyl)phenyl)amino)benzoyl)-1*H*-indol-3-yl)acetate (150): Following general procedure B, 238 mg (96%) of **150** were isolated as an off-white solid by triturating the crude residue with pentane (x3). R_f = 0.34 (20% EtOAc/hexanes); Mp: 153–154°C; ^{1}H-NMR (400 MHz, $CDCl_3$) δ 7.68 (d, J = 8.4 Hz, 2H), 7.46 (t, J = 7.8 Hz, 1H), 7.43 (s, 1H), 7.37 (d, J = 8.0 Hz; 1H), 7.32 (d, J = 7.6 Hz, 1H), 7.05 (d, J = 8.4 Hz, 2H), 7.19 – 6.96 (m, 2H), 6.70 (dd, J = 8.8, 2.4 Hz, 1H), 6.42 (s, 1H), 3.86 (s, 3H), 3.73 (s, 3H), 3.71 (s, 2H), 2.45 (s, 3H); ^{13}C-NMR (100 MHz, $CDCl_3$) δ 171.6 (+), 168.6 (+), 155.6 (+), 147.4 (+), 141.3 (+), 136.1 (+), 132.6 (–), 132.0 (+, q, $^2J_{CF}$ = 31.2 Hz), 131.1 (+), 130.2 (+), 130.1 (–), 126.7 (+), 123.8 (+, q, $^1J_{CF}$ = 272.7 Hz), 122.9 (–), 119.5 (–, q, $^3J_{CF}$ = 3.5 Hz), 116.5 (–, q, $^3J_{CF}$ = 3.3 Hz), 115.2 (–), 114.7 (–), 111.4 (–), 111.3 (+), 100.9 (–), 55.7 (–), 52.1 (–), 30.2 (+), 13.0 (–); HRMS (EI) [M^+] calcd. for $C_{27}H_{23}F_3N_2O_4$ 496.1610; found 496.1625.

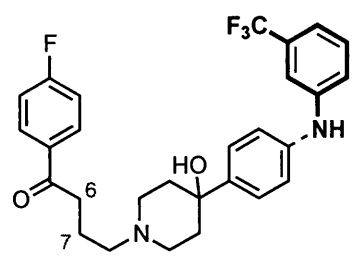

1-(4-fluorophenyl)-4-(4-hydroxy-4-(4-((3-(trifluoromethyl)phenyl)amino)phenyl)piperidin-1-yl)butan-1-one (151): Following general procedure B with the exception that the reaction was heated at 45°C, 229 mg (91%) of **151** were obtained as an off-white solid by triturating the crude residue with pentane (x3) then by purification of the resulting solid via flash chromatography (pre-adsorbed onto Celite, gradient: CH_2Cl_2→5%→10% MeOH/ CH_2Cl_2, R_f = 0.19 in 6% MeOH/CH_2Cl_2). Mp: 137–139°C; ^{1}H-NMR (400 MHz, CD_3OD) δ 8.12 – 8.08 (m, 2H), 7.42 (d, J = 8.8 Hz, 2H), 7.36 (t, J = 8.2 Hz, 1H), 7.27 – 7.21 (m, 4H), 7.13 (d, J = 8.4 Hz, 2H), 7.04 (d, J = 7.6 Hz, 1H), 3.12 – 3.05 (m, 2H), 2.98 (d, J = 11.2 Hz, 2H), 2.74 (t, J = 11.4 Hz, 2H), 2.67 (t, J = 7.6 Hz, 2H), 2.13 (dt, J = 13.1, 3.5 Hz, 2H), 2.04 (quint, J = 7.6 Hz, 2H), 1.82 (d, J = 13.2 Hz, 2H) [exchangeable OH and NH protons were not observed]; ^{13}C-NMR (100 MHz, CD_3OD) δ 198.4 (+), 165.7 (+, d, $^1J_{CF}$ = 252.6 Hz), 145.0 (+), 141.2 (+), 141.0 (+), 133.4 (+, d, $^4J_{CF}$ = 3.0 Hz), 131.0

(+, q, $^2J_{CF}$ = 31.7 Hz), 130.5 (–, d, $^3J_{CF}$ = 9.1 Hz), 129.4 (–), 125.6 (–), 124.3 (+, q, $^1J_{CF}$ = 271.4 Hz), 118.6 (–), 118.0 (–), 115.1 (–, d, $^2J_{CF}$ = 22.1 Hz), 114.9 (–, q, $^3J_{CF}$ = 4.0 Hz), 111.5 (–, q, $^3J_{CF}$ = 4.0 Hz), 69.4 (+), 57.1 (+), 49.0 (+), 36.7 (+), 35.4 (+), 20.2 (+). ^{19}F-NMR (376 MHz, $CDCl_3$) δ -64.3 (s, 3F), -107.8 (m, 1F); HRMS (EI) [M^+] calcd. for $C_{28}H_{28}F_4N_2O_2$ 500.2087; found 500.2069. Note that complete ^{1}H-^{2}H exchange of the ketone α-protons at C6 occurs over a period of 24 h after dissolution in CD_3OD, resulting in the disappearance of the ^{1}H resonance at 3.12 – 3.15 ppm and a change in the multiplicity of the resonance at 2.04 ppm from a quintet to a triplet. Similarly, the disappearance of the ^{13}C resonance at 35.4 ppm and the appearance of an equal-intensity triplet at 34.7 ppm (J_{CD} = 18.1 Hz) was observed.

5.7 – X-ray Crystallography of Pd-PEPPSI Complexes

X-ray data for complexes **73** and **75** – **78** were collected by Dr. Alan J. Lough (University of Toronto) on a Bruker Kappa APEX-DUO diffractometer using monochromated Mo-Kα radiation (0.71073 Å; Bruker Triumph) and were measured using a combination of φ scans and ω scans at 147 K. The data were processed using APEX2 and SAINT.[130] Absorption corrections were carried out using SADABS.[130] The structure was solved and refined using SHELXTL for full-matrix least-squares refinement that was based on F^2 atoms were included in calculated positions and allowed to refine in riding-motion approximation with U~iso~ tied to the carrier atom.[131]

Table 13. Crystal data and structure refinement for **73**

Space group	P n m a	
Unit cell dimensions	a = 18.2385(13) Å	a= 90°.
	b = 17.1739(12) Å	b= 90°.
	c = 10.4158(8) Å	g = 90°.
Volume	3262.5(4) $Å^3$	
Z	4	
Density (calculated)	1.523 Mg/m^3	
Absorption coefficient	1.005 mm^{-1}	
F(000)	1528	
Crystal size	0.19 x 0.17 x 0.05 mm^3	
Theta range for data collection	2.23 to 27.54°	
Reflections collected	16270	
Independent reflections	3886 [R(int) = 0.0535]	
Completeness to theta = 27.54°	99.7 %	
Absorption correction	Semi-empirical from equivalents	
Max. and min. transmission	0.9514 and 0.8319	
Data / restraints / parameters	3886 / 0 / 206	
Goodness-of-fit on F^2	1.030	
Final R indices [I>2sigma(I)]	R1 = 0.0320, wR2 = 0.0691	
R indices (all data)	R1 = 0.0517, wR2 = 0.0776	
Largest diff. peak and hole	0.906 and -0.524 $e.Å^{-3}$	

Table 14. Crystal data and structure refinement for **75**

Space group	P -1	
Unit cell dimensions	a = 9.8594(9) Å	a= 75.639(2)°.
	b = 13.7360(11) Å	b= 70.790(2)°.
	c = 14.9054(13) Å	g = 71.738(2)°.
Volume	1786.4(3) $Å^3$	
Z	2	
Density (calculated)	1.542 Mg/m^3	
Absorption coefficient	2.823 mm^{-1}	
F(000)	830	
Crystal size	0.32 x 0.17 x 0.05 mm^3	
Theta range for data collection	1.47 to 27.56°.	
Reflections collected	18119	
Independent reflections	8177 [R(int) = 0.0290]	
Completeness to theta = 27.56°	98.9 %	
Absorption correction	Semi-empirical from equivalents	
Max. and min. transmission	0.7456 and 0.6293	
Data / restraints / parameters	8177 / 0 / 380	
Goodness-of-fit on F^2	1.073	
Final R indices [I>2sigma(I)]	R1 = 0.0335, wR2 = 0.0807	
R indices (all data)	R1 = 0.0507, wR2 = 0.0856	
Largest diff. peak and hole	0.758 and -0.999 $e.Å^{-3}$	

Table 15. Crystal data and structure refinement for **76**

Space group	P -1	
Unit cell dimensions	a = 9.6333(18) Å	a= 76.447(4)°.
	b = 13.685(3) Å	b= 72.353(4)°.
	c = 14.804(3) Å	g = 72.800(4)°.
Volume	1754.1(6) $Å^3$	
Z	2	
Density (calculated)	1.339 Mg/m^3	
Absorption coefficient	0.783 mm^{-1}	
F(000)	732	
Crystal size	0.21 x 0.18 x 0.12 mm^3	
Theta range for data collection	1.46 to 27.55°.	
Reflections collected	34972	
Independent reflections	8058 [R(int) = 0.0353]	
Completeness to theta = 27.55°	99.4 %	
Absorption correction	Semi-empirical from equivalents	
Max. and min. transmission	0.7455 and 0.6910	
Data / restraints / parameters	8058 / 0 / 380	
Goodness-of-fit on F^2	1.054	
Final R indices [I>2sigma(I)]	R1 = 0.0319, wR2 = 0.0746	
R indices (all data)	R1 = 0.0401, wR2 = 0.0779	
Largest diff. peak and hole	1.177 and -0.539 $e.Å^{-3}$	

Table 16. Crystal data and structure refinement for **77**.

Space group	P 21/n	
Unit cell dimensions	a = 12.213(2) Å	a= 90°.
	b = 18.246(3) Å	b= 92.310(4)°.
	c = 17.091(3) Å	g = 90°.
Volume	3805.5(12) $Å^3$	
Z	4	
Density (calculated)	1.413 Mg/m^3	
Absorption coefficient	0.736 mm^{-1}	
F(000)	1664	
Crystal size	0.41 x 0.36 x 0.14 mm^3	
Theta range for data collection	1.63 to 27.53°.	
Reflections collected	33538	
Independent reflections	8746 [R(int) = 0.0323]	
Completeness to theta = 27.53°	99.7 %	
Absorption correction	Semi-empirical from equivalents	
Max. and min. transmission	0.7456 and 0.6908	
Data / restraints / parameters	8746 / 0 / 450	
Goodness-of-fit on F^2	1.040	
Final R indices [I>2sigma(I)]	R1 = 0.0250, wR2 = 0.0573	
R indices (all data)	R1 = 0.0321, wR2 = 0.0608	
Largest diff. peak and hole	0.415 and -0.511 $e.Å^{-3}$	

Table 17. Crystal data and structure refinement for **78**.

Space group	P -1	
Unit cell dimensions	a = 11.300(5) Å	a= 95.213(9)°.
	b = 12.698(5) Å	b= 92.716(8)°.
	c = 14.640(6) Å	g = 100.168(9)°.
Volume	2054.8(14) $Å^3$	
Z	2	
Density (calculated)	1.391 Mg/m^3	
Absorption coefficient	0.808 mm^{-1}	
F(000)	892	
Crystal size	0.38 x 0.18 x 0.08 mm^3	
Theta range for data collection	1.64 to 27.56°.	
Reflections collected	25544	
Independent reflections	9368 [R(int) = 0.0330]	
Completeness to theta = 27.56°	98.8 %	
Absorption correction	Semi-empirical from equivalents	
Max. and min. transmission	0.7456 and 0.6991	
Data / restraints / parameters	9368 / 0 / 450	
Goodness-of-fit on F^2	1.021	
Final R indices [I>2sigma(I)]	R1 = 0.0284, wR2 = 0.0619	
R indices (all data)	R1 = 0.0377, wR2 = 0.0666	
Largest diff. peak and hole	0.413 and -0.501 $e.Å^{-3}$	

CHAPTER 6: References

1. Johansson Seechurn, C. C. C.; Kitching, M. O.; Colacot, T. J.; Snieckus, V. *Angew. Chem Int. Ed.* **2012**, *51*, 5062-5085.
2 "The Nobel Prize in Chemistry 2010". Nobelprize.org. 26 Mar 2013, http://www.nobelprize.org/nobel_prizes/chemistry/laureates/2010/
3. Hartwig, J. F. *The Organometallic Chemistry of the Transition Metals: From Bonding to Catalysis*; University Science: Sausalito, CA: 2010.
4. *Metal-catalyzed cross-coupling reactions*, 2nd ed.; de Meijere, A., Diederich, F. Eds.; Wiley: New York, 2004.
5. (a) Mizoroki, T.; Mori, K.; Ozaki, A. *Bull. Chem. Soc. Jpn.* **1973**, *46*, 1505–1508. (b) Mizoroki, T.; Mori, K.; Ozaki, A. *Bull. Chem. Soc. Jpn.* **1971**, *44*, 581. (c) Dieck, H. A.; Heck, R. F. *J. Am. Chem. Soc.* **1974**, *96*, 1133–1136; (d) Heck, R. F.; Nolley, J. P. Jr. *J. Org. Chem.* **1972**, *37*, 2320–2322.
6. *Catalyzed Carbon-Heteroatom Bond Formation*, 1st ed.; Yudin, A. K. (Ed.); Wiley: New York, 2011.
7. For selected examples of Pd-catalyzed C-O coupling of phenols, see: (a) Aranyos, A.; Old, D. W.; Kiyomori, A.; Wolfe, J. P.; Sadighi, J. P.; Buchwald, S. L. *J. Am. Chem. Soc.* **1999**, *121*, 4369; (b) Mann, G.; Incarvito, C.; Rheingold, A. L.; Hartwig, J. F.; *J. Am. Chem. Soc.* **1999**, *121*, 3224; (c) Harkal, S.; Kumar, K.; Michalik, D.; Zapf, A.; Jackstell, R.; Rataboul, F.; Riermeier, T.; Monsees, A.; Beller, M. *Tetrahedron Lett.* **2005**, *46*, 3237; (d) Burgos, C. H.; Barder, T. E.; Huang, X.; Buchwald, S. L. *Angew. Chem. Int. Ed.* **2006**, *45*, 4321; (e) Hu, T.; Schulz, T.; Torborg, C.; Chen, X.; Wang, J.; Beller, M.; Huang, J. *Chem. Commun.* **2009**, 7330.
8. For selected examples of Pd-catalyed C-O coupling of aliphatic alcohols, see: (a) Shelby, Q.; Kataoka, N.; Mann, G.; Hartwig, J. F.; *J. Am. Chem. Soc.* **2000**, *122*, 10718; (b) Parrish, C. A.; Buchwald, S. L. *J. Org. Chem.* **2001**, *66*, 2498; (c)

Kuwabe, S-I.; Torraca, K. E.; Buchwald, S. L. *J. Am. Chem. Soc.* **2001**, *123*, 12202; (d) Wu, X.; Fors, B. P.; Buchwald, S. P. *Angew. Chem. Int. Ed.* **2011**, *50*, 9943.

9. For a recent review of metal-catalyzed C-S coupling, see: Bichler, P.; Love, J. A. *Top. Organomet. Chem.* **2010**, *31*, 39–64.
10. For recent reviews on metal-cataluzed C-P bond formation, see: (a) Tappe, F. M. J.; Trepohl, V. T.; Oestreich, M. *Synthesis* **2010**, *18*, 3037–3062; (b) Gleuck, D. S. *Top. Organomet. Chem.* **2010**, *31*, 65–100.
11. For selected examples of Pd-catalyzed aminations forming biologically active compounds, see: (a) Decker, M.; Si, Y.-G.; Knapp, B. I.; Bidlack, J. M.; Neumever, J. L.; *J. Med. Chem.* **2010**, *53*, 402–418; (b) Sandanayaka, V.; Mamat, B.; Mishra, R. K.; Winger, J.; Krohn, M.; Zhou, L.-M.; Keyvan, M.; Enache, L.; Sullins, D.; Onau, E.; Zhang, J.; Hallorsdottir, G.; Sigthorsdottir, H.; Thorlaksdottir, A.; Sigthorsson, G.; Thorsteinnsdottir, M.; Davies, D. R.; Stewart, L. J.; Zembower, D. E; Andresson, T.; Kiselvov, A. S.; Singh, J.; Gurney, M. E. *J. Med. Chem.* **2010**, *53*, 573–585.
12. For select reviews on the use of cross-coupling in total synthesis, see: (a) Nicolaou, K. C.; Bulger, P. G.; Sarlah, D.; *Angew. Chem. Int. Ed.* **2005**, *44*, 4442–4489; (b) Torborg, C.; Beller, M. *Adv. Synth. Catal.* **2009**, *351*, 3027–3043.
13. Adapted from ref. 1.
14. Larsen, R. D.; King, A. O.; Chen, C. Y.; Corley, E. G.; Foster, B. S.; Roberts, F. E.; Yang, C.; Liebermann, D. R.; Reamer, R. A.; Tschaen, D. M.; Verhoeven, T. R.; Reider, P. J.; Lo, Y. S.; Rossano, L. T.; Brookes, A. S.; Meloni, D.; Moore, J. R.; Arnett, J. F. *J. Org. Chem.* **1994**, *59*, 6391–6934.
15. de Koning, P. D.; McAndrew, D.; Moore, R.; Moses, I. B.; Boyles, D. C.; Kissick, K.; Stanchina, C. L.; Cuthbertson, T.; Kamatani, A.; Rahman, L.; Rodriguez, R.; Urbina, A.; Sandoval (née Accacia) A.; Rose, P. R. *Org. Proc. Res. Dev.* **2011**, *15*, 1011–1026.

16. (a) Shinkai, I.; King, A. O.; Larsen, R. D.; *Pure Appl. Chem.* **1994**, *66*, 1551–1556; (b) King, A. O.; Corley, E. G.; Anderson, R. K.; Larsen, R. D.; Verhoeven, T. R.; Reider, P. J.; Xiang, Y. B.; Belley, M.; Leblanc, Y.; Labelle, M.; Prasit, P.; Zamboni, R. J.; *J. Org. Chem.* **1993**, *58*, 3731–3735; (c) Higgs, G.; *Chem. Ind.* **1997**, 827–830.

17. a) Smith III, A. B.; Beauchamp, T. J.; LaMarche, M. J.; Kaufman, M. D.; Qiu, Y.; Arimoto, H.; Jones, D. R.; Kobayashi, K. *J. Am. Chem. Soc.* **2000**, *122*, 8654–8664; b) Smith III, A. B.; Kaufman, M. D.; Beauchamp, T. J.; LaMarche, M. J.; Arimoto, H. *Org. Lett.* **1999**, *1*, 1823–1826.

18. a) Nicolaou, K. C.; Rao, P. B.; Hao, J.; Reddy, M. V.; Rassias, G.; Huang, X.; Chen, D. Y.-K.; Snyder, S. A. *Angew. Chem. Int. Ed.* **2003**, *42*, 1753–1758; b) Nicolaou, K. C.; Hao, J.; Reddy, M. V.; Rao, P. B.; Rassias, G.; Snyder, S. A.; Huang, X; Chen, D. Y.-K.; Brenzovich, W. E.; Giuseppone, N.; Giannakakou, P.; O'Brate, W. E. *J. Am. Chem. Soc.* **2004**, *126*, 12897–12906.

19. Lebsack, A. D.; Link, J. T.; Overman, L. E.; Stearns, B. A. *J. Am. Chem. Soc.* **2002**, *124*, 9008–9009.

20. For a detailed account of the development of modern ancillary ligands in Pd-catalyzed cross-coupling reactions, see: Lundgren, R. J.; Stradiotto, M. *Chem. Eur. J.* **2012**, *18*, 9758–9769.

21. Tolman, C. A. *Chem. Rev.* **1977**, *77*, 313–348.

22. For a review on the TEP and other methods for the measurement of net donor properties of phosphines, NHCs, and related ligands, see: Gusev, D. G. *Organometallics* **2009**, *28*, 763–770.

23. Kharamov, D. M.; Lynch, V. M.; Biewlawski, C. W.; *Organometallics* **2007**, *26*, 6042–6049.

24. Crabtree, R. H. *The Organometalic Chemistry of the Transition Metals;* 5th ed.; Wiley and Sons, **2009.**

25. For an account of the development of conditions for cross-coupling aryl chlorides and other traditionally unreactive electrophiles, see: (a) Fu, G. C. *Acc. Chem. Res.* **2008**, *41*, 1555–1564; (b) Littke, G. C.; Fu, G. C. *Angew. Chem. Int. Ed.* **2002**, *41*, 4176–4211.

26. (a) Littke, A. F.; Fu, G. C. *Angew. Chem. Int. Ed.* **1998**, *37*, 3387–3388; (b) Nishiyama, M.; Yamamoto, T.; Koie, Y. *Tetrahedron Lett.* **1998**, *39*, 2367–2370.

27. Zapf, A.; Ehrentraut, A.; Beller, M. *Angew. Chem. Int. Ed.* **2000**, *39*, 4153–4155.

28. QPhos ligand: (a) Shelby, Q.; Kataoka, N.; Mann, G.; Hartwig, J. F. *J. Am. Chem. Soc.* **2000**, *122*, 10718–10719; JosiPhos ligand: (b) Shen, Q.; Shekhar, S.; Stambuli, J. P.; Hartwig, J. F. *Angew. Chem. Int. Ed.* **2005**, *44*, 1371–1375; (c) Alvaro, E.; Hartwig, J. F. *J. Am. Chem. Soc.* **2009**, *131*, 7858–7868. (d) Review: Hartwig, J. F. *Acc. Chem. Res.* **2008**, *41*, 1534–1544.

29. For a review of the Buchwald family of dialkybiaryl phosphines, see: Martin, R.; Buchwald, S. M. *Acc. Chem. Res.* **2008**, *41*, 1461–1473.

30. Dixon, D.A.; Dobbs, K. D.; Arduengo III, A. J.; Bertrand, G. *J. Am. Chem. Soc.* **1991**, *113*, 8782

31. (a) *Handbook of Metathesis*; Grubbs, R. H. Ed.; Wiley-VCH: Weinheim, Germany, 2003; Vols 1–3; (b) Blechert, S.; Connon, S. J. *Angew. Chem., Int. Ed.* **2003**, *42*, 1900–1923; (c) Schrock, R. R.; Hoveyda, A. H. *Angew. Chem., Int. Ed.* **2003**, *42*, 4592–4633.

32. (a) Lee, H. M.; Jiang, T.; Stevens, E. D.; Nolan, S. P. *Organometallics* **2001**, *20*, 1255–1258; (b) Hillier, A. C.; Lee, H. M.; Stevens, E. D.; Nolan, S. P. *Organometallics* **2001**, *20*, 4246–4252; (c) Vasquez-Serrano, L. D.; Owens, B. T.; Buriak, J. M. *Chem. Commun.* **2002**, 2518–2519.

33. (a) Markó, I. E.; Stérin, S.; Buisine, O.; Mignani, G.; Branlard, P.; Tinant, B.; Declerq, J.-P. *Science* **2002**, *298*, 204–208; (b) Díez-Gonzalez, S.; Kaur, H.; Kauer Zinn, F.; Stevens, E. D.; Nolan, S. P. *J. Org. Chem.* **2005**, *70*, 4784–4798.

34. (a) For a recent review, see: Kantchev, E. A. B.; O'Brien, C. J.; Organ, M. G. *Angew. Chem. Int. Ed.* **2007**, *46*, 2768–2813; (b) Herrmann, W. A.; Öfele, K.; Preysing, D. V.; Schneider, S. K. J. *Organomet. Chem.* **2003**, *687*, 229–248; (c) Navarro, O.; Kelly, R. A., III; Nolan, S. P. *J. Am. Chem. Soc.* **2003**, *125*, 16194–16195; (c) Marion, N.; Ecarnot, E. C.; Navarro, O.; Amoroso, D.; Bell, A.; Nolan, S. P. *J. Org. Chem.* **2006**, *71*, 3816–3821; (d) Organ, M. G.; Chass, G. A.; Fang, D.-C.; Hopkinson, A. C.; Valente, C. *Synthesis* **2008**, *17*, 2776–2797.

35. De Lewis, A. K.; Caddick, S.; Cloke, F. G. N.; Billingham, N. C.; Hitchcock, P. B.; Leonard, J. *J. Am. Chem. Soc.* **2003**, *125*, 10066–10073

36. (a) *N-heterocyclic Carbenes in Transition Metal Catalysis and Organocatalysis*. Cazin, C. S. J., Ed.; Springer: New York, 2011; (b) Glorius, F. (Ed.); *Top. Organomet. Chem.* **2007,** *21*, 1–20.

37. Trnka, T. M.; Grubbs, R. H. *Acc. Chem. Res.* **2001**, *34*, 18–29.

38. Altenhoff, G.; Würtz, S.; Glorius, F. *Tetrahedron Lett.* **2006**, *47*, 2925–2928.

39. Organ, M. G.; Çalimsiz, S.; Sayah, M.; Hoi, K. H.; Lough, A.J. *Angew. Chem. Int. Ed.* **2009**, *48*, 2383–2387.

40. Berthon-Gelloz, G.; Siegler, M. A.; Spek, A. L.; Tinant, B.; Reek, J. N. H.; Markó, I. E. *Dalton Trans.* **2010**, *36*, 1444–1446.

41. (a) Wu, L.; Drinkel, E.; Gaggia, F.; Capolicchio, S.; Linden, A.; Falivene, L.; Cavallo, L.; Dorta, R. *Chem. -Eur. J.* **2011**, *17*, 12886–12890; (b) Luan, X.; Mariz, R.; Gatti, M.; Costabile, C.; Poater, A.; Cavallo, L.; Linden, A.; Dorta, R. *J. Am. Chem. Soc.* **2008**, *130*, 6848–6858.

42. Wanzlick, H. W.; Schoenherr, H. J. *Angew. Chem., Int. Ed. Engl.* **1968,** *7,* 141.

43. Öfele, K. *J. Organomet. Chem.* **1968**, *12*, 42.

44. (a) Hillier, A. C.; Sommer, W. J.; Yong, B. S.; Peterson, J. L.; Cavallo, L.; Nolan, S. P. *Organometallics* **2003**, *22*, 4322–4326; For an online application that can be used to compute $\%V_{Bur}$, see: (b) Poater, A.; Cosenza, B.; Correa, A.; Giudice, S.; Ragone,

F.; Scarano, V.; Cavallo, L. *Eur. J. Inorg. Chem.* **2009**, 1759–1766. <http://www.molnac.unisa.it/OMtools/sambvca.php>

45. Dorta, R.; Stevens, E. D.; Scott, N. M.; Costabile, C.; Cavallo, L.; Hoff, C. D.; Nolan, S. P. *J. Am. Chem. Soc.* **2005**, *127*, 2485–2495.
46. (a) Clavier, H.; Nolan, S. P. *Chem. Commun.* **2010**, *46*, 841–861; (b) Diebolt, O.; Fortman, G. C.; Clavier, H.; Slawin, A. M. Z.; Escudero-Adán, E. C.; Benet-Buchholz, J.; Nolan, S. P. *Organometallics* **2011**, *30*, 1668–1676.
47. Chianese, A. R.; Li, X.; Janzen, M. C.; Faller, J. W.; Crabtree, R. H. *Organometallics* **2003**, *22*, 1663–1667.
48. Chianese, A. R.; Kovacevic, A.; Zeglis, B. M.; Faller, J. W.; Crabtree, R. H. *Organometallics* **2004**, *23*, 2461–2468.
49. (a) Altenhoff, G.; Goddard, R.; Lehmann, C. W.; Glorius, F. *J. Am. Chem. Soc.* **2004**, *126*, 15195–15201; (b) Altenhoff, G.; Goddard, R.; Lehmann, C. W.; Glorius, F. *Angew. Chem. Int. Ed.*, **2003**, *42*, 3690– 3693.
50. Frey, G. D.; Rentzshe, C. F.; von Preysing, D.; Scherg, T.; Muehlhofer, M.; Herdtweck, E.; Herrmann, W. A. *J. Organomet. Chem.* **2006**, *691*, 5725–5738.
51. Kelly III, R. A.; Clavier, H.; Giudice, S.; Scott, N. M.; Stevens, E. D.; Bordner, J.; Samardjiev, I.; Hoff, C. D.; Cavallo, L.; Nolan, S. P. *Organometallics* **2008**, *27*, 202–210.
52. For a recent review of the electronic properties of NHC ligands, see: Nelson, D. J.; Nolan, S. P. *Chem. Soc. Rev.* **2013**, *42*, 6723–6753.
53. Khramov, D. M.; Lynch, V. M.; Biewlawski, C. W. *Organometallics* **2007**, *26*, 6042–6049.
54. Leuthuäßer, S.; Schwarz, D.; Plenio, H. *Chem. Eur. J.* **2007**, *13*, 7195–7203.
55. For a detailed review of modern phosphine and NHC-Pd pre-catalysts, see: Li, H.; Johansson Seechurn, C. C. C.; Colacot, T. J. *ACS Catal.* **2012**, *2*, 1147–1164.

56. Organ, M. G.; Avola, S.; Dubovyk, I.; Hadei, N.; Kantchev, E. A. B.; O'Brien, C. J.; Valente, C. *Chem. Eur. J.* **2006**, *12*, 4749–4755.

57. Valente, C.; Baglione, S.; Candito, D.; O'Brien, C. J.; Organ, M. G. *Chem. Commun.* **2008**, 735–736.

58. Organ, M. G.; Abdel-Hadi, M.; Avola, S.; Hadei, N.; Nasielski, J.; O'Brien, C. J.; Valente, C. *Chem. Eur. J.* **2007**, *13*, 150–157.

59. Organ, M. G.; Abdel-Hadi, M.; Avola, S.; Dubovyk, I.; Hadei, N.; Kantchev, E. A. B.; O'Brien, C. J.; Valente, C. *Chem. Eur. J.,* **2008**, *14*, 2443–2452.

60. For a review on the development of the second generation of Pd-PEPPSI complexes, see: Valente, C.; Calimsiz, S.; Hoi, K. H.; Mallik, D.; Sayah, M.; Organ, M. G. *Angew. Chem. Int. Ed.* **2012**, *51*, 3314–3332.

61. (a) Organ, M. G.; Calimsiz, S.; Sayah, M.; Hoi, K. H.; Lough, A. J. *Angew. Chem. Int. Ed.* **2009**, *48*, 2383–2387; (b) Farmer, J. L.; Hunter, H. N.; Organ, M. G. *J. Am. Chem. Soc.* **2012**, *134*, 17470–174473

62. (a) Calimsiz, S.; Sayah, M.; Mallik, D.; Organ, M. G. *Angew. Chem. Int. Ed.* **2010**, *49*, 2014–2017; (b) Calimsiz, S.; Organ, M. G. *Chem. Commun.* **2011**, *47*, 5181–5183.

63. Dowlut, M.; Mallik, D.; Organ, M. G. *Chem. Eur. J.* **2010**, *16*, 4279–4283.

64. (a) Hoi, K.H.; Calimsiz, S.; Froese, R. D. J.; Hopkinson, A. C.; Organ, M. G. *Chem. Eur. J.* **2011**, *17*, 3086–3090; (b) Hoi, K.H.; Calimsiz, S.; Froese, R. D. J.; Hopkinson, A. C.; Organ, M. G. *Chem. Eur. J.* **2012**, *18*, 145– 51.

65. Sayah, M.; Calimsiz, S.; Organ, M. G. **2008**, *Unpublished work.*

66. (a) Arduengo III, A. J.; Davidson, F.; Dias, H. V. R.; Goerlich, J. R.; Khasnis, D.; Marshall, W. J.; Prakasha, T. K. *J. Am. Chem. Soc.* **1997**, *119*, 12742–12749; (b) Arduengo III, A. J.; Krafczyk, R.; Schumutzler, R.; Craig, H. A.; Goerlich, J. R.; Marshall, W. J.; Unverzagt, M. *Tetrahedron* **1999**, *55*, 14523–14534.

67. Gaillard, S.; Bantreil, X.; Slawin, A. M. Z.; Nolan, S. P. *Dalton Trans.* **2009**, 6967–6971.
68. Sanderson, M. D.; Kamplain, J. W.; Bielawski, C. W. *J. Am. Chem. Soc.* **2006**, *128*, 16514–16515
69. Mendoza-Espinosa, D.; Donnadieu, B.; Bertrand, G. *J. Am. Chem. Soc.* **2010**, *132*, 7264–7265.
70. For a review of the use of N-F electrophilic fluorinating reagents, see: Lal, G. S.; Pez, G. P.; Syvret, R. G. *Chem. Rev.* **1996,** *96*, 1737–1755.
71. For a concise review of *N*-fluoropyridinium chemistry, see: Kiselyov, A. S. *Chem. Soc. Rev.* **2005**, *34,* 1031–1037.
72. Hayashi, H.; Sonoda, H.; Fukumura, K.; Nagata, T. *Chem. Commun.* **2002**, 1618–1619.
73. Tang, P.; Wang, W.; Ritter, T. *J. Am. Chem. Soc.* **2011,** *133*, 11482–11484.
74. Solovyev, A.; Lacôte, E.; Curran, D. P. *Org. Lett.* **2011**, *13*, 6042–6045.
75. Ueng, S-H.; Brahmi, M. M.; Derat, É.; Fensterbank, L.; Lacôte, E.; Malacria, M.; Curran, D. P. *J. Am. Chem. Soc.* **2008**, *130*, 10082–10083.
76. For selected examples of the use of NFSI (**49**) in fluorination of organomagnesium and organolithium reagents, see: (a) Yang, M-H.; Matikonda, S. S.; Altman, R. A. *Org. Lett.* **2013**, *15*, 3894–3897; (b) Yamada, S.; Gavryushin, A.; Knochel, P. *Angew. Chem. Int. Ed.* **2010**, *49*, 2215–2218; (c) Snieckus, V.; Beaulieu, F.; Mohri, K.; Han, W.; Murphy, C. K.; Davis, F. A. *Tetrahedron Lett.* **1994**, *35*, 3465–3468.
77. *Organolithiums: Selectivity for Synthesis*; Clayden, J; Tetrahedron Organic Chemistry Series, Volume 23; Elsevier Science: Oxford, UK, 2002.
78. Schuh, K.; Glorius, F. *Synthesis* **2007**, *15*, 2297–2306.
79. Sayah. M.; **2010**, *Unpublished Work.*
80. The details of the synthesis of this aniline are outlined in Part II of this thesis.
81. Sayah, M.; Calimsiz, S.; Mallik, D.; Organ, M. G.; *Unpublished work.*

82. Viciu, M. S.; Kissling, R. M.; Stevens, E. D.; Nolan, S. P. *Org. Lett.* **2002**, *4*, 2229–2231.

83. Dowlut, M.; Organ, M. G. **2009**, *Unpublished Work.*

84. Clavier, H.; Correa, A.; Cavallo, L.; Escudero-Adán, E. C.; Benet-Bucholz, J.; Slawin, A. M. Z.; Nolan, S. P. *Eur. J. Inorg. Chem.* **2009**, 1767–1773.

85. A similar variation in $\%V_{Bur}$ was noted when moving from the linear [(NHC)Au(I)Cl] complexes to square planar [(NHC)Au(III)Cl_3] complexes: Gaillard, S.; Slawing, A. M. Z.; Bonura, A. T.; Stevens, E. D.; Nolan, S. P. *Organometallics* **2010**, *29*, 394–402.

86. Drug Information Online. Top 200 Drugs of 2012 .http://www.drugs.com/stats/top100/2012/sales (accessed Jul 20, 2013).

87. Lovering, F.; Bikker, J; Humblet, C. *J. Med. Chem.* **2009**, *52*, 6752–6756.

88. For a thorough review on the cross-coupling of alkyl organometallic reagents, see: Jana, R.; Pathak, T. P.; Sigman, M. S. *Chem. Rev.* **2011**, *111*, 1417–1492

89. Hayashi, T.; Konishi, M.; Kobori, Y.; Kumada, M.; Higuchi, T.; Hirotsy, K. *J. Am. Chem. Soc.,* **1984,** *106*, 158–163.

90. Dreher, S. D.; Dormer, P. G.; Sandrock, D. L.; Molander, G. A. *J. Am. Chem. Soc.* **2008**, *130*, 9257–9259.

91. van den Hoogenband, A.;. Lange, J. H. M.; Terpstra, J. M.; Koch, M.; Visser, G. M.; Visser, M.; Korstanje, T. J.; Jastrzebski, J. T. B. H. *Tetrahedron Lett.* **2008**, *49*, 4122–4124.

92. Han, C.; Buchwald, S. L. *J. Am. Chem. Soc.*, **2009**, *131*, 7532–7533.

93. Çalimsiz, S.; Organ, M. G. *Chem. Commun.* **2011**, *47*, 5181–5183.

94. Krasovskiy, A.; Malakhov, V.; Gavryushin, A.; Knochel, P.; *Angew. Chem. Int. Ed.* **2006**, *45*, 6040–6044.

95. In the case of 3-pentylzinc bromide, any product arising from BHE and MI into an adjacent carbon atom will be an isomer of the desired product, whereas in the case of

2-butylzinc bromide, re-insertion into the adjacent secondary carbon will result in the same product after RE.

96. Pompeo, M; Froese, R. D. J.; Hadei, N.; Organ, M. G. *Angew. Chem. Int. Ed.* **2012**, *51*, 1–5.

97. For selected examples, see: (a) Hooper, M. W.; Hartwig, J. F. *Organometallics* **2003**, *22*, 3394–3403; (b) Hooper, M. W.; Utsunomiya, M.; Hartwig, J. F. *J. Org. Chem.* **2003**, *68*, 2861–2873; (c) Su, M; Buchwald, S. P. *Angew. Chem. Int. Ed.* **2012**, *51*, 4710–4713.

98. Calculations performed at The Dow Chemical Company, Midland, MI 48674 (USA) at the B3LYP level with LANL2TZ(F) on Pd and 6-31G* on the remaining atoms

99. Using the Eyring equation, the following expression relating experimental selectivities and computed $\Delta\Delta E^{\ddagger}$ values can be derived: $\ln(n(E)/n(B)) = \ln(k_E/k_B) = \Delta\Delta E^{\ddagger}/RT$ where n(E)/n(B) is the molar ratio of regioisomers formed during the reaction (ie. the experimental selectivity) and k_E/k_S is the ratio of the rate constants associated with forming E and B, respectively. For a complete derivation, see the Supporting Information in ref. 98.

100. (a) Urgaonkar, S.; Xu, J.-H.; Verkade, J. G.; *J. Org. Chem.* **2003**, *68*, 8416–8423; b) Reddy, C. V.; Kingston, J. V.; Verkade, J. G.; *J. Org. Chem.* **2008**, *73*, 3047–3062.

101. Rataboul, F.; Zapf, A.; Jackstell, R.; Harkal, S.; Riermeier, T.; Monsees, A.; Dingerdissen, U.; Beller, M. *Chem. Eur. J.* **2004**, *10*, 2983–2990.

102. So, C. M.; Zhou, Z.; Lau, C. P.; Kwong, F. Y. *Angew. Chem. Int. Ed.* **2008**, *47*, 6402–6406.

103. Lundgren, R. J.; Peters, B. D.; Alsabeh, P. G.; Stradiotto, M.; *Angew. Chem. Int. Ed.* **2010**, *49*, 4071–4074

104. For some representative examples, see: (a) Ikawa, T.; Barder, T. E; Biscoe, M. R.; Buchwald, S. L. *J. Am. Chem. Soc.* **2007**, *129*, 13001–13007; (b) Ref. 59.

105. For some representative examples, see: (a) Hamann, B. C.; Hartwig, J. F.; *J. Am. Chem. Soc.* **1998**, *120*, 7369–7360; (b) Old, D. W.; Wolfe, J. P.; Buchwald, S. L. *J. Am. Chem. Soc.* **1998**, *120*, 9722–9723; (c) Shen, Q.; Shekhar, J. P.; Hartwig, J. F. *Angew. Chem. Int. Ed.* **2005**, *44*, 1371–1375; (d) Shen, Q.; Ogata, T.; Hartwig, J. F. *J. Am. Chem. Soc.* **2008**, *130*, 6586–6596.

106. Wolfe, J. P.; Buchwald, S. L. *Tetrahedron Lett.* **1997**, *38*, 6359–6362.

107. For a representative example, see: Meyers, C.; Maes, B. U. W.; Loones, K. T. J.; Bal, G.; Lemiere, G. L. F.; Dommisse, R. A. *J. Org. Chem.* **2004**, *69*, 6010–6017 and references therein.

108. Fors, B. P.; Krattiger, P.; Strieter, E.; Buchwald, S. L. *Org. Lett.* **2008**, *10*, 3505–3508.

109. For a review, see: Surry, D. S.; Buchwald, S. L. *Chem. Sci.* **2011**, *2*, 27–50.

110. Hoi, K. H.; Coggan, J. A.; Organ, M. G. *Chem. Eur. J.* **2013**, *19*, 843–845.

111. Sayah, M.; Lough, A. J.; Organ, M. G. *Chem. Eur. J.* **2013**, *19*, 2749–2756.

112. Fantasia, S.; Nolan, S. P. *Chem. Eur. J.* **2008**, *14*, 6987–6933.

113. Still, W.C.; Kahn, M.; Mitra, A. *J. Org. Chem*, **1978**, *43*, 2923–2925

114. Hintermann, L. *Beilsten J. Org. Chem.* **2007**, *3*, 1–5.

115. Hirano, K.; Urban, S. Wang, C.; Glorius, F. *Org. Lett.* **2009**, *11*, 1019–1022

116. Krasovskiy, A.; Knochel, P. *Synthesis* **2006**, *5*, 890-891.

117. Sulpizio, A.; Mella, M.; Albini, A. *Tetrahedron* **1989**, *45*, 7545–7552.

118. Joshi-Pangu, A.; Ganesh, M.; Biscoe, M. R. *Org. Lett.* **2011**, *13*, 1218–1221.

119. Corley, E. G.; Conrad, K.; Murry, J. A.; Savarin, C.; Holko, J.; Boice, G. *J. Org. Chem.* **2004**, *69*, 5120–5123.

120. 3-bromobenzofuran was prepared from benzofuran in two steps according to: Juhl, K.; Kehler, J.; Norgaard, M. B. U.S. Patent US 2006/0287386 A1, Dec 21, 2006.

121. *tert*-Butyl 3-bromo-1*H*-indole-1-carboxylate was prepared in 98% yield from *tert*-butyl 1*H*-indole-1-carboxylate according to: James, C. A.; Coelho, A. L.; Gevaert, M.; Forgione, P.; Snieckus, V. *J. Org. Chem.* **2009**, *74*, 4094–4103.

122. 1-Bromoindene was prepared in 26% yield from 1-indanone according to: Spaggiari, A.; Vaccari, D.; Davoli, P.; Torre, G.; Prati, F. *J. Org. Chem.* **2007**, *72*, 2216–2219.

123. 2-Bromobenzo[*b*]thiophene was prepared in 59% yield from benzo[*b*]thiophene according to: Krajewski, K.; Zhang, Y.; Parrish, D.; Deschamps, J.; Roller, P. P.; Pathak, V. K. *Bioorg. Med. Chem. Lett.* **2006**, *16*, 3034–3038.

124. 2-Bromobenzofuran was prepared in two steps from salicylaldehyde in 39% overall yield according to: Newman, S. G.; Aureggi, V.; Bryan, C. S.; Lautens, M. *Chem. Commun.* **2009**, 5236–5238.

125. *tert*-Butyl 2-bromo-1*H*-indole-1-carboxylate was prepared in 91% yield from *tert*-butyl 1*H*-indole-1-carboxylate using the procedure for the iodide counterpart found in: Roy, S.; Gribble, G. W.; *Tetrahedron Lett.* **2005**, *46*, 1325–1328, substituting I_2 with $(CCl_2Br)_2$.

126. McNulty, J.; Cheekoori, S.; Bender, T. P.; Coggan, J. A. *Eur. J. Org. Chem.* **2007**, 1423–1428.

127. Zhu, X.; Su, L.; Huang, L.; Chen, G.; Wang, J.; Song, H.; Wan, Y. *Eur. J. Org. Chem.* **2009**, 635–642.

128. Anderson, K. W.; Mendez-Perez, M.; Priego, J.; Buchwald, S. L. *J. Org. Chem.* **2003**, *68*, 9563–9573.

129. See ref. 64b.

130. Bruker **2007**, APEX2, SAINT, and SADABS, Bruker AXS Inc., Madison, Wisconsin, USA.

131. Sheldrick, G. M. *Acta Cryst. A* **2008** *64*, 112–122.

PART II: TOWARDS A SCALABLE SYNTHESIS OF NHC PRECURSOR 2,6-DI(3-PENTYL)ANILINE

CHAPTER 7: Introduction

7.1 – Preparation of Pd-PEPPSI Complexes

Following the initial success of Pd-PEPPSI-IPent (**5**) as an effective pre-catalyst for the synthesis of sterically-encumbered biaryls,[1] large quantities of the complex were required in order to further evaluate its efficacy in other difficult cross-coupling reactions. Pd-PEPPSI complexes can be easily prepared in high yields by heating a mixture of N,N-diarylimidazolium or imidazolinium chloride salt, K_2CO_3, and $PdCl_2$ in neat 3-chloropyridine (Scheme 1).[1a,2]

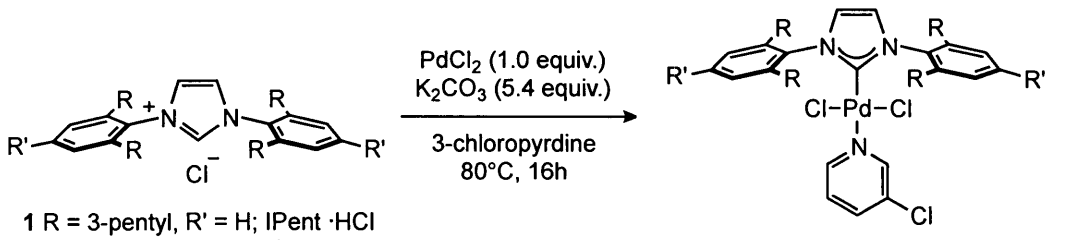

1 R = 3-pentyl, R' = H; IPent ·HCl
2 R = iPr, R' = H; IPr ·HCl
3 R = Et, R' = H; IEt ·HCl
4 R = R' = Me; IMes ·HCl

5 R = 3-pentyl, R' = H; PEPPSI-IPent; 65%
6 R = iPr, R' = H; PEPPSI-IPr; 97%
7 R = Et, R' = H; PEPPSI-IEt; 98%
8 R = R' = Me; PEPPSI-IMes; 91%

Scheme 1. Representative synthesis of Pd-PEPPSI complexes.

Numerous synthetic methods for the preparation of N,N-diarylimidazolium salts **2** – **4** and related congeners have been developed and reviewed.[3] The most commonly employed approach, originally disclosed by Arduengo and co-workers,[4] involves the cyclization of N,N-diaryldiimines with chloromethylethyl ether, however other cyclization strategies have been developed which make use of paraformaldehyde in the presence of a Bronsted acid (HCl)[5] or Lewis acid (TMSCl).[6] Invariably, the N,N-diaryldiimine precursor is generated via a simple acid-catalyzed condensation reaction between glyoxal and an appropriately substituted alkylaniline (Scheme 2). During efforts directed towards the preparation of IPent·HCl (**1**), a significantly more sterically congested NHC precursor, Organ and co-workers discovered that current methodology could be successfully applied with only minor alterations. However, unlike with salts **2** –

4, the aniline required for the preparation of **1** is not commercially available, thus a fast, cost-effective, and scalable synthesis of 2,6-di(3-pentyl)aniline (**9**) was required in order to procure significant quantities of pre-catalyst **5**.

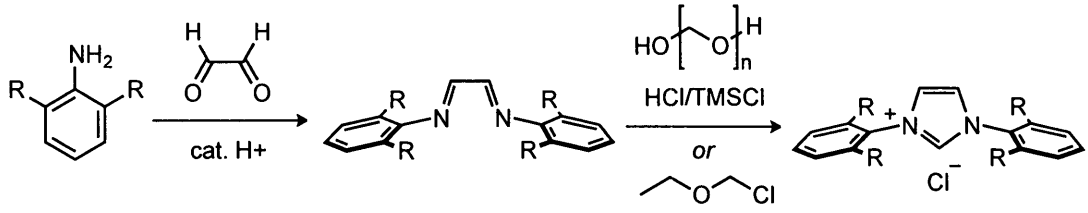

Scheme 2. Traditional preparation of imidazolium salts **2** – **4** and related congeners.

7.2 – Literature Precedent for the Preparation of 2,6-di(3-pentyl)aniline

The only literature precedent for the preparation of **9** was reported in 2007 by Steele and co-workers and involves benzylic deprotonation followed by alkylation of inexpensive 2,6-dimethylaniline using the superbase BuLi/LiK($OCH_2CH_2NMe_2$)$_2$ under an atmosphere of ethylene (Equation 1).[7] Although this process is reported to generate the desired aniline as the sole product in good yield, the requirement for a high-pressure reactor and the safety concerns associated with the use of such harsh reaction conditions on large scale prompted Organ to investigate milder alternatives.

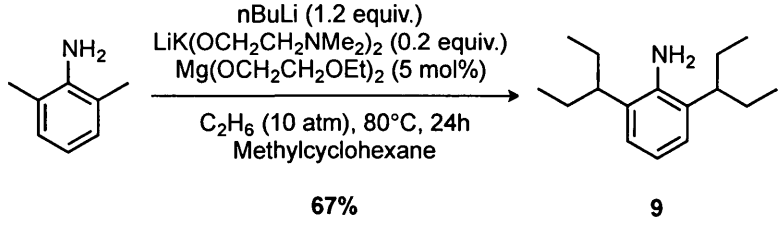

(1)

7.3 – Organ's First-Generation Synthesis of 2,6-di(3-pentyl)aniline[8]

The initial synthetic route developed by Organ for the preparation of **9** featured an *in situ* Shapiro-Suzuki sequence in which hydrazone **12** was first converted to alkenylboronic acid **14** via alkenyllithium **13**, which was then cross-coupled to 2,6-dibromoaniline to generate unsaturated aniline **16** in 70% overall yield (Scheme 3). Catalytic hydrogenation

of **16** with Crabtree's catalyst ([Ir(COD)(PCy$_3$)py]PF$_6$) furnished desired aniline **9** quantitatively.

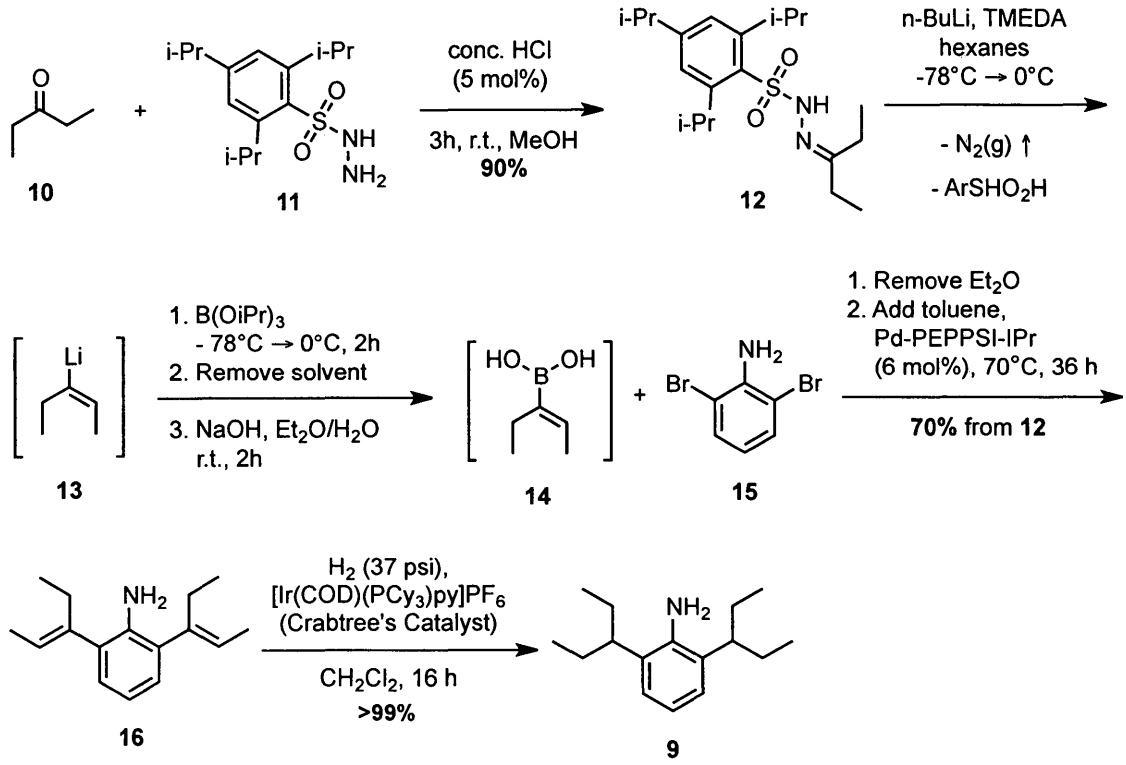

Scheme 3. Organ's first generation synthesis of 2,6-di(3-pentyl)aniline (**9**)

Organ and co-workers discovered that, although gram quantities of **9** could be synthesized in good yield, the Shapiro-Suzuki sequence was tedious, time-consuming, and prohibitively expensive due to the high cost of Crabtree's Catalyst (Aldrich $794/g) and **11** (Aldrich $133/g). Additionally, the scalability of the Shapiro reaction was limited due to the requirements for cryogenic cooling and chromatographic purification as well as the safety concerns associated with rapid extrusion of N_2 gas from the reaction mixture upon warming. Moreover, due to the extremely poor atom economy of the reaction in which 80% of the mass of hydrazone **12** is lost, the potential to conduct the process on large scale was constrained by the vast quantities of **12** that would be required on scale. For example, to generate only 100 g of **9**, nearly 700 g of **12** would be required at a cost

of nearly $100,000! In light of these glaring deficiencies, Organ sought an alternative protocol in which large-scale production of **9** was the primary objective.

7.4 – Organ's Second-Generation Synthesis of 2,6-di(3-pentyl)aniline[9]

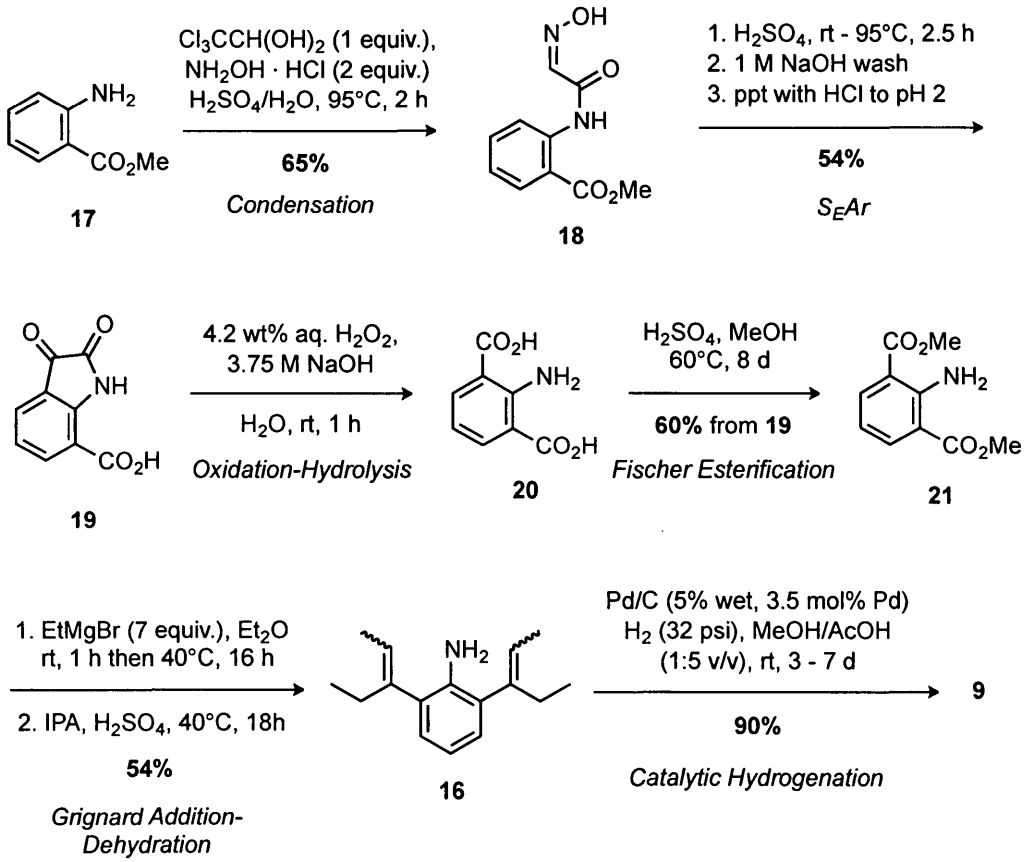

Scheme 4. Organ's second generation synthesis of 2,6-di(3-pentyl)aniline (**9**)

The second-generation synthesis of **9**, devised and optimized in 2009, began with methyl anthranilate (**17**), an inexpensive reagent available in bulk quantities (Scheme 4). Acid-mediated condensation of **17** with chloral hydrate and $H_2NOH{\cdot}HCl$ led to hydroxyimino acetamide **18**, which was then subjected to more strongly acidic conditions to initiate an intramolecular Friedel-Crafts reaction, yielding 2-carboxyisatin (**19**) after hydrolysis. Subsequent Baeyer-Villager oxidation and *in situ* base-mediated hydrolysis furnished diacid **20**, which was then esterified to diester **21** under acidic conditions. Treatment of

21 with excess ethylmagnesium bromide followed by acid-mediated elimination of the resultant tertiary benzylic alcohol yielded **16** as a mixture of geometric isomers. Finally, catalytic hydrogenation with Pd/C proceeded to generate **9** in excellent yield.

Despite the high step count and the lower overall yield relative to the first-generation strategy, this new process was conducted successfully on scale to furnish >200 g of **9**. However, during the scale-up, it became evident that this procedure would not be suitable to deliver larger quantities of **9** due to persistent difficulties associated with purification of intermediate **16**, which negatively affected the efficiency and reproducibility of the subsequent hydrogenation step. This, in addition to the extended time required to complete the synthesis (18 – 22 days), led us to re-examine alternative synthetic protocols for the large-scale preparation of **9**.

7.5 – Plan of Study

Consistent with the requirement for multi-gram quantities of state-of-the-art cross-coupling catalyst Pd-PEPPSI-IPent (**5**), the aim of this work is to develop a process-ready synthesis of 2,6-di(3-pentyl)aniline (**9**) that is fast, inexpensive, and readily scalable. In order to verify the effectiveness of the new protocol, a scale-up campaign will be performed with the objective of preparing kilogram-scale quantities of **9** that can then be used to generate **5** in quantities sufficient for further evaluation and distribution to chemists in academia and industry.

CHAPTER 8: Towards a Scalable Synthesis of 2,6-di(3-pentyl)aniline

8.1 – First Alternative Synthetic Approach to 2,6-di(3-pentyl)aniline

Although Organ's first synthetic strategy was ultimately deemed unsuitable for scale-up, it aptly demonstrated that alkenylboronic acids were competent nucleophiles in the Suzuki-Miyaura reaction with 2,6-dibromoaniline to generate unsaturated aniline **16**. Thus we thought it sensible to revisit this cross-coupling approach with added emphasis placed on devising a more user-friendly and scalable preparation of the intermediate alkenylboronic acid coupling partner. Rather than relying on the Shapiro reaction to generate **14** and related derivatives **24** and **25** (Scheme 5), we envisioned converting alkenyl halides **26** – **28** or pseudo-halide **29**, derived from readily available 3-pentanone, to alkenylboronic acid pinacol ester **24** via Pd-catalyzed Miyaura borylation. Ester **24** can then be cross-coupled directly to 2,6-dihaloaniline or first converted to the more reactive free boronic acid **14** or potassium trifluoroborate salt **25**.

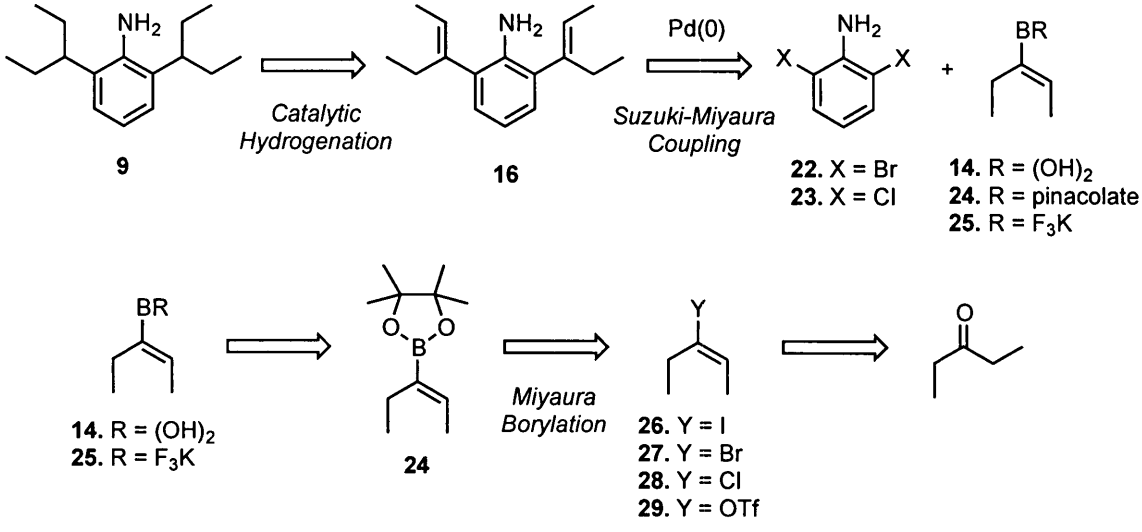

Scheme 5. First alternative retrosynthesis of 2,6-di(3-pentyl)aniline (**9**).

8.1.1 – Choice of Vinyl Halide or Pseudo-halide

Considering their high reactivity profiles in cross-coupling chemistry, vinyl iodide **26** or bromide **27** would be the immediate choice for this key intermediate. However, in light of our previous extensive research towards their synthesis, it was determined that these substrates would not meet our requirements for a cost-effective and scalable protocol.[10] Conversely, although literature precedent exists for the large-scale preparation of chloride **28**,[11] its reactivity profile in the Miyaura borylation is much too low to proceed without the use of expensive phosphine ligands.[12] As a result, we focused our initial efforts on preparing alkenyltriflate **29**, which was deemed to be considerably more facile than either the iodide or bromide counterparts.

8.1.2 – Triflation of 3-pentanone: Optimization and Scale-up

Since their introduction in the late 1960s by Stang and co-workers,[13,14] aryl and alkenyl triflates have become common intermediates in organic synthesis as coupling partners in transition-metal catalyzed cross-coupling reactions,[15,16] and as sources of vinyl cations[17] and alkylidene carbenes.[18] Alkenyl triflates are commonly prepared by either quenching a carbonyl metallo-enolate with a triflating agent such as *N*-phenyltriflimide, or treating the carbonyl compound directly with triflic anhydride in the presence of a non-nucleophilic base such as 2,6-di-*tert*-butylpyridine.[19] Unfortunately, given the prohibitive cost of *N*-phenyltriflimide and the practical difficulties associated with large-scale ketone enolization at -78°C, triflation using triflic anhydride in the presence of various amine bases was seen as a cost-effective and scalable alternative (Table 1).

We were pleased to discover that within 16 h, greater than 90% conversion to the desired triflate **29** could be achieved using 1.8 equivalents of triflic anhydride and either 2,6-lutidine or N,N-diisopropylethylamine (DIPEA) in CH_2Cl_2 (entries 3 and 4). The ammonium triflate salts that formed upon mixing base and triflic anhydride are soluble in CH_2Cl_2 and do not hinder stirring or reaction kinetics. Unexpectedly, the use of pyridine resulted in a much cleaner reaction mixture and a similarly high conversion to product

(>90%) was achieved, however a much longer reaction time (>40 h) was required due to the poor solubility of the generated pyridinium triflate salts (Entry 5). Using less than 1.8 equivalents of triflic anhydride or inorganic bases such as Cs_2CO_3 resulted in incomplete conversion (<70%) to product (Entries 1 and 2).

Table 1. Optimization Studies towards the Synthesis of **29**

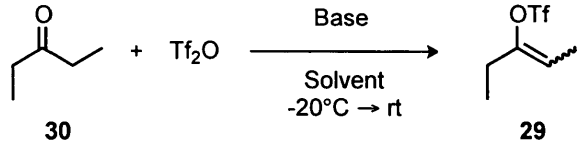

30 **29**

Entry	Solvent	Base	Equiv. Base/Tf_2O	Time (h)	Conversion (%)[a]	Yield (%)[b]
1	CH_2Cl_2	Cs_2CO_3	1.4	24	51	44
2	CH_2Cl_2	2,6-lutidine	1.5	24	71	-
3	CH_2Cl_2	2,6-lutidine	1.8	24	92	60[c]
4	**CH_2Cl_2**	**DIPEA**	**1.8**	**16**	**90**	**67[c]**
5	CH_2Cl_2	Pyridine	1.8	44	92	68
6	pentane	2,6-lutidine	1.8	16	62	51

[a] Determined by ^{1}H-NMR spectroscopy; [b] After evaporation of solvent, filtration through a pad of silica, washing with pentane unless noted otherwise; [c] Isolated as a mixure of geometric isomers in a ratio of 79 (*Z*) : 21 (*E*).

Given that the R_f value of 3-pentanone in pentane is low (0.1) relative to **29** (0.5), removal of unreacted 3-pentanone via silica filtration was thought to be ideal. Initially, the crude reaction mixture was diluted with pentane and filtered through a pad of silica gel, however to our dismay, the dark red pyridinium salt by-products were also drawn through the silica by CH_2Cl_2. To remedy this, CH_2Cl_2 was evaporated prior to filtration and the resulting red residue was taken up in pentane and then filtered, leading to isolation of pure **29** after careful removal of pentane. Although this purification method allowed for the isolation of pure **29** without the need for chromatography or distillation,

the disparity between the conversion determined by ^{1}H-NMR spectroscopy and the isolated yield was significant (20–30 %). We reasoned this to be due to the volatility of **29** and the requirement for two separate reduced-pressure evaporation events. This led us to perform the analogous reaction in pentane rather than CH_2Cl_2, which would allow us to eliminate the first evaporation step. Unfortunately, the reaction kinetics were much slower in pentane and a conspicuous red semi-solid precipitated from the reaction mixture after addition of Tf_2O that severely hindered stirring (Table 1, Entry 6). In light of these unsuccessful attempts, the use of 1.8 equivalents of Tf_2O and DIPEA in CH_2Cl_2 was adopted as the primary protocol suitable for scale-up using a simple silica gel filtration for purification.

*8.1.3 – Borylation and Cross-coupling of Triflate **29***

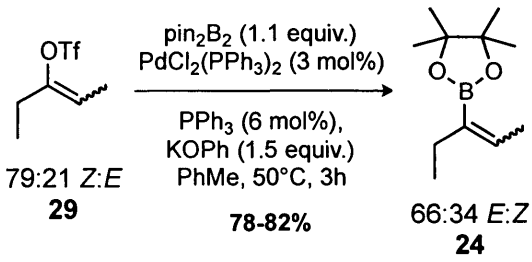

(2)

Having developed a method for the large-scale synthesis of **29**, Pd(0)-catalyzed Miyaura borylation with bis(pinacolato)diboron was undertaken (Equation 2).[20] With minor modifications to the published work-up procedure, this protocol was implemented smoothly and reproducibly on scales greater than 20 g with isolated yields up to 82%. Filtration of the crude mixture through a pad of silica gel, eluting with 2% ether in pentane was sufficient to isolate the boronic acid pinacol ester **24** in >95% purity as a mixture of geometric isomers in a ratio of 66:34 *E*:*Z*. We have demonstrated this procedure to be both inexpensive and scalable – two essential requirements for the synthesis of our desired aniline **9.**

With ester **24** in hand, we then decided to investigate the Suzuki-Miyaura coupling of **24** directly to 2,6-dibromoaniline (Table 2). Oxidative hydrolysis to the free boronic acid

was forgone given the difficulties associated with isolation and characterization of low-molecular weight boronic acids.[21] Optimization of this coupling began with the use of our own Pd-PEPPSI-IPr catalyst (**6**) owing to its availability and ease of synthesis. At the outset, we explored the use of a solvent system consisting of equal parts toluene, ethanol, and water, which had been known in our lab to work effectively for aryl boronic acid pinacol esters using **6**.[22] A number of bases were screened monitoring the progress of the reaction by GC/MS.

Table 2. Optimization Studies Towards the Synthesis of Unsaturated Aniline **16**

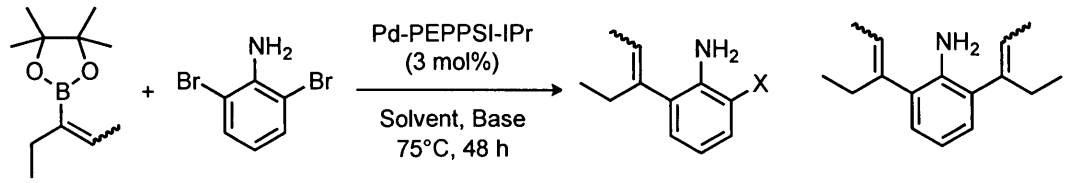

24 3.0 equiv. | **22** 1.0 equiv. | **30**, X = Br; **31**, X = H | **16**

Entry	Solvent[a]	Base	Equiv. Base	Result
1	A	Na_2CO_3	5	Incomplete Conversion[b]
2	A	K_2CO_3	5	Incomplete Conversion[b]
3	A	Cs_2CO_3	5	Incomplete Conversion[b]
4[c]	A	K_2CO_3	15	Incomplete conversion[d]
5	A	K_3PO_4	5	Incomplete conversion[e]
6	A	NaOH	5	Incomplete conversion[e]
7	A	KOH	5	Incomplete conversion[e]
8[f]	B	K_2CO_3	5	**Complete conversion** to **16**

[a] Solvent A: toluene/EtOH/H_2O (1:1:1); Solvent B: Toluene/H_2O (1:1) [b] Significant amount of **24** remaining, **22** completely consumed, 2:1 **30**:**16**; [c] Catalyst loading increased to 6 mol%; [d] 5:1 **16**:**31**; [e] **24** completely consumed, **22** Major, Dehalogenated **22** and **31** significant; [f] 2.5 equiv. **24** used.

In all cases employing the three component solvent system, the reaction did not proceed to completion (Entries 1 – 7). With carbonate bases, a 2:1 ratio of mono-coupled product

30 to desired aniline **16** was observed along with small amounts of dehalogenated mono-coupled product **31** (Entries 1-3). Keeping K_2CO_3 as the base, increasing the catalyst loading to 6 mol% and the amount of base to 15 equiv. did result in the consumption of all available electrophile, yet a significant amount (ca. 20%) of **31** was also produced (Entry 4), necessitating chromatographic purification of **16**, a procedure not amenable to large-scale implementation.

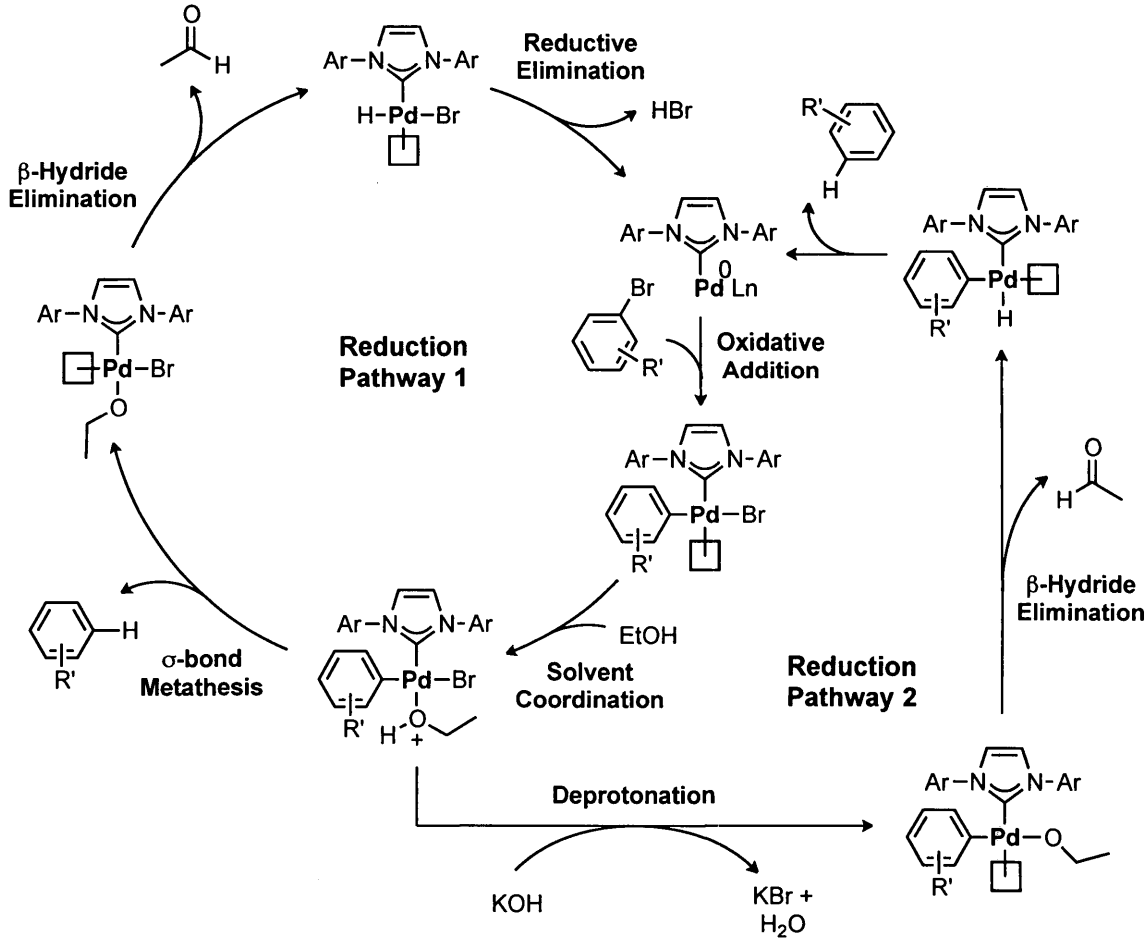

Figure 1. Proposed mechanism for electrophile dehalogenation with EtOH co-solvent

Although initially reluctant to remove the ethanol component from the solvent system since we have demonstrated its importance in similar couplings, we suspected that it was responsible for the widespread reduction being observed. Electrophile dehalogenation can

be thought to occur via two mechanistic pathways, both of which implicate protic solvents as the terminal reductant (Figure 1). If the transmetalation step is slow, EtOH can intercept the oxidative addition complex forming a Pd(II) oxonium species which can undergo σ-bond metathesis to generate **31** directly (Pathway 1), or be converted to a Pd(II) alkoxide, similarly furnishing **31** following β-hydride elimination and reductive elimination (Pathway 2). Consistent with this hypothesis, when the ethanol component was removed and a solvent system consisting of 1:1 toluene/water was employed using K_2CO_3 as the base, complete conversion to desired aniline **16** was observed within 48 h at 80°C without any significant reduction (Table 2, Entry 8). Reducing the amount of **24** from 3 equiv. to 2.5 and the amount of base from 10 equivalents to 5 had no effect on the conversion and allowed for significant cost and material savings (Table 2, Entry 8).

Since **16** and **24** are of similar polarity, removal of excess **24** via filtration through silica gel was not a viable option. Instead, we opted for an acid-base extraction wherein the aniline was extracted into aqueous HCl then subsequently deprotonated with NaOH. Although ultimately effective, this extraction procedure proved somewhat difficult considering the unexpectedly high solubility of the anilinium salt in organic media.[23] Nonetheless, the coupling and extraction has been applied successfully on a 5 g scale and generates the desired aniline cleanly in isolated yields consistently above 80%. Subsequent hydrogenation with palladium on charcoal (Pd/C) in the presence of excess acetic acid yields pure saturated aniline **9** quantitatively.

Altogether, this process route has the potential to provide **9** in multi-gram quantities as required, however the cost associated with the use of 1.8 equivalents of triflic anhydride and palladium catalysts over three steps would be problematic on larger scales. Since efforts to perform the borylation and cross-coupling steps in one pot with the same Pd source were not fruitful, we set our sights on improving the synthesis of pinacol ester **24** and reducing the overall number of Pd-catalyzed processes.

8.2 – Second Alternative Synthetic Approach to 2,6-di(3-pentyl)aniline

Having exhausted all possible efforts towards the synthesis and functionalization of alkenyl iodides, bromides, and triflates derived from 3-pentanone, our last remaining approach relied on the use of the corresponding chloroalkene **28**, which unlike the previous intermediates can be prepared easily on scale. Synthesis of **28** from 3-pentanone followed by reductive lithiation would afford alkenyllithium **13** that could be quenched with a source of electrophilic boron, such as pinacol isopropyl borate (pinBOiPr) to generate ester **24** (Scheme 6).

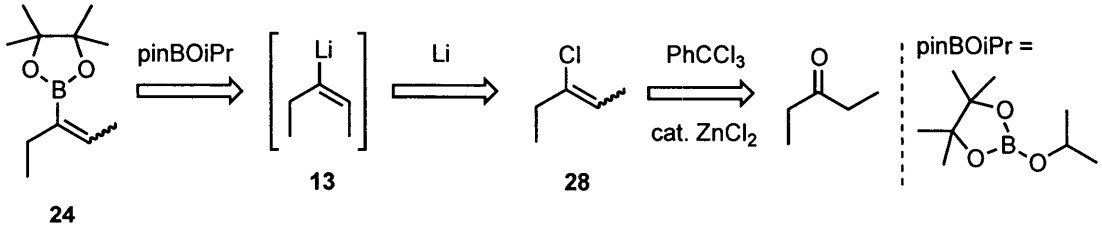

Scheme 6. Improved synthetic approach towards **24**

8.2.1 – Synthesis and Borylation of Chloroalkene 28

Following an account in the patent literature disclosed by Lanet in 1975,[11] **28** was successfully synthesized on a 1 mol scale in 61% yield as a 91:9 *Z:E* mixture (Scheme 7). After the reaction had proceeded to completion, **28** could be recovered in >98% purity by a simple ambient-pressure distillation. The two reaction by-products are either gaseous (HCl) or high-boiling (PhCOCl) thus facilitating easy product isolation. This approach has been shown to be both highly scalable and inexpensive, two essential requirements for the synthesis of desired aniline **9**.

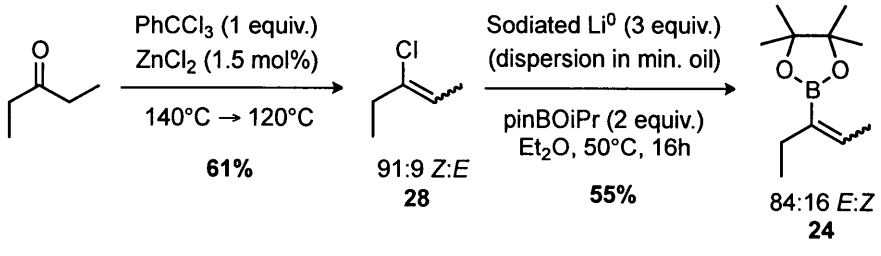

Scheme 7. Optimized Synthesis of Pinacol Ester **24** from chloroalkene **28**

With a scalable synthesis of **28** secured, we focused our efforts on activation of the C-Cl bond. Since aryl and alkenyl chlorides are known to be essentially inert to lithium halogen exchange[24] and much less reactive towards magnesium[25] and zinc insertion due to the relatively high bond dissociation energy (81 kcal/mol), we directed our attention towards homolytic activation with an alkali metal. In the past, Organ and co-workers had experimented successfully with the use of Na metal in the presence of triisopropylborate to form the corresponding alkenyl boronic acid isopropyl ester.[26] However, extended reaction times in excess of 48 hours were required and acceptable product yields could not be obtained unless greater than 6 equivalents of the metal were used. In response, we decided to investigate activation with the less caustic alkali metal, lithium.

Solutions of cyclic alkenyllithiums have been prepared in the literature from cyclic chloroalkenes using 2-3 equivalents of lithium metal with high sodium content (2%) in refluxing ether.[27] It has been shown that both the physical characteristics and sodium content of the Li metal are important features in determining the success of the reaction. Specifically, in 1990, Brandsma and co-workers reported that the standard conditions for this transformation are poorly reproducible unless the reaction was made to occur using sodiated lithium in the presence of pieces of broken glass.[28] This observation was rationalized from the assumption that the glass shards were mechanically scraping the insoluble LiCl by-product from the unreacted Li metal thereby resulting in improved reaction kinetics and reproducibility. Accepting this rationale, our initial experimentation made use of 3-4 equiv. of sodiated lithium wire (0.5% - 1.0% Na) which was flattened and cut into small rectangular pieces (1 cm x 0.2 cm x 0.1 cm) in the presence of irregularly shaped glass shards ranging in length from 0.1 cm – 1 cm derived from 9" Pasteur pipettes. To ensure a consistent "concentration" of glass shards, one pipette per 10 mmol **28** was used. In order to prevent E2 elimination of **28** by nascent alkenyllithium, we opted to perform an *in situ* quench by stirring the Li metal together with the desired boron electrophile, trapping the alkenyllithium as soon as it is generated (Table 3).

Table 3. Optimization Studies for the Lithiation-Borylation of **28**

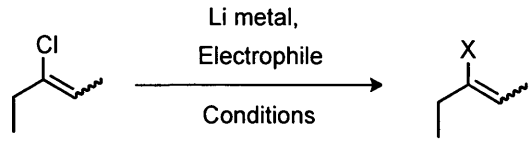

28

X = B(pin), **24**
X = BF_3K, **25**

Entry	Li Source (equiv.)	% Sodium	Electrophile	Solvent	Temp. (°C)	Time (h)	% Conv.[a]	% Yield[b]
1	Ribbon, >99% (3.0)[c]	ppm (<0.01%)	pinBO^{i}Pr	Et_2O	55	20	67	-
2	Wire, 98% (4.0)[c]	0.5-1.0	pinBO^{i}Pr	Et_2O	55[d]	49	100	49
3	Wire, 98% (4.0)[c]	0.5-1.0	pinBO^{i}Pr	THF	70	44	100	31
4	Wire, 98% (4.0)[c]	0.5-1.0	pinBO^{i}Pr	DME	80	20	0	0
5	25% Disp. in Oil (3.0)	0.5	pinBO^{i}Pr	Et_2O	50	22	100	55[e]
6	25% Disp. In Oil (3.0)	0.5	$B(O^iPr)_3$ then KHF_2	Et_2O	50	17	100	42[f]

[a] Percent conversion of **28** to **24/25** determined by ^{1}H-NMR spectroscopy by filtering a 100 – 200 μL aliquot through a plug of Celite before diluting with $CDCl_3$; [b] After flash chromatography; [c] Using one broken 9" pipette/10 mmol **28**; [d] Only 2.5% conversion to product observed after 24h at 40°C; [e] After distillation in vacuo at ~60 mmHg; [f] Alkenyl potassium trifluoroborate salt **25** isolated after crystallization.

To our dismay, stirring **28** with 4.0 equiv. of sodiated Li wire and 2.0 equiv. of isopropyl pinacolborate (pinBO^{i}Pr) in gently refluxing (40°C) diethyl ether, afforded only 2.5% conversion to product after 24h. However, upon increasing the temperature of the oil bath to 55°C, complete conversion to product was observed after stirring for an additional 20 h (Entry 2). Removal of excess Li via Celite filtration followed by aqueous work-up afforded a clear, yellow oil in 76% crude yield. Analysis of the crude mixture via ^{1}H-NMR spectroscopy revealed essentially pure product with the exception of a large unidentifiable peak at δ1.2 ppm. Purification via flash chromatography furnished pure

ester **24** in 49% yield as an 84:16 *E*:*Z* mixture, implying >90% retention of olefin geometry. Unfortunately, the significant by-product that may have formed as a result of anionic or radical-mediated polymerization, could not be isolated.

Switching the solvent to THF resulted in complete consumption of **28** within a similar time frame yet only 31% of the desired ester was isolated after chromatography and a number of unidentifiable by-products in addition to the one observed with Et_2O were prominent. This result may be attributed to the increased reactivity of THF towards organolithiums relative to Et_2O at temperatures above ambient.[25,24,29] For example at 35°C, the half-life of nBuLi in Et_2O has been measured to be 31 h whereas in THF it is only 10 min. In an attempt to improve reaction kinetics, DME was employed as solvent with the assumption that oxygen chelation might increase solubility of the LiCl by-product. Unfortunately, no product was observed (Entry 4), consistent again with stability trends of organolithium reagents in this solvent.

Disappointed with the low yields of **24** and the stirring difficulties that would inevitably arise on scale-up, we sought to investigate alternative Li sources. Consistent with a literature precedent for the synthesis of cyclopentenyllithium,[30] we opted to investigate the use of a sodiated dispersion of Li in mineral oil. In light of the finely dispersed nature of the Li particles, we thought that the increase in effective surface area would dramatically improve reaction kinetics and obviate the need for mechanical removal of LiCl. Indeed, when this dispersion was employed in Et_2O at 50°C, complete conversion to the desired pinacol ester **24** was observed within 22 h. Filtration and extractive work-up led to isolation of a yellow oil in 66% crude yield which after vacuum distillation at 60 mmHg afforded 55% of **24** as a colourless oil in >99% purity. NMR analysis of the viscous distillation mother liquor revealed the presence of the same unidentifiable by-product with a characteristic sharp singlet at δ1.2 ppm. Pleased with the reduction in reaction time and the simplification of the experimental procedure, we deemed the moderate yield acceptable given the relatively low cost of the reagents involved.

Using this procedure, replacing pinBO^{i}Pr with B(O^{i}Pr)$_3$ and an aqueous KHF_2 work-up, trifluoroborate salt **25** was also isolated in 42% yield after crystallization from acetone. These salts exhibit similar reactivity patterns to boronic acids and as solids, dramatically simplify purification relative to liquid boronic acid pinacol esters such as **24**.[32]

8.2.2 Re-optimization of the Suzuki-Cross Coupling

With ester **24** and trifluoroborate salt **25** in hand, we decided to re-investigate the Suzuki-Miyaura coupling with 2,6-dichloroaniline instead of 2,6-dibromoaniline as the former is significantly less costly (Aldrich $0.73/g vs. $10.7/g) and more readily available in bulk quantities (Table 4).

Applying the conditions previously optimized for 2,6-dibromoaniline led to mixtures of desired aniline **16** and mono-coupled product **33** along with unreacted **24** even at 100°C (Entries 1, 2). Changing the base from 5 M aqueous K_2CO_3 to KOH afforded complete conversion to **16** with no **33** or **31** detectable by GC/MS (Entry 3). Reducing the catalyst loading from 3.0 to 2.0 mol% could be accomplished without any deleterious effects, however further reduction to 1.0 mol% resulted in incomplete conversion (Entries 4,5). Since unreacted **24** could not be easily removed from **16** (identical R_f values), we then attempted to determine the minimum amount of **24** required for the reaction to proceed to completion without any excess remaining (Entries 6–9). We were pleased to discover that full conversion to **16** could be achieved with as little as 2.1 equiv. of **24** with no trace of the ester remaining after work-up. However, formation of metallic Pd in the reaction mixture invariably accompanied by trace amounts of reduction (<1%) was commonly observed after 24 h. To remedy this, the amount of base and temperature were reduced from 10 equiv. to 5 equiv. and from 80°C to 70°C, respectively (Entry 11). Under these conditions, complete conversion and 98% yield of **16** was obtained after work-up and silica filtration on a 5.6 g scale as a mixture of 2 major geometric isomers *(Z,Z)*-**16** and *(E,Z)*-**16** in a ratio of 69:31. A trace amount of the *(E,E)*-isomer was also formed but could not be quantified by ^{1}H-NMR spectroscopy.

Table 4. Optimization Study of Suzuki-Miyaura Coupling of **32** with **24**[a]

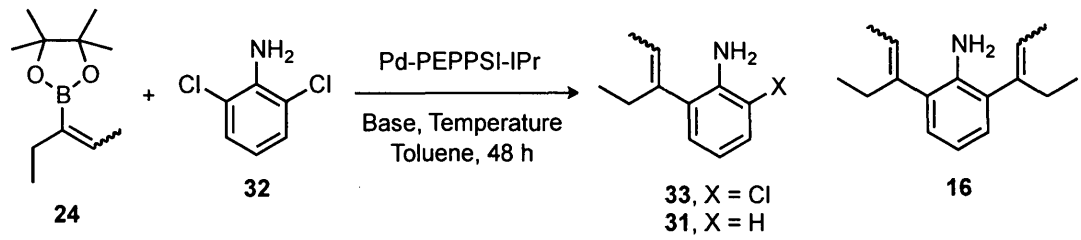

Entry	mol% PEPPSI	Base (equiv.)	equiv. 24	Temp. (°C)	Results[b]	Yield (%)
1	3.0	5 M K_2CO_3 (10.0)	3.0	80	**33** (minor), **16** (major), unreacted **24**	-
2	3.0	5 M K_2CO_3 (10.0)	3.0	100	**33** (minor), **16** (major), unreacted **24**	-
3	3.0	5 M KOH (10.0)	3.0	80	Complete conv. to **16**, unreacted **24**	-
4	2.0	5 M KOH (10.0)	3.0	80	Complete conv. to **16**, unreacted **24**	-
5	1.0	5 M KOH (10.0)	3.0	80	**33** (minor), **16** (major), unreacted **24**	-
6	2.0	5 M KOH (10.0)	2.5	80	Complete conv. to **16**, 20% unreacted **24**	-
7	2.0	5 M KOH (10.0)	2.25	80	Complete conv. to **16**, 3.6% unreacted **24**	-
8	2.0	5 M KOH (10.0)	2.20	80	Complete conv. to **16**, 1.8% unreacted **24**	-
9	2.0	5 M KOH (10.0)	2.10	80	Complete conv. to **16**, no unreacted **24**	95[b]
10	2.0	5 M KOH (5.0)	2.10	80	Complete conv. to **16**, no unreacted **24**	-
11	**2.0**	**5 M KOH (5.0)**	**2.10**	**70**	**Complete conv. to 15, no unreacted 23**	**98**[c]

[a]All reactions performed on a 0.5 mmol scale unless otherwise noted. [b] Qualitative GC/MS analysis of crude mixture after aqueous work-up; % **24** remaining determined by ^{1}H-NMR spectroscopic analysis; [c] 10 mmol scale (2.3 g), after flash chromatography; [d] 24.3 mmol scale (5.6 g scale), after work-up and silica filtration.

Unexpectedly, 1% of some NHC-based Pd complex without ligated 3-chloropyridine was also recovered after filtration. Treatment with Norit SX neutral activated charcoal effectively decolourized the product but the NHC species remained intact (Figure 2). Conversely, stirring an aliquot with Quadrapure TU Pd scavenger resulted in the disappearance of all NHC signals, confirming the nature of the impurity as an NHC-ligated Pd complex rather than an imidazolium salt. Interestingly, after the Pd impurity had been removed, a trace amount of two 3-substituted pyridines in a ratio of 1.9:1 became visible, which were likely the coupling products of *(E/Z)*-**24** and 3-chloropyridine. However, removal of the NHC-Pd impurity in the end was deemed unnecessary since the hydrogenation step required the use of Pd, thus the crude mixture was used without further purification. Fortuitously, after hydrogenation, no traces of NHC were detected in the product.

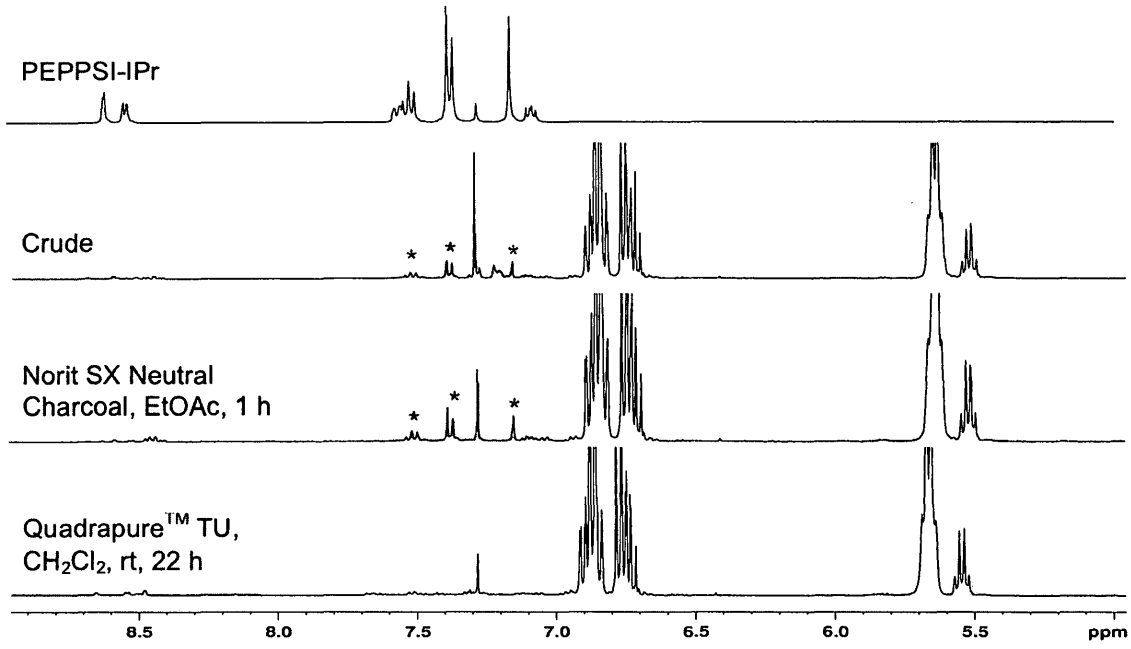

Figure 2. ^{1}H-NMR spectra of Pd-removal attempts from **16**

Pushing forward, we decided to determine a set of optimized conditions for the coupling of trifluoroborate salt **25** with **32** (Table 5). Beginning with previously optimized conditions for the coupling of these substrates with Pd-PEPPSI-IPr,[31] 3 equiv. of **25** were

heated with 6 equiv. of either K_2CO_3 or $K_3PO_4 \cdot H_2O$ in methanol at 60°C for 48 h (Entries 1,2). Unfortunately, although the starting aniline had been completely consumed, ~1:1 mixtures of **16** and **33** were observed along with a small amount of **31**. Using a harsher hydroxide base did push the reaction in the direction of **16**, yet significant amounts of **31** were also observed (Entry 3). These high levels of reduction are likely diagnostic of a slow rate of transmetalation. One can envision that if, after oxidative addition, transmetalation of **26** is slow, a reduction of the electrophile can occur via the pathways outlined in Figure 1.

Table 5. Optimization Study of Suzuki-Miyaura Coupling of **32** with **25**[a]

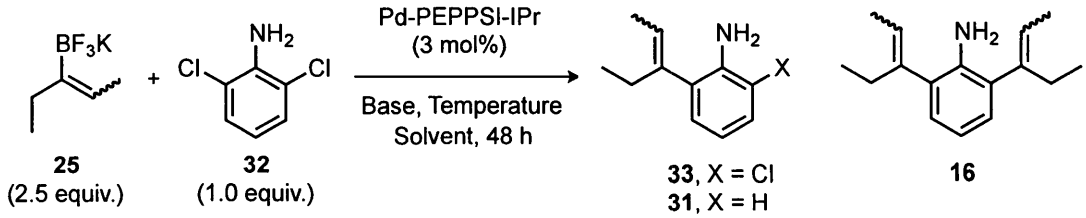

25 (2.5 equiv.) + **32** (1.0 equiv.) → **33**, X = Cl; **31**, X = H; **16**

Entry	Solvent	Base (equiv.)	T (°C)	Results[b]
1	MeOH	K_2CO_3 (6.0)	60	**33**:**16** (1:1), trace **31**
2	MeOH	$K_3PO_4.H_2O$ (6.0)	60	**33**:**16** (1:1), trace **31**
3	MeOH	KOH (6.0)	60	**16** (major), **33** (minor) **31** significant
4	Toluene	5 M KOH (7.5)	70	**33** (major), **16** (minor) **31** significant

[a] Reactions performed with 3 equiv. **25** on 0.5 mmol scale in HPLC grade MeOH (0.25 M); [b] Qualitative GC/MS analysis of crude mixture after aqueous work-up

In an attempt to suppress the observed reduction, methanol was replaced with the biphasic toluene/water solvent system that was found to work effectively in the coupling of ester **24** (Entry 4). Ultimately, no improvements were observed and reduction remained rampant. Since these trifluoroborate salts are known to be poor transmetalating

agents in the absence of protic conditions,[32] we reasoned that suppression of reduction would be challenging. This, in addition to the observed poor shelf life of **25**,[33] led us to forgo further optimization studies and adhere to the protocol successfully developed for the coupling of pinacol ester **24**.

8.2.3 – Scaling Up the Lithiation-Borylation Step

Since the synthesis of **28** is readily scalable, the main challenge associated with the second alternative synthetic strategy laid in the synthesis of ester **24**. Specifically, we were faced with two main difficulties during our attempts to scale up this process: (1) Removal of the mineral oil from the lithium dispersion; and (2) Removal of the LiCl and LiO^{i}Pr salt by-products from the reaction mixture. To evaluate the scalability of the reaction, we conducted our first large-scale trial on a 0.3 mol scale (31.4 g **28**).

We discovered that, although the mineral oil did not impede the efficiency of the reaction, it could not be reliably separated from **24** via fractional distillation.[34] In light of this, we opted to remove the oil by washing with dry Et_2O before adding the other reagents, a process complicated by the low density of Li, which floats on Et_2O. To this end, the reaction flask was charged with the Li dispersion, stirred with Et_2O for 1 min. then allowed to stand for 20 min. after which the supernatant was carefully removed via cannula. To be sure that the mineral oil had been completely removed, this process was repeated a total of three times. Later, once the lithiation-borylation had gone to completion, we were faced with the task of removing excess Li metal as well as LiCl and LiO^{i}Pr generated during the course of the reaction. We were reluctant to perform an aqueous work-up due to the presence of highly reactive Li particles still suspended in solution, thus we opted to perform a Celite filtration instead. The filtration proceeded smoothly and the Li particles remaining in the filter cake were quenched by slow addition into 2-propanol.

Pleased to have solved the immediate practical challenges associated with the scale-up, we were disappointed to discover that on this scale, a significant and reproducible drop in

yield from nearly 60% to 20% was observed. Given that all process parameters (temperature, concentration, solvent) had been kept constant, we were unsure why the yield had dropped so precipitously. In light of this new development, we could no longer justify pursuing this strategy as a viable means for the large-scale synthesis of **9**.

*8.2.4 – Differential Reactivity of (Z)-**24** vs. (E)-**24***

Before beginning the search for a third alternative synthetic protocol, we opted to cross-couple all remaining **24** with **32** using the earlier optimized conditions. As expected, **24** derived from chloroalkene **28** coupled quantitatively, furnishing **16** in >95% yield, however we were surprised to find that when employing **24** derived from alkenyltriflate **29** the coupling did not proceed to completion even after extended reaction times. The only difference between the two batches was the ratio of *(E)*-**24** to *(Z)*-**24**: 84:16 E:Z (made from **28**) vs. 66:34 *E*:*Z* (made from **29**). This could imply either that *(Z)*-**24** transmetalates more slowly than the *E*-isomer when coupling to an aryl chloride or that *(Z)*-**24** is less stable under these reaction conditions than the *E*-isomer.

Upon close examination of the transmetalation step, it might be reasonable to expect that the steric repulsion between the terminal methyl group in *(Z)*-**24** and the aryl ligand might disfavour the coordination event that is likely required for transmetalation to occur (Figure 3). Since the terminal methyl in *(E)*-**24** is directed away from the metal, this isomer may be more likely to coordinate to the metal and thus may irreversibly transmetalate to Pd at a faster rate than the *(Z)*-isomer. This is an argument for kinetic control since the *(E)*-alkenyl-Pd species generated from transmetalation of *(E)*-**24** is likely higher in energy than that of the *(Z)* derivative on steric grounds.

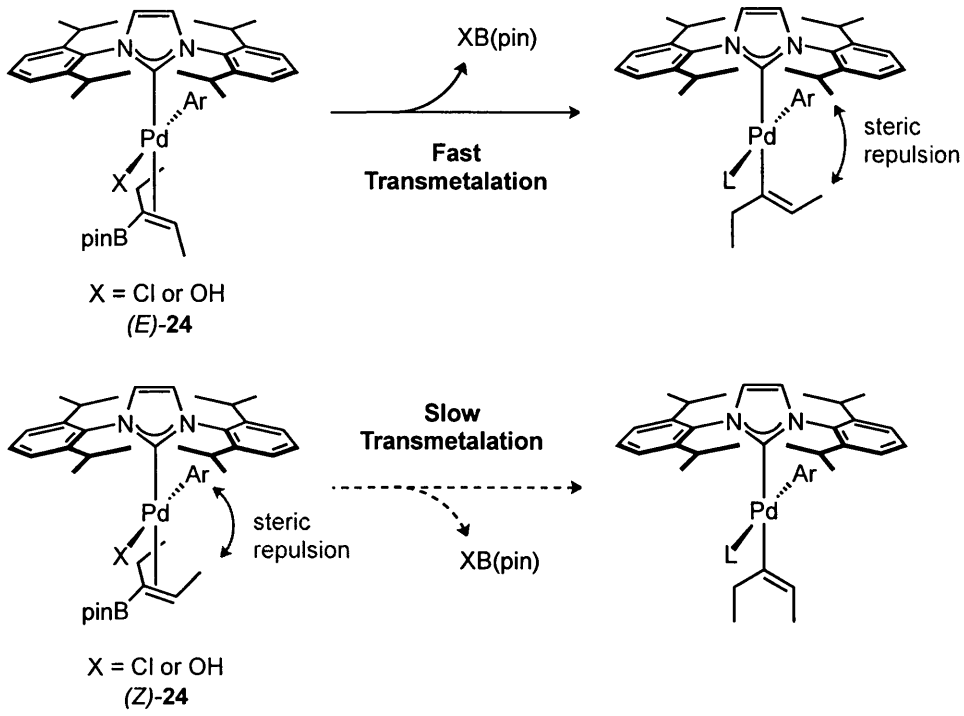

Figure 3. Proposal for the impaired transmetalating ability of *(Z)*-**24** relative to *(E)*-**24**.

If this proposal were indeed true, the olefin-geometry of the cross-coupled product (**16**) should be *(E)*-enriched especially during the initial stages of the reaction when the concentration of the *(E)*-isomer is at its highest. However, examination of the ^{1}H-NMR spectra of the incomplete reaction after 48 h using *(Z)*-enriched **24** (made from triflate **29**) revealed the ratio of isomers in products **33** and **16** to be 68:32 Z:E, implying essentially no change from the ratio of isomers in the starting material (66:34). Surprisingly the amount of unreacted *(Z)*-**24** had decreased significantly relative to the *(E)*-isomer to 93:7 *E*:*Z*. Since the "missing" *(Z)*-isomer was not incorporated into the cross-coupled product, we can conclude that *(Z)*-**24** is slightly less stable than *(E)*-**24** under these reaction conditions. For example, due to less steric congestion around the B atom, it may be that *(Z)*-**24** is more likely to be intercepted by OH- ions forming the water-soluble borate, which is unavailable to react.

8.3 – Third Alternative Synthetic Approach to 2,6-di(3-pentyl)aniline

Having repeatedly failed to design a scalable and inexpensive synthesis of boronic acid pinacol ester **24** and related congeners, we decided to attempt a more direct approach in which alkenyllithium **13** derived from chloroalkene **28** was directly cross-coupled to 2,6-dihaloaniline. Using 2.1 equiv. of the sodiated dispersion of Li metal in mineral oil found to work well for the lithiation-borylation sequence, we successfully prepared a solution of organolithium **13** in Et_2O (Equation 3). Analysis of the organolithium via No-D ^{1}H-NMR spectroscopy indicated complete consumption of **28**, forming **13** with 97% retention of olefin geometry.

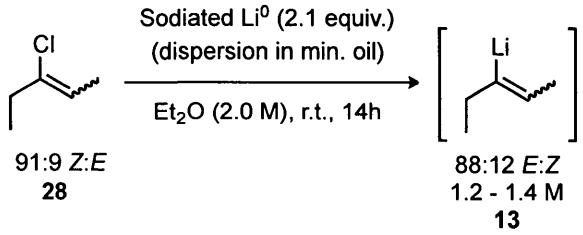

(3)

We then attempted to cross-couple the organolithium to both **22** and **32** using PEPPSI-IPr and PEPPSI-SIPr (Table 6). Unfortunately, no reaction was observed when we attempted a direct coupling of **13** and **32** alone in Et_2O (Entry 1). We proceeded next to perform a Negishi cross-coupling of the organozinc derivative of **13**, formed from transmetalation with $ZnCl_2$. When NMP was used as a co-solvent, the reaction with dibromide **30** proceeded to completion, however the analogous reaction with less costly dichloride **32** was less effective (Entries 2,3). We were surprised to find though that Et_2O and NMP were immiscible under these conditions leading to a biphasic reaction mixture, which would inevitably lead to stirring and mixing challenges on scale-up. Our next step was to perform a Kumada-Tamao-Corriu (KTC) coupling between the *in situ*-generated Grignard reagent and **22/32**, which has been reported to work well in THF alone (Entries 4–9).[35] When $MgBr_2$ was used as the transmetalating agent, incomplete conversions to **16** were obtained in all cases. Interestingly, when $MgCl_2$ was used instead, complete conversion to **16** was observed when coupling to dibromide **30**. Switching to the

dichloride **32** was less successful as mostly mono-coupled product **33** was observed. Since reductive elimination is occurring from the same complex regardless of the magnesium salt used, it is likely that the Grignard reagent generated from $MgCl_2$ is a more effective transmetalator than that generated from $MgBr_2$. A similar rate acceleration was observed by Organ and co-workers when employing arylzinc chlorides generated from Grignard transmetalation with $ZnCl_2$ relative to $ZnBr_2$.[36] In this case, purported changes in organozinc aggregation state were invoked to explain the improved transmetalating ability.[37]

Table 6. Optimization Study of Cross-coupling Organolithium **13**

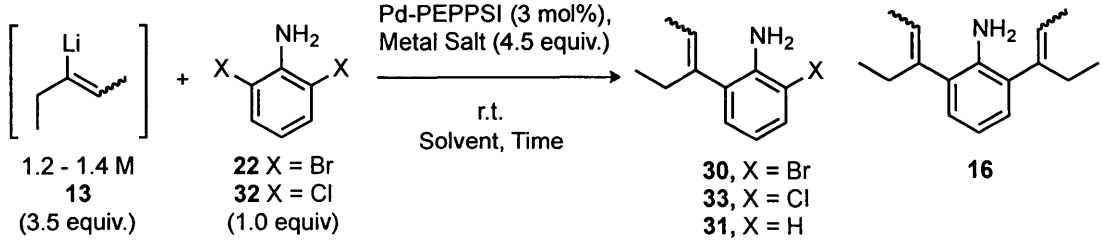

1.2 - 1.4 M **13** (3.5 equiv.) | **22** X = Br, **32** X = Cl (1.0 equiv) | **30**, X = Br; **33**, X = Cl; **31**, X = H | **16**

Entry	X	PEPPSI catalyst	Metal Salt	Solvent	Time (h)	Results[a]
1	Cl	IPr	None	Et_2O	24	No reaction
2	Br	IPr	$ZnCl_2$	NMP	41	Complete conv. to **16**
3	Cl	IPr	$ZnCl_2$	NMP	41	Incomplete conv.; **31** and **33** significant
4	Br	IPr	$MgBr_2$	THF	18	**16** (Major); **30** (Minor)
5	Br	SIPr	$MgBr_2$	THF	18	**16** (Major); **30** (Minor)
6	Cl	IPr	$MgBr_2$	THF	18	**32**, **33** (Major)
7	**Br**	**IPr**	**$MgCl_2$**	**THF**	**18**	**Complete conv. to 16**

8	Cl	IPr	$MgCl_2$	THF	18	**33** (Major); **16** (Minor)
9	Cl	SIPr	$MgCl_2$	THF	18	**33** (Major); **16** (Minor)

[a] Determined via qualitative GC/MS analysis of a reaction aliquot after the indicated time.

8.4 – Scaling up the Kumada-Tamao-Corriu (KTC) Process

*8.4.1 – Large-scale synthesis of chloroalkene **28***

Given the straightforward nature of the process, we immediately proceeded to conduct the chlorination reaction on a 0.8 Kg (7.7 mol) scale using overhead mechanical stirring and 5 L glassware. On this scale, extra provisions were made to trap the HCl gas by-product as it evolved from the reaction by employing a series of NaOH and water traps positioned at the reactor outlet. Heating a suspension of $ZnCl_2$ (1.5 mol%) in $PhCCl_3$ to 135°C for ca. 2 h resulted in a dark red solution to which an equimolar amount of 3-pentanone was added dropwise over 8 h. As the addition progressed, a vigorous reflux was observed and the internal temperature of the reaction stabilized at 120°C. After stirring for an additional 19 h, the reaction mixture was sampled and checked by ^{1}H-NMR spectroscopy. On small scale, >99% conversion to product is usually observed at this time, however on this scale, the reaction had only proceeded to 94% completion. Considering the similar boiling points of 3-pentanone (102°C) and **28** (94°C), driving the reaction to completion is of utmost importance in order to isolate **28** in pure form. To our dismay, after stirring for an additional 24 h, the reaction had stalled.

At this stage, we decided to commence distillation of the ketone/product mixture and attempt to remove the unreacted ketone at a later stage. Surprisingly, only 295 g of distillate was collected, which corresponded to an unusually low product yield of 36%, contaminated with 7% ketone and 1% PhCOCl. Given the slight solubility of 3-pentanone in water, we thought it worthwhile to investigate the possibility of removing the ketone via extraction. Washing an aliquot with 1:1 v/v H_2O or 5:1 v/v H_2O was ineffective at removing both ketone and PhCOCl, yet washing with an equal volume of

28% $NH_4OH_{(aq)}$ removed only PhCOCl. Since aqueous extraction proved unsuccessful, we thought stirring the mixture with an appropriate hydride reducing agent might reduce the ketone and the PhCOCl to their corresponding metal alkoxides, from which we could then distill the product. Stirring an aliquot with $NaBH_4$ (1.5 equiv. hydride required to react with ketone and PhCOCl) for 2 h at 75°C was completely ineffective, likely due to the poor solubility of the salt in **28**. However, stirring with $LiAlH_4$ at rt for 2 h resulted in the complete consumption of both **28** and PhCOCl. Redistilling the entire mixture over $LiAlH_4$ furnished pure **28** in >90% recovery, however since >600g **28** were required to perform the lithiation-coupling sequence, the chlorination step was repeated.

During the first run, we noticed a vigorous reflux during ketone addition which led us to suspect that the reason for the poor conversion was that much of the ketone was in the gas phase in the headspace of the reactor and thus was unavailable to react. In an effort to improve the yield of **28**, we decided to reduce the internal temperature of the reaction to between 100°C - 110°C and reduce the headspace volume by doubling the scale of the reaction using the same 5 L round-bottom flask. Implementing these changes led to >98% conversion to **28** a mere 6 h after completion of ketone addition. After distillation, 802 g (51%) of **28** were collected and shown to contain <1% of both 3-pentanone and PhCOCl, sufficiently high purity to use without further purification in the subsequent step. The chlorination protocol has been successfully repeated twice on this scale to provide nearly 2 Kg of **28**.

8.4.2 – Large-scale reductive lithiation and Kumada-Tamao-Corriu Coupling

With a sufficient quantity of **28** in hand, we set our sights on scaling up the lithiation-coupling sequence. After successfully repeating the protocol to furnish 10 g of **16**, we opted to scale up by a factor of 10. Reductive lithiation of **28** proceeded well on a 2 mol (210 g) scale providing a 1.35 M solution of organolithium **13** in Et_2O after replicate titration with 1,3-diphenylacetone *p*-tosylhydrazone.[38] Of note, due to the highly reactive nature of the **13**, we elected to use magnetic stirring rather than mechanical stirring as it

would have been impossible to obtain an air-tight seal with the latter. Mineral oil removal was accomplished by washing three times with Et_2O as described earlier in Section 8.2.3.

Next we performed the KTC coupling on a 0.4 mol scale, which would produce ca. 91 g of **16** (Scheme 8). Using mechanical stirring and 5 L glassware, **13** was added slowly to a suspension of $MgCl_2$ in THF over 2 h forming Grignard **34**. We had earlier verified by No-D ^{1}H-NMR spectroscopy that transmetalation proceeds to completion within 2 h. Cooling of the reaction vessel was accomplished using compressed air, however we were surprised to find that the exotherm associated with $MgCl_2$ solvation was greater than that from the transmetalation. A THF solution of PEPPSI-IPr and **22** was then slowly added to the suspension of **34** adjusting the rate of addition to prevent a runaway exotherm. Since the heat generated from the deprotonation of **22** is likely required to drive the cross-coupling to completion, we avoided cooling the reaction too drastically. Once the addition had completed, the orange suspension was allowed to stir for 16 h at which time, GC/MS analysis indicated complete conversion to **16**. Interestingly, we also noticed the presence of 2 higher boiling compounds in the reaction mixture, which corresponded to the mass of **16** with an additional pentenyl group. Upon further investigation, we discovered that commercially available **22** contained 1–2 % of 2,4,6-tribromoaniline which led to the formation of an equivalent amount of tricoupled aniline **35**. We deemed this to be an acceptable impurity since an extra 4-substituted 3-pentyl group should not significantly affect the steric or electronic character of the NHC into which it will be incorporated.

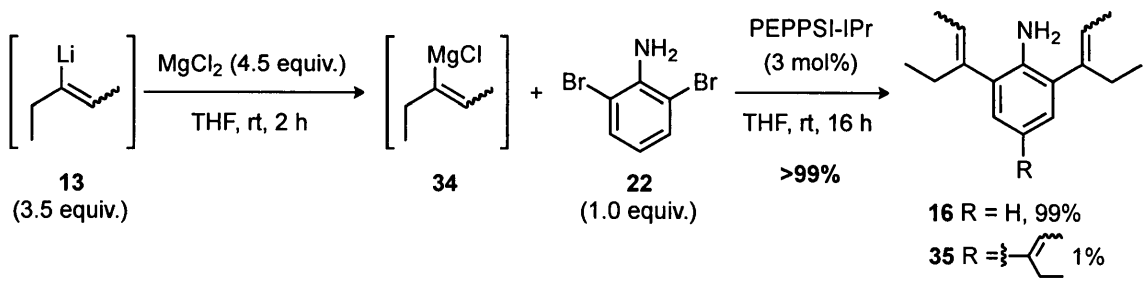

Scheme 8. Synthetic route to unsaturated aniline **16**.

Once completed, we proceeded to quench the reaction by slow addition of chilled 1 M aqueous HCl. From our earlier experiences on small scale, we were aware that slow addition was necessary in order to avoid the formation of intractable Mg^{2+} slurries, thus the addition was made to proceed over a period of 2 h until the pH of the aqueous layer was ca. 4. At this point, the mixture was biphasic and nearly homogeneous with a conspicuous black emulsion present at the layer interface (likely colloidal Pd). Simply diluting with water was enough to break up the emulsion. The mixture was transferred to a separatory funnel and subjected to a standard extractive work-up. The product-rich organic layer was dried and decolourized by stirring with anhydrous $MgSO_4$ and Norit SX neutral activated charcoal. The suspension was then filtered though silica gel and the solvent stripped under reduced pressure to yield a brown oil shown to be **16** as a mixture of geometric isomers by GC/MS analysis, with a yield of 104%. Analysis of the crude product via ^{1}H-NMR spectroscopy revealed the presence of two additional impurities that were not detected by GC: (1) 1–2% of some NHC-ligated Pd complex (similar to the one observed after coupling ester **24** with **22**); and (2) various geometric isomers of dimerized **13**. From earlier studies, we knew the NHC-Pd complex decomposes to easily-removable products during the subsequent catalytic hydrogenation so we made no effort to remove it at this stage. Removal of dimerized **13** was accomplished by repeated azeotroping with either acetonitrile or toluene. Drying the residue under high vacuum furnished 93.0 g (102%) of **16** containing the above-mentioned impurities, which was used directly in the next step.

Given the success of the KTC trial run, we further scaled up the process by a factor of 3, limited only by the availability of larger glassware. The reductive lithiation and cross-coupling steps were made to occur in 5 L and 12 L round-bottom flasks respectively, furnishing 264 g (102%, 1.13 mol) of **16** with the same impurity profile as on the small-scale run. This sequence was repeated twice on this scale, providing 528 g of **16**. Since its initial development in the summer of 2011, >0.7 Kg of **16** has been successfully prepared using this process route.

8.4.3 – Large-scale catalytic hydrogenation

Using our earlier optimized procedure,[39] catalytic hydrogenation of **16** was accomplished with Pd/C (3.3 mol%) in a binary solvent system of MeOH/AcOH under 60 psi of H_2 with yields typically in the range of 90-92% (Equation 4). Due to the volume limitations of the high-pressure reactor (2 L), the largest scale on which these reductions could be performed was 125 g.[40]

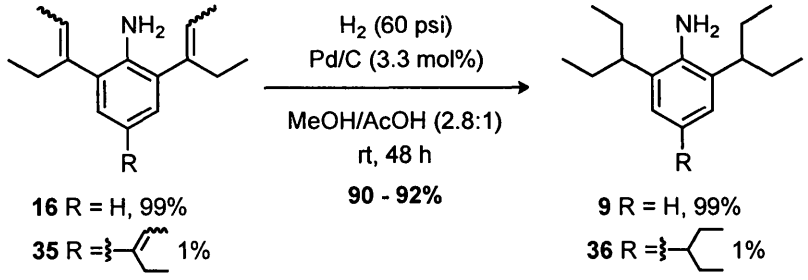

(4)

Work-up and isolation of these reactions was straightforward and predictable. Once deemed complete by GC/MS analysis, the Pd/C was removed via filtration through Celite and the filtrate was stripped of MeOH and as much AcOH as possible. The residue thus obtained was taken up in Et_2O and slowly basified with a solution of 3M NaOH until the pH of the aqueous layer reached ca. 12. After extraction with Et_2O, the product-rich organic layer was filtered through a pad of silica gel and the resulting filtrate concentrated to yield **9** as a light orange oil. The only impurity visible by ^{1}H-NMR spectroscopy and GC/MS analysis was 2,4,6-tri(3-pentyl)aniline (**36**), which carried over from the previous step.

8.5 – Conclusions

In order to prepare large quantities of state-of-the-art coupling catalyst Pd-PEPPSI-IPent (**1**), a cost-effective and scalable synthesis of 2,6-di(3-pentyl)aniline (**9**) was required. A number of synthetic routes were investigated which featured a key cross-coupling step between a 3-metallo-2-pentene fragment and 2,6-dihaloaniline to generate unsaturated

analogue **16**, which could be easily reduced to **9**. While the Suzuki-Miyaura coupling of boronic acid pinacol ester **24** proceeded well with inexpensive 2,6-dichloroaniline, preparing this intermediate on large scale proved either prohibitively expensive or practically challenging. In light of these difficulties, we discovered a method for the cross-coupling of organolithium **13**, derived from easily accessible chloroalkene **28**, with 2,6-dibromoaniline. This process was conducted on large-scale to furnish **16** in single batches as large as 264 g. Catalytic hydrogenation of **16** with Pd/C provided desired aniline **9** in yields >90% and in purities >97%. Since its inception in late 2011, this process has been successfully employed to generate nearly 0.7 Kg of **9** and subsequently 0.4 Kg of **1**. This new process undoubtedly has the potential for larger scale implementation.

CHAPTER 9: Experimental Procedures

9.1 – General Experimental

All experiments were conducted under an atmosphere of dry argon in oven-dried or flame-dried glassware using standard Schlenk techniques. Experiments performed in an oil bath were done using Fisher Scientific silicone oil in a Pyrex crystallizing dish on top of an IKA RCT basic model magnetic hotplate stirrer with an ETS-D5 electronic contact thermometer. Glovebox manipulations were performed in an MBraun Unilab glove-box under an atmosphere of dry argon. All reagents were purchased from Sigma-Aldrich, Alfa Aesar, or Strem and were used without further purification unless noted otherwise. THF and Et_2O were distilled under argon over sodium-benzophenone ketyl prior to use whereas toluene and dichloromethane were distilled under argon over calcium hydride prior to use. All reaction vials (screw-cap threaded, caps attached, 15x45 mm) were purchased from Fisher Scientific. Analytical Thin Layer Chromatography (TLC) was performed on EMD 60 F254 pre-coated glass plates and spots were visualized with UV light (254 nm) or a $KMnO_4$ staining solution. Column chromatography purifications were carried out using the flash technique on EMD silica gel 60 (230 - 400 mesh).[41] NMR spectra were recorded on Bruker 300 AVANCE, Bruker 400 AVANCE, and Bruker 600 DRX spectrometers. The chemical shifts for ^{1}H-NMR spectra are given in parts per million (ppm) referenced to the residual proton signal of the deuterated solvent; coupling constants are expressed in Hertz (Hz). ^{13}C-NMR spectra were referenced to the carbon signals of the deuterated solvent. The following abbreviations are used to describe peak multiplicities: s = singlet, br s = broad singlet, d = doublet, br d = broad doublet, t = triplet, br t = broad triplet, q = quartet, quint = quintet, sext = sextet, sept = septet, dd = doublet of doublets, tt = triplet of triplets, qt = quartet of triplets, qd = quartet of doublets, and m = multiplet. For ^{13}C-APT NMR spectra, quaternary carbons and carbons with an even number of attached protons produce a positive (+) signal whereas peaks with a negative (–) signal arise from carbons attached to an odd number of protons. Gas chromatographic analysis was performed on Varian Series GC/MS/MS 4000 System.

Melting points were determined using a Fisher-Johns melting point apparatus and are uncorrected. High Resolution Mass Spectrometry (HRMS) analysis was performed by the Mass Spectrometry and Proteomics Unit at Queen's University in Kingston, Ontario.

9.2 – Experimental Procedures

9.2.1 – Suzuki-Miyaura Route via alkenyltriflate (29)

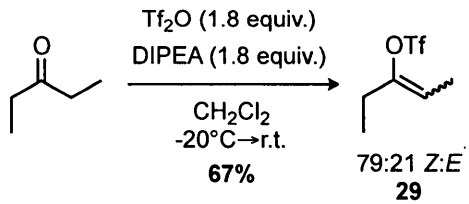

Synthesis of pent-2-en-3-yl trifluoromethanesulfonate (29). In a 2-neck 500 mL round-bottom flask equipped with magnetic stir bar and pressure-equalizing addition funnel, a solution of 3-pentanone (5.3 mL, 50 mmol) and N,N-diisopropylethylamine (15.7 mL, 90 mmol) in CH_2Cl_2 (250 mL) at ca. -20°C was charged with freshly distilled Tf_2O (15.1 mL, 90 mmol) dropwise over 30 min. During this time, a colour change from light yellow to brown was observed. The mixture was then allowed to warm slowly to rt overnight. Monitoring by ^{1}H-NMR spectroscopy for the disappearance of ketone, the reaction was deemed to be complete within ca. 20 h (>90% conversion). At this time, the solvent was evaporated under reduced pressure (aspirator rotary evaporator, bath temperature = 10°C) and the dark red residue thus obtained was diluted with 150 mL pentane and stirred for 10 min. The mixture was filtered over a 2.5 cm pad of silica covered with a 1 cm pad of celite in a 150 mL coarse-porosity fritted glass funnel and the filter cake washed thoroughly with pentane. The filtrate was concentrated to yield 7.72 g of a light yellow oil shown to be **29** in 95% w/w purity (67% yield) as a mixture of geometric isomers, which was used directly without further purification. The ration of isomers was determined to be 79:21 *Z*:*E* determined by a 2D-NOESY NMR experiment. ***Z*-isomer:** ^{1}H-NMR (400 MHz, $CDCl_3$) δ 5.35 (q, J = 6.8 Hz, 1H), 2.44 – 2.35 (m, 2H), 1.76 (d, J = 6.4 Hz, 3H), 1.14 (t, J = 7.0 Hz, 3H); ^{13}C-NMR (100 MHz, $CDCl_3$) δ 151.7

(+), 118.5 (+, q, $J_{C\text{-}F}$ = 319.0 Hz), 114.5 (–), 26.7 (+), 11.0 (–), 10.9 (–); ^{19}F-NMR (282 MHz, $CDCl_3$) δ -74.6. ***E*-isomer:** ^{1}H-NMR (400 MHz, $CDCl_3$) 5.56 (q, J = 7.2 Hz, 1H), 2.44 – 2.35 (m, 2H), 1.72 (d, J = 7.2 Hz, 3H), 1.15 (t, J = 7.0 Hz, 3H); ^{13}C-NMR (100 MHz, $CDCl_3$) δ 152.0 (+), 118.6 (+, $J_{C\text{-}F}$ = 320.0 Hz), 115.8 (–), 22.9 (+), 11.5 (–), 10.8 (–); ^{19}F-NMR (282 MHz, $CDCl_3$) δ -74.0. HRMS (EI) [M^+] calcd. for $C_6H_9F_3O_3S$ 218.0225; found 218.0231.

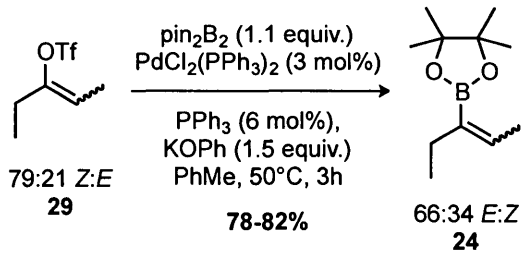

Synthesis of 4,4,5,5-tetramethyl-2-(pent-2-en-3-yl)-1,3,2-dioxaborolane (24). A 1 L round-bottom flask equipped with magnetic stir bar was charged with triflate **13** (30.0 g, 137 mmol), $PdCl_2(PPh_3)_2$ (2.9 g, 4.1 mmol), PPh_3 (2.2 g, 8.2 mmol), bis(pinacolato)diboron (38.3 g, 151 mmol), and potassium phenoxide (27.2 g, 206 mmol) in air. The flask was evacuated and backfilled with Ar (x3) after which toluene (400 mL) was added. The flask was then immersed in a pre-heated 50°C oil bath and the resulting off-white suspension stirred vigorously at this temperature until ^{19}F-NMR analysis indicated complete consumption of **29**. After 3 h, the reaction was cooled to room temperature, diluted with 100 mL Et_2O, and filtered through a 2.5 cm pad of silica gel covered with a 1 cm pad of celite in a 150 mL coarse-porosity fritted glass funnel, washing the filter cake thoroughly with 350 mL Et_2O. The resulting brown filtrate was washed with 250 mL portions of 1 M NaOH (x3) and brine (x1), dried over anhydrous $MgSO_4$, filtered, and concentrated under reduced pressure to yield 29.79 g of a brown oil. This crude oil was taken up in a minimum amount of pentane and filtered through a 5 cm pad of silica gel eluting with pentane (400 mL) then 2% Et_2O/pentane (1.2 L) to yield 22.9 g (82 %) of ester **24** as a light yellow-brown oil as a mixture of geometric isomers in 96% w/w purity, which was used without further purification. The ratio of isomers was

determined to be 69:31 *E:Z* by a series of 1D-NOESY NMR experiments. R_f = 0.48 (E), 0.43 (Z) (2% Et_2O/pentane). ***E*-isomer:** ^{1}H-NMR (300 MHz, $CDCl_3$) δ 6.11 (q, *J* = 6.6 Hz, 1H), 2.11 (q, *J* = 7.4 Hz, 2H), 1.89 (d, *J* = 6.6 Hz, 3H), 1.29 (s, 12 H), 0.98 (t, *J* = 7.5 Hz, 3H). ^{13}C-NMR (75 MHz, $CDCl_3$) δ 139.5, 82.8, 29.9, 24.8, 17.2, 14.9 [quaternary carbon adjacent to B not detected]; ^{11}B-NMR (96 MHz, $CDCl_3$) δ -35.5. ***Z*-isomer:** ^{1}H-NMR (300 MHz, $CDCl_3$) δ 6.39 (q, *J* = 6.9 Hz, 1H), 2.16 (q, *J* = 7.4 Hz, 2H), 1.72 (d, *J* = 6.9 Hz, 3H), 1.27 (s, 12H), 0.95 (t, *J* = 7.5 Hz, 3H); ^{13}C-NMR (75 MHz, $CDCl_3$) δ 139.6, 82.9, 24.7, 21.3, 14.4, 13.9 [quaternary carbon adjacent to B not detected]; ^{11}B-NMR (96 MHz, $CDCl_3$) δ -35.5. HRMS (CI) [M^+] calcd. for $C_{11}H_{21}BO_2$ 196.1635; Found 196.1635.

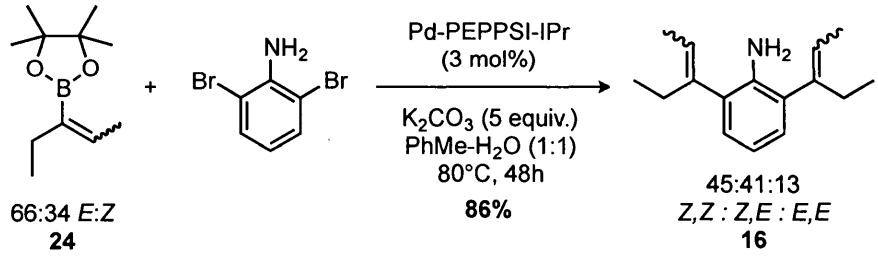

Synthesis of 2,6-di(pent-2-en-3-yl)aniline (16), representative procedure. A 25 mL round-bottom flask equipped with magnetic stir bar was charged with pinacol ester **24** (1.18 g, 6 mmol), Pd-PEPPSI-IPr (40.8 mg, 0.06 mmol), 2,6-dibromoaniline (0.5 g, 2 mmol), and K_2CO_3 (2.76 g, 20 mmol) in air. The flask was evacuated and backfilled with Ar (x3), charged with toluene (5 mL) and de-ionized water (5 mL), then sealed and allowed to stir at 80°C under a static atmosphere of Ar. After 48 h, the reaction was cooled to room temperature, diluted with Et_2O, and filtered through a short pad of celite, washing with Et_2O. The filtrate was washed with an equal volume of brine then the organic layer was extracted with 30 mL portions of 6 M HCl (x4) after which the combined extracts were basified with NaOH pellets to a pH of *ca.* 12. Subsequent extraction with Et_2O (100 mL x 3), washing with H_2O (100 mL x 2), drying over anhydrous $MgSO_4$, filtration, and concentration under reduced pressure yielded 394 mg

(86%) of **16** as an orange oil as a mixture of 3 major geometric isomers according to GC/MS analysis. The ratio of isomers was determined to be ca. 45:41:13 *Z,Z:Z,E:E,E* by ^{1}H-NMR and 2D-NOESY NMR analysis. ***Z,Z*-isomer:** ^{1}H-NMR (600 MHz, $CDCl_3$, 23°C) δ 6.88 (d, *J* = 7.2 Hz, 2H), 6.78 (t, *J* = 7.5 Hz, 1H), 5.69 – 5.64 (m, 2H), 2.41 – 2.39 (m, 4H), 1.55 – 1.48 (m, 6H), 1.10 – 1.01 (m, 6H); ^{13}C-NMR (100 MHz, $CDCl_3$, 60°C) δ 141.5, 140.3, 127.3, 126.4, 121.4, 117.2, 31.4, 14.2, 12.7. ***Z,E*-isomer:** ^{1}H-NMR (600 MHz, $CDCl_3$, 23°C) δ 6.91 (dd, *J* = 7.5 and 1.5 Hz, 1H), 6.86 (dd, *J* = 7.5 and 1.5 Hz, 1H), 6.75 (t, *J* = 7.5 Hz, 1H), 5.69 – 5.64 (m, 1H), 5.54 (q, *J* = 6.8 Hz, 1H), 2.51 – 2.40 (m, 2H), 2.41 – 2.39 (m, 2H), 1.85 – 1.81 (m, 3H), 1.55 – 1.48 (m, 3H), 1.10 – 1.01 (m, 3H), 0.99 (t, *J* = 7.5 Hz, 3H); ^{13}C-NMR (100 MHz, $CDCl_3$, 60°C) δ 141.8, 140.6, 130.1, 127.8, 127.3, 126.7, 123.5, 121.5, 117.1, 31.3, 24.0, 14.2, 13.3, 12.8, 12.6. ***E,E*-isomer:** ^{1}H-NMR (400 MHz, $CDCl_3$, 23°C) δ 6.91 (d, *J* = 7.2 Hz, 2H), 6.72 (t, *J* = 7.4 Hz, 1H), 5.56 (q, *J* = 6.8 Hz, 2H), 3.80 (br s, 2H), 2.45 (m, 4H), 1.85 (d, *J* = 6.8 Hz, 6H), 1.02 (t, *J* = 7.6 Hz, 6H); ^{13}C-NMR (100 MHz, $CDCl_3$, 23°C) δ141.3, 140.7, 130.2, 127.6, 123.7, 116.8, 23.9, 13.4, 12.8; HRMS (EI) [M^+] calcd. for $C_{16}H_{23}N$ 229.1830; found 229.1822.

*9.2.2 – Suzuki-Miyaura Route via alkenylchloride (**28**)*

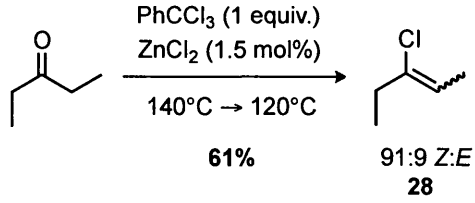

3-chloropent-2-ene (28) (Medium-Scale Synthesis): A 3-neck 500 mL round-bottom flask equipped with stir bar, reflux condenser, and pressure-equalizing addition funnel was charged with anhydrous $ZnCl_2$ (2.0 g, 15 mmol). The flask was then evacuated and backfilled with Ar (x3) and charged with α,α,α-trichlorotoluene (142 mL, 1 mol) via syringe. The resulting suspension was immersed in a pre-heated 140°C oil bath and allowed to stir vigorously at this temperature for 35 min during which time a colour

change from light yellow to deep violet was observed. The temperature of the oil bath was then lowered to 110°C and the addition funnel charged with 3-pentanone (106 mL, 1 mol). The ketone was added dropwise over ca. 1h and evolution of an acidic gas began immediately. After stirring for 16 h at 110°C, ^{1}H-NMR spectroscopic analysis ($CDCl_3$) revealed complete consumption of 3-pentanone. The flask was removed from the oil bath and allowed to cool over 10 min during which time the addition funnel was removed and the reflux condenser replaced with a simple distillation apparatus. The flask was then re-immersed in the oil bath and the temperature of the bath increased until a clear, colourless liquid began to distill (bath temp: 135-140°C, boiling point 94°C). 63.6 g (61%) of this liquid was collected and shown to be **28** in 98% purity as a mixture of geometric isomers The ratio of isomers was determined to be 91:9 *Z:E* with a 2D-NOESY NMR experiment. The distillate was contaminated with approximately 1% each of residual 3-pentanone and reaction by-product benzoyl chloride. On this scale, the product obtained after the initial distillation was used without further purification in subsequent reactions. To remove any dissolved HCl, the liquid was stored over K_2CO_3 and activated 4Å MS at -15°C under Ar. ***Z*-isomer:** ^{1}H-NMR (400 MHz, $CDCl_3$) δ 5.53 (q, J = 6.4 Hz, 1H), 2.35 (q, J = 7.2 Hz, 2H), 1.73 (d, J = 6.0 Hz, 3H), 1.13 (t, J = 7.4 Hz, 3H); ^{13}C-NMR (100 MHz, $CDCl_3$) δ 137.3 (+), 118.5 (–), 32.8 (+), 13.9 (–), 12.6 (–). ***E*-isomer:** ^{1}H-NMR (400 MHz, $CDCl_3$): δ 5.61 (q, J = 7.2 Hz, 1H), 2.38 (q, J = 7.2 Hz, 2H), 1.67 (d, J = 7.2 Hz, 3H), 1.13 (t, J = 7.4 Hz, 3H); ^{13}C-NMR (100 MHz, $CDCl_3$) δ 135.9 (+), 121.2 (–), 26.8 (+), 13.6 (–), 12.1 (–); HRMS (EI) [M^+] calcd. for C_5H_9Cl 104.0393; found 104.0389.

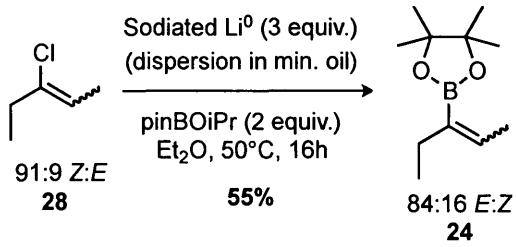

4,4,5,5-tetramethyl-2-(pent-2-en-3-yl)-1,3,2-dioxaborolane (23): A two-neck 1 L round-bottom flask equipped with reflux condenser and magnetic stir bar was charged with Li (12.5 g, 450 mmol, 25% dispersion in mineral oil) under positive Ar pressure via the side neck. The mineral oil was removed by adding 100 mL Et_2O via cannula, stirring the resulting suspension for 30 s, then withdrawing the Et_2O via cannula after all the Li had floated to the top (10 min – 20 min). After repeating this three times, 450 mL of Et_2O was added to the oil-free Li via cannula followed by pinBO^{i}Pr (61.2 mL, 300 mmol) and **28** (15.7 g, 150 mmol) via syringe. The grey suspension was allowed to stir at rt for 30 min then the flask was immersed in a pre-heated 50°C oil bath and stirred vigorously at this temperature for 22 h. A 300 μL aliquot was withdrawn, filtered through a short plug of Celite, and diluted with $CDCl_3$. ^{1}H-NMR spectroscopic analysis indicated complete consumption of **28** thus the reaction was cooled to r.t. The suspension was filtered through a 1 cm pad of Celite in a 150 mL coarse-porosity fritted glass funnel washing the pink filter cake with ca. 150 mL of Et_2O. The resulting light-yellow, turbid filtrate was washed successively with 500 mL portions of 0.5 M HCl, H_2O, and brine, then dried over anhydrous $MgSO_4$, filtered, and concentrated under reduced pressure at 30°C to yield 19.5 g of a light-yellow oil. Distillation in vacuo (p~60 mmHg, bp = 75°C) afforded 16.2 g (55%) of **24** as a clear, colourless oil as a mixture of geometric isomers, which was stored under Ar at -5°C. The ratio of isomers was determined to be 84:16 *E*:*Z* by a series of 1D-NOESY NMR experiments. Analytical data was consistent with that reported in Section 9.2.1 (*vide supra*).

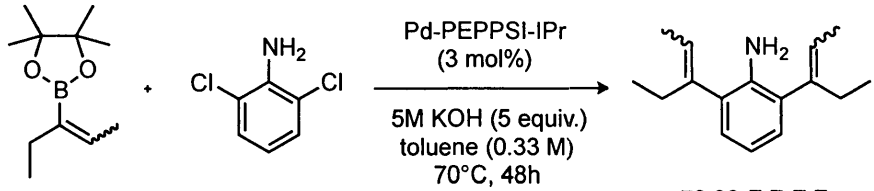

2,6-di(pent-2-en-3-yl)aniline (16): In air, an Ar-purged, oven-dried 200 mL round-bottom flask equipped with magnetic stir bar and reflux condenser was charged with pinacol ester **24** (11.12 g, 56.7 mmol), Pd-PEPPSI-IPr (550 mg, 0.81 mmol), and 2,6-dichloroaniline (4.37 g, 27 mmol). The flask was then evacuated and backfilled with Ar (x3) and charged with toluene (81 mL) and an aqueous 5 M KOH solution (27 mL, 135 mmol KOH). The resulting biphasic mixture was allowed to stir vigorously in a pre-heated 70°C oil bath overnight under Ar. Within 2-3 h, the colour of the organic layer changed from light yellow to orange with a grey emulsion present at the interface. After 48 h, a 300 μL aliquot was withdrawn from the brown organic layer and passed through a short plug of Celite covered with anhydrous $MgSO_4$, washing with EtOAc. GC/MS analysis indicated complete conversion of **24** to **16**, thus the reaction was cooled to rt. The biphasic mixture was filtered through a 1 cm pad of Celite in a 60 mL medium-porosity fritted glass funnel, washing with EtOAc until the filtrate was completely colourless. The filtrate was then transferred to a separatory funnel and the aqueous layer removed. The organic layer was washed with 100 mL portions of 1 M NaOH (x3), sat'd aq NH_4Cl (x1), and brine (x1), dried over anhydrous $MgSO_4$, and finally decolourized by stirring with 5 heaping spatulas of Norit SX-2 neutral activated charcoal for 30 min. The resulting suspension was filtered through a 1 cm pad of silica gel covered with a 1 cm pad of Celite washing with EtOAc. The filtrate was concentrated and 5.47 g (98%) of **16** were obtained as a yellow-orange oil as a mixture of 2 major geometric isomers according to GC/MS analysis. The ratio of isomers was determined to be approximately 70:30 *Z,Z*:*E,Z* using 2D-NOESY NMR analysis. A small amount of the *E,E*-isomer was

also visible by GC/MS analysis. Analytical data for the two isomers is consistent with that reported in Section 9.2.1 (*vide supra*).

*9.2.3 – Kumada-Tamao-Corriu Route via alkenylchloride (**28**)*

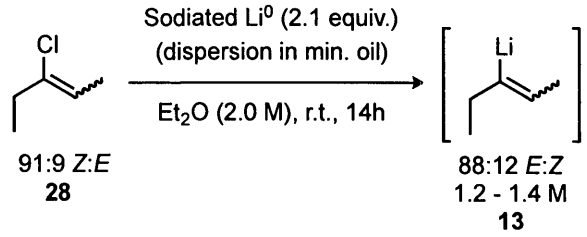

Pent-2-en-3-yllithium (13) (Medium-Scale Synthesis): A 2-neck 250 mL round-bottom flask equipped with reflux condenser and magnetic stir bar was charged with Li (12.8 g, 462 mmol, 25% dispersion in mineral oil) via the side neck under positive Ar pressure, rinsing with ca. 10 mL Et_2O as necessary. To remove the mineral oil, Et_2O (50 mL) was added and the resulting grey suspension stirred for 30 s then allowed to stand until the Li particles had floated to the surface (ca. 20 min), at which time the supernatant was carefully removed via cannula. This process was repeated a total of three times. To the oil-free Li was added Et_2O (90 mL), then the flask was fitted with an oven-dried pressure-equalizing addition funnel under positive Ar pressure. The addition funnel was charged with a solution of **28** in 20 mL Et_2O and dropwise addition began over a period of one hour to the gently stirring, grey suspension. Within 10 min, a gentle reflux was observed which became more vigorous after 30 min. After the addition was complete, the addition funnel was rinsed with 2-3 mL Et_2O and the vigorously refluxing suspension was allowed to stir overnight. After 16 h, the insoluble LiCl salt byproduct was allowed to settle leaving a dark orange solution of **13** ranging in concentration from 1.2 – 1.4 M, as determined by titration with 1,3-diphenylacetone p-tosylhydrazone.[38]

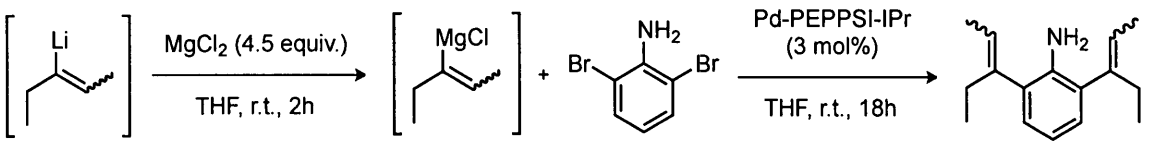

88:12 *E*:*Z*
13

78:22 *Z,Z*:*E,Z*
16

2,6-di(Pent-2-en-3-yl)aniline (16): A 3-neck 500 mL round-bottom flask equipped with magnetic stir bar, reflux condenser (L-neck), 250 mL pressure-equalizing addition funnel (C-neck), and rubber septum (R-neck) was charged with anhydrous $MgCl_2$ (15.9 g, 167 mmol), which had been pre-weighed in a glovebox, via the R-neck under positive Ar pressure. The flask was then evacuated and backfilled with Ar (x3), after which THF (45 mL) was added forming a white suspension (slight exotherm). The addition funnel was charged with a 1.3 M solution of **13** in Et_2O (100 mL, 130 mmol) *via* cannula and dropwise addition of this solution was initiated over a period of 35 min, during which an exothermic reaction was apparent. The addition funnel was rinsed with 2-3 mL Et_2O and the resulting light-yellow suspension was allowed to stir for 2 h. To the addition funnel was added a solution of 2,6-dibromoaniline (9.31 g, 37.1 mmol) and Pd-PEPPSI-IPr (757 mg, 1.11 mmol) in 40 mL THF, which was then added dropwise to the reaction over 15 min, initiating a vigorously exothermic reaction. The funnel was rinsed with 5 mL THF and the yellow/orange mixture was allowed to stir overnight under Ar. After 16 h, a 200 μL aliquot was withdrawn from the orange suspension, quenched into sat'd aq. NH_4Cl and extracted into EtOAc. The extract was filtered through a short plug of silica gel with EtOAc and analyzed for completion *via* GC/MS, which indicated complete conversion of starting material to desired product, *m/z* 229 (2 major geometric isomers) along with a trace amount (<1%) of 2,4,6-tri(pent-2-en-3-yl)aniline, *m/z* 281 (2 major geometric isomers), originating from an equivalent amount of 2,4,6-tribromoaniline present in the starting material. The flask was fitted with a clean 250 mL addition funnel and charged with 80 mL of a cold (4-5°C) 1 M HCl solution. The first 30 mL were added at a rate of 0.75 mL/minute with vigorous stirring, resulting in a vigorously exothermic reaction and the formation of a dense beige precipitate. Once the exotherm had subsided, the addition

rate was increased to ca. 3 mL/min until the remainder of the solution had been added. After the addition was completed, the precipitate had fully dissolved and the mixture was biphasic with the aqueous layer at a pH of 3 – 4. The contents of the flask were transferred to a separatory funnel, diluting with H_2O as necessary to break up a black Pd emulsion in the aqueous layer. The organic layer was collected and the aqueous layer extracted with Et_2O (x2). The combined organic extracts were washed with brine then stirred with anhydrous $MgSO_4$ and Norit SX neutral activated charcoal (10 g) for 16 h. The suspension was then filtered over a 2 cm pad of silica gel in a 150 mL M-porosity fritted glass funnel washing the filter cake with Et_2O until the filtrate became colourless. The light-yellow filtrate was concentrated under reduced pressure and the resulting oil azeotroped with toluene (100 mL x 3) to remove excess water and any traces of dimerized Grignard reagent. After drying for 16 h under high vacuum, 8.83 g (104%) of **16** were obtained as a dark-orange oil, as a mixture of 2 major geometric isomers according to GC/MS analysis. The ratio of isomers was determined to be 78:22 *Z,Z*:*E,Z* using ^{1}H-NMR and 2D-NOESY NMR spectroscopic analysis. According to ^{1}H-NMR analysis, the product was contaminated with 1 – 2 % of some NHC-ligated palladium complex, however the crude was used directly without further purification since this catalyst by-product is effectively removed during the subsequent catalytic hydrogenation. Analytical data for the two isomers is consistent with that reported in Section 9.2.1 (*vide supra*).

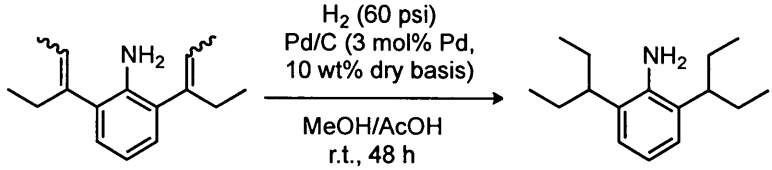

78:22 *Z,Z*:*E,Z*
16

9

2,6-di(pentan-3-yl)aniline (9): An oven-dried hydrogenation flask was charged with **16** (9.7 g, 42.3 mmol), glacial acetic acid (31 mL), HPLC-grade methanol (85 mL), and Pd/C (10 wt% Pd, dry basis, 1.35 g, 1.27 mmol) in portions. The flask was transferred to

a Parr shaker, evacuated and backfilled with H_2 (x4), then allowed to shake under H_2 (60 psi) for 48 h, at which time GC/MS analysis indicated complete conversion of **16** to **9**. The reaction mixture was filtered through a pad of Celite, washing the filter cake copiously with MeOH. The volatiles were then evaporated under reduced pressure at 55°C and the resulting light-brown residue was diluted with Et_2O. With stirring, a solution of 2M NaOH was added to the mixture until the pH of the aqueous layer was 10 – 12. The biphasic mixture was transferred to a separatory funnel and the organic layer collected. The aqueous layer was extracted with Et_2O (x2) and the combined organic extracts were washed with brine, dried over anhydrous $MgSO_4$, then filtered through a 2 cm pad of silica gel in a 60 mL M-porosity fritted glass funnel, washing the filter cake with Et_2O until the filtrate became colourless. The filtrate was concentrated under reduced pressure and dried under high vacuum for 16 h to yield 9.34 g (95%) of **9** as a light-orange oil. ^{1}H-NMR (400 MHz, $CDCl_3$) δ 6.94 (d, J = 7.6 Hz, 2H), 6.81 (t, J = 7.6 Hz, 1H), 3.66 (br s, 2H), 2.53 (quint, J = 6.6 Hz, 2H), 1.81-1.58 (m, 8H), 0.88 (t, J = 7.6 Hz, 12H). ^{13}C-NMR (100 MHz, $CDCl_3$) δ 142.5 (+), 130.0 (+), 123.8 (–), 118.4 (–), 42.3 (–), 28.0 (+), 12.0 (–). These spectral data are consistent with those reported in the literature.[7]

CHAPTER 10: References

1. (a) Organ, M. G.; Calimsiz, S.; Sayah, M.; Hoi, K. H.; Lough, A. J. *Angew. Chem. Int. Ed.* **2009**, *48*, 2383–2387; (b) Calimsiz, S.; Sayah, M.; Mallik, D.; Organ, M. G. *Angew. Chem. Int. Ed.* **2010**, *49*, 2014–2017.
2. (a) O'Brien, C. J.; Kantchev, E. A. B.; Valente, C.; Hadei, N.; Chass, G. A.; Lough, A.; Hopkinson, A. C.; Organ, M. G. *Chem. Eur. J.* **2006**, *12*, 4743–4748.
3. For a recent review on the synthesis of N-heterocyclic carbene precursors, see: (a) Benhamou, L.; Chardon, E.; Lavigne, G.; Cesar, V. *Chem Rev.* **2010**, *111*, 2705–2733. (b) Hahn, F. E.; Jahnke, M. C. *Angew. Chem. Int. Ed.* **2008**, *47*, 3122–3172.
4. Arduengo, A. J.; Krafczyk, R.; Schmutzler, R. *Tetrahedron* **1999**, *55*, 14523–14534.
5. Jafarpour, L.; Stevens, E. D.; Nolan, S. P. *J. Organomet. Chem.* **2000**, *606*, 49–54.
6. L. Hintermann, *Beilsten J. Org. Chem.* **2007**, *3*, 1–5.
7. Steele, B. R.; Georgakopoulos, S.; Micha-Screttas, M.; Screttas, C. G. *Eur. J. Org. Chem.* **2007**, *19*, 3091–3094.
8. Sayah, M.; Calimsiz, S.; Organ, M. G. *Unpublished Results.*
9. Mallik, D.; Tsimerman, M.; Organ, M. G. *Unpublished Results.* Adapted from Tsimerman, M. PhD Thesis, York University, 2013.
10. Pompeo, M. *CHEM 4000 Undergraduate Research Thesis*, **2009**, unpublished results.
11. Lanet, J. C. US Patent 3,899,532, August 12, 1975.
12. Billingsley, K. L.; Barder, T. E.; Buchwald, S. L. *Angew. Chem. Int. Ed.* **2007**, *46*, 5359–5363.
13. Stang. P. J.; Summerville, R. J. *J. Am. Chem. Soc.*, **1969**, *91*, 4600–4601.
14. For a concise review, see (a) Ritter, K. *Synthesis*, **1993**, *8*, 735–762; for a more general review of triflate chemistry, see (b) Stang, P. J.; Hanack, M.; Subramanian, L. R. *Synthesis*, ***1982***, 85–126.
15. (a) Ohe, T.; Miyaura, N.; Suzuki, A. *J. Org. Chem.*, **1993**, *58*, 2201–2208; (b) Ishiyama, T.; Murata, M.; Miyaura, N. *J. Org. Chem.*, **1995**, *60*, 7508–7510; (c)

Ishiyama, T.; Itoh, Y.; Kitano, T.; Miyaura, N. *Tetrahedron Lett.* **1997**, *19*, 3447–3450; (d) Takagi, J.; Takahashi, K.; Ishiyama, T.; Miyaura, N. *J. Am. Chem. Soc.*, **2002**, *124*, 8001–8006.

16. For reviews involving the use of vinyl triflates in cross-coupling reactions, see: (a) Stille, J. K. *Pure Appl. Chem.*, **1985**, *57*, 1771–1780.; (b) Stille, J. K. *Angew. Chem. Int. Ed.*, **1986**, *25*, 508–524; (c) Scott, W. J.; Stille, J. K. *J. Am. Chem. Soc.*, **1986**, *108*, 3033–3040; (d) Kalinin, V.N. *Synthesis*, **1992**, 413–432; (e) Mitchell, T. N.; *Synthesis*, **1992**, 803–815; (f) Sheiper, B.; Bonnekessel, H. K.; Furstner, A. *J. Org. Chem.* **2004**, *69*, 3943–3949.
17. Stang. P. J.; Rappaport, Z.; Hanack, M.; Subramanian, L. R. *Vinyl Cations;* Academic: New York, **1979**.
18. Stang, P.J.; *Acc. Chem. Res.*, **1978**, *11*, 107–114.
19. (a) Stille, J. K., *Pure Appl. Chem.*, **1985**, *57*, 1771–1780; (b) Scott, W. J.; McMurry, J. E. *Acc. Chem. Res,* **1988**, *21*, 47–54; (b) McMurry, J. E.; Scott, W. J. *Tetrahedron Lett.* **1983**, *24*, 979–982; (c) Stang, P. J.; Treptow, W. *Synthesis*, **1980**, 283–284.
20. Takagi, J.; Takahashi, K.; Ishiyama, T.; Miyaura, N. *J. Am. Chem. Soc.* **2002**, *124*, 8001–8006.
21. Hall, D. G., ed. *Boronic Acids: Preparation, Applications in Organic Synthesis and Medicine.* **2005**, Wiley.
22. Calimsiz, C.; Organ, M. G. *Unpublished Results.*
23. In ref. 7, the solubility of **9**·HCl was reported to be greater in hexanes than in water, demonstrating the immense lipophilic character of the ortho-alkyl substituents.
24. Clayden, J. *Organolithiums: Selectivity for Synthesis.* **2002**, Elsevier Science, Ltd, Oxford.
25. Wakefield, B. J. *Organomagnesium Methods in Organic Chemistry.* **1995**, Elsevier Science, Ltd., Oxford.
26. Calimsiz, S.; Organ, M. G. *Unpublished Results*

27. Braude, E. A.; Forbes, W. E. *J. Chem. Soc.* **1951**, 1755–1761.

28. Brandsma, L; Verkruijsse, H. D. *Synth. Comm.* **1990**, 21, 3367–3369.

29. Stannety, P.; Koller, H.; Mihovilovic, M. *J. Org. Chem.* **1992**, *57*, 6833–6837.

30. Smith, D. B.; Waltos, A. M.; Loughhead, D. G.; Weikert, R. J.; Morgans, Jr., D. J.; Rohloff, J. C.; Link, J. O.; Zhu, R. *J. Org. Chem.* **1996**, *61*, 2236–2241.

31. O'Brien, C. J.; Kantchev, E. A. B.; Valente, C.; Hadei, N.; Lough, A.; Hopkinson, A. C.; Organ, M. G. *Chem. Eur. J.* **2006**, *12*, 4743–4748.

32. For a review on the use of potassium trifluoroborate salts see: Molander, G. A.; Canturk, B. *Angew. Chem. Int. Ed.* **2009**, *48*, 9240–9261.

33. After storage in a desiccator over $P_2O_5/CaCl_2$ for two weeks, the solid went from flocculent and white to sticky and yellow accompanied with some decomposition as observed by ^{1}H-NMR spectroscopic analysis.

34. The lower-boiling components of the mineral oil began to co-distil with **24** towards the end of the distillation.

35. Organ, M. G.; Abdel-Hadi, M.; Avola, S.; Hadei, N.; Nasielski, J.; O'Brien, C. J.; Valente, C. *Chem. Eur. J.* **2007**, *13*, 150–157.

36. Sayah, M. PhD Dissertation, York University, Toronto, ON, Canada, 2013.

37. Jin, L.; Liu, C.; Liu, J.; Hu, F.; Lan, Y.; Batsanov, A. S.; Howard, J. A. K.; Marder, T.; Lei, A. *J. Am. Chem. Soc.* **2009**, *131*, 16656–16657.

38. Lipton, M. F.; Sorensen, C. M.; Sadler, A. C.; Shapiro, R. H.; *J. Organomet. Chem.* **1980**, *186*, 155–158.

39. Hydrogenation procedure optimized by Dr. Debasis Mallik.

40. Hydrogenation performed by Dr. Subakar Paramanantham and Dr. Evgeny Kuzakov at Dalton Pharma Services, 349 Wildcat Rd., Toronto, ON M3J 2S3, Canada.

41. Still, W.C.; Kahn, M.; Mitra, A. *J. Org. Chem*, **1978**, *43*, 2923–2925.